Low Energy, Passive Acoustic Sensing for Wireless Underwater Monitoring Networks

Gavin James Lowes

School of Engineering
Newcastle University

This dissertation is submitted for the degree of
Doctor of Philosophy

Newcastle University May 2022

Abstract

This thesis presents the research conducted to develop low energy passive acoustic monitoring (PAM) algorithms. There are many signal processing techniques and machine learning systems which are capable of detecting and classifying target signals. However, this project aims to produce PAM detection and classification results using a low energy budget. The benefit of using this approach is that physical devices can be developed and deployed in open sea for several months using only battery power. This opens up the deployment area to very deep water where power sources are not readily available. Using passive acoustic communication to relay the detection data produced by the algorithm, it is expected that these systems could form an underwater network of sensor nodes.

There are three targets for passive acoustic detection/classification included in this thesis, which are motorised surface vessels, cetacean clicks and cetacean whistles. The surface vessel detection method is based on a low energy implementation of Detection of Envelope Modulation On Noise (DEMON). Vessels produce high frequency modulated noise during propeller cavitation which the DEMON method aims to extract for the purposes of automated detection. The vessel detector design has different approaches with mixtures of analogue and digital processing, continuous and duty-cycled sampling/processing. The detector has been integrated with a low cost/power acoustic modem platform to provide acoustic communication of data in near real time. The vessel detector has been deployed at 20m depth for a total of 84 days in the North Sea providing a large data set, which the results are based on.

Open sea field trial results have shown the detection of single and multiple vessels with a 94% corroboration rate with local Automatic Identification System (AIS) data. Results have shown additional information about the detected vessel, such as the number of propeller blades, can been extracted solely based on the detection data. The attention to energy efficiency has led to an average power consumption of 11.4mW enabling long term deployments of up to 6 months using only four alkaline C cells. Additional battery packs and a modified enclosure could enable a longer deployment duration. As the detector was still deployed during the first UK lockdown, the impact of Covid-19 on North Sea fishing activity has been captured in the results.

Cetacean click detection is based on identifying and classifying the high frequency impulsive click trains created by cetaceans during navigation and foraging. A low energy method of detecting these vocalisations is proposed alongside a statistical based method of classification. The algorithm developed was tested using real recordings of cetacean activity and comparisons have been conducted against a commercially available cetacean monitoring system. The results show that the energy efficient algorithm produces comparable results to the commercial system when real recordings are processed.

The cetacean whistle detection algorithm is based on a low energy phase locked loop (PLL) technique. PLL methodology has been adapted for this project to aid in developing a low energy approach to detecting cetacean whistles by tracking the sweeps in frequency they produce. Results are based on offline processing using real recordings of these animals. The results have shown a 75% success rate when comparing against human analysis of the recording.

Future work includes the further development of the cetacean related algorithms into fully deployable, battery-powered, nodes for open sea field trails. The future work related to vessel detection includes adding a tracking feature to the passive acoustic monitoring technology.

I would like to dedicate this thesis to the memory of my father,
Anthony James Lowes (1956-2016).

Acknowledgements

There are a number of people and organisations I would like acknowledge and thank for supporting this project.

Firstly, I would like to thank Newcastle University and the School of Engineering for providing me with the opportunity and facilities to undertake this research project.

I would like to acknowledge the project sponsor, Engineering and Physical Sciences Research Council (EPSRC), for funding this project. I would like to thank the project collaborators, University of York, Herriet-Watt University, Technip FMC, Imenco UK Ltd and Subsea 7.

I owe thanks to the members of the Sensors, Electromagnetics and Acoustics Laboratory (SEALab) for their support during this project, including Jeff Neasham, Ben Sherlock, Richie Burnett, Dave Graham and Lindsay Smith. The open knowledge sharing in this laboratory has been invaluable to my progression as a researcher.

I would like to pay special thanks to my project supervisor Jeff Neasham for not only awarding me this opportunity but also for supporting my learning aspirations during this project. I would also like to thank my second supervisor Charalampos Tsimenidis for his support during this PhD.

I would like to give special thanks to my friends who have encouraged me during the challenges of completing a PhD including David Stephenson, Craig Crosby, Christopher Melrose and Conor McCue.

I owe thanks to my family who have supported me throughout this journey, Michelle, Jon-Paul, Phil and Jimmy. I would also like to thank my dog Jasper because he is great and I want his name in my thesis.

I owe a special thank you to my partner Annie for supporting me during the ups and downs of this journey. She has always encouraged me to keep going during the tough times and has supported me every step of the way.

Finally, I would like to thank my mother, Susan Lowes, who has believed in me from day one and without her support I would not have completed this PhD journey. I will be forever grateful to her.

Table of contents

List of figures

List of tables

Nomenclature

Acronyms / Abbreviations

ADC Analogue to digital converter

AGC Automatic Gain Control

AIS Automatic Identification System

ANGY Acoustic Network Gateway

ANN Artificial Neural Network

CADD Continuous Analogue and Digital Detection

CART Classification and Regression Trees

CDA Cetacean Detection Algorithm

CIC Cascaded Integrator-Comb

DEMON Detection of Envelope Modulation On Noise

DMA Direct Memory Access

DSP Digital Signal Processing

FFT Fast Fourier Transform

FPR False Positive Rate

FT Fourier Transform

GPS Global Positioning System

ICI Inter-click Interval

JNCC Joint Nature Conservation Committee

LDA Linear Discriminant Analysis

MARS Monterey Accelerated Research System

MMSI Maritime Mobile Service Identity

NBHF Narrow Band High Frequency

NCDD Non-Continuous (duty-cycled) Digital Detection

NCO Numerically Controlled Oscillator

NEPTUNE Northeast Pacific Undersea Networked Experiments

NERC Natural Environment Research Council

NIFCA Northumberland Inshore Fisheries and Conservation Authority

NMV3 NanoModem V3 - Underwater acoustic modem developed by SEALab

PAM Passive Acoustic Monitoring

PCB Printed Circuit Board

PLL Phase Locked Loop

RADAR Radio Detection and Ranging

RHIB Rigid-Hulled Inflatable Boats

RNLI Royal National Lifeboat Institution

ROC Receiver Operating Characteristic

RSD Relative Standard Deviation

SEALab Newcastle University's Sensors Electromagnetics and Acoustics Laboratory

SEOE Standard Error Of the Estimate

SOLAS Safety Of Life At Sea

SONAR Sound Navigation And Ranging

SOSUS Sound Surveillance System

SVM Support Vector Machine

TDOA Time Difference Of Arrival

TPR True Positive Rate

USMART Smart dust for large scale underwater wireless sensing

WT Wavelet Transform

Chapter 1

Introduction

Passive acoustic monitoring (PAM) is used to measure, monitor and identify the source of incoming signals. Signals are captured and processed to identify unique features related to the target. A wide variety of PAM techniques have been produced by researchers to identify targets such as vessels, cetaceans, submarines, remotely operated vehicles etc. In many of these publications, targets have been identified with the help of a high degree of processing power. Often signals of interest are in the 100's of kHz, such as some species of cetaceans. This requires a high sample rate to capture the signal and in turn will require significant processing capabilities. The overall aim of this project is to identify the same targets as other research but in such a way that maximises power efficiency. To give context to the term power efficiency, this project aims to develop low power/cost hardware and software to automatically detect a variety of targets using a power budget of approximately 10 mW. It is hoped that using this low power budget, detection and classification of targets can still be reliably achieved when compared to the best available ground truth.

The algorithms presented in this thesis are related to three passive acoustic monitoring targets. They are cetacean whistles, cetacean clicks and surface vessels. In the algorithms developed for each of these targets, various degrees of implementation have been achieved. In the research related to PAM of cetacean clicks and whistles, algorithms have been evaluated against real recordings using offline processing. In the surface vessel research, algorithms have not only been developed and tested offline, they have also been implemented into custom hardware and deployed in open sea field trials.

1.1 Contributions

The research presented in this thesis has contributed to the development of underwater acoustic wireless sensor networks by producing energy-efficient detection and classification

algorithms. Integration of the presented algorithms into practical hardware nodes for remote deployment at sea is a major focus of the work presented. The following list states the main contributions of this research project:

1. Develop passive acoustic detection algorithms that can be implemented with very low energy processing (in the order of 10 mW).
2. Evaluate the performance of detection algorithms by using recorded data of the target compared against the best available ground truth.
3. Adapt an existing low cost/power acoustic modem platform (the NanoModem V3 (NMV3) developed by SEALab at Newcastle University) to implement an embedded wireless detection device.
4. Demonstrate underwater acoustic transmission of detection information related to the target.
5. Evaluate system performance in a realistic offshore environment.

1.2 Publications

The following publications are a result of the research carried out in this thesis:

1. Lowes, G. J., Neasham, J., Burnett, R., Sherlock, B., and Tsimenidis, C. (2022). Passive acoustic detection of vessel activity by low-energy wireless sensors. *Journal of Marine Science and Engineering*, 10(2):248
   DOI: 10.3390/jmse10020248
2. Lowes, G. J., Neasham, J. A., Burnett, R., and Tsimenidis, C. C. (2019). Low energy, passive acoustic sensing for wireless underwater monitoring networks. In *OCEANS 2019 MTS/IEEE SEATTLE*, pages 1–9. IEEE.
   DOI: 10.23919/OCEANS40490.2019.8962399

1.3 Thesis Outline

This section provides an outline of the thesis by giving a short description of each chapter. There are three main technical chapters related to the three passive acoustic targets which are cetacean clicks, cetacean whistles and surface vessels. Figure 1.1 outlines the structure of the technical chapters including the level of development for each passive acoustic target.

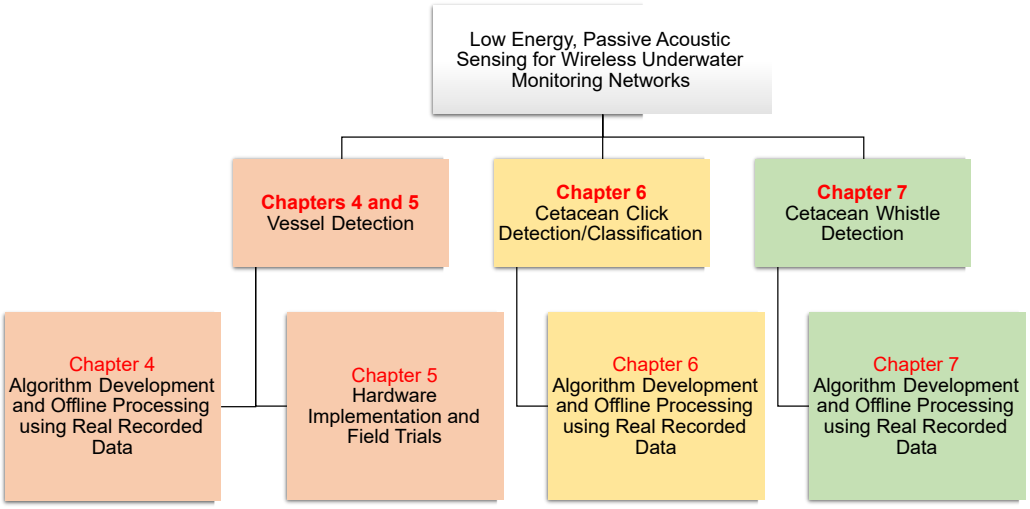

Fig. 1.1 Thesis structure diagram to illustrate the three areas of technical content.

Chapter 2 gives the fundamental background information related to the field of underwater acoustics and PAM. It also includes information related to the specific passive acoustic targets of this research. This includes cetacean acoustic information which covers areas such as the definition of cetacean whistles and clicks. Information related to vessel acoustics and in particular the sounds created during propeller cavitation is also included in this chapter.

In Chapter 3, the literature related to this research is presented and analysed. The literature falls under the two main categories of passive acoustic target, cetaceans and vessels. The literature presented shows the methods in which authors have approached acoustic detection and classification of cetaceans and vessels. It also discusses the current state-of-the-art technology available to monitor these acoustic targets.

Chapters 4 and 5 are related to a vessel detection algorithm, which has been both developed and practically implemented into custom designed hardware. These chapters demonstrate the development of the vessel detector from initial algorithm to a fully prototyped sensor node, deployed in open sea field trials. Chapter 4 contains the research carried out to develop the vessel detection algorithm. This includes the offline processing of vessel recording to aid development and testing of the algorithm. The results of this chapter led to the implementation of the algorithm in custom hardware, which is detailed in chapter 5. The following chapter outlines the extensive field trial results and the analysis of the algorithm's performance.

Chapter 6 is related to cetacean click detection and classification. Algorithms are presented which aim to detect and classify these signals using a power efficient approach. The algorithms developed are tested using offline processing in which real cetacean recordings are used to evaluate performance.

Chapter 7 is the second of the cetacean technical sections is related to whistle detection. A low energy method of detecting whistles using frequency tracking is presented. The algorithm developed is evaluated using real recordings of cetacean activity compared against human manual analysis of the same recording.

Chapter 8 outlines the conclusion and recommendations derived from this thesis. It details the concluding contributions this work has made to the research community. The final part of this chapter is the recommended future work to take this research further.

Chapter 2

Background

2.1 Introduction

This chapter provides the background information related to the research conducted in this thesis. As this project is related to underwater PAM techniques and technology, an overview of underwater acoustics is included. It is important to not only understand how sound travels underwater but also the challenges that the channel/environment can create. This first section on underwater acoustics is then followed by more specific topics related to the PAM targets, which are surface vessels and cetaceans.

2.2 Underwater Acoustics

In this section, key concepts related to underwater sound are introduced to give the reader an understanding and appreciation of the challenges faced during this project. The underwater environment is unpredictable in its nature with many sources of interference, both natural and man-made. As the main theme of this project is related to developing passive acoustic detection techniques, the underwater acoustic environment is an essential area of consideration during design.

Acoustics have been utilised as the preferred method for data transfer and localisation underwater by both humans and cetaceans. The advantage of using sound as opposed to light or radio waves for underwater applications is due to the propagation characteristics of each method. In sea water, sound waves suffer far less attenuation and travel considerably further than that of light or radio waves [90]. Humans have used underwater acoustics for detection purposes as far back as the 15^{th} century. Leonardo Di Vinci documented PAM by stating, *"If you cause a ship to stop, and place the head of a long tube in the water and place*

the outer extremity to your ear, you will hear ships at a greater distance from you" [15]. This simple method has since evolved into the development of both passive and active underwater acoustic monitoring systems. PAM systems became critical tools during times of war to detect approaching enemy vessels. The United States of America adopted passive technology on a large scale during the Cold War by deploying many hydrophone arrays on the seabed along the coastline. The system was named SOSUS, which stood for Sound Surveillance System [50]. Research in active acoustic detection was intensified after the sinking of the Titanic in 1912, with hopes of locating the wreckage acoustically [50]. To achieve reliability in terms of passive acoustic detection and classifications, it is important to understand the physical properties of acoustic propagation in the underwater channel.

2.2.1 Speed of sound

The speed of sound may seem like a trivial consideration given the well documented bench mark of $1500\,\mathrm{m\,s^{-1}}$ [50]. This is a good approximation but does not give the full picture. The speed that an acoustic wave travels through a medium, such as sea water, is directly related to the local characteristics of the medium itself. Specifically, the propagation speed c $(\mathrm{m/s})$ is related to the density ρ $(\mathrm{kg/m^3})$ and compressibility χ $(\mathrm{Pa^{-1}})$ of the transmission medium. This relationship is described in Equation 2.1.

$$c = \sqrt{\frac{1}{\chi\rho}} \tag{2.1}$$

In sea water, the density ρ and compressibility χ are not constant. Density ρ varies with the chemical composition of the water and compressibility χ varies with both temperature and pressure. The variation of temperature, salinity and pressure are all contributing factors which influence the speed of sound underwater. As Figure 2.1 shows, all three of these contributions vary with depth, which can make the speed of sound difficult to predict.

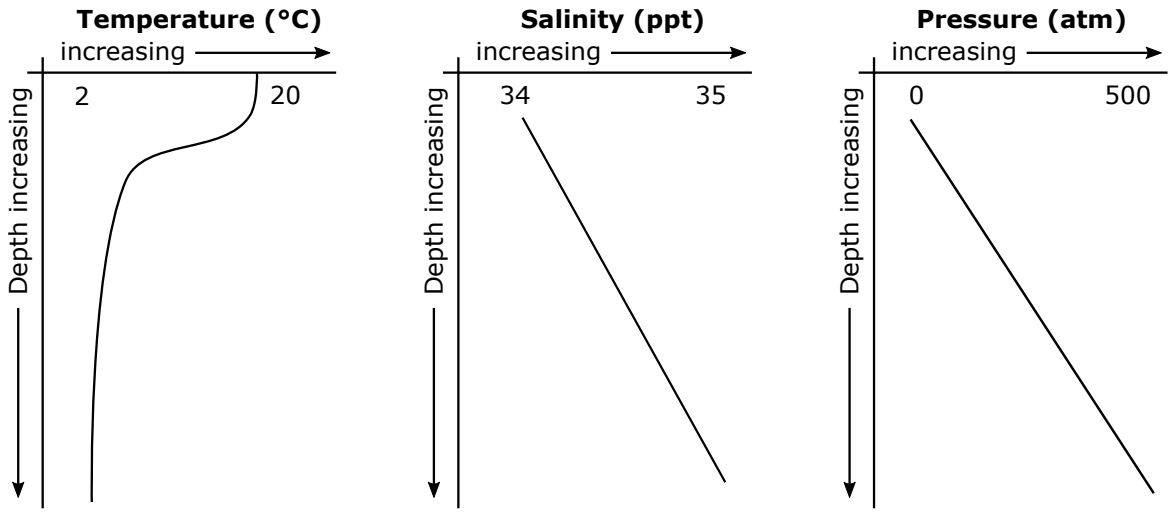

Fig. 2.1 Impact of temperature, salinity and pressure on sound speed as a function of depth.

A typical sound speed profile is shown in Figure 2.2. As illustrated, there is a noteable non-linear change in the speed of sound as depth is increased.

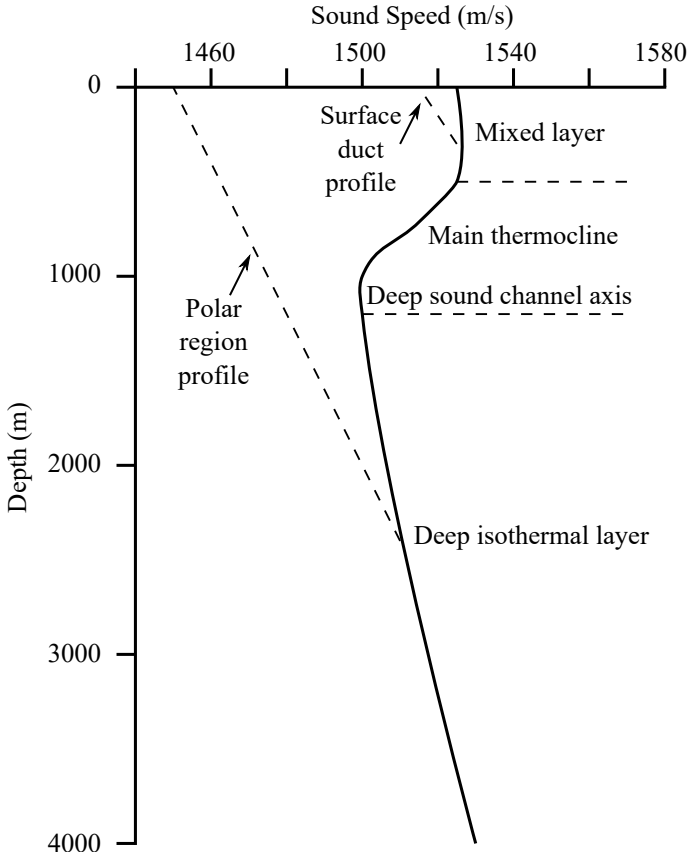

Fig. 2.2 Example of a typical underwater sound speed profile for varying depth [1].

It must be noted that Figure 2.2 provides only a generic overview of the speed of sound as a function of depth. It does not show the potential variation in sound speed due to factors such as geographical location or season. These variations are shown in Figure 2.3, which provides example sound speed profiles for different locations during contrasting seasonal conditions. Example 'E' in figure 2.3 is one of the most variable sound speed profiles illustrated, which is caused by a warm and cold water infusion between Atlantic and Mediterranean waters. The impact of a strong thermocline layer on acoustic propagation can be severe as sound can be refracted back towards the colder regions. This can cause problems if a receiving hydrophone is not deployed deep enough to avoid this warm water layer. Examples 'G' to 'J' also illustrate that sound speed profiles in shallow water can be just as variable as the deeper water examples.

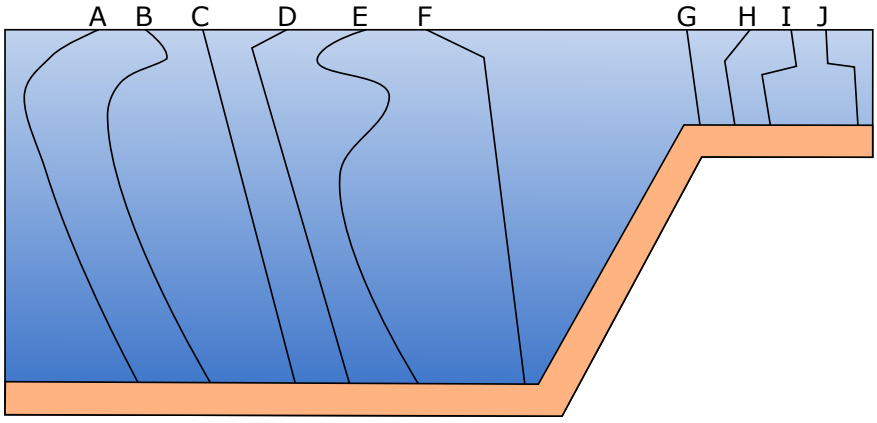

A - Summer SOFAR Channel
B - Winter SOFAR Channel
C - Winter Mediterranean
D - Summer Mediterranean
E - NE Atlantic with Mediterranean Water Intrusion
F - Polar
G - Winter Shallow Water
H - Summer Shallow Water
I - Autumn Shallow Water
J - Shallow Water with Fresh Water at the Surface

Fig. 2.3 An illustration of the high variability of sound speed in different depths, seasons and locations [50].

As this section illustrates, the speed of sound can vary depending on a variety of factors and should not be assumed to be constant nor predictable without analysing the medium in which the sound is travelling.

2.2.2 Sound Propagation

When an acoustic wave propagates through sea water, it is subject to losses due to spreading and absorption. Spreading losses are a measure of the energy lost as the signal propagates

away from the source. Absorption losses relate to the dissipative nature of sea water in that energy from the acoustic wave is absorbed into the sea water and dissipated through chemical reaction [50].

Spreading losses can be sub categorised due to the limiting boundaries of the subsea environment. A point acoustic source will transition from an initial spherical spreading, with increasing radius over time, to cylindrical spreading due to the surface and seabed boundaries.

An example of spherical spreading in illustrated in Figure 2.4 which shows a point source S with omni-directional spreading.

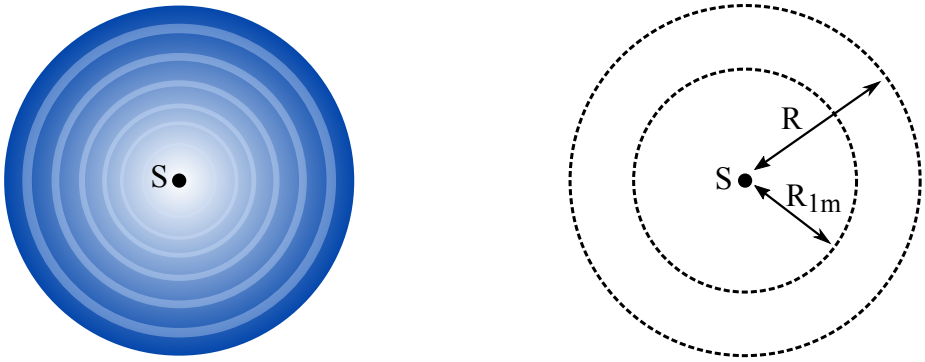

Fig. 2.4 An illustration of spherical spreading from a point source to complement Equation 2.2.

There are two radius measurements shown which relate to a one metre reference R_{1m} and a point of measurement radius R, both measured in metres. Using these radii values along with a correction for absorption α related attenuation, the transmission loss TL measured in decibel dB can be calculated using Equation 2.2.

$$TL = 20\log(R/R_{1m}) + \alpha R \tag{2.2}$$

The transmission loss equation is true for spherical spreading, however once a transition is made into cylindrical spreading there is a change in the average transmission loss calculation. Figure 2.5 illustrates the transition from a spherical spreading signal to that of a cylindrical spreading signal. Assuming the source is positioned at mid-height of variable H, the transition range r_0 (i.e. the spherical propagation region prior to transitioning to cylindrical propagation defined by the surface and seabed boundaries) is represented by Equation 2.3.

$$r_0 = \frac{H}{2tan\beta_0} \tag{2.3}$$

Figure 2.5 also shows that regions exist near to the source where sound waves of sufficiently large angle β_0, become negligible due to bottom reflection losses.

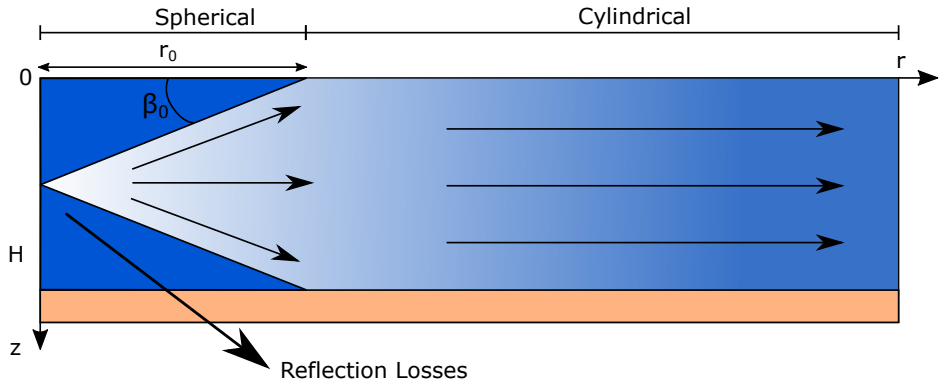

Fig. 2.5 Transition from spherical spreading to cylindrical spreading transmission loss due to the physical barrier of the ocean.

As Figure 2.5 shows, the spherical spreading signal transforms due to the sea surface and sea floor. The impact of this transition on transmission loss is highlighted in Equation 2.4 which shows a decrease in transmission loss intensity when cylindrical spreading occurs.

$$\begin{aligned} TL &= 20 + \alpha r & r < r_0 \\ TL &= 10\log(rr_0) + \alpha r & r > r_0 \end{aligned} \tag{2.4}$$

When discussing underwater propagation loss it is important to state that signal attenuation is not linear over all frequencies. This is particularly important when using signal frequency analysis for the purposes of classification. For example, a white beaked dolphin produces echolocation clicks over a wide frequency band, typically 20-150kHz [71]. Depending how far the animal is away from the hydrophone, the received frequency spectrum will be altered as higher frequency signals attenuate quicker than lower frequency signals. Figure 2.6 illustrates the transmission loss experienced as a function of range for a selection of frequencies.

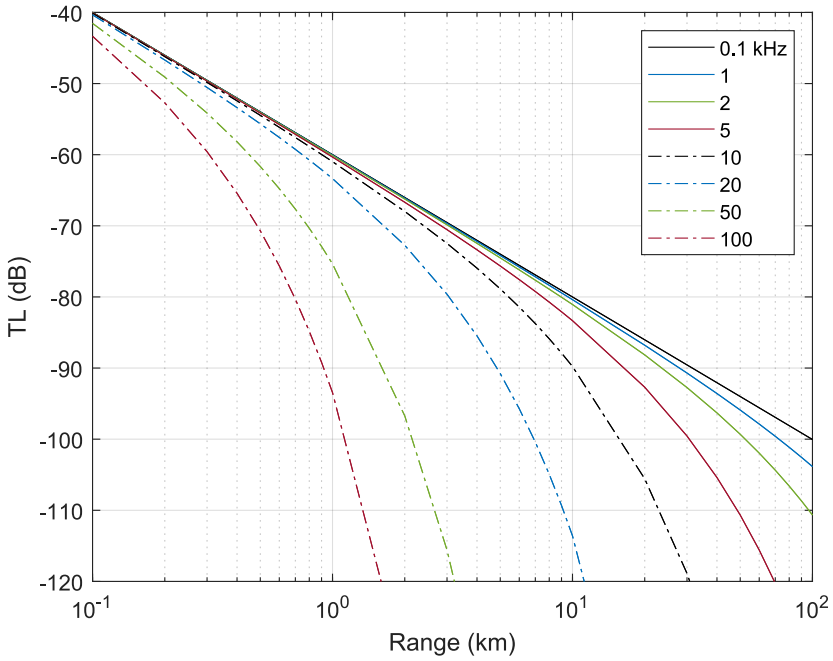

Fig. 2.6 Transmission loss as a function of range for various frequencies [50]

2.2.3 Multipath

Taking a cross-section of the ocean there are two distinct limiting regions which impact acoustic propagation. The surface and seabed act as reflective surfaces which can create the potential for multiple signal paths (Multipath). An example of multipath is illustrated in Figure 2.7, which shows a receiver intercepting several signal trajectories from the same source. The impact of receiving multiple signal paths is further detailed in the lower plot of Figure 2.7. This shows the receiver signal which contains multiple peaks depending on the path taken during propagation [50]. Having this potential variability in the received signal can cause problems when utilising underwater acoustics for applications such as data transfer. This is because in theory there could be so many signal paths that the direct path becomes unobtainable at the receiver.

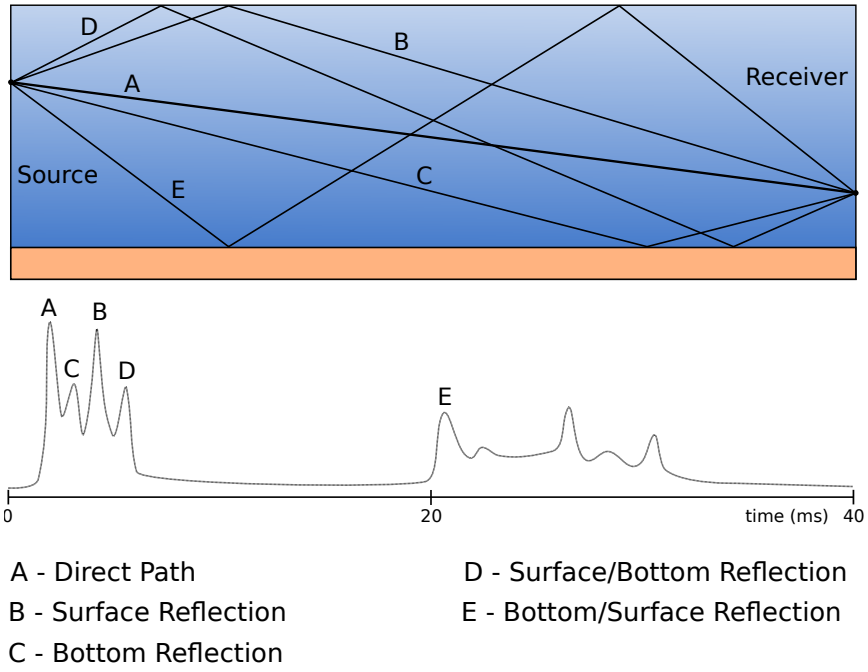

Fig. 2.7 An illustration showing the potential impact of multipath on a received signal.

The impact of multiple signal paths is not limited to distortion of the received time domain signal. A signal's frequency spectrum can also be distorted due to frequency selective fading. This is when multiple signal paths interact to cause partial cancellation of the received signal [50]. An example of when this can be problematic is when attempting to track a sweep in frequency such as a dolphin whistle. Frequency selective fading can create short nulls in the time-frequency plot which can cause issues when attempting to track frequency consistently over time.

2.2.4 Doppler Effect

If an underwater sound producing source is fixed relative to a moving target then the reflected signal from the target received back at the source will differ from what was produced initially. This process of frequency distortion due to movement is known as a Doppler shift [15]. The frequency seen at the moving target f_1 can be related to the frequency produced at the fixed source f_0 by considering the speed at which the target is moving v and the speed of sound c of the medium itself. This is illustrated in Equation 2.5 from [15].

$$f_1 = f_0(1 - \frac{v}{c}) \tag{2.5}$$

Now considering that the moving target will also reflect a signal f_2 back to the fixed sound producing source, an additional Doppler shift will occur, this relationship is described in Equation 2.6.

$$f_2 = f_0 \frac{1 - v/c}{1 + v/c} \tag{2.6}$$

The difference between the received frequency at the source and the frequency transmitted initially f_d is described in Equation 2.7 from [15].

$$f_d = f_2 - f_0 = -\frac{2v f_0}{c} \left(1 - \frac{v}{c}\right)^{-1} \tag{2.7}$$

2.2.5 Noise and Interference

The main theme of the work presented in this thesis involves passive acoustic monitoring (PAM) of signals for purposes of detection and classification. Noise and Interference are key aspects for consideration when designing PAM systems. Some of the categories identified as 'noise' in this section are actually the signals this project is interested in detecting by use of custom designed signal processing algorithms. As big as our oceans are they can be very congested and noisy environments to conduct PAM activities. A great overview of the different potential noise sources active in our oceans is provided by the much published Wenz curves in Figure 2.8 originally produced in 1962 by Gordon M. Wenz [92].

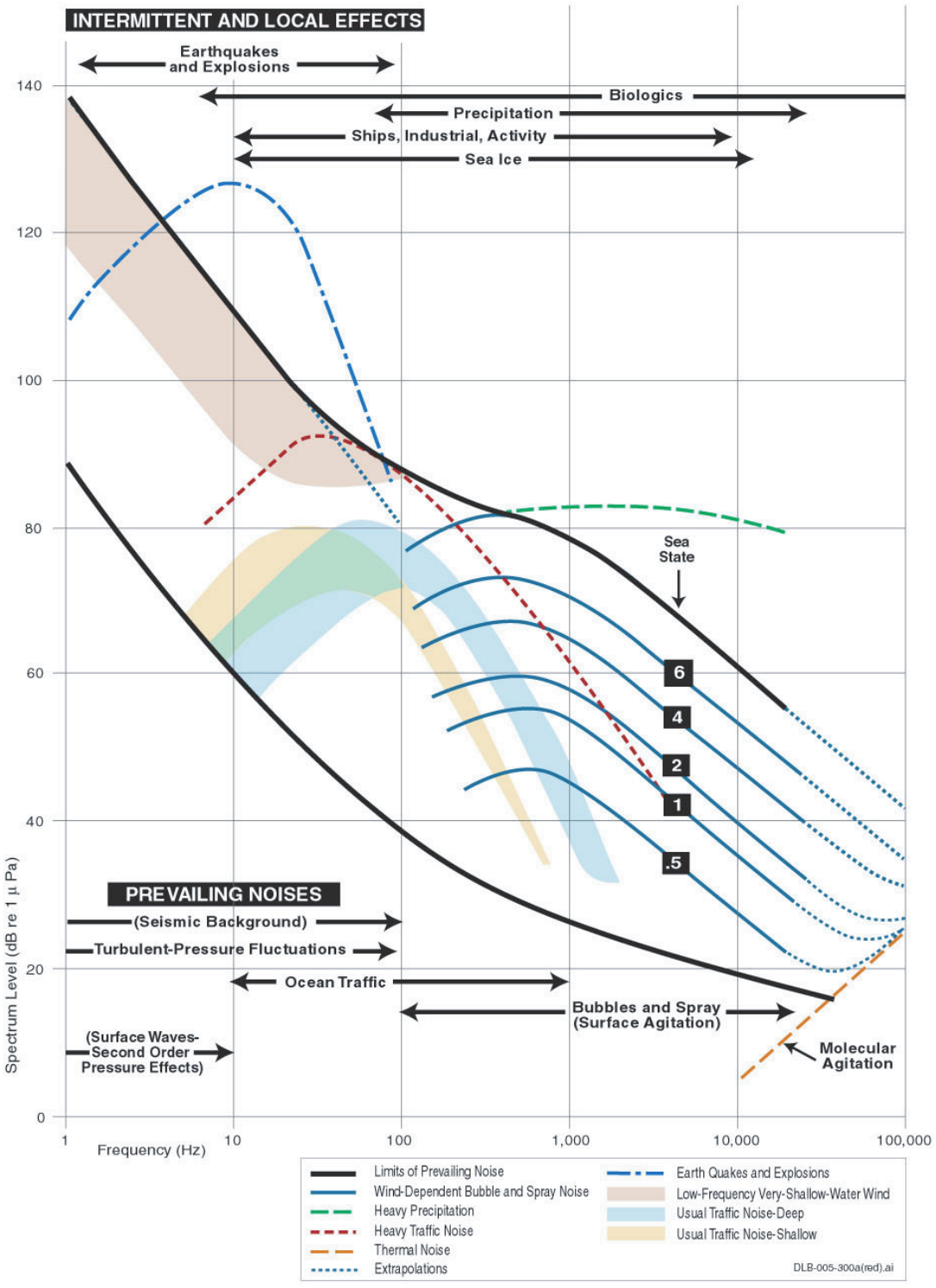

Fig. 2.8 Wenz curves detailing the intensity of marine ambient noise stemming from sources such as wind, weather, geological activity and shipping [27].

2.2.5.1 Natural/Biological Ambient Noise

Ambient noise, often referred to as background noise, is defined as noise other than that which is being monitored [90]. Sources of ambient noise can be categories as natural/biological and synthetic as discussed below.

Natural ambient noise sources include seismic activity, wind, rain, waves and thermal activity of water molecules. Seismic activity tends to occupy the very low frequency region below 5 Hz whilst wave turbulence take the low frequency region of 5-20 Hz. Atmospheric activity such as wind and rain are active from 200 Hz to 100 kHz. Thermal noise occupies the high frequency end of the natural ambient noise spectrum with activity above 100 kHz [58].

Biological sources of ambient noise include snapping shrimp, croakers and cetaceans [15]. Snapping shrimp use their claws to create a quite broadband noise between 500 and 20 kHz whilst croakers oscillate their swim bladder to make sound in an action which mimics the beating of a drum. Croakers produce a lower frequency noise in the sub 1 kHz band.

Cetacean is the collective name given to whales, dolphins and porpoises. Sounds produced by these animals vary depending on activity and species. Cetacean activity sounds tend to be categorised as either 'echolocation clicks' or 'communication signals'. An example of the stark difference in frequency band used for different species can be seen in dolphin and porpoise echolocation clicks. Dolphin's tend to produce a very broadband click around 40 to 130 kHz whilst a porpoise will produce a very narrow-band click in the 120 to 150 kHz region [88].

2.2.5.2 Synthetic Ambient Noise

Synthetic ambient noise relates to sources of noise created by human-made components. These include shipping activity and industrial work (harbours, shipyards, wind farms, oil and gas etc). The overriding contributor of synthetic ambient noise stems from global shipping activity. The sounds produced cover a frequency range of 10 Hz up to 1 kHz. Shipping sound is produced by areas of the vessel such as the propeller during cavitation, on-board machinery during operation or flow noise whilst travelling [50].

2.2.5.3 Self Noise

As the name suggests, self-noise is caused by the actual system deployed underwater. The noise created by the platform itself includes examples such as rigging (clinking chains during movement), flow noise (external structure creating bubble) or electrical noise (created by the housed electronic components) [50]. All of these self-noise sources are theoretically

controllable and should be considered to minimise there impact when designing underwater systems.

2.2.5.4 Interference

Acoustic interference relates to other human-made underwater acoustics systems. The predominant user of such systems is the shipping industry. Most large scale vessels will have a selection of acoustic systems on-board with the most common being SONAR. SONAR (Sound Navigation And Ranging) is the process of detecting objects using acoustic signals [90]. Multiple vessels using various acoustic systems can lead to jamming between systems. This is why the design of a robust filtering stage to reject as much of the spectrum as possible and leave only the signals of interest is so important in underwater acoustics.

2.3 Underwater Acoustic Monitoring

This section formally introduces the types of underwater acoustic monitoring which are used in many industries such as defence, marine conservation, oil and gas. There are two types of acoustic monitoring techniques which are classified as active and passive. Both are used for the purposes of detecting objects using acoustic signals which is a process known as SONAR.

2.3.1 Active Acoustic Monitoring

Active SONAR uses sound waves to locate objects of interest similar to the method used by dolphins to hunt for food. A transmitter and receiver are used to estimate the range of an object as illustrated in Figure 2.9. The diagram shows a hull mounted acoustic transmitter/receiver which produces pulses of sound and then records the echo received. This allows for objects to be detected and range information can be calculated. Active SONAR can be very effective in locating objects of interest but does not fit well with low power applications. This is because the process of producing sound using electrical energy can by high, especially if the proposed system is designed to operate using battery power for several months.

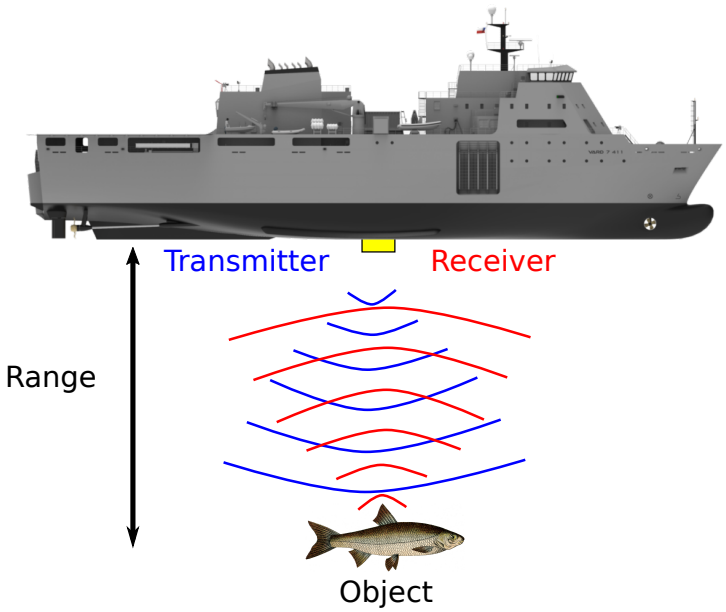

Fig. 2.9 Diagram of an active SONAR system deployed on a ships hull to identify object below.

2.3.2 Passive Acoustic Monitoring

Passive SONAR is a much more energy efficient method of detecting objects as a system can simply listen. Passive sonar uses signal processing techniques to identify objects which produce sound waves underwater such as dolphins or propeller cavitation. Figure 2.10 illustrates the process of passive SONAR. This example shows a towed receiver array which could consist of several elements to enable direction information related to the target to be calculated. As the passive system does not transmit any sound waves it can be considered a more echo-friendly system for marine life when compared to active SONAR.

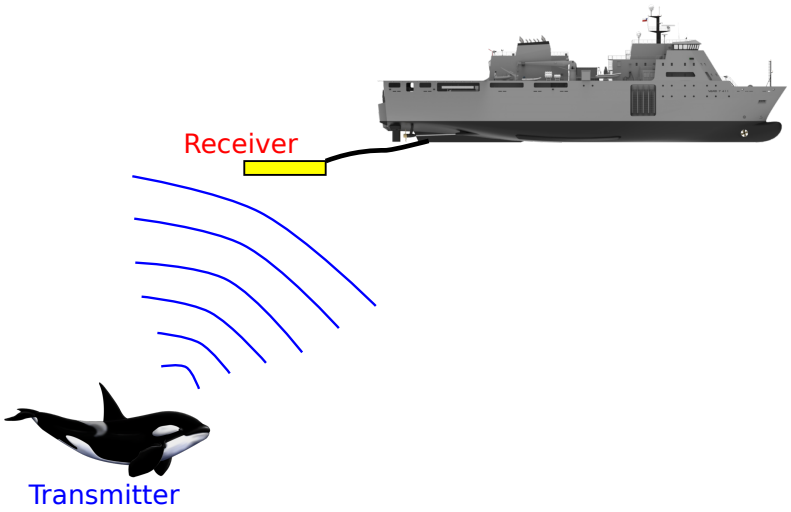

Fig. 2.10 Diagram of a passive SONAR system deployed on a towed array behind a ship.

2.4 Vessel Detection

This section provides a background of the sounds produced by a vessel. Understanding these signals is crucial to developing a successful detection algorithm. This section also shows the current technology to give the reader context as to what is already available and where this project will sit amongst these devices. The motivation for aiming to detect these vessels in a passive acoustic manner is also discussed, which leads to the aims of this area of research.

2.4.1 Propeller Cavitation

Marine vessels produce noise from a variety of sources including propellers, electric motors, diesel generators, auxiliary machinery and water flow. The most intense source of noise often stems from the propeller during rotation [75]. As the propeller rotates through the water, cavitation occurs which is the formation and dissipation of air bubbles over time. Bubbles are formed due to a drop in the local static pressure and once the water pressure exceeds that of the bubble vapour pressure the bubble will implode causing a local pressure wave to be emitted. This pressure wave is the noise that is associated with propeller cavitation.

Looking deeper into the propeller itself there are a variety sources of cavitation noise including tip vortex, blade type, hub vortex, wake induced pressure pulses, blade rotation induced pressure pulses and finally resonance between the blade's natural frequencies and trailing edge vortices. These sources of cavitation noise are illustrated in Figure 2.11.

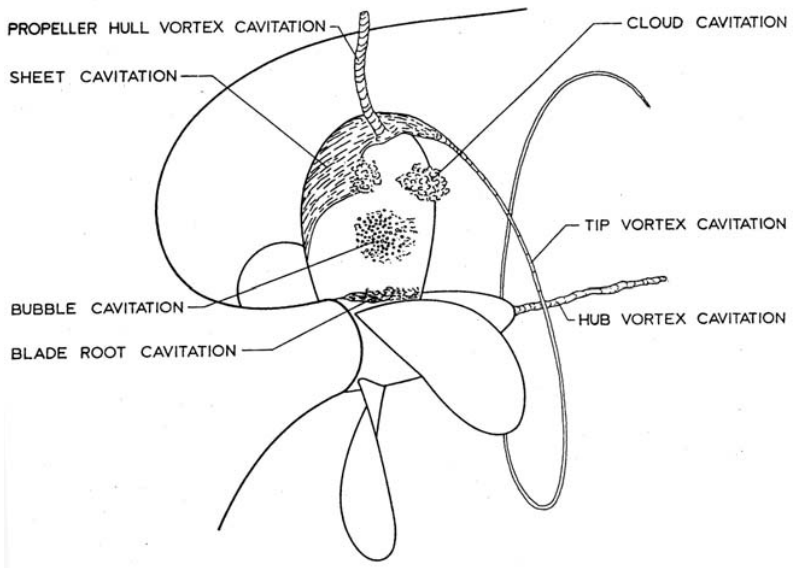

Fig. 2.11 An illustration of the various types of propeller cavitation [2].

Propeller cavitation noise is load dependent in that at low load the propeller is operating in a non-cavitating state. In this state the strongest source of noise can often stem from alternative areas such as auxiliary machinery. When the load is increased cavitation begins to occur and propeller noise will begin to increase and often dominate other ship noise sources. Figure 2.12 shows various ship produced noise sources and how they relate to a ship's speed.

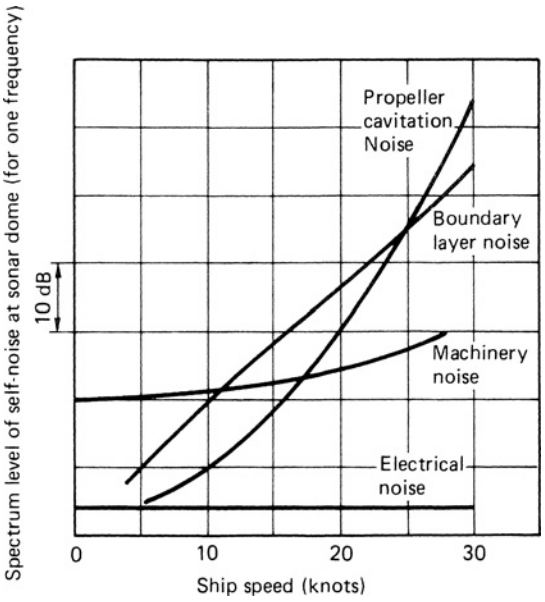

Fig. 2.12 The various sources of noise produced by a vessel as a function of vessel speed [17].

The vortices detailed in Figure 2.11 are created due to the pressure difference between the suction and pressure sides of the propeller blade. Over time these vortices begin to cavitate, which subsequently produces a broadband signal that radiates through the sea water. An example of the sound produced by a vessel underwater is shown in Figure 2.13.

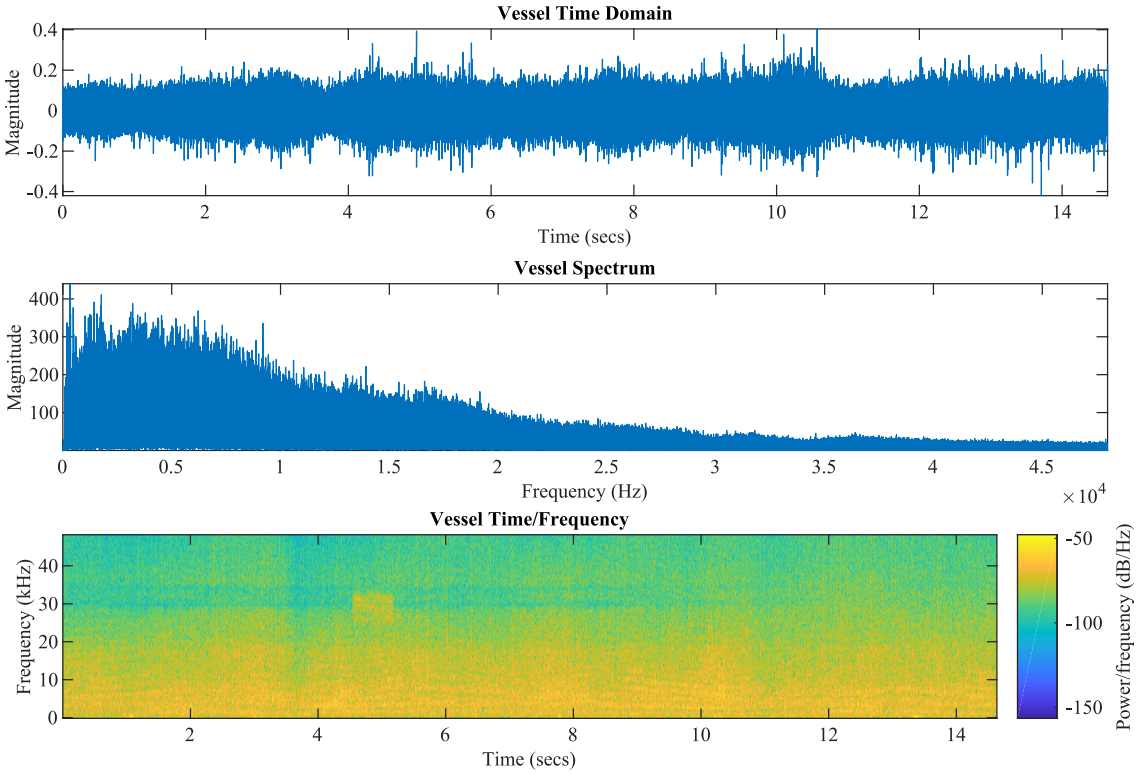

Fig. 2.13 An example of a vessel signal recorded in the North Sea in both time and frequency domains.

In ships which have two propellers, interference can occur between the two noise sources and as a consequence the combined signal can become very directional [2].

2.4.2 Problem Statement

Monitoring vessels may seem like a task which has already been addressed with technology such as Automatic Identification System (AIS) and Global Positioning System (GPS), further discussed in Section 2.4.3. However, these technologies are only going to be utilised by a vessel which either wants to be identified or has the means to invest in such equipment.

2.4.3 Current Technology

There are a variety of technologies available for the purposes of vessel tracking, the most popular is AIS. This automated system transmits important data related to the vessel such as position, speed, course and the vessel's unique Maritime Mobile Service Identity (MMSI) number. AIS transponders capture positional data by using the GPS and transmit this information using the AIS transponder as part of a packet every 2 to 10 seconds. AIS devices

are relatively low cost ranging from £150 to £500 for a basic model and can be powered by the vessel with battery backup. As stated by the safety of life at sea (SOLAS) regulation V/19, AIS systems are a legal requirement for *"all ships of 300 gross tonnage and upwards engaged on international voyages and cargo ships of 500 gross tonnage and upwards not engaged on international voyages and passenger ships irrespective of size"* [43].

2.4.4 Motivation

Vessel detection is an important area of research as it can be used for useful applications such as boat traffic monitoring, a search and rescue tool to aid the Royal National Lifeboat Institution (RNLI), and a means of detecting and reporting surface and sub-sea threats. One of the key applications where this technology could be useful would be for defence purposes. The safety and security of the United Kingdom's coastline has recently been a media focal point, due to the increase in illegal attempts to cross the English Channel in small rigid-hulled inflatable boats (RHIB) [13, 80]. With an area of approximately 75,000 km^2, the English Channel is a challenging zone for anyone to effectively police 24 hours a day. Even excluding this factor, there are obstacles such as harsh weather conditions and poor visibility to contend with. The size of a single RHIB, on average 0.016 km^2, in the potential search area is comparable to searching for a "needle in a haystack". As these vessels are being used for illegal crossings, stealth is a major factor for those onboard. As such, it is reasonable to assume that any standard automatic identification system (AIS) would be disabled. However, one detection feature that is difficult or even impossible to hide is the acoustic emissions produced from the RHIB's propeller during cavitation. Therefore, this project will demonstrate that constructing a low power, cost effective system to detect acoustic emissions, could provide a viable solution to this increasing problem.

2.4.5 Research Aims

In order to achieve a vessel detection system which addresses the limitations identified, this project aims to:

- Develop passive acoustic vessel detection algorithms that can be implemented with very low energy processing (of the order of 10 mW).
- Compare different approaches with mixtures of analogue and digital processing, continuous and duty-cycled sampling/processing.
- Adapt an existing low cost/power acoustic modem platform (NMV3) to implement a wireless vessel detection device.

- Demonstrate underwater acoustic transmission of vessel detection information.
- Evaluate system performance in a realistic offshore environment.

2.5 Cetacean Monitoring

This section provides a comprehensive background of cetacean vocalisations, why there is a need to detect these animals and how they are currently detected. Cetacean is the collective term used to describe whales, dolphins and porpoises. The classification of marine life can be further broken down into two sub-categories which are Mysticeti (Baleen) and Odontoceti (Toothed). The main difference being the method of feeding used by each species. Baleen whales have a comb-like structure which hangs from the upper jaw, allowing them to filter out prey in preparation for consumption. Alternatively, a toothed whale or dolphin will feed in a more conventional manner similar to that of a carnivore [94].

2.5.1 Vocalisations

The production method of cetacean acoustic emissions is widely debated within literature. Cetaceans, similar to that of humans, have a well-developed larynx which is certainly capable of creating sound. However, there is strong suggestion within marine biology research that the source of sound production for cetaceans stems from the nasal passage. It is suggested that air is forced past overlapping flaps of muscle which are named ‘phonic lips’. As the air passes through the phonic lips, the two muscular structures hit each other creating a sound source [28].

Creation of sound is only one aspect of a cetacean’s acoustic emissions given that the sound beam shape produced is very directional. The reason for a directional beam pattern is for tracking purposes similar to a military SONAR. How a cetacean achieves such a directional beam width of around 6-10 degrees is widely debated in literature. A large number of publications agree that a fatty area of tissue in the animal’s forehead, named the ’melon’, plays a role in focusing the sound produced into the narrow beam shape [7]. The melon contains a unique fat which has matched sound velocity to that of the surrounding sea water. There are authors who suggest that the skull also plays a role in focusing the beam by means of reflections coupled with refraction in the soft tissue [6]. Figure 2.14 illustrates the anatomy of a dolphin including the ’phonic lips’ for sound production and melon/skull for

beam forming. It is also worth noting the lower jaw and associated 'acoustic window' soft tissue in Figure 2.14. This is the cetacean's receiver, which captures the echoes of sound for processing of range and direction.

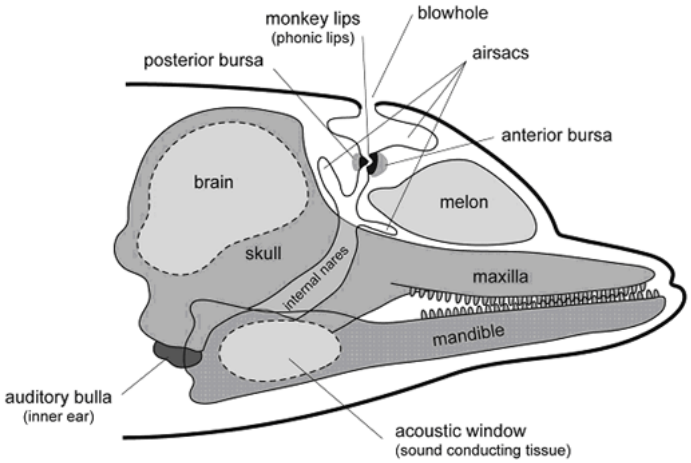

Fig. 2.14 An example of the anatomy of a dolphin used to illustrate the mechanism used by the animal to produce sound for the purposes of navigation and foraging [28]

Cetaceans can produce a variety of sound types for various applications. Cetacean sounds have been characterised in literature as moans, grunts, knocks, thumps, shrieks, shot-guns, buzzes, creaks, clicks, pulses, up or down calls etc. To loosely characterise this variety of cetacean sound interpretations, two categories are generally used when describing vocalisations. These are echolocation clicks and communication signals. Echolocation clicks tend to be short high-intensity pulses which are very directional for the the purposes of locating food, similar to that of a submarine's SONAR pulse used for locating objects. Echolocation clicks are used by toothed whales and provide the animal with information regarding location, range and direction of an object. Communication signals tend to be more familiar with humans as they are the whistles and moans often associated with cetaceans as they take place within the human audible band. Communication signals are used by baleen whales and dolphins and tend to be tonal signals which have low directionality [95]. The difference between a communication 'whistle' and an echolocation 'click' is illustrated in Figure 2.15. The time/frequency plots are very distinctive with the whistle resembling a linear sweep from 6 to 12 kHz and the clicks showing sharp vertical lines spanning a large frequency range but over a short duration.

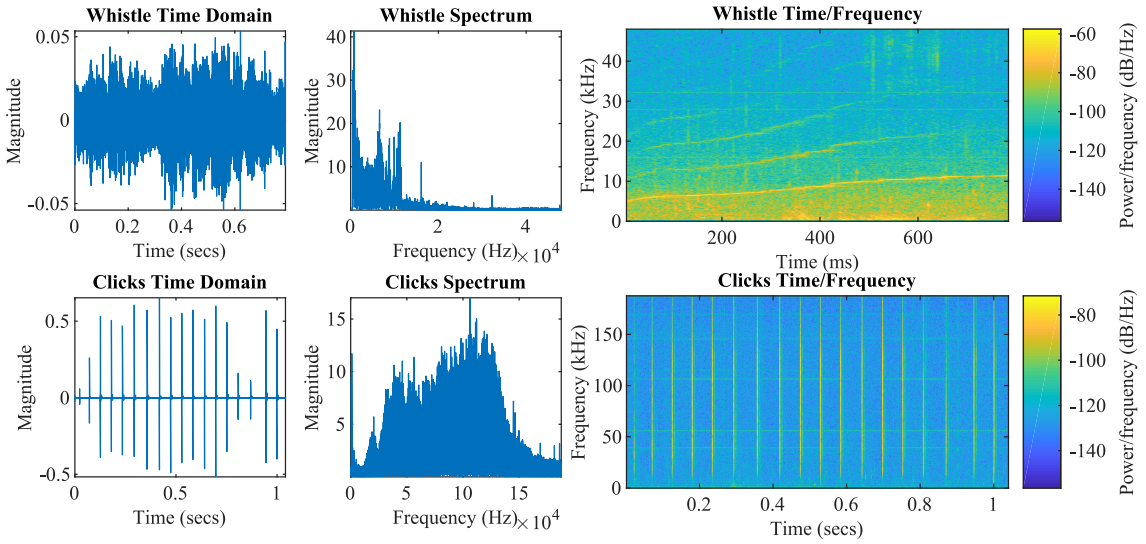

Fig. 2.15 An example of a dolphin whistle (top row of plot) versus a dolphin click train (bottom row of plots).

Another factor to consider when receiving cetacean signals is the impact that the animals orientation, relative to the receiver, has on the received signal. In 2004, Rasmussen *et al.* conducted field trials to estimate the transmission beam patter of White Beaked Dolphin clicks in Icelandic waters [72]. Findings indicated that at an off-axis angle of only $\pm 10^{\circ}$ results in a minus 18 dB attenuation in the signal's intensity compared with an on axis 0° transmission. This demonstrates the highly directional signals produced by white beaked dolphin and must be considered in any detection system.

2.5.1.1 Cetacean Hearing

In addition to producing sound, cetaceans also receive sound, which in 'normal operation' allows them to target food sources. Normal operation refers to an environment free from outside sources of excessive interfering noise. The ocean can be a very noisy environment with noise produced from naturally occurring sources such as seismic activity but also from many anthropological sources. Examples of anthropogenic noise sources include shipping, offshore drilling, SONAR, wind farms and anti-fouling devices. Just like humans, cetaceans have a frequency range and an intensity which will cause them discomfort in the wild. This is a key area to consider when designing any underwater technology so as not to impact the main residents of the ocean. The effects caused by anthropogenic noise on marine mammals can be summarised in the following categories [88]:

- Threshold Shift - A temporary/permanent shift in the hearing threshold of the marine mammal.
- Behaviour Alterations - This can be in the form of course alteration and avoidance of areas.
- Stress - An increase in the stress hormone of the marine mammal.
- Masking - The masking of potentially important marine mammal signals such as communication/echolocation.
- Standings - Naval SONAR has often been associated with mass standings due to the frequency and intensity.
- Indirect Effects - This refers to masking of the signals produced by marine mammals prey to avoid being targeted.

2.5.2 Problem Statement

Monitoring of cetacean activity can be incredibly difficult given the unpredictable nature of these animals and the incredibly large monitoring area which may need to be covered.

2.5.3 Current Technology

There are several methods employed to monitor cetaceans which are chosen depending on species and available resources. Methods are generally based on either visual or acoustic monitoring or a combination of both. The cost implication of either method will vary depending on the scale and duration of the monitoring program. It is possible to visually monitor cetacean activity in a low cost manner by taking positions on coastal areas or by using opportunistic vessels such as passenger ferries or tourist style cetacean vessels [31]. Visual surveys play a vital role in monitoring cetacean activity, however, they are both labour and time intensive with many surveys conducted by volunteer organisations. A technique often employed for conducting cetacean surveys is the use of aerial vehicles to identify the animals as they come to the surface [63]. This technique can be advantageous as large areas can be covered quicker than using a surface vessel. However, this comes at the disadvantage of a high costs for aircraft time. In addition, this method relies on animals coming to the surface with many cetacean capable of long periods without surfacing [69]. A more invasive technique to monitor cetacean activity is physically tagging the animal with a tracking and

data relay device. This allows for very accurate data but comes at the obvious cost of potential harm and distress caused by tagging the animal [5].

PAM of cetacean is a technique used throughout the marine biology community. Figure 2.16 shows two examples of different PAM technology actively used for cetacean monitoring.

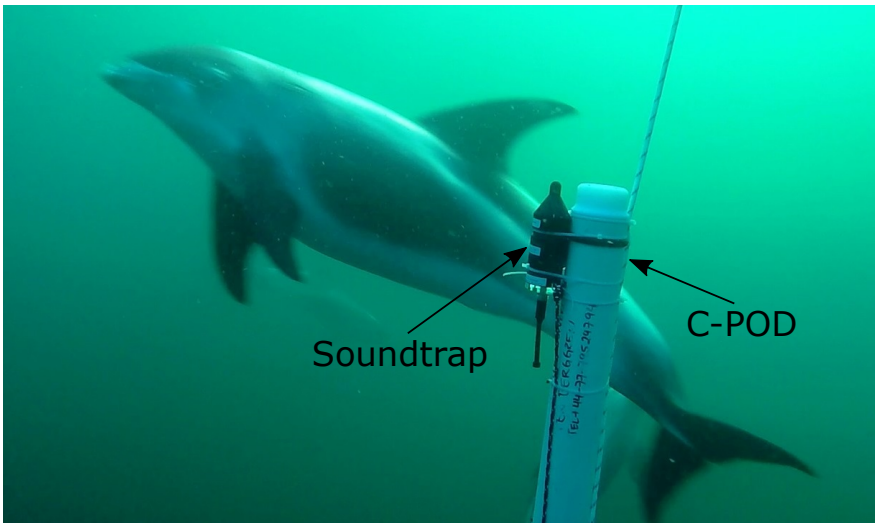

Fig. 2.16 The SoundTrap is a compact self-contained underwater sound recorder for ocean acoustic research. It offers high frequency recording to capture sound upto 150kHz underwater [61]. A C-POD is a self-contained cetacean click train detector, manufactured by Chelonia Limited, which stores its findings locally [21].

PAM of cetacean activity offers both advantages and disadvantages. Firstly it is a far less invasive technique than methods such as tagging because PAM is based on listening for cetacean calls. Secondly it is far less labour intensive than visual surveys as the detection system can be deployed at sea for long durations depending on power efficiency. Finally, depending on the budget it would be possible to monitor large areas using multiple PAM units. The only limiting factor in terms of the amount of units required would be each individual unit's detection range sensitivity. There are disadvantages to PAM of cetacean activity which starts with the reliance on an animal to produce sound within range of a monitoring system. These animals are unpredictable in nature so there are no guarantees that clicks or whistles will be produced. The second obstacle with PAM is that data is often stored locally on the device which results in delayed findings and potential for the device to be lost at sea. Thirdly, the current commercially available systems can be costly, therefore it would be expensive to distribute many units over a large area. Finally the reliability of the PAM system is only as good as the decision making algorithm which operates within, therefore, strong reliability testing using the best ground truth available is a key aim of a PAM system.

2.5.4 Motivation

Monitoring of cetacean activity is important to ensure the conservation of these animals and aid industry/governments to make informed decisions when encroaching on the ocean environment. By logging the population size of cetacean species in the wild it provides the possibility to identify the cause of any sudden drop in numbers that may occur and prevent a species become endangered or even extinct [31]. The oceans are becoming more congested every year with increased shipping, new industrial infrastructure such as oil and gas platforms and a sharp rise in wind farm installations. All of this activity creates more sources of noise and disruption which can have a profound impact of cetaceans. In the past ten years there has been a sharp rise in the number of cetacean mass stranding events [4]. There is a strong suggestion that high powered naval SONAR could be one cause of mass stranding events [64]. As discussed in Section 2.5.1.1, cetaceans experience pain and discomfort when their comfortable hearing threshold is breached. This breach is believed to be the main culprit when stranding events occur as audio related injuries have been identified during autopsy deceased mass standing cetaceans [46]. A less extreme example of the benefit of cetacean monitoring is to provide a greater understanding of the impact of human actions in the ocean. This information can enable more informed decisions to be made by humans to minimise impact. There has been a sharp increase in both investment and physical installations of offshore wind farms especially around the United Kingdom [30]. It is important to monitor these installation sites before, during and after installations to provide marine life impact data so that there can be constant improvements made to minimise and negative impact.

2.5.5 Research Aims

In order to achieve a cetacean monitoring system which addresses the limitations identified, this project aims to develop a system which can:

- Reliably detect cetacean acoustic signals (whistles or clicks).
- Transmit detection results acoustically and in a bio-friendly manner.
- Distinguish between species based on the acoustic signals received.
- Achieve a low power design to enable units to remain deployed for long periods.
- Maintain a low-cost design approach throughout.

Chapter 3

Literature Review

3.1 Introduction

In this section, research related to cetacean/vessel detection is reviewed. The focus of the literature review is centred on three key areas. The first is instrumentation, which is the physical systems that have been used to perform PAM of cetacean/vessels. The second area is related to the actual algorithm/signal processing techniques used to detect these signals of interest. The final area of the literature review is focused on how researchers have classified the detected signals of interest.

3.2 Passive Acoustic Monitoring of Vessels

This section presents literature related to passive acoustic monitoring of vessels. The first section relates to the instrumentation currently employed to monitor vessel activity. The second section highlights the detection methods used by researchers to identify a vessel. The final section details the methods of classification that have been used to identify characteristics about the detected vessel.

3.2.1 Vessel Detection Instrumentation

There are many technologies available for the purposes of detecting and tracking a vessel's activity at sea. Typical examples include RADAR (Radio Detection and Ranging), air surveillance, passive acoustics, AIS and Active SONAR. The focus of this section will be to review passive instrumentation used for detecting/tracking a vessel to align with the project aims. There is already instrumentation available in which a vessel can be monitored passively such as air surveillance. However, this method does not satisfy the low cost, long term

monitoring aim of the project. This section will instead concentrate on passive technologies which could be realistically adopted for low cost and long term deployment system.

The first suitable technology adopted by many researchers to detect and sometimes classify a vessel is using passive acoustic monitoring. This method usually involves a hydrophone connected to a digitised system such as a recording device or an embedded detection algorithm. Much like the examples shown in the cetacean detection instrumentation section of this document (Section 3.3.1) there are both wired and wireless variations of passive acoustic vessel detection instrumentation.

Wired systems typically consist of either a single or array of hydrophones deployed at sea with a cable link back to shore [9, 86]. The cable provides both mains power and high speed communication to the the subsea system. Sutin et al. developed a wired acoustic monitoring system named the Stevens Passive Acoustic Detection System (SPADES). The system consists of an array of four hydrophones deployed at sea with a fibre optic communication link back to shore. The system is aimed at passively detecting surface/underwater threats such as vessels and deep sea divers. Trials were carried out using a variety of surface vessels and human divers to record sound emissions for development of detection and classification algorithms [86]. The SPADES system developed by the Stevens Institute of Technology has been adopted by a selection of other researchers [23, 24, 65]. A wired link system offers obvious advantages such as an uninterrupted 24-hour a day monitoring node, which can be used to process data in real time using complex algorithms. The disadvantages of a wired system include the limited deployment location, as it would be unrealistic to deploy a cable from shore to remote and deep water locations. Another drawback is the emphasis on the cable link itself. If it becomes damaged then monitoring would stop and it could be both time consuming and costly to repair.

Wireless PAM systems come in many variations but the main distinction is whether the system processes data on board using an integrated detection algorithm. In contrast, some systems are designed to simply store the raw audio for post processing on shore once the unit has been retrieved. Sorensen et al. uses a self contained continuous-recording passive acoustic sensor called SOREN sensor. This system is capable of recording for a period of one month at a sample rate of 44.1 kHz using battery power. To enable the raw audio data to be easily retrieved, the mooring was made to be positively buoyant and an acoustic release system was added to release the unit on command back to the surface [82]. Tesei et al. use a self contained passive acoustic monitoring system that is housed within an autonomous underwater vehicle (AUV) called a Slocum glider [51]). The system comprises of a hydrophone array to provide directionality capabilities and an on board computer to process data. The detection algorithm is running in real time on the AUV with detection

results being relayed via satellite once the vehicle surfaces [87]. Each of the wireless PAM systems described exhibit their own advantages and disadvantages. A wireless system which stores raw acoustic data benefits from being fairly simple in its design and also it enables almost limitless post-processing power of the raw acoustic data. This processing power enables complex algorithms to be performed which may enable a more accurate end result. The alternative wireless system whereby the data is processed on board and relayed back to shore enables the end user to receive a near real time stream of detection results. This disadvantage of this approach is that the results received back at shore are only as accurate and robust as the algorithm itself. In addition, there is a significant reliance placed on the data transfer method used to connect with the shore side computer. One method of addressing this shortfall is by using a distributed network of PAM units which can all communicate with each other and have multiple communication routes back to shore.

A single PAM unit is limited by the area in which it is sensitive enough to detect the target signal. An isolated unit is also in danger of being lost or damaged especially when deployed at sea which can often be extreme, highly changeable environments. By adding additional units, as part of a network, opportunities arise to increase reliability using dual redundancy and multi hop communication.

Networking of nodes is not limited to passive acoustics and researchers have experimented with networks of magnetic detection units [78]. An alternative method of passively detecting the presence of a vessel without the use of acoustics and in a relatively low-power, low-cost manner is the use of Magnetic Anomaly Detection (MAD). MAD is a method used to detect changes in the earth's magnetic field. Holmes documents the evolution of MAD technology used during World War Two to detect the magnetic field signatures of enemy naval vessels [42]. The theory of MAD is that if a large steel vessel passed over a magnetometer then the normally stable ambient magnetic field measurement would be altered by the vessel. This is because the vessel produces its own magnetic field, which would momentarily overcome the earth's ambient magnetic field and become the dominant force from the perspective of the magnetometer. One of the major benefits of MAD is its ability to effectively detect objects which are hidden, such as sea mines covered by sand or silt [53].

3.2.2 Vessel Detection Algorithms

In this section the various algorithms developed by researchers for the purposes of passive acoustic detection of vessels are presented. To recap, passive acoustic detection of vessels is based on propeller cavitation as introduced in Section 2.4.1.

3.2.2.1 Wavelet Analysis

One method of detecting vessel activity in the presence of noise is by using a wavelet based detection algorithm [9, 82]. A Wavelet Transform (WT) provides both time and frequency information simultaneously for a given input signal as opposed to a Fourier Transform (FT) which can provide time or frequency information depending on the direction of the transform.

Sorensen et al. presents a discrete wavelet decomposition algorithm to identify vessel acoustics in the presence of background noise. This is then followed by a harmonic extraction tool to characterise the ship. The author has created self contained data acquisition nodes to monitor the underwater acoustic environment. The data is sampled at 44.1 kHz and can record for a period of one month using on board batteries. The nodes are then manually collected and data processed on shore. Results show that deployments achieved a true positive rate (TPR) of 93% for false positive rates (FPR) of below 40% for vessel detection, validated against a human acoustic specialist [82].

Whilst this method provides a high TPR, the associated FPR is also quite high, which may be down to the validation method employed. Where possible, using visual identification or the AIS on board vessels could reduce potential error in audible verification. Processing data on shore definitely has the advantage of unrestricted processing power, however, the ability to detect and report the presence of a vessel in near real time would be lost. This ability may be application specific as for defence purposes it would be a desirable feature, however, for non critical applications may not be so important. Deployment and retrieval of data acquisition nodes is also an expensive process as boat time can be very costly, which may be an issue for some less funded target applications. The author concludes that an area of future work would be the incorporation of the algorithm into a large scale underwater network with the ability to communicate between sensors.

3.2.2.2 Detection of Envelope Modulation on Noise

The fundamental methodology behind Detection of Envelope Modulation on Noise (DEMON) has widely been used in literature for the purposes of vessel detection [24, 26, 65, 66]. The DEMON method for vessel detection relates to detecting the almost rhythmic high frequency noise produced during propeller cavitation. Propeller cavitation, as detailed in Section 2.4.1, is the formation and collapse of air pockets due to the rotation of the propeller through the water. The process of detecting this periodic high frequency noise is generally carried out using the method illustrated in Figure 3.1.

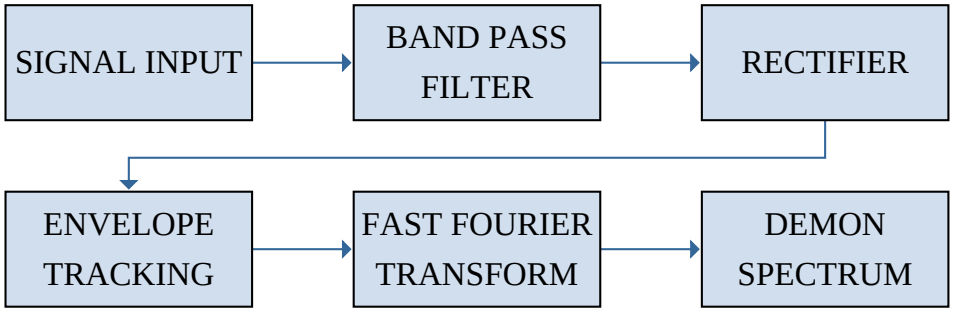

Fig. 3.1 Flow chart describing the DEMON algorithm.

The final stage spectrum of Figure 3.1 will indicate the rate at which the high frequency propeller noise is occurring within the water. This can give an indication to the speed at which a vessel may be travelling and whether the vessel is increasing of decreasing its speed.

Chung et al. illustrates the use of the DEMON algorithm for the detection of ships within a busy harbour environment. The author uses a cross-correlation method from multiple hydrophone sources to establish both the ship's bearing but also as a tool to isolate individual ship signatures [24]. To carry out field trials of the algorithm, the author used a piece of hardware developed by the Stevens Institute of Technology specifically for passive acoustic detection purposes. The SPADES consists of four hydrophones connected with a central storage and processing hub [86]. This can then be linked via an underwater cable to a shore-side computer to provide power and communication of results.

Clark et al. documents another variation on the DEMON algorithm in which the acoustic signal produced by a ship is processed using sub-band filtering. The author shows that by using this method the modulation harmonics related to propeller cavitation can be emphasised improving the signal-to-noise ration by as much as 3.2dB [26].

Pollara et al. present several improvements on the widely used DEMON algorithm for vessel detection. The author firstly uses two hydrophones to indicate the Time Difference Of Arrival (TDOA) of a vessel based on phase delay. Results show that the TDOA of a vessel can be used as a method of vessel bearing tracking. Secondly the DEMON spectrum of several small vessels are collected and analysed to establish potential classification characteristics. Results show that the number of peaks along with their magnitudes could provide a tool for classification in small vessels. Finally, the author discusses the dependence of the DEMON algorithm on the high frequency carrier signal it aims to demodulate. Results show that the selection of passband for DEMON analysis has a large bearing on the success of detection and classification [65].

The papers discussed demonstrate that the DEMON algorithm in its most basic form is widely used and achieves detection results. There are many credible lines of improvement presented in the papers discussed, however, many would require a significant processing and power supply ability. As the Stevens Institute of Technologies SPADES equipment demonstrates, a permanent power cable is required when processing and communicating data in isolated underwater areas. To be truly effective in monitoring our oceans for vessel activity, a fully wireless system capable of detecting and communicating results that carries a self contained power source would potentially address many of the practical deployment issues highlighted.

3.2.3 Vessel Classification Algorithms

Vessel classification using PAM involves identifying vessel characteristics, such as the type or size, based solely on the acoustic signal received. Researchers have used various approaches to achieve classification of vessels using PAM.

3.2.3.1 Neural Networks/Machine learning

The use of neural networks/machine learning is quite a popular approach to classifying vessel signatures. Leal et al. uses artificial neural networks (ANNs) with backward propagation to classify signals [47]. This involves training the neural network to recognise patterns in correct classifications. In addition, support vector machines (SVMs) were used as part of the classification process. An SVM is a supervised machine learning model which is used to separate data into classes by outputting hypeplanes. A hyperplane is a plane of separation based on the data set which distinguishes one class from another. The algorithm was developed in Matlab and achieved classification accuracy of 92%. Axelsson and Rhén uses neural networks based on features from multi-sensor created signatures [10]. The signature is made up of underwater acoustic, electric potential and magnetic sensor data. These signatures are then used to train the neural network to recognise differences and identify unique features to vessel types. Using this approach, accuracy of 87.4% was achieved when classifying a vessel according to size. Averbuch et al. uses a combination of Linear Discriminant Analysis (LDA) and Classification and Regression Trees (CART) to perform vessel classification [9]. LDA is used to separate the data into classes by identifying unique features in the vessel signature. The CART uses decision trees which use the same unique features to make a prediction. The final results of the LDA and CART are then compared to make a final decision on the classification. This method relies on training the classifiers using large data sets but results did show detection and classification of vessels were achieved. Sierra and

Contreras uses spectrum feature extraction to train a fuzzy logic classifier using fast-boat acoustic signatures. Fuzzy logic is a classification process which replaces a boolean, true or false, concept of entities either being members of a set or not with the notion that membership can be 'fuzzy' i.e. that entities can have 'degrees of membership' of a set. For example, an entity could have a 90% membership function which means it is likely to belong to the set in question but it is not possible to say for certain. In the paper the author uses six different types of 'go-fast' boats to test the detection and classification algorithm. Results showed a detection/classification accuracy of between 67 and 90% depending on the degree of membership to the right class.

In this section neural network and machine learning techniques have been shown to produce high accuracy classification results. A common requirement shown is the need to train the classifier which calls for large data sets. This would require time and processing power alongside accurately classified data sets to train the algorithm. In a limitless system in terms of power and processing ability, neural network/machine learning would potentially outperform most low power systems. However, if a detection/classification system is required to be deployed at sea, using only battery power to operate, then neural network/machine learning may not be a suitable approach.

3.2.3.2 Detection of Envelope Modulation on Noise

Detection of envelope modulation on noise (DEMON) is a well established method of passive acoustic detection of vessels previously introduced in Section 3.2.2.2. In addition to the detection capabilities, the DEMON method can also offer classification information based on the DEMON spectrum. Pollara et al. shows methods of identifying physical parameters related to the detected vessel based on spectral analysis [67]. Using cepstrum analysis and the DEMON spectrum, parameters including shaft/engine rate, number of propellers and blades, and engine firing rate can be identified. Pollara et al. showed that the DEMON spectrum peaks are related to the rate of rotation of the propeller shaft and also the blade rate. This information can help to identify the type of vessel such as whether it is likely to be a large or small vessel. The relationship used to calculate the number of blades is shown in Equation 3.1. Periodic increase in cavitation intensity results in amplitude modulated noise (Blade rate). Imperfections in the blades often results in a dominant cavitating blade which also results in amplitude modulated noise (Shaft Rate).

$$\text{No. Blades}(N) = \frac{\text{Blade Rate}(Fb)}{\text{Shaft Rate}(Fs)} \tag{3.1}$$

Sutin et al. also used the DEMON approach to detect and classify vessels. The author used a controlled experiment comprising of six vessels to test the algorithm. Results showed that the DEMON spectrum indicated vessel parameters such as shaft rotation frequency, propeller rotation frequency and blade frequency.

This section shows that the DEMON passive acoustic method of detection can also used to provide additional information about the vessel detected. This information can lead to a prediction about the type of vessel which may aid the end user depending on the application.

3.2.4 Summary

This section provides a summary of the literature discussed highlighting the strengths and limitations of each category. Table 3.1 shows a summary for vessel monitoring instrumentation, detection and classification algorithms.

Categories		Strengths	Limitations
Instrumentation	Wired Systems	High Speed Communication	Limited Deployment Range
		Mains Power Supply	Costly to setup and deploy
		Real Time Signal Processing	High reliance on cable link
	Wireless Systems	Can be deployed in remote locations	No real time data link with wireless data logger system
		Data stored locally can be processed offline	Deployment duration limited by battery life
		Can utilise wireless communication to relay data such as Satellite/ LoRaWAN/ Acoustics	Limited on-board processing power restricts the complexity of detection algorithms
		Data loggers can be cheap to manufacture relative to a wired system	Costly to deploy and retrieve nodes using vessels
			Remote deployments are vulnerable to harsh sea conditions and can be lost or destroyed.
Detection Algorithms	Wavelet Analysis	Provides both time and frequency data which is beneficial for vessel detection	Not deployed as a real time detection system which delays data for the end user
		High TPR when detecting vessels using offline data processing	High FPR using human specialists to validate data
	DEMON Algorithm	Widely used in passive acoustic monitoring to detect vessels	Complexity of detection algorithm can add to processing load
		Computationally light processing stages to achieve DEMON spectrum using fixed-point FFT	Offline processing of data may not be suited to industries such as defence
Classification Algorithms	Neural Networks/ Machine Learning	Strong detection accuracy for many machine learning based vessel classification systems	High processing power required to produce classification results
			Not suitable for battery operates system
			Reliance on large data sets to train the classifier
	DEMON Algorithm	Can be used to identify the number of propeller blades, indication vessel type	Classification results rely on DEMON spectrum resolution
		Classification results are based on existing DEMON spectrum data	

Table 3.1 Summary table of vessel monitoring instrumentation, detection and classification algorithms.

3.3 Passive Acoustic Monitoring of Cetacean

In this section, literature related to passive acoustic monitoring of cetaceans is presented. This includes the different types of instrumentation used such as wired/wireless systems. It also includes methods used to detect different types of cetacean signals such as 'clicks' and 'whistles'. In the final part of this section, methods of classifying whistles and clicks into specific species is presented.

3.3.1 Monitoring Instrumentation

There is a wide variety of instrumentation that has been used for the purposes of cetacean monitoring within the research community. These range from fixed seabed deployments with wired links back to shore to fully wireless units capable of wireless data transfer. In this section, an overview of the different approaches used by researchers is presented and discussed.

3.3.1.1 Wired Systems

Wired passive acoustic monitoring systems usually consist of a number of fixed hydrophones with a wired links back to shore. The most well known fixed PAM system is likely the Sound Surveillance System (SOSUS) developed by the Americans during the Cold War as a means of detecting enemy submarines [50]. The SOSUS network is deployed along large sections of the United States coastline and allows for the supply of acoustic data in near real time. SOSUS has since been declassified and is now used primarily by researchers including those interested in PAM of cetaceans. Stafford et al. used signals recorded by the SOSUS network to detect and locate blue whales based on their calls using a matched filter approach. U.S. Navy aircraft were deployed to visually validate that whales were present in the area along with the analyses of local recordings from the site to prove the animals were indeed vocalising [85].

A more recent installation of a fixed wired PAM platform is the Northeast Pacific Undersea Networked Experiments (NEPTUNE) ocean observatory. The NEPTUNE system is an 800 km fibre optic subsea loop which contains a wide variety of sensor technology including acoustics. Some of the NEPTUNE systems most sought after underwater facilities include an abundant power supply and high speed data transfer. These facilities enable more computationally intensive tasks such as real time imagery and audio feeds [11].

Another smaller example of a wired ocean observatory is the Monterey Accelerated Research System (MARS). This system contains a 52 km high speed data and power line

which has been used for the purpose of PAM. Ryan et al. connected an omnidirectional hydrophone to the MARS infrastructure, which is capable of capturing acoustic signals between 10 Hz and 200 kHz. This facility was used to examine what acoustic signals dominated different frequency bands such as vessel traffic, cetacean activity and weather [76].

An underwater wired system provides many advantages especially in terms of power and data transfer as shown in the projects discussed. The ability to transfer and store data securely onshore in real time is a major advantage in underwater research as there is always the possibility that the device deployed may be lost or damaged. There are also disadvantages to deploying a fixed wired system to conduct underwater acoustic research. For many projects, a major drawback of a wired approach is the cost involved in hiring a vessel to deploy the device and install a cable link back to shore. The cable link itself can also be limiting factor as it may restrict the deployment to shallow water near to the coast. Overall, this approach is suited to well funded projects that require a relatively small monitoring area around a coastal location, such as monitoring a port or estuary.

3.3.1.2 Wireless Systems

Devices designed for PAM of cetaceans come in many variations but the two main distinctions are whether the data is stored locally or relayed wirelessly back to shore. The 'data' involved can also be a distinguishing category as data may be in the form of audio recordings to be processed onshore or the data could be actual detection results based on on-board processing of detection algorithms.

Wiggins and Hildebrand demonstrate a battery powered system which can operate remotely for long periods of time by storing acoustic sounds locally on several disk drives totalling a 2 TB capacity. The system uses a sample rate of 200 kHz to capture the high frequency content that cetaceans are capable of emitting. This sample rate would allow for around 55 days of continuous recording and the underwater enclosure design allowed for depths of up to 6600 m [93]. A commercially available example of this type of wireless acoustic recorder is the Soundtrap by Ocean Instruments, which was introduced briefly in Section 2.5.3. The Soundtrap is a high frequency battery powered sound recorder capable of recording at up to 150 kHz. Deployment duration is limited only by battery life and storage capacity which both depend on the user's configurations such as sample rate and duty cycle [61].

A slight variation on the method employed by Wiggins and Hildebrand is a system which is battery powered but detection data is stored as opposed to raw audio recordings. This means that a detection algorithm is implemented on the device itself as opposed to onshore.

There are many examples of this method as one of the most popular commercially available systems is based on an on-board processing/storage system [22, 59, 73]. The C-POD was briefly introduced in Section 2.5.3 and features an on-board cetacean click based detection algorithm with results stored locally [21].

Brunoldi et al. shows an example of a more permanent wireless installation which benefits from the use of solar power and high speed data. The installation contains an array of hydrophones at various depths with audio data transferred wirelessly back to shore using a transparent WiFi bridge (72 MB s^{-1} bandwidth) [14]. This system can almost be categorised as a hybrid system as it has similar limitations to many wired installations. The cost involved is likely to be high due to the choice of components such as solar charged batteries, 30 t mooring with 60 m wire and an array of 740 Hz to 68 kHz omnidirectional hydrophones. The WiFi link offers high speed real time data transfer across 4 km back to shore. However, with any WiFi link there will be a range limitation involved depending on the equipment used and this can restrict deployments to near shore locations.

In contrast to the wireless transmission of audio data, Matsumoto et al. created a prototype real time killer whale detection system capable of relaying detection data via a combination of underwater acoustic communication and an Iridium satellite connection. The system comprised of a PAM unit with on-board detection algorithm that communicated with a central gateway via underwater acoustic communication. This data was then relayed to shore by the central gateway using an Iridium satellite link to shore[52].

The use of wireless technology in underwater PAM projects allows for greater portability in deployment. It allows for projects to be conducted in remote locations and also in deep water using the on-board battery pack. As illustrated in this section, there are a wide variety of PAM systems, each with their own advantages and disadvantages. A wireless system which stores data locally benefits from the simplicity in its design. There is no requirement to transmit any data and therefore the system can be simply designed to record for the maximum amount of time for which the on-board memory and battery will allow for. The deployment time allowance of a PAM storage device is often a key area of consideration as the frequency in which you need to service each deployment will inevitably increase the project costs in terms of vessel time. One of the biggest issues with locally stored data systems is that there is limited safeguarding of the data itself. Data is the most valuable asset to the researcher and if it is corrupted or lost there is no backup with a locally stored system. These disadvantages can be addressed in a wireless PAM system which is capable of relaying data periodically or in near real time. Data can be received onshore and placed into a suitable safeguarding procedure, which will ensure that no data is lost and the research can continue as planned. However, there are also disadvantages to this approach as the facility to wirelessly transfer

data will come at a cost of increased power consumption. Long-term underwater PAM research projects require the instrumentation to be extremely power efficient and therefore every additional feature must be considered carefully.

3.3.1.3 Networked Systems

Our oceans cover 70% of the planet's surface, therefore monitoring such a expansive area is incredibly difficult as each PAM device will have a limited monitoring radius. One solution to this problem is to use multiple sensor devices, which have acoustic networking capabilities. This approach allows for data to make its way through the network back to a secure shore side location. Using multiple devices also gives the added bonus of redundancy. If a device is lost of damaged, the data can still make its way back to shore using an alternative route. The main challenges of developing an underwater acoustic sensor network is the design of reliable communication signals and the routing of data through the network [3, 83].

The research of this thesis is part of the USMART (Smart dust for large scale underwater wireless sensing) project which is aimed at developing underwater sensing networks based on ultra-low-cost wireless communication and sensing nodes [89]. An illustration of the underwater network of nodes is shown in Figure 3.2.

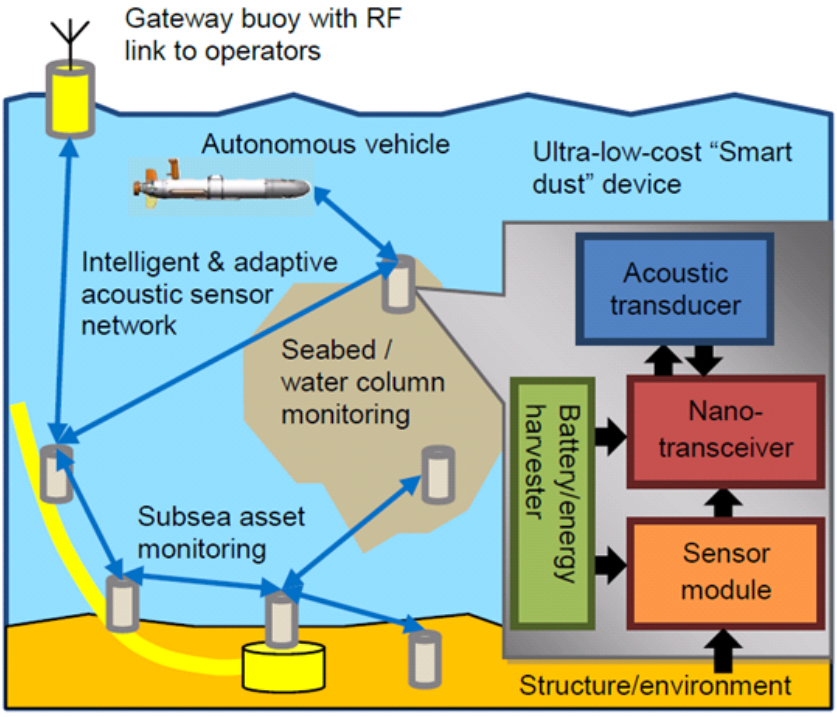

Fig. 3.2 Project illustration of USMART [89]. The figure shows a wireless underwater network of sensor nodes all linked via acoustic communication to a central gateway buoy. This buoy provides a RF link to relay data back to shore for analysis.

3.3.2 Vocalisation Detection Algorithms

In this section, methods employed by researchers for the detection of cetacean calls are discussed. As introduced in Section 2.5.1, there are two main categories of cetacean calls which are 'clicks' and 'whistles'. The methods of detecting these calls tend to be very different therefore this section has been split in two sub-sections which concentrate on each cetacean call category. To recap, a click refers to a high frequency impulsive sound, which tends to be very short in time when compared to a whistle. A click often appears multiple times in quick succession which is referred to as a 'click train'. A whistle refers to a tonal sound in which the frequency is varied in a linear like pattern over time. A whistle which increases in frequency over time is often referred to as an 'up-call' or 'up-sweep'.

As with most automated detection systems there is every effort to assign a gold standard for decision making. In the case of cetacean detection the closest 'ground truth' system that exists is the interpretation of a trained human specialist. A human operator was used by Clark et al. to identify calls made by bowhead whales during field trial recordings [25]. This method is extremely labour intensive and not very practical for long term studies which

would amount many hours of recording. Therefore, advancements in automated cetacean detection systems have been active within the research community.

3.3.2.1 Clicks

A cetacean click is a high frequency impulsive event, which can be detected in both the time and frequency domains. Figure 3.3 shows an example of a typical echolocation click from a white beaked dolphin in both the time and frequency domain.

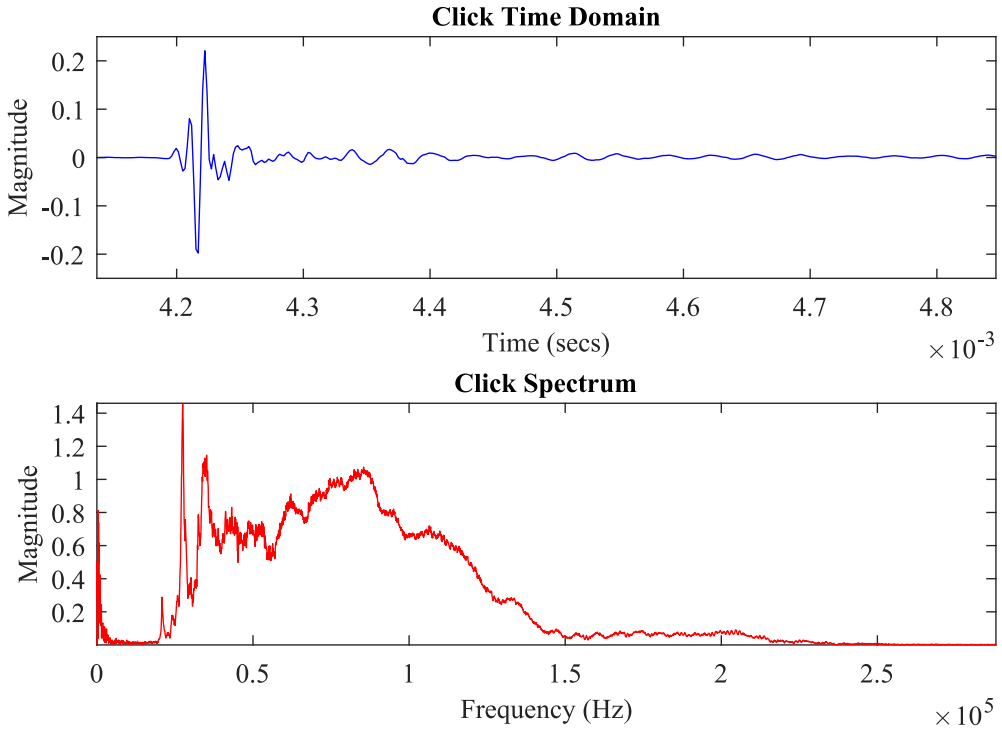

Fig. 3.3 Example of a single click by a White Beaked Dolphin.

As Figure 3.3 shows, a click event creates features which could be used for the purposes of automated detection. In the time domain a click has a high peak to average amplitude ratio and the the click event is over within a fraction of a second. The frequency domain plot in red is also quite distinctive as the click event contains a high frequency broadband spectrum.

One of the most popular commercial click detectors used by many marine biologists in their published cetacean related work is the C-POD which was introduced in Section 2.5.3 [18, 19, 35, 73, 77]. The C-POD is an automated passive acoustic detector of porpoises, dolphins and and other toothed whales (except sperm whales) developed by Chelonia Limited [21]. Unfortunately, the C-POD is a 'black box' system in that there is no information about

the detection method used to process the signals received. It is important to introduce this device as it does serve as a standard with which to compare against due to its adoption by the research community.

In contrast to C-POD, which uses on-board processing to create its detection results, there are options which process audio onshore. The first is PAMGUARD which is an open source piece of software which provides cetacean passive acoustic monitoring (PAM) capabilities [40, 62]. Using PAMGUARD the user can batch process audio recordings to identify clicks and whistles based on user configurable detection criteria. The following list gives examples of the user defined criteria used to automatically detect cetacean clicks:

- Pre-filter - Used to isolate the band of interest where clicks are likely to be present for a specific species.
- Inter click interval - This is a measurement of time between clicks during a train of clicks.
- Number of clicks - Impulsive sounds are not uncommon with animals such as snapping shrimps. Therefore placing a minimum number of clicks can be beneficial for detection of cetacean click trains.

Another popular choice of software, which is also aimed at processing large audio data sets quickly, is the Integrated System for Holistic Multi-channel Acoustic Exploration and Localisation (ISHMAEL) [54]. ISHMAEL provides a variety of automated detection methods including energy summation, matched filtering and cross-correlation. There are also threshold options to trigger events, which like PAMGUARD are configurable by the user for their particular application.

There are examples of researchers who have attempted to develop their own click detection systems which don't utilise commercial hardware/software. Gillespie and Chappell used a high frequency hydrophone connected to three different band limiting filters with envelope tracing to detect harbour porpoises. The low frequency envelope signals were then digitised and detection decisions were based on the relative amplitudes of the signals in each of the three bands [39].

Cetacean detection algorithms tend to be tuned by user defined thresholds based on knowledge of the target. The systems presented in this section will rely on the end user having a good grasp of cetacean acoustics to operate them effectively. The exception is the C-POD which offers an automated system but does not reveal its methodology. A system which fits in the middle of these two areas could serve both the research community and general commercial end users.

3.3.2.2 Whistles

The methods used by researchers to detect cetacean whistles are varied but tend to be focused on the spectral pattern created by a whistle. Figure 3.4 shows an example of a whistle in both time and frequency domains.

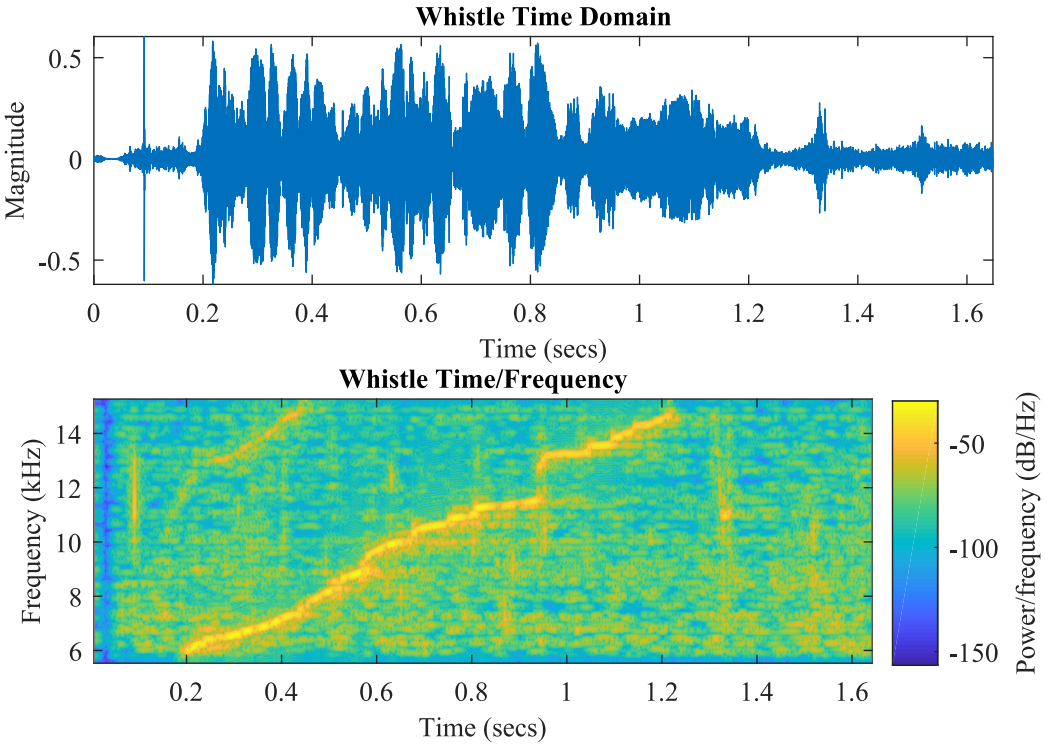

Fig. 3.4 Example of a single whistle.

As Figure 3.4 illustrates, there is a very distinctive pattern in the frequency domain with a near linear increase in frequency over time. There are various methods which have been developed to detect cetacean whistles. One method used for the detection of whistles is to use a matched filter approach. The main principle behind this approach is to create a known signal based on knowledge of the target. This signal is then correlated with the incoming unknown signal to detect the presence of the known signal in the incoming signal. Bouffaut et al. used a variation of this technique to detect antarctic blue whale calls using a stochastic matched filter. Results showed an increase in detections for low signal to noise signals when compared to a more standard matched filter approach [12]. Stafford also used a matched filter approach to detect blue whales recorded by the Unites States Navy's SOSUS array which was previously introduced in Section 2.2. The results showed that providing the matched

filter was based on field data it was possible to detect calls and even determine localisation of the animal providing multiple hydrophone data sources are available [84].

A second method used by researchers to detect dolphin whistles is the implementation of a neural network. A neural network is a collection of algorithms with the aim of identifying relationships within data. Potter et al. used a large selection of marine mammal sounds to train the neural network algorithm. A second equally large set of data was used to test the neural network's approach to detect marine mammal calls. Results showed a significant improvement on detection error percentage over alternative methods with only 1.5% error rate [68]. More recently Jiang et al. explored the use of convolutional neural networks to detect and classify whale calls. Convolutional neural networks are a type of deep learning algorithm commonly used to analyse images for the purposes of automated recognition. The main advantage of this approach is that minimal user input is required to train the algorithm, aside from providing a substantial training data set. Jiang et al. found that using this approach achieved a 97% correct detection rate for whale calls [45].

A third method of detecting whistles uses an edge detection algorithm on a whistles spectrogram. Gillespie detects calls made by a whales by first smoothing its spectrogram by convolving it with a Gaussian kernel. The smoothed spectrogram is then passed through an edge detection algorithm which singles out the outline of potential whistles. From this process a set of parameters can be extracted such as bandwidth and duration to compare with expected values for the target to be detected. Results showed a high number of correctly detected calls based on comparison with a human specialist operator. False alarms detected during trials were low with only one or two per day [36]. Datta and Sturtivant also used an edge detection algorithm for the purposes of detecting dolphin whistles. In this example a detected whistle is split into segments based on the trend of the segment (i.e. rising, falling, flat etc). This was then used as a means of distinguishing one whistle from the next for the purposes of classification [29].

A final method of whistle detection is by using spectrogram cross correlation on acoustic data. In this method a synthetic signal or 'kernel' is created based on prior knowledge of the target. The kernel is then cross-correlated with the incoming spectrogram data to establish whether a match for the kernel is present in the data. Mellinger and Clark used this method to identify low-frequency bowhead whale calls with a success rate of 97.5% [55]. Munger et al. investigated the performance of a spectrogram cross-correlation method to detect right whale calls in long term recordings. In this example a human specialist was used to provide a gold standard with which to compare the detection algorithm against. Results showed high false detections but it was concluded that this method could be adopted by human specialists to aid their data processing efficiency [56].

Each of the whistle detection methods presented offers the end user a strong degree of reliability in its results. The potential pitfall is the implementation of each system for long term deployments in remote locations. Unless a fixed power source is present in addition to a data relay system then the practicalities of operating remotely for long durations are unrealistic. Designing an algorithm which could operate at very low power and relay data without the need for costly infrastructure would address many of the obstacles presented by cetacean monitoring in open sea.

3.3.3 Species Classification Algorithms

Alongside the detection of cetaceans it is also incredibly important to classify the targets detected. Species classification provides a greater depth of data for the end user, which can help to understand things such as interaction between species and migration patterns. In this section, methods of species classification based on clicks and whistles are discussed.

3.3.3.1 Clicks

The echolocation clicks produced by cetaceans tend to be high frequency impulsive events. On the surface they may seem to be fairly similar sounds between species but there can often be distinguishable features. A good example of this is the difference in spectrum of a white beaked dolphin and a harbour , as illustrated in Figure 3.5. A SONAR signal is included to illustrate how a human made signal can appear similar to a cetacean signal. In this example the spectral shape of a harbour porpoise and SONAR click are not too dissimilar.

As Figure 3.5 illustrates, distinctions made between underwater sound sources are based around common identifying features in the time and frequency domains. Soldevilla et al. uses unique spectral features to classify the presence of Risso/Pacific White-Sided dolphin based on their echolocation clicks. The first stage of classification is based on identifying a distinctive spectral peak and notch pattern which is associated with the presence of each species of dolphin. It is shown that no such pattern exists for other species such as the bottlenose or common dolphin. The second stage separates the Risso and Pacific White-Sided dolphin by analysing the spectral peak mean and spectral notch mean values for the signals received. It is shown that these values are consistently distinctive between each species of dolphin, therefore providing a means of classification [81].

Another example of using spectral features as a means of classifying a cetacean is shown by Gillespie and Caillat. The author uses parameters such as peak/mean frequency, click duration, width of primary spectral peak and relative spectral energy in neighbouring frequency bins to aid classification. The author uses two methods of statistical classification.

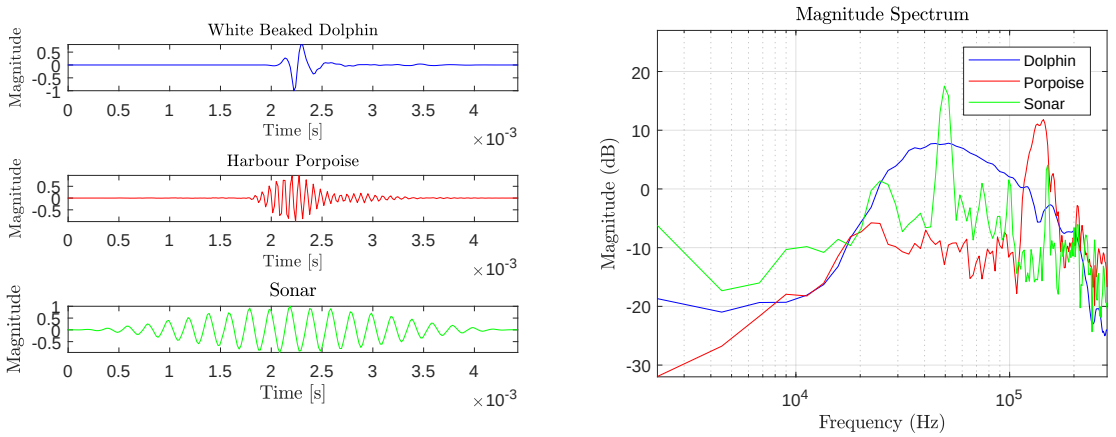

(a) Time domain comparison

(b) Frequency domain comparison

Fig. 3.5 Example of the distinguishing features between cetacean species in both time and frequency. SONAR has also been included to illustrate how synthetic human made signals could be mistaken for cetacean produced signals.

The first method is based around a statistical tree classifier, which sets limits around each of the identifying parameters (e.g. click duration, peak frequency ...etc) in the attempt to identify a species once all parameters have been considered. The second method uses a multivariate classifier based on the spectral energy of 32 frequency bins of width 1.5 kHz. The first method yielded an error rate of 20 to 30% and the second method showed promise in detecting beaked whales based on post human analysis of the detected signals [37].

Roch et al. uses a different approach by using cepstrum feature extraction to represent identified clicks in place of the more standard spectrum. Cepstrum analysis is based on calculating the inverse Fourier transform of the logarithm of the estimated signal spectrum. It is often used in speech analysis to determine voice pitch and also for separation of sound sources (i.e. voiced and unvoiced sources) [70]. The click features extracted are then classified into species using Gaussian mixture models by providing large data sets to train the classifier. This approach achieved a mean error rate of 22% for the whole experiment with the classification of Curvier beaked whale clicks showing the best performance in terms of error rate with less than 2% [74].

The cetacean click classification methods presented show that signal based features can inform the end user about the species which has been detected. Each method shows various degrees of accuracy using spectral and cepstrum based analysis. The main consideration

for this project is whether each method would be suitable for a low-energy application. Using a low-energy click detection method could control access to the more power hungry classification methods presented.

3.3.3.2 Whistles

The classification of cetacean whistles is based on a commonly held opinion within the research community that some species produce "signature whistles" [16]. A signature whistle is one that is unique and repeatable by an individual to identify itself within its group. The whistle can then be classified by developing algorithms which can pick out the unique identifying feature produced by each species. One example of whistle feature extraction used for the purposes of species classification is shown by Datta and Sturtivant. The author works in the frequency domain and uses an edge detection algorithm to identify the whistles against background noise. This edge detection result is then smoothed using a contour following routine in an attempt to clean up any imperfections and produce an accurate representation of the original whistles shape. To quantify the shape of the whistle the author splits the detected whistle up into segments in order to detect whether the segment in question is rising, falling or flat. The individual segment shape detection is achieved using a least mean square algorithm to calculate a quadratic equation which represents the segment shape. This collection of quadratic equations form the digital signature of a whistle, which can then be compared to other whistles detected to identify any commonalities. The classification of whistles using the digital signatures detected was carried out using Hidden Markov Models trained with previous data sets [29].

Gillespie et al. uses an initial spectrogram based detection algorithm to identify whistles based on a pre-determined signal to noise ration threshold. The author identifies a common weakness in this approach where whistles are often detected in fragments and do not always include the complete whistle. To address this issue, the author breaks down all detected whistles into uniformly sized whistle fragments, which can then be further analysed. The fragments are classified using a Linear Discriminant Analysis, which attempts to maximise the separation of each of the statistical parameters extracted from the fragments. Extracted parameters include the mean frequency, slope of the frequency change over time and the curvature of the fragment. This method has showed a correct classification rate of 94% for four species of cetacean. The author also states that this high rate of classification is dependant on the number of species included in the classifier mix with a considerable drop when more species are included [38].

Cetacean whistle classification tends to be based around the spectrogram of the target signal. This is due to its fairly unique pattern and good signal to noise ration. The automated

detection of the pattern can be quite computationally intensive. As discussed in the click classification section, there must be a layer of control so that energy is not wasted trying to classify signals on the fly. Once a whistle has been detected, access to the classification algorithm would be granted. The methods presented in this section are all valid in that they are capable of classifying cetaceans but may not all be well suited to a low-energy application. This is due to the processing power required in classification methods involving a spectrogram, or those requiring large data sets for machine learning. Low-power methods of classifying cetaceans is key to this project's success as the overall aim is to implement the algorithm's developed in practical low-power embedded hardware/software.

3.3.4 Summary

This section provides a summary of the literature discussed highlighting the strengths and limitations of each category. Table 3.2 shows a summary for cetacean monitoring instrumentation, detection and classification algorithms for both cetacean clicks and whistles.

Categories		**Strengths**	**Limitations**
Instrumentation	Wired Systems	Permanent power supply	High installation costs
		High speed data transfer	Restricted deployment range
		Real time data processing	Dependency on power/data cable link
	Wireless Systems	Data can be transferred to shore via Satellite/ LoRaWAN/ Acoustics	Locally stored data may be lost in harsh sea environment
		Unrestricted deployment range with a wireless system	Limited deployment duration due to battery power consumption
		Data loggers are simple and cheap compared with a wired system	Limited storage capacity especially at high sample rates
		Can achieve low power consumption depending on design complexity	Deployment and servicing costs can be high due to vessel time required
Click Detection Algorithms	Commercial Systems (C-POD, Pamguard)	Widely used by marine biology research community	Some systems are 'black box' systems with no detail on method of detection
		Software systems can batch process recordings using offline processing	Setup can require extensive acoustic knowledge of cetaceans to choose tuning parameters in software
			Expensive to purchase commercials systems and software
	Envelope Tracing	Low-power analogue front end design	Detection algorithm not embedded in hardware
		System performs detection and classification	Limited to harbour porpoises

Whistle Detection Algorithms	Matched Filer	Shown to detect calls and determine localisation	Requires prior knowledge of a known target signal
		Could be implemented in low power electronics	No implemented on embedded system for remote deployments
	Neural Network	Low detection error rate	Requires a large training data set
		Can be improved over time with additional training data	Not suitable for embedded platform due to computation load
	Edge Detection	Low false alarm rate for whale calls	Requires spectrogram calculation which can be computationally intensive
		Widely used in offline processing with strong detection results	Not suitable for remote low-power deployments
	Cross Correlation	High detection success in whale calls	Requires synthetic signal based on prior knowledge of target
		Could be implemented in embedded hardware depending on system complexity	High false detection's in whale calls
Click Classification Algorithms	Spectral Feature Extraction	Shown to separate dolphin species	Spectral analysis may not be suitable for low power applications
		Can be used to identify spectral features for statistical classification	High error rate in detecting beaked whales
	Cepstrum Feature Extraction	Low error rate for Curvier beaked whales	Computationally intensive to calculate Cepstrum
		Click classifier could be implemented with a lower power detection system to limit unnecessary power consumption	May not be suitable for embedded platform for real time classification due to complexity
Whistle Classification Algorithms	Hidden Markov Model	Can be constantly updated with further data to improve accuracy of training data	Requires large training data set to perform classification
			Uses edge detection to provide data to the classifier which may not be realistic in an embedded system
	Linear Discriminant Analysis	High classification rate when limiting the number of species included in classifier	Spectrogram based detection shown to detect only part of a whistle
		Classifier can work on fragmented whistles to extract classification features	

Table 3.2 Summary table of cetacean monitoring instrumentation, detection and classification algorithms for both cetacean clicks and whistles.

Chapter 4

Vessel Detector Algorithm Development

4.1 Introduction

This chapter presents the development of a low energy passive acoustic vessel detector to work as part of a wireless underwater monitoring network. The vessel detection method is based on a low energy implementation of DEMON. Vessels produce high frequency modulated noise during propeller cavitation which the DEMON method aims to extract for the purposes of automated detection. The vessel detector design has different approaches with mixtures of analogue and digital processing, continuous and duty-cycled sampling/processing. The detector has been integrated with the low cost/power NMV3 to provide acoustic communication of data in near real time.

4.2 Overall System Design and Methodology

The design of the vessel detector is based on the aims and objectives set out for this project as identified in 2.4.5. The project aims specifically related to vessel detection are to:

- Develop passive acoustic vessel detection algorithms that can be implemented with very low energy processing (of the order of 10 mW).
- Compare different approaches with mixtures of analogue and digital processing, continuous and duty-cycled sampling/processing.
- Adapt the existing low cost/power NMV3 platform to implement a wireless vessel detection device.
- Demonstrate underwater acoustic transmission of vessel detection information.

- Evaluate system performance in a realistic offshore environment.

To achieve these aims, the vessel detector is based on the DEMON methodology whilst also maximising power efficiency as much as possible during the design. The DEMON method of detecting propeller cavitation is summarised in the flow chart in Figure 4.1.

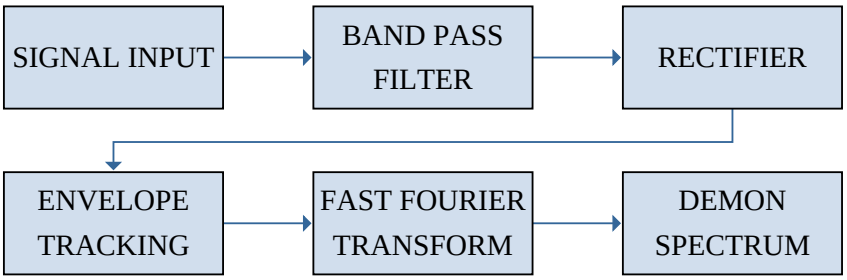

Fig. 4.1 Flow chart describing the DEMON algorithm.

The practical implementation of the DEMON method is based on a mix of low power analogue electronics and power efficiency inspired digital signal processing. Figure 4.2 summarises the design of the vessel detector using a flow diagram.

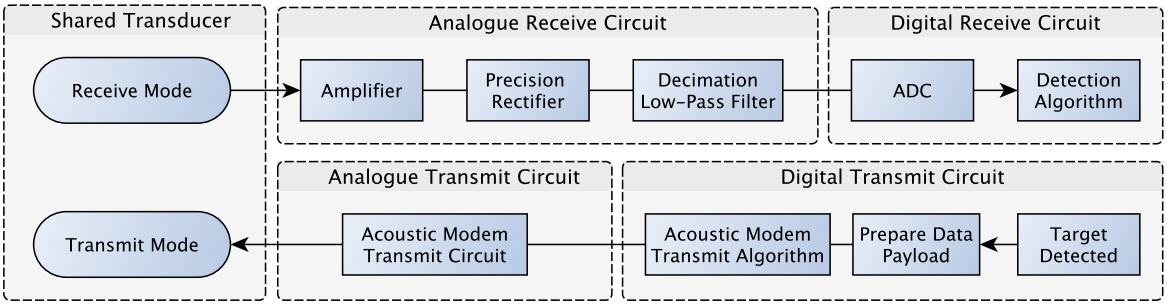

Fig. 4.2 Vessel detector system diagram showing the the stages of design from receiving a signal to sending a detection result using the same transducer element.

The receiver circuit design of the vessel detector is based on the previously documented DEMON method. To detect the envelope of the modulated noise created by a propeller during cavitation, the system uses three stages of analogue electronics illustrated in Figure 4.2. The aim of the three stages is simply to extract the received signal's envelope whilst also providing significant amplification. The envelope is then sampled at a suitable rate to capture the band of interest and subsequently processed through the detection algorithm. Once a vessel has been detected by the algorithm the data payload is prepared and sent using

an integrated acoustic communication device developed by Newcastle University's Sensors Electromagnetics and Acoustics Laboratory (SEALab). Both the received vessel signal and acoustic data payload use the same transducer element, which is one of many cost saving design features of the vessel detector.

Further detail on each stage of the vessel detectors design is included in the following sections of this report.

4.3 Software Design

This section presents each of the software modes developed for vessel detection are presented. They include the Continuous Analogue and Digital Detection (CADD) mode and the Non-continuous (duty-cycled) digital detection (NCDD).

4.3.1 Continuous Analogue and Digital Detection (CADD)

The CADD mode is the main method used for many of the vessel detection results. This includes the long term deployment experiments conducted over several months. Parts of the CADD mode have already been introduced in Section 4.2. This section aims to describe the detection mode in greater detail including the actual decision making algorithm.

The first stage of the CADD mode is the analogue signal processing circuit. This is used to extract the envelope of high frequency noise created during propeller cavitation. This is a key requirement of the DEMON algorithm, as discussed in Section 4.2. At the end of the analogue process is the analogue to digital conversion (ADC) using the shared communication devices on board microcontroller. The shared microcontroller is a Kinetis KL16 48MHz Cortex-M0+ Ultra-Low Power MCU, 256KB Flash, 32KB SRAM, 64-LQFP [60]. This microcontroller includes pins capable of 16-bit ADC resolution. The stages which follow from the ADC form the completion of the DEMON method as well as the vessel detection decision making algorithm. These stages are illustrated in Figure 4.3.

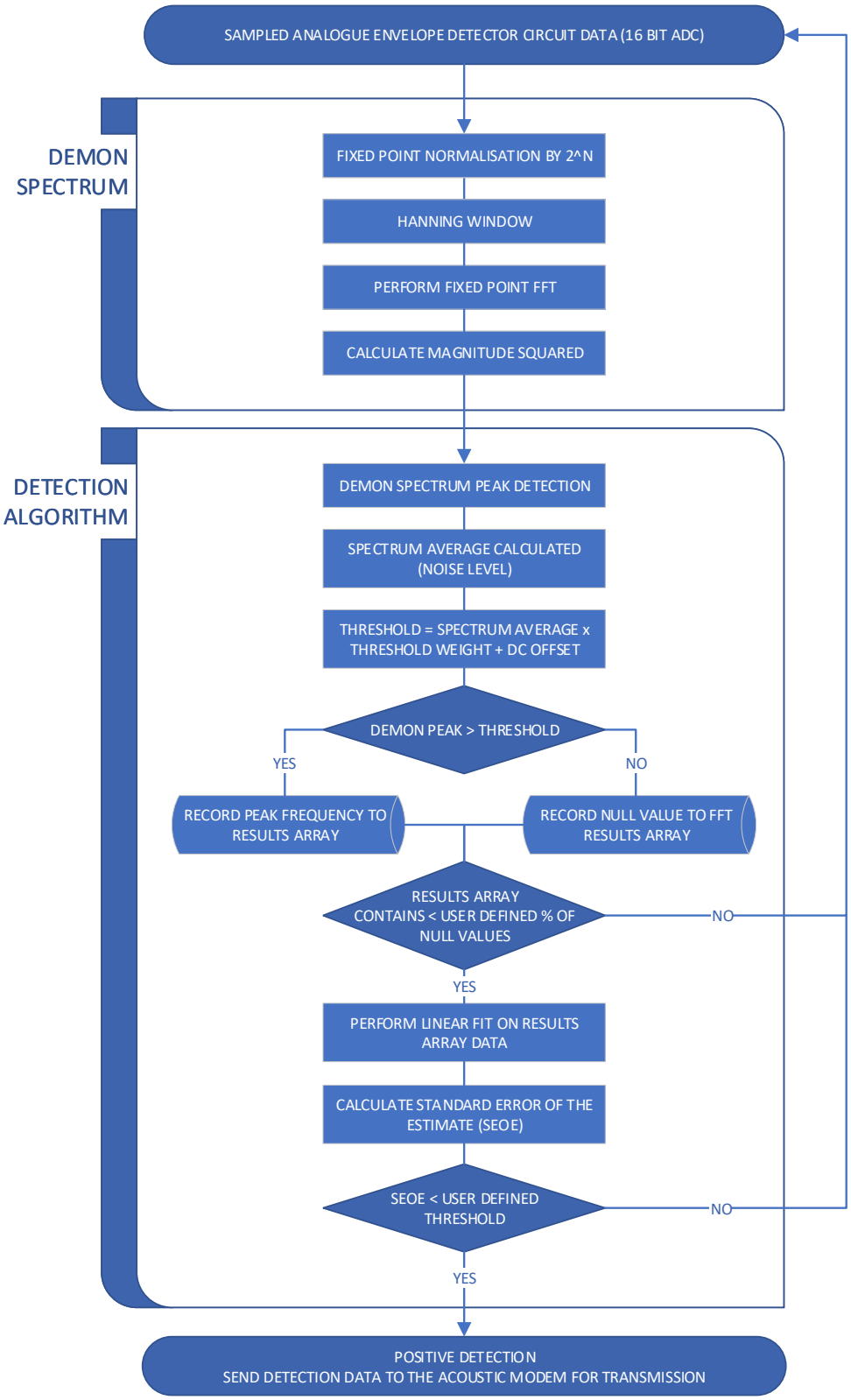

Fig. 4.3 Flow chart to illustrate the main stages of the CADD vessel detection mode.

Expanding on the overview provided by Figure 4.3, the following list provides a detailed description of all stages of the low power detection algorithm starting with the sampling of the analogue signal.

1. Sample Rate - The incoming signal is sampled at 256 Hz to capture spectral energy between 0 and 127 Hz. This is the band of interest for propeller cavitation detection using the DEMON method. Sampling is undertaking using the Direct Memory Access (DMA) facility on the KL16Z microcontroller. Samples are read into a Buffer A which is 256 samples in length. At the same time as these samples are being read into Buffer A, Buffer B is being processed by the detection algorithm. Upon completion of sampling to Buffer A the DMA controller switches the destination of its samples to Buffer B and now Buffer A is processed by the detection algorithm. This method of double buffers is known as 'ping-pong' buffering and allows for increased efficiency of the microcontroller's resources.

2. Remove DC Bias - As the ADC cannot sample a negative voltage using a single ended setup, the incoming signal includes a fixed DC bias. This DC bias is now removed by subtracting the mean value ($\bar{x}$) of the current block of 256 samples (x_i where i is the sample index). The reason for removing the DC bias is that it was added during the analogue signal processing stage and does not represent the signal of interest.

$$\bar{x} = \frac{1}{n}\sum_{i=1}^{n} x_i \tag{4.1}$$

$$x[n] := x[n] - \bar{x} \tag{4.2}$$

3. Data Shift - The microcontroller used is limited to 16-bit arithmetic with a maximum stored number size of 32-bit. In order to preserve the accuracy of data during calculation, data values are left shifted prior to the calculation being carried out. For example, if the maximum data value was 600 in decimal, it would be possible to left shift 5 places giving a new value of 19200. However, shifting 6 places would result in a value of 38400 which is greater that the 2^{15} limit of 32768. This larger value could cause binary overflow in the planned calculation as the maximum number size for the result is 2^{32}. It is very important to ensure overflow does not occur as this can destroy both the data and end results.

4. Hanning Window - Before the data is passed to the fixed point FFT (Fast Fourier Transform) routine it is first windowed to prevent spectral leakage. The Hanning window used has a fixed amplitude of 2^{15} to ensure that there is no chance of binary

overflow during windowing calculation. This is because both of the maximum values to be multiplied do not exceed 2^{15}, therefore the maximum result of the calculation must be 2^{30} or below. Once the windowing function has been implemented on the data a shift correction is performed to right shift data back to a maximum of 2^{16} ready for the FFT routine.

5. Fixed Point FFT - The KL16Z microcontroller used to implement the detection algorithm uses fixed point arithmetic. Therefore, a fixed point 16-bit FFT algorithm has been designed to work with the hardware available. The main advantage of fixed point arithmetic is the speed at which it can be completed and the minimal strain it puts on the microcontroller. The big disadvantage is the potential loss in accuracy during calculation as lower resolution bits can be lost due to the limited number size. As implemented prior to the windowing stage, binary shifting is big part of the FFT routine to preserve accuracy. The fixed point FFT is based on Equation 4.3 with modifications to enable fixed point arithmetic and maintain data resolution.

$$x[k] = \sum_{n=0}^{N-1} X[n] W_N^{kn} \qquad k = 0, 1, ..., N-1 \tag{4.3}$$

$W^{kn} = e^{-j\frac{2\pi kn}{N}}$, *k = Index of Frequency, n = Index of Signal, N = Block Size*

6. FFT Magnitude - The result of the fixed point FFT is a real and imaginary array. Using these arrays, the DEMON magnitude squared is calculated using Equation 4.4. The reason there is no square root in the magnitude formula is because it would be computationally intensive to complete and it is not required for the end result. As in previous stages, data resolution is maintained by shifting data to maximise the dynamic range available.

$$X_{Magnitude} = (X_{Real} \times X_{Real}) + (X_{Imaginary} \times X_{Imaginary}) \tag{4.4}$$

7. DEMON Spectrum Peak Detection - Now that we have the DEMON spectrum resulting from the FFT, the remain stages represent the decision making part of the vessel detection algorithm. The aim is to identify consistent above threshold spectral peaks in the DEMON spectrum. Therefore the first task is to identify the peak magnitude and which of the 128 frequency bin's it occurs in. Each of these frequency bins represents 1 Hz of resolution. In addition to the largest peak present in the DEMON spectrum, the second largest peak is also identified for the purposes of post processing analysis.

8. Magnitude Threshold - The first user defined threshold is related to the magnitude of the DEMON peaks detected. The threshold is currently based on a multiple of the spectrum average. The spectrum average is currently calculated using Equation 4.5.

$$Magnitude\ Threshold = \frac{1}{n}\sum_{i=1}^{n} X_i \tag{4.5}$$

$$X = DEMON\ Spectrum\ Magnitude,\ n = Number\ of\ Frequency\ Bin's,$$
$$i = Index\ of\ Signal$$

Once the peak magnitude threshold has been calculated it is compared with the detected peak magnitude. If the relationship shown in Equation 4.6 is not satisfied then a zero value is recorded in the linear fit array to indicate a negative result.

$$Detected\ Peak\ Magnitude > Calculated\ Magnitude\ Threshold \tag{4.6}$$

9. Linear Fit - As discussed in the previous stage, each time a DEMON spectrum is calculated, the peak magnitude and frequency are recorded for comparison against a user defined threshold. The frequency data that is recorded after each DEMON spectrum is calculated it is also subject to regression analysis. A line of best fit, represented by $\hat{y}$, is calculated for the frequency data recorded to establish is a consistent trend exists over time. The formulae used to calculate the line of best fit are shown in Equations 4.7, 4.8 and 4.9.

$$\hat{Y}_i = b_0 + b_1 X_i \tag{4.7}$$

$$b_1 = \frac{\sum(X_i - \bar{X})(Y_i - \bar{Y})}{\sum(X_i - \bar{X})^2} \tag{4.8}$$

$$b_0 = \bar{Y} - (b_1 \bar{X}) \tag{4.9}$$

An example of the linear fit applied to frequency data is shown in Figure 4.4. To quantify the level of trend that exists within the frequency data, a Standard Error Of the Estimate (SEOE) calculation is carried out as discussed in the next stage.

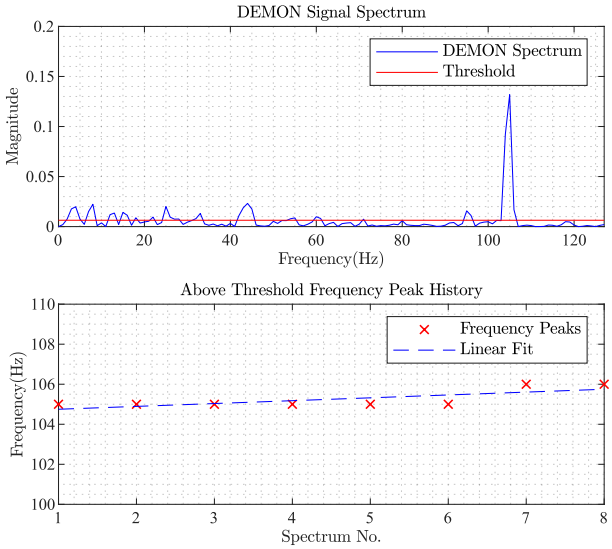

Fig. 4.4 Example of a positive detection spectrum and historical frequency peak record with calculates SEOE.

10. Standard Error Of the Estimate (SEOE) - To identify if a consistent trend in the DEMON peak record exists over a given timeframe, a line of best fit is applied to the data set and the SEOE is calculated (*see Figure 4.4*). The SEOE is a measure of how well the actual recorded samples relate to the line of best fit or estimated samples. The SEOE calculation is shown in Equation 4.10, where $\hat{y}$ is the estimated samples and y is the actual samples.

$$SEOE = \sqrt{\sum_{i=0}^{n} \frac{(\hat{Y}_i - Y_i)^2}{n-2}} \tag{4.10}$$

If the calculated SEOE is below a user defined threshold this would constitute a positive detection as shown in Equation 4.11.

$$Calculated\ SEOE < SEOE\ Threshold \tag{4.11}$$

11. Detection Decision - Once the previous stages of the algorithm have been satisfied, the last part of the process is to package useful data to relay back to the end user. The vessel detector makes use of a communication device developed by SEALab to send data acoustically through the water. There are two messages which the vessel may send depending on which mode the device is in at the time. The first message type relates to a vessel being detected and the second message is a periodic diagnostic message used for condition monitoring. Both of these message types contain a selection of the following items within the message payload.

- Message ID - Used to distinguish itself from other deployments using the same communication technology.
- Node Address - A unique address specific to a single node.
- Sequence - An on-board message sequence number used to identify missed data on the receiver end.
- Magnitude - Contains the magnitude data from the on-board FFT calculation for both the first and second largest peak.
- Frequency - Contains the frequency bin to which the first and second largest peak relate to in the calculated FFT.
- SEOE - A measure of how well the calculated frequency samples relate to a line of best fit using SEOE.
- Threshold - The magnitude threshold at the time of detection.
- Battery Voltage - A measure of the current battery voltage on the attached battery pack.

A 'vessel detected' message contains all of the items previously listed but the data is compressed to take up only 24 bytes to maximise efficiency. This data is sent through the water and using a data acknowledgement feature of the communication device it is possible to confirm its delivery. Should this acknowledgement not arrive back at the vessel detector, the algorithm has been designed to re-transmitted data for a specified number of attempts before the message is abandoned. This mode is one of the additional features included in the vessel detector, more detail of this and other features included are shown below.

1. Vessel Detection Time Out - Once a vessel has been detected there is a time out period of one minute. During this period no positive detections will be sent unless the current frequency detected is sufficiently different from the previously detected frequency at the start of the one minute time out. In the current setup the new frequency must be ± 5 Hz of the previously detected frequency. The one minute mode helps to prolong the battery life of the unit as many repeated detections are avoided whilst still identifying potential different vessels or a notable change in propeller speed.

2. Vessel Frequency Threshold - To reject any unrealistic propeller frequencies, a threshold has been placed on the allowable frequency which can be detected. In the current setup any frequency which is below 2 Hz is deemed unrealistic and therefore rejected from producing a positive detection result.

3. Periodic Diagnostic Message - As the vessel detector is designed to operate in total isolation for a period of several months at sea, a periodic diagnostics mode has been added. In this mode, a short message including battery voltage and the last message sequence number is sent every six hours. This provides not only a reliable source of battery condition data but also shows that the unit is still operating correctly.

4. Acoustic Retrieval Mode - One of the biggest challenges with deploying devices underwater is the potential for equipment to go missing or become dislodged from its mooring. This is a concern as equipment will inevitably has a cost involved but also because losing equipment at sea would only add to the already alarming plastics pollution in our oceans. To safeguard against loosing the device the vessel detection utilises the acoustic communication devices ping and return function. In this mode an estimated range is provided based on the speed of sound underwater. In the vessel detector's low power mode, the system will enter a 'ping-mode' after every periodic diagnostics message for a period of 5 minutes. This allows for the device to be pinged repeatedly from a surface vessel to establish its location and retrieve the device.

4.3.2 Non-continuous (duty-cycled) digital detection (NCDD)

The NCDD mode provides an alternative approach to the previous CADD mode in that the detection process is fully digital and the period of active detection is duty cycled. To make these two modes comparable the total average power consumption is matched and the overall vessel detection algorithm has not changed. In the NCDD mode the signal is sampled at 80 kHz which captures all of the amplified input signal in the 0 to 40 kHz range. High frequency noise produced during propeller cavitation is typically found in the 20 to 30 kHz range which satisfies the Nyquist criteria for this mode. The stages of the NCDD mode are illustrated in Figure 4.5.

As shown in Figure 4.5 the amplified signal is sampled at 80 kHz and the first stage of filtering is the removal of the D.C. bias added by the analogue amplifier. The reason for this bias is so that the ADC can capture the entire signal as it is not capable of capturing a negative voltage. Once the signal is sampled the bias is removed and the absolute value is taken. This is to rectify the signal similar to the analogue precision rectifier in the CADD mode. The next two stages both aim to decimate and low-pass filter the signal to capture the envelope of the now rectifier signal. The reason for starting with a Cascaded Integrator-Comb (CIC) decimation filter is due to the high sample rate of 80 kHz. A CIC filter is a very computationally efficient filter as it involves only additions and subtractions. The decimation rate is set to 32 which adds to efficiency as only every 32^{nd} sample is considered

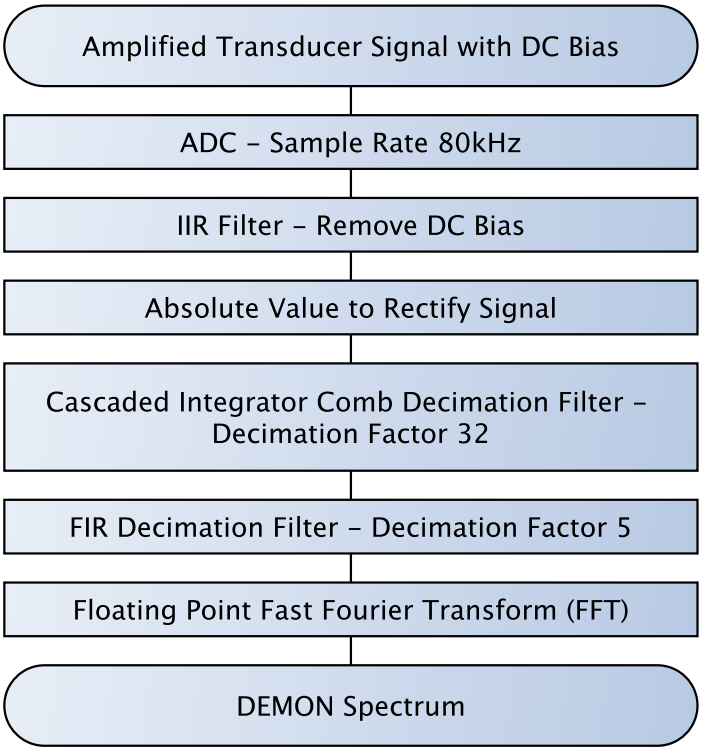

Fig. 4.5 Illustration of the NCDD mode signal processing method, used to produce the DEMON spectrum. The method combines different digital filtering/decimation techniques in order to maximise processing efficiency and retain spectral resolution.

for calculation in the CIC stage. These efficiency measures are at the expense of a less than ideal low pass filter response. This is illustrated in Figure 4.6 which shows the filter response of both the CIC filter and the following FIR decimation filter.

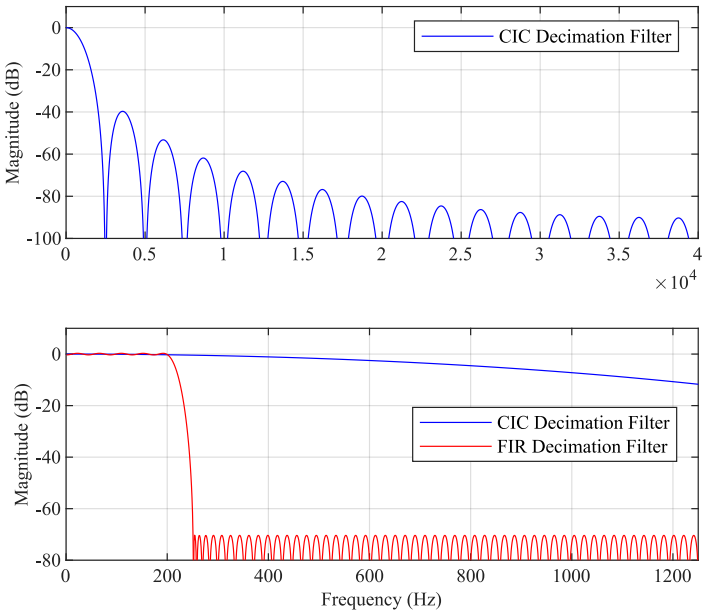

Fig. 4.6 Filter response of the NCDD mode digital signal processing stage. The plot shows the filter response of a CIC filter followed by an FIR filter, both of which have stages of decimation. The end result is a tightly bound filter response but the computational load is greatly reduced by using this combination of filters.

The FIR decimation filter is more complex computationally than the CIC filter as it involves both multiplications and additions. However, this filter is now running at 1/32 of the 80 kHz sample rate due to the CIC decimation stage. The FIR filter is set to decimate by a factor of 5 so it only considering every 160th sample of the original 80 kHz sample rate. That FIR output signal has now been decimated and low pass filtered down from 80 kHz to 500 Hz which preserves spectral content below 250 Hz due to the Nyquist criteria. The final stage in Figure 4.5 shows a floating point FFT which calculates the spectral content of the signal.

One of the key features of the NCDD mode is the improved precision gained using a floating point FFT to produce the DEMON spectrum. This improved precision can be a great advantage in detecting very small signals from distant vessels.

4.4 Algorithm Offline Processing Results

This section contains offline processing results for the vessel detection algorithm. The testing was carried out using real field trial recordings of passing vessels. The acoustic recordings were taken using the same piezoceramic ring used in the vessel detector. This is to ensure

that the MATLAB based vessel detection algorithm sees the same signal as the physical device would.

The recordings taken for development of the detection algorithm were obtained using a hydrophone deployed at shore side which recorded sounds made by passing vessels. This limits knowledge regarding the vessel itself as these were not controlled experiments using known vessels. Information related to vessel speed, orientation and engine type would be useful for algorithm development purposes. One trial using a University owned RHIB was conducted but the data-set was limited to only a few passing's in the port of Blyth. Using a richer data set would be advantageous in future developments of this research to expand development capabilities.

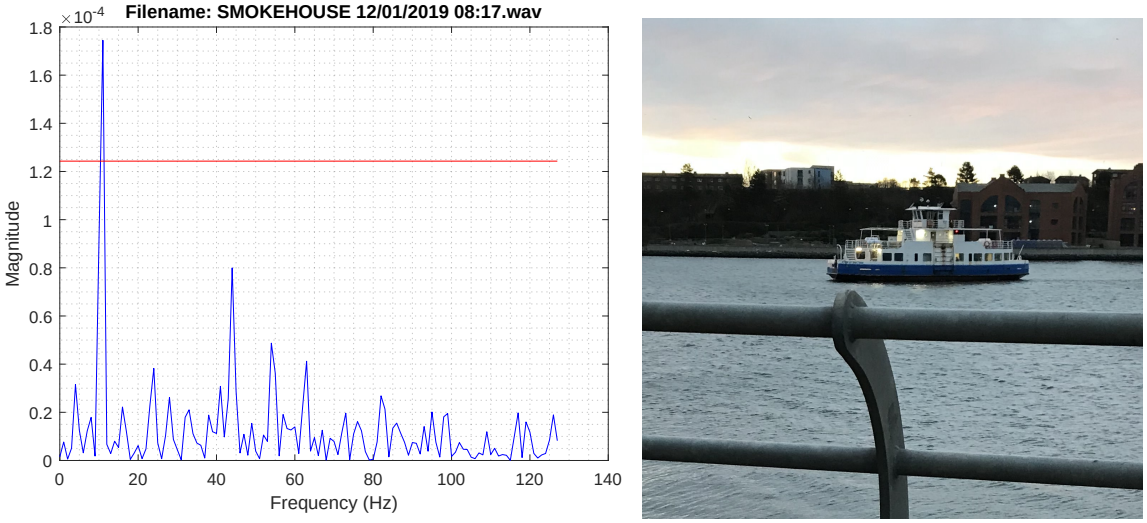

Fig. 4.7 Passenger ferry DEMON spectrum

Figure 4.7 shows a passenger ferry which crosses the Tyne River as part of a local transportation network. Upon detection the algorithm shows the DEMON spectrum contains a low frequency peak at 10Hz. This frequency result has been typical during trials for this vessel potentially due to speed restrictions on the river and short navigation path.

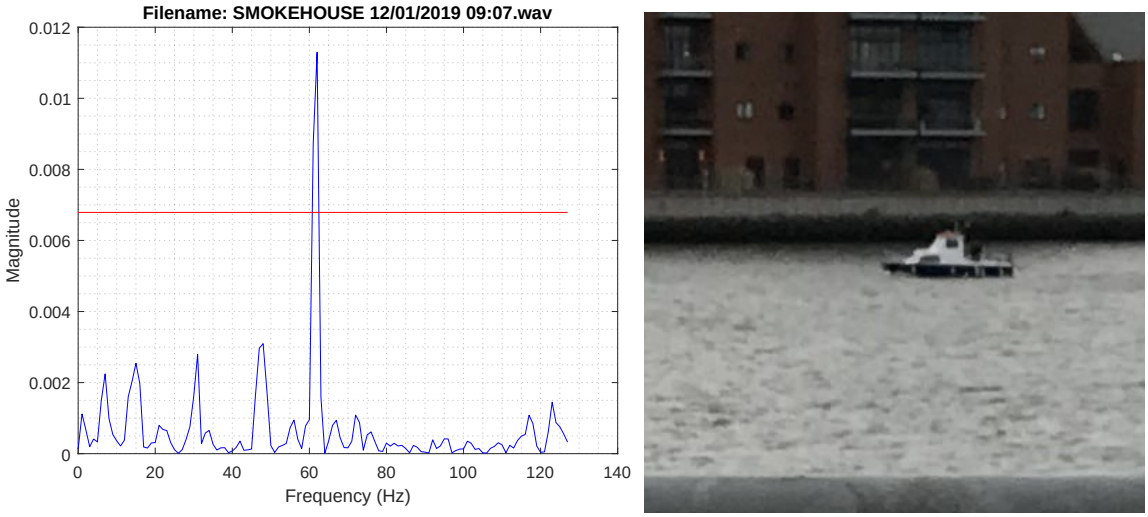

Fig. 4.8 Small recreational vessel DEMON spectrum

Figure 4.8 shows a small recreational fishing vessel. The associated spectrum shows a higher frequency peak which would indicate the rotational rate of the propeller is higher than the previous passenger ferry. During trials it is also characteristic of smaller vessels travelling along the river to have a higher frequency peak than that of the larger vessels. This may be down to the propeller size with larger vessels requiring fewer revolutions per minute to produce thrust.

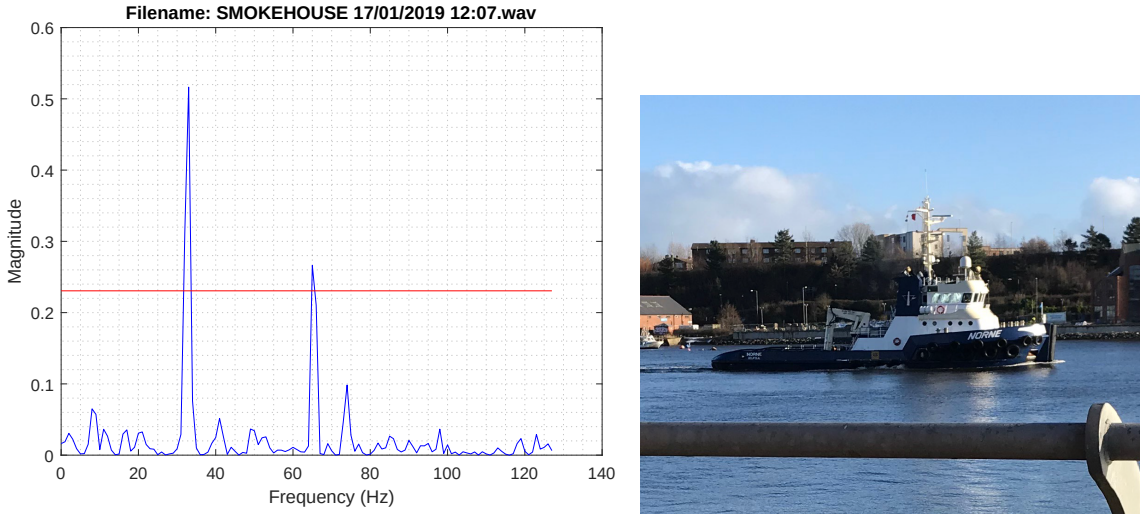

Fig. 4.9 Tug boat DEMON spectrum

Figure 4.9 is an interesting recording as there was a second vessel in the area at the time which may explain the secondary peak. The ability to deal with multiple vessels during

detection is an area which will form part of the future work of this project.

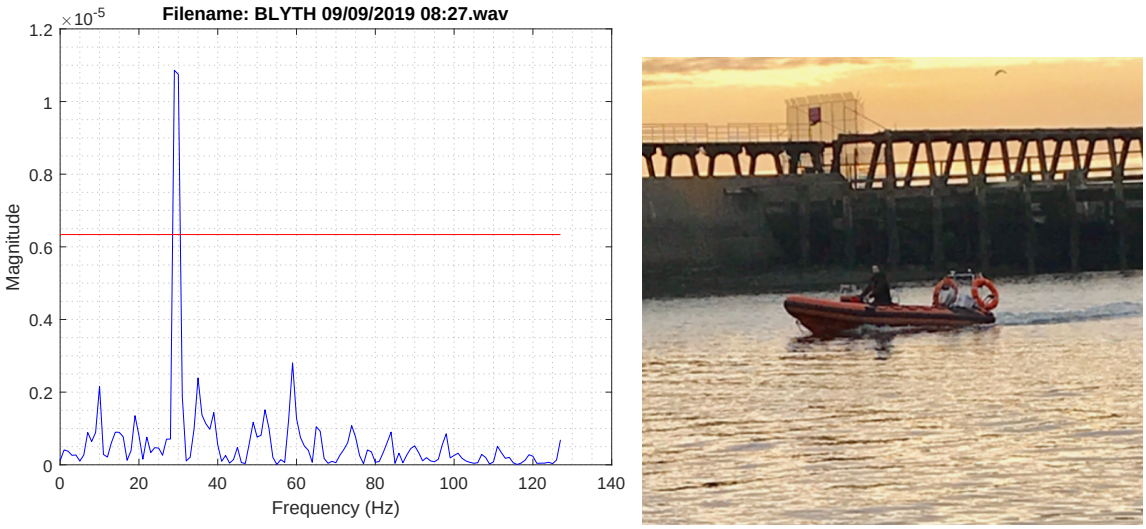

Fig. 4.10 Rigid-hulled inflatable boat (RHIB) DEMON spectrum

Figure 4.10 represents the main target for the vessel detection system. The RHIB is a small vessel which is often used for illegal activity. As the result shows the detection algorithm developed has detected the vessel acoustically with a peak at 27 Hz. This vessel belongs to Newcastle University and will be a key asset for future trials.

4.4.1 Threshold Optimisation

The vessel detection algorithm has three main user defined thresholds which influence the detection result. They include threshold weight, detection time frame and SEOE threshold. Threshold weight refers to the user defined value that is multiplied by the spectral mean to calculate the overall magnitude threshold. Equation 4.12 illustrates the magnitude threshold calculation. In the event that the spectral energy does not exceed this threshold then the algorithm will not record a detection result and move on to the next data set.

$$Threshold = Threshold\ Weight\ X\ Spectral\ Mean \tag{4.12}$$

The detection time frame refers to the amount of time that will be considered when calculating the linear fit and SEOE. This can be an important user defined variable as the deployment location can impact the value chosen. During trials within a port location, it has been observed that vessels often make minor thrust adjustments as opposed to prolonged

engine thrusts. These minor adjustments indicate that the detection time frame must be reduced to detect the small engine adjustments. Out in open sea this would be the opposite situation as vessels are often running engines at a constant speed to maintain heading against the sea conditions.

The SEOE threshold is a level of acceptable tolerance for the calculated linear fit result. This user defined threshold impacts the quality of a detection decision as increasing this value would result in a decision based on a poor linear fit.

To effectively select the optimal user defined variables, a MATLAB based algorithm has been produced to evaluate each combination of the three user defined variables using the same acoustic recording. In executing this algorithm it is important to know the ground truth value of expected true positive detections. This makes it clear to identify if either false positive or false negative detection results have occurred. Figures 4.11, 4.12, 4.13 show the optimisation results for one acoustic recording that contains 60 seconds of known vessel noise and 60 seconds of known background noise. The reason for the added background noise signal is to establish if the algorithm produces any false positive results. In the examples illustrated, a maximum true positive result would be around 60 on the 'No. of Detection' axis based on the number of seconds of known boat activity.

Figure 4.11 shows that the optimum user defined variable for threshold weight and detection time frame would be 5 and 7 respectively to achieve the best possible true positive detection result. Figure 4.12 shows that the optimum user defined variable for threshold weight and SEOE threshold would be 5 and 10 respectively to achieve the best possible true positive detection result. Figure 4.13 shows that the optimum user defined variable for detection time frame and SEOE threshold would be 5 and 10 respectively to achieve the best possible true positive detection result.

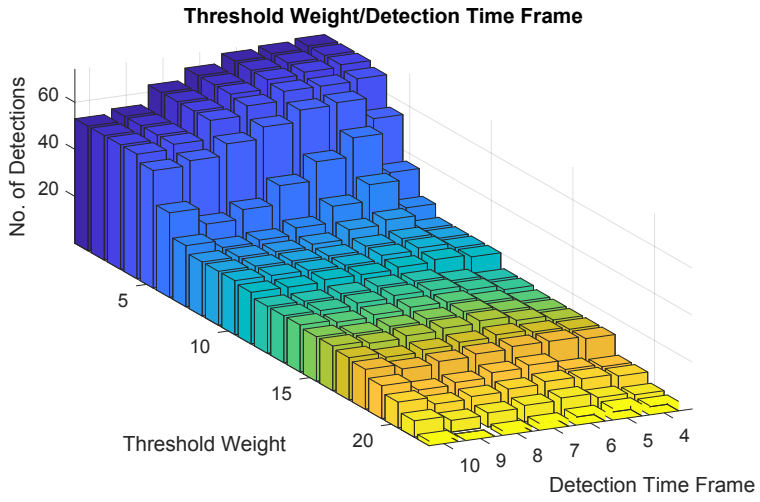

Fig. 4.11 Comparison of the number of detections identified for various threshold weight/detection timeframe values.

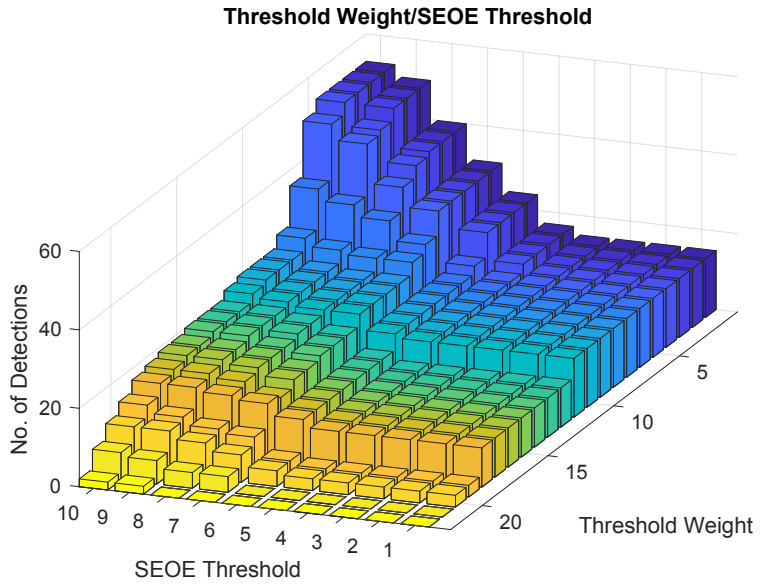

Fig. 4.12 Comparison of the number of detections identified for various threshold weight/SEOE threshold values.

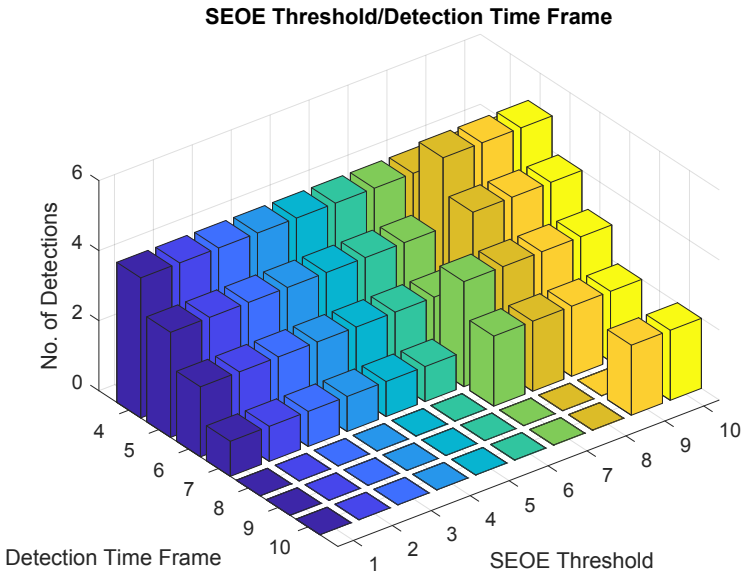

Fig. 4.13 Comparison of the number of detections identified for various detection time frame/SEOE threshold values.

To further evaluate the optimum thresholds to be used within the systems design, Receiver Operating Characteristic (ROC) curves have been calculated. ROC curves help to evaluate the performance of a classification-based system such as the vessel detector. To do this the true positive rate (TPR) is plotted against false positive rate (FPR) for varying thresholds. In figures 4.14 and 4.15 two thresholds are varied against each other to cover all possible combinations of threshold values. For example, figure 4.14 shows varying SEOE threshold values against a set of varying threshold weights. Using each of the ROC curves plotted, it is possible to select the optimum set of thresholds to achieve the highest TPR for the lowest FPR. This is because each plotted point represents two threshold values, therefore, the best possible TPR for the lowest FPR for each of the three threshold categories can be evaluated.

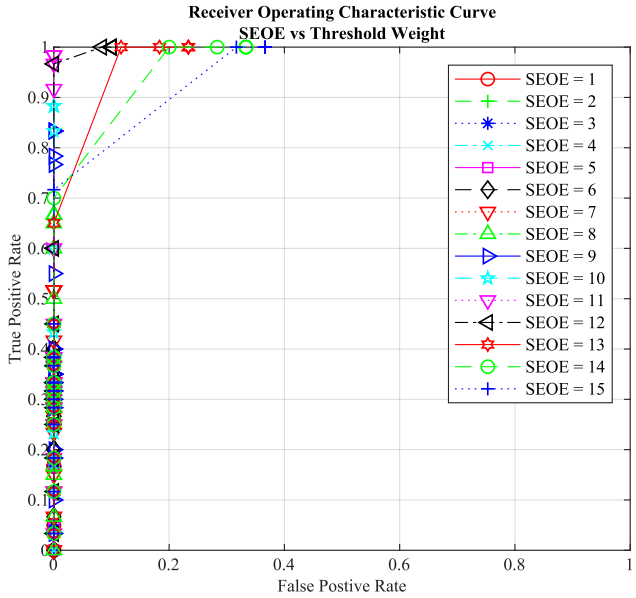

Fig. 4.14 Receiver Operating Characteristic (ROC) curve comparing SEOE against threshold weight.

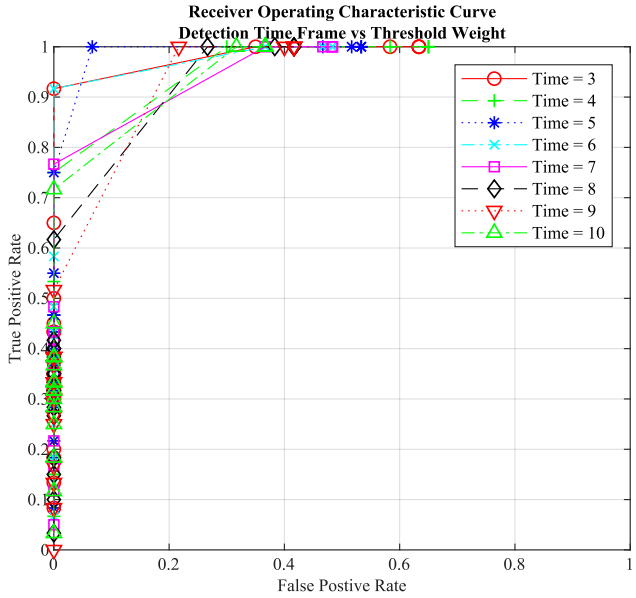

Fig. 4.15 Receiver Operating Characteristic (ROC) curve comparing detection time frame against threshold weight.

Based on figures 4.11, 4.12, 4.13, 4.14 and 4.15 the optimal user defined values for this example acoustic recording have been found to be:

- Threshold Weight = 5.
- Detection Time Frame = 6 Seconds.
- SEOE Threshold = 11 Hz.

The results of the optimisation algorithm shown only include one example of a vessel recording, in practice this process has been repeated with multiple vessels. This is to create a more generalised robust configuration based on a large data set.

4.5 Summary

The aim of this section was to develop an algorithm which is able to detect the presence of a vessel using only the acoustic emissions created during propeller cavitation.

Methods of detection have been presented using a variety of digital and analogue signal processing. Each of the detection methods are specifically tailored around a low energy implementation. This is evident by the low energy analogue electronics and digital fixed point arithmetic used within the CADD algorithm. A fully digital approach is used within the NCDD algorithm, with the caveat that it operates at a duty cycle to match the power budget of the CADD mode.

During offline processing using recorded vessel data, the CADD mode showed that a strong spectral peak can be detected using the DEMON based detection algorithm. In addition to these initial offline detection results, optimisation of the user defined thresholds within the algorithm has been carried out using a ground truth recording.

In summary, the Matlab-based algorithms developed have shown encouraging results, which warrant implementation in an embedded based microcontroller system.

Chapter 5

Vessel Detector Algorithm Implementation

5.1 Introduction

This chapter describes the implementation of the vessel detection algorithm into custom low power hardware and the results of the long duration subsea field trials. The aim of this section is to demonstrate the practical deployment of the vessel detector and show the potential of forming a very low energy wireless underwater sensor network.

The key contributions for this chapter of work is the deployment of a energy efficient embedded vessel detection algorithm for long term deployments at sea. To evaluate each of these contributions, techniques have been adopted to maximise accuracy whilst operating within the practical limitations of long term analysis at sea. One of the key challenges for this chapter was establishing the best possible ground truth to compare detection results against. The best possible solution would be a full visual survey of vessel activity 24-hours. However, this would be impractical, not just from a logistics point of view but also because the conditions at sea can severely limit visual surveys such as during the night and in heavy fog. The methods adopted in this chapter to establish a ground truth have been a mixture of local AIS data, inline acoustic recorders and some visual confirmation.

For long term deployments, AIS data has been key to evaluating detection reliability with the acknowledgement that AIS is not legally required to be carried by all vessels. To further evaluate reliability, data related to local weather conditions has been used as a means of monitoring performance during poor acoustic conditions caused be severe weather.

Energy efficiency is an important metric for this project and key to long term deployments at sea using only battery power. Energy efficiency is measurable at shore for each stage of

the system. However, for long term deployments of an event driven system it becomes more complex and reasonable predictions can be made using the knowledge of the system stages.

5.2 System Design

This section presents the key enabling technology used to facilitate the long duration field trials which have taken place. In particular, the NMV3 is presented which has enabled wireless communication of the detection data produced by the algorithm. In addition, the evolution of the vessel detector system is described to show the journey from a shore based prototype to a fully wireless underwater sensor node.

5.2.1 Integrated Communication Device

To achieve a wireless underwater monitoring network capable of long term deployments, the vessel detection system will be integrated with an existing piece of hardware developed by SEALab. Figure 5.1 shows a low-cost, low-power, miniature underwater acoustic communication device, capable of transmitting and receiving data reliably up to a distance of 2km in a single hop.

Fig. 5.1 Acoustic communication device (pre-encapsulation) developed by SEALab.

Using a 5V supply, the NMV3 consumes a maximum of 300 *mA* in its transmit mode. However, this transmission lasts only a fraction of a second, depending on the amount of data to be sent. Aside from transmitting, the NMV3 can operate in receive/listening mode which consumes 5/2.5 mA respectively. At a manufacturing cost of less than £30, in quantities of more than 200 units, this technology is a key enabler behind producing an underwater

network of sensor nodes. A full technical specification of the acoustic communication device's capabilities is shown in Figure 5.2.

Supply voltage	3 – 6.5V dc (5V or 6V supply recommended)
Supply current (5V supply)	Listening: 2.5 mA Receiving: 5mA Transmitting: max 300mA
Acoustic frequency	24-32kHz
Acoustic source level	~168 dB re 1uPa @ 1m
Acoustic directivity	Near omnidirectional (reduction around cable entry of potted unit).
Physical layer	Aperiodic orthogonal code keying with BPSK modulation and error correction code.
Acoustic data rate (raw)	640 bits/s, unicast and broadcast data messages up to 64 bytes in length.
Acoustic throughput (max)	463 bits/s
Addressing	Up to 256 units (addresses 0-255)
Ranging increment	4.7 cm (c=1500m/s)
Ranging variance	~10 cm
Maximum Range	> 2 km
RS232 interface	9600 Baud, 8-bit, no parity, 1 stop bit, no flow control

Fig. 5.2 NMV3 technical specification

Figure 5.3 shows the basic hardware building blocks which make up the NMV3. This project builds upon the communication capability by modifying the acoustic communication device's receiver setup. This is achieved by adding low cost analogue components and re-programming the on board micro-controller with a new vessel detection algorithm. Sharing the piezoceramic transducer to both receive signals for detection and transmit the resulting data will further work towards reducing the overall cost.

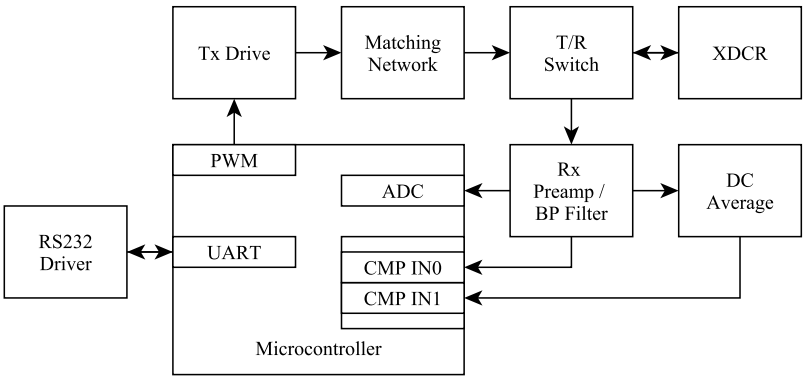

Fig. 5.3 NMV3 Hardware Block Diagram shows the design stages from the transducer signal (XDCR) to the received serial data via UART.

5.2.2 Design Evolution

Over the three years of this project, the vessel detector has evolved and through many iterations with refinements made after each field trial. To illustrate the design and development over time, Figures 5.4, 5.5 and 5.6 have been included with a short description of the changes implemented after each iteration.

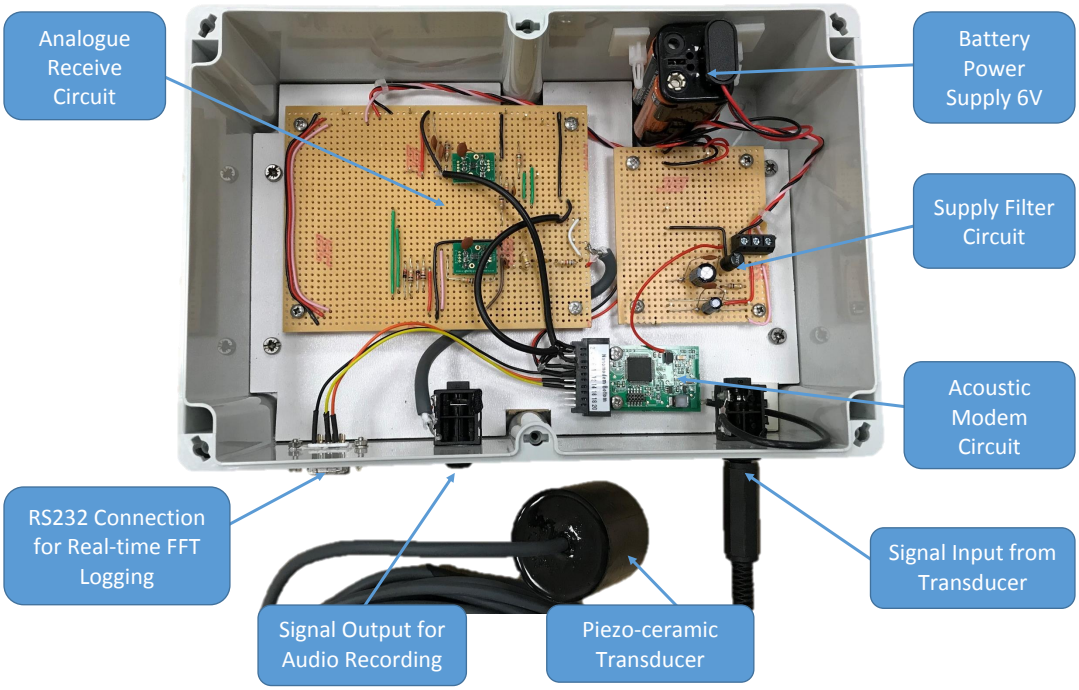

Fig. 5.4 Vessel detector version 1.0 used during initial onshore development field trials at the River Tyne.

Figure 5.4 shows the first vessel detector system. This version was designed to connect directly to a laptop for a shore side deployment. The only part of this version of the vessel detector to be deployed under the water was a transducer element, which is encapsulated and attached to an underwater rated cable. The benefits of this initial design was that all of the electronics were accessible during field trials along with real time data linked via RS-232. This allowed for rapid changes to be made to refine the performance of the vessel detector during field trials and using real vessel signals.

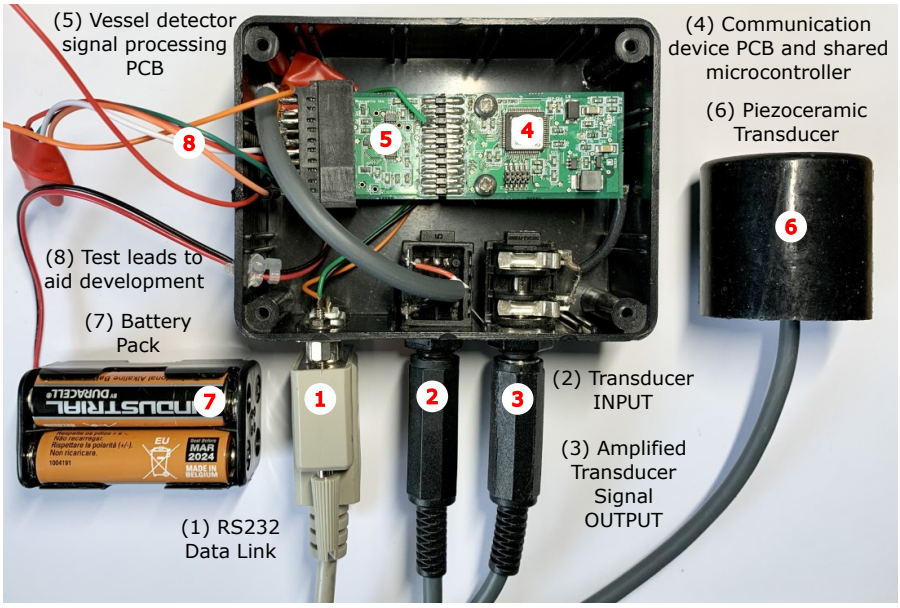

Fig. 5.5 Vessel detector version 2.0 with added signal processing Printed Circuit Board (PCB) used during the development of the detection algorithm.

The next version of the vessel detector is shown in Figure 5.5. In this version a new PCB is added which performs all of the vessel detector's analogue signal processing. To recap, the analogue stage of the design was used to amplify the incoming signal and extract the envelope of this signal in line with the DEMON methodology.

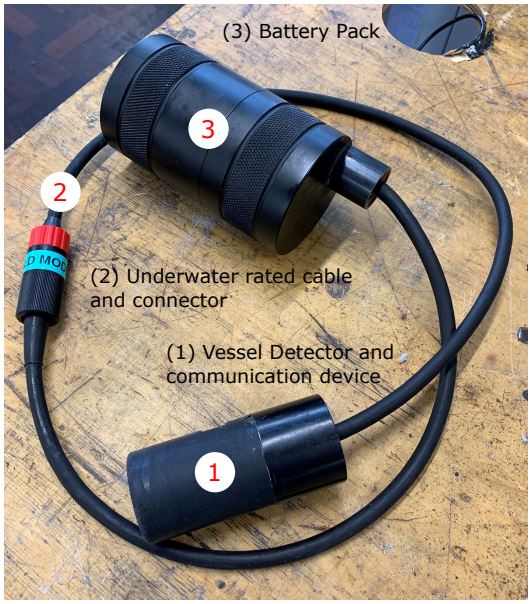

Fig. 5.6 Vessel detector version 3.0 fully enclosed in depth rated materials ready for long term subsea deployment.

The final version of the vessel detector is shown in Figure 5.6. The Figure shows the complete wireless arrangement which is ready for subsea deployment.

5.2.3 Field Trial Infrastructure

To facilitate field trial work, the SEALab team at Newcastle University have developed a WiFi gateway data buoy. The gateway buoy, shown in Figure 5.7, has been deployed 3km off the UK's North East coast aligned with Newcastle University's Marine Station in Blyth, Northumberland.

Fig. 5.7 Newcastle University WiFi Gateway Data Buoy.

The data buoy contains two hydrophones and two acoustic communication devices as illustrated in Figure 5.8. It operates using an on-board Raspberry Pi which is linked to a high gain Wi-Fi antenna. The buoy uses solar panels to charge on-board batteries which enables year round operation.

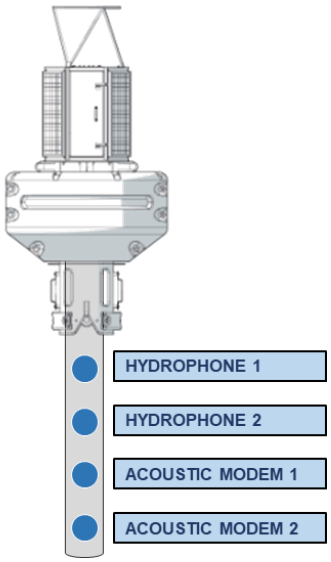

Fig. 5.8 Newcastle University Wi-Fi Gateway Buoy Diagram.

The buoy works as part of the Newcastle University Acoustic Network Gateway (ANGY) which is illustrated in Figure 5.9.

Fig. 5.9 Newcastle University ANGY system.

The ANGY system provides a Wi-Fi link between Newcastle University's computer network and the gateway buoy. This allows for real time access to data received on either of the two acoustic communication devices. In addition, access to a live audio stream from either of the two hydrophones mounted on the gateway buoy is possible. Having this system in place allows for a long term deployment of vessel detector units around the central gateway buoy for long term data analysis.

5.3 Hardware Design

In this section, a detailed description of the vessel detector's hardware design is presented. There are significant challenges in creating a system capable of capturing underwater acoustics from distant sources. Moreover, creating an reliable enclosure to withstand the harsh sea conditions is key to the success of the system.

5.3.1 Analogue Signal Processing Circuit Design

One of the main aims of this project is to create sensor applications which can be deployed for several months using only battery technology to provide power. The design of the vessel detector has attempted to address this aim by using low power analogue electronics to perform parts of the DEMON process, as opposed to using a completely digital approach. The benefits of using analogue electronics, aside from the low power consumption, is that the rate at which the signal needs to be sampled by the ADC can be greatly reduced. To recap, the DEMON method extracts the envelope modulation of high frequency noise. The envelope frequency is often in the sub-150 Hz as opposed to the high frequency noise which occurs in the kHz range. This allows for a much reduced sample rate to capture the envelope. This envelope signal is detected by the analogue circuit shown in Figure 5.10. The circuit shown fits into the overall system design presented in Figure 4.2 where the output of the low pass filter feeds into the microcontroller ADC for sampling.

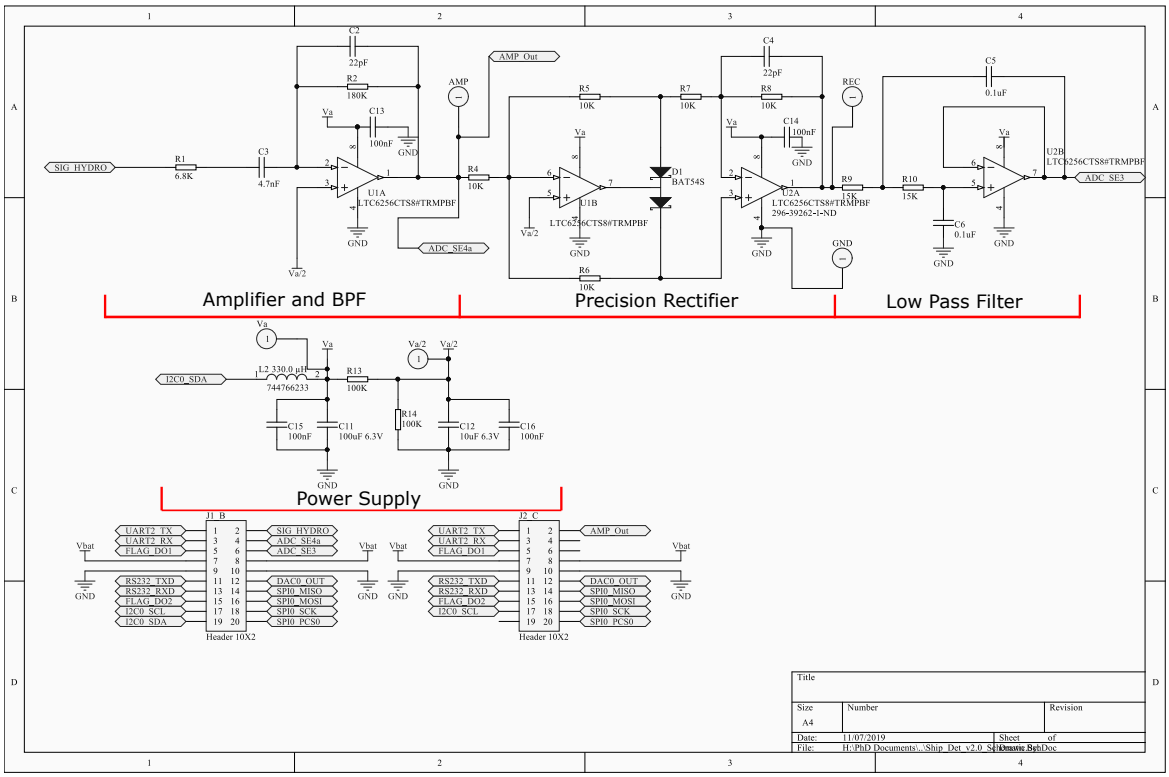

Fig. 5.10 Circuit schematic showing the key stages of the analogue signal processing design for the vessel detector.

To enable both mass manufacturing potential and prototype testing, a PCB has been created for the circuit in Figure 5.10. The PCB design was created by the author using Altium design suite as shown by the 3D images in Figure 5.11.

(a) PCB Top - Power Supply

(b) PCB Bottom - Analogue Signal Processing

Fig. 5.11 A 3D generated image of the two sided add-on PCB prior to manufacture.

The PCB was designed to separate power supply components from signal processing components by using both sides of the board. This can be seen in the 3D Atlium genrated images in Figure 5.11 as well as the final completed board shown in Figure 5.12.

(a) PCB Top - Power Supply

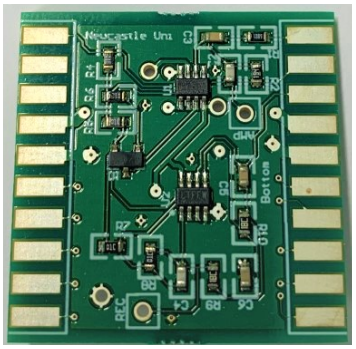

(b) PCB Bottom - Analogue Signal Processing

Fig. 5.12 A photo of the completed PCB design once manufactured.

5.3.2 Circuit Simulations

To further illustrate the design of the analogue circuit introduced in Section 5.3.1, simulations have been included which were carried out using LTspice. Figure 5.13 shows the impact of each stage of the front-end analogue circuit design. Stages include:

- Input - Signal input from transducer element.
- Sig_Hydro - Output of first stage amplifier on communication device.
- Amp_Out - Output of custom vessel detector PCB analogue amplifier.
- Rectify - Output of custom vessel detector PCB precision rectifier.
- ADC_SE3 - Input to microcontroller single ended ADC.

As the simulation shows, the incoming signal goes through significant amplification before it is then rectified and finally low pass filtered. This final low pass filter stage is what produces the envelope signal of interest which is then sampled at a much reduced rate of 256 Hz. This sample rate is in place of the potential 80 kHz sample rate which would be needed should a digital implementation of the DEMON method be used. This is because the high frequency noise created during propeller cavitation tends to occur up to 40 kHz, therefore Nyquist criteria demand this higher sample rate to capture the band of interest.

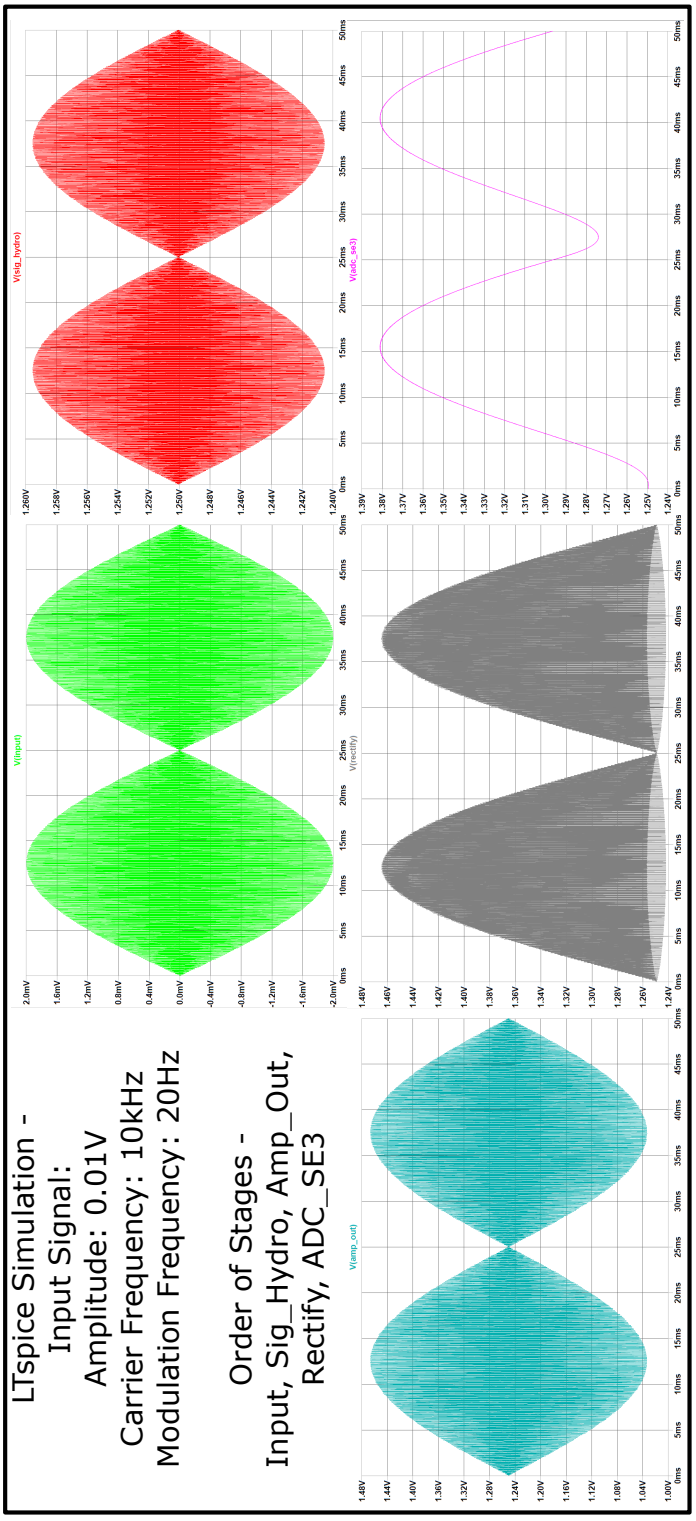

Fig. 5.13 LTSpice simulation of the analogue front end circuit.

Figure 5.13 includes one stage of the process which is not shown on the previous schematic in Figure 5.10. The PCB is designed to integrate with the existing acoustic communication device developed by Newcastle University as discussed in Section 5.2.1. To do this, one stage of amplification/filtering is utilised on the existing communication device circuit prior to the signal reaching the vessel detector's amplification stage. These two levels of amplification/filtering are illustrated by the bode plot in Figure 5.14. The level of gain illustrated in Figure 5.14 (approx. 40 dB), has been chosen to maximise the performance of following stage rectifier circuit, in addition to utilising as much of the dynamic range of the ADC as possible.

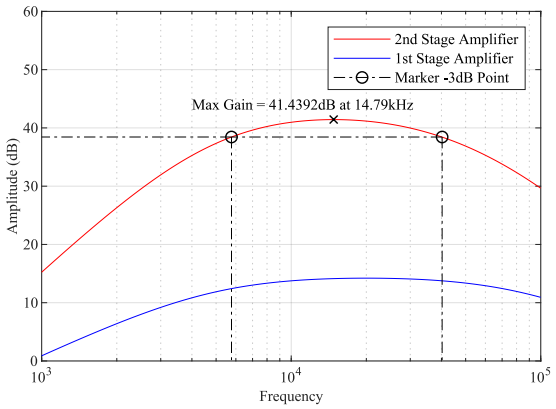

Fig. 5.14 LTspice simulation results showing the frequency response of the vessel detectors analogue circuit design.

5.3.3 Bespoke Underwater Enclosure

The vessel detector enclosure has been custom designed to enable a deployment duration of up to one year at a minimum depth of 20m. In addition, the enclosure must be low-cost to enable the unit to be mass manufactured to form an affordable network of sensor nodes. Considerable thought has gone into designing a low cost reliable enclosure which is easily reproduced using mass manufacturing techniques such as injection moulding. Off the shelf components have been used wherever possible and any custom processes have been designed with portability to full scale manufacturing in mind. Figure 5.15 shows an example of a bespoke 3D component created to aid the encapsulation process of the detectors PCB and transducer. The 3D component also includes a cable gland and mounting holes in anticipation of producing nodes on a large scale.

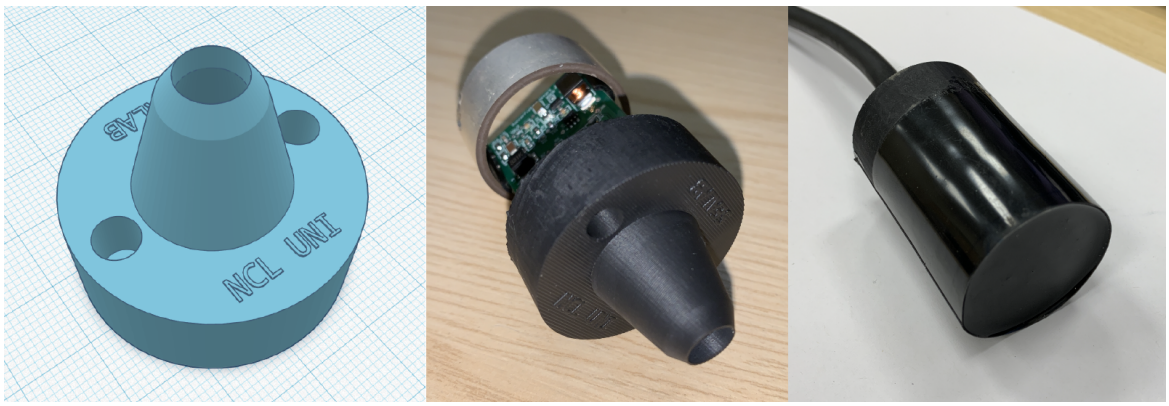

Fig. 5.15 This figure shows the design and construction of a 3D printer encapsulation component. This shows progress made to enable mass production of the potted vessel detector/communication device. Key design aspects in the 3D printed design include; cable gland, mounting holes, PCB holder and transducer end potting process.

5.3.4 System Build Process

The vessel detector is designed to work alongside an acoustic communication device developed by SEALab. Whilst many components of the communication device are shared with the vessel detector, such as the microcontroller, there is an additional PCB design solely for the vessel detector. The motivation for this integrated design is to both save cost and also to expand the communication device's capabilities to include a passive acoustic monitoring of passing vessels. Figure 5.16 shows the existing PCB connected to the add-on board prior to encapsulation. The left hand PCB, relative to the soldered connection, is the acoustic communication device whilst the right hand PCB is the PAM add-on board designed to perform the analogue signal processing stages of the DEMON method.

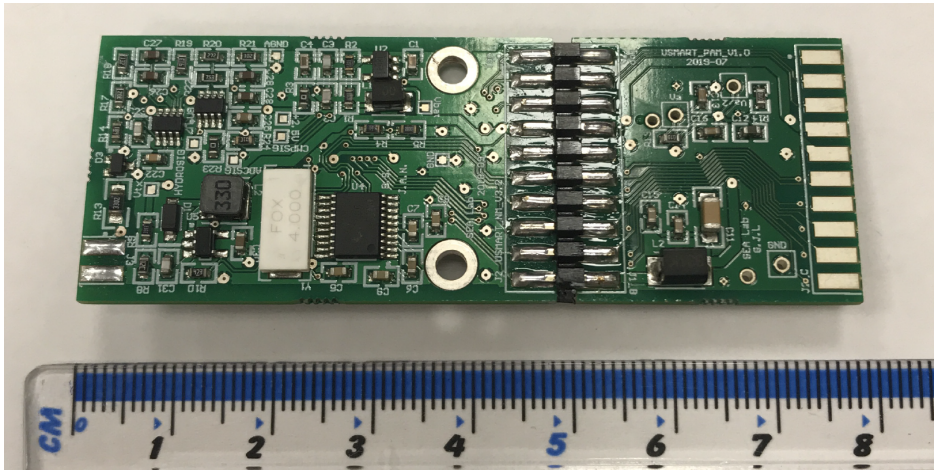

Fig. 5.16 Assembly - NMV3 PCB (Left) and PAM Add-On PCB (Right)

Figure 5.17 shows the addition of the piezoceramic ring and underwater rated cable. The underwater cable can be connected to a battery pack to create a total self contained deployment node for underwater vessel detection. In this mode data is sent acoustically through the water to another location. The cable can also be connected to a laptop, as done during field trials, to receive real time FFT data and also the raw acoustic signal data.

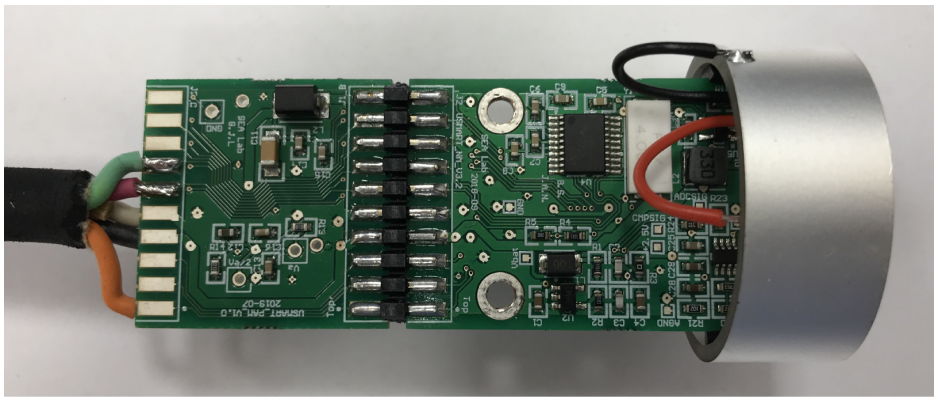

Fig. 5.17 Assembly - Piezoceramic Transducer Ring and Underwater Rated Cable

Figure 5.18 shows the encapsulated vessel detection and communication system. This encapsulation was constructed using a purpose built mould tool and potted with specifically chosen Polyurethane to achieve a good acoustic impedance match to the surrounding water.

Fig. 5.18 Assembly - Encapsulated Vessel Detection System in Polyurethane

To finalise the design for field trials, a low cost submersible power source was required. Figure 5.19 shows the complete enclosure design prior to a long term subsea deployment.

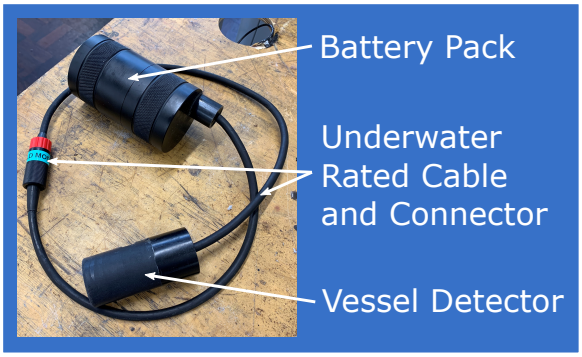

Fig. 5.19 Illustration of the Vessel detector set up prior to a sub sea deployment. The detector is connected via an underwater rated cable to a depth rated battery pack.

Figure 5.19 shows a larger battery pack holder which is made from a modified diver enclosure. Leading from this is the underwater rate cable which connects the smaller enclosure which houses the vessel detector electronics. This smaller enclosure is made from an acoustically favourable polyurethane material using a potting process perfected by SEALab. This encapsulation material and method maximises acoustic performance whilst also delivering a low-cost, durable end product.

5.3.5 Power Consumption

In this section the vessel detector is broken down into the stages first introduced in overall system design in Figure 4.2. The key stages of the vessel detector are:

- Analogue Receive Circuit - Amplifier, Precision Rectifier and Decimation Low Pass Filter
- Digital Receive Circuit - Remove DC offset, Fixed Point FFT, Detection Algorithm

The vessel detector has a custom analogue front end PCB which is specifically designed to minimise current consumption during operation. The aim of the circuit is to extract the received signal envelope to enable the DEMON spectrum to be calculated. Figure 5.20 shows that the circuit design consumes only 0.6 mW of power when isolated from the digital system.

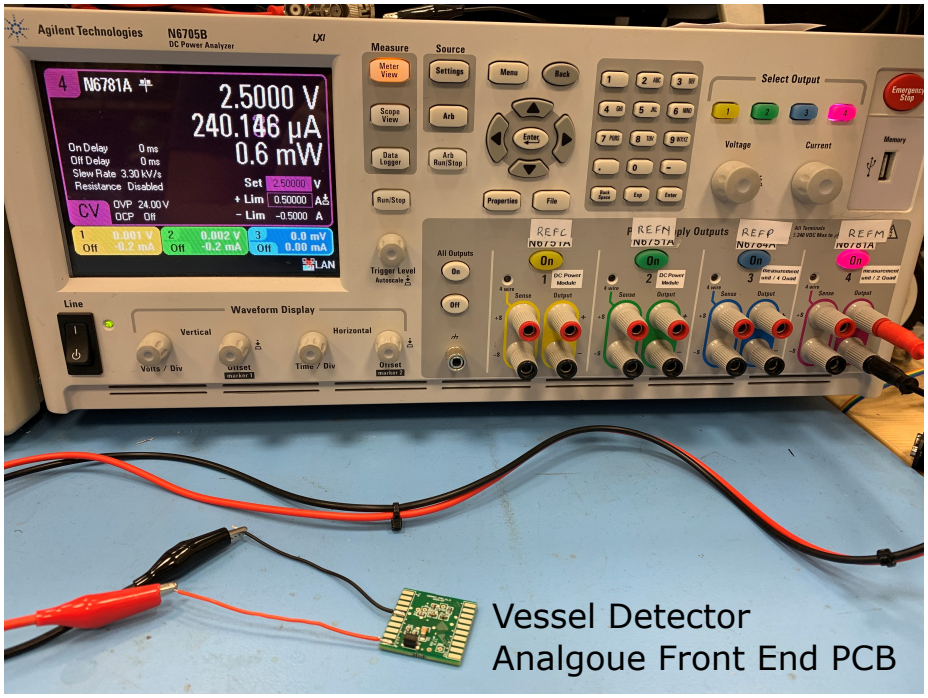

Fig. 5.20 Power consumption of the vessel detectors analogue front end PCB in isolation.

In the digital receive circuit the PCB includes components related to the communication device, which are important to the overall design methodology of providing near real time detection data transfer. The average power consumption for the analogue and digital circuit running the vessel detectors CADD mode is shown in Figure 5.21 at 11.1 mW.

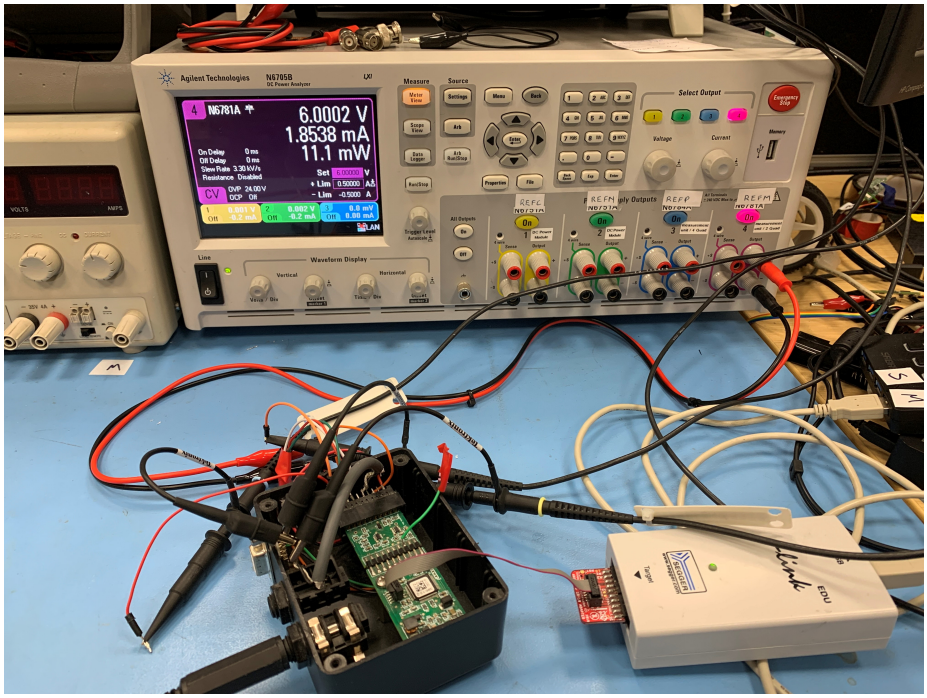

Fig. 5.21 Power consumption of vessel detector hardware running in CADD mode.

To further analyse the inner working of the vessel detector's CADD mode, timings for each stage have been captured in Figure 5.22. This shows the timings related to the acquisition and processing of samples in one of the two 'ping-pong' styles buffers. A 'ping-pong' buffer works on the idea that whilst one buffer of samples is being acquired, the other buffer's samples are being processed. The timings captured in Figure 5.22 show that the actual digital signal processing part of the detection algorithm has been designed to be efficient and is completed in less than 200 ms.

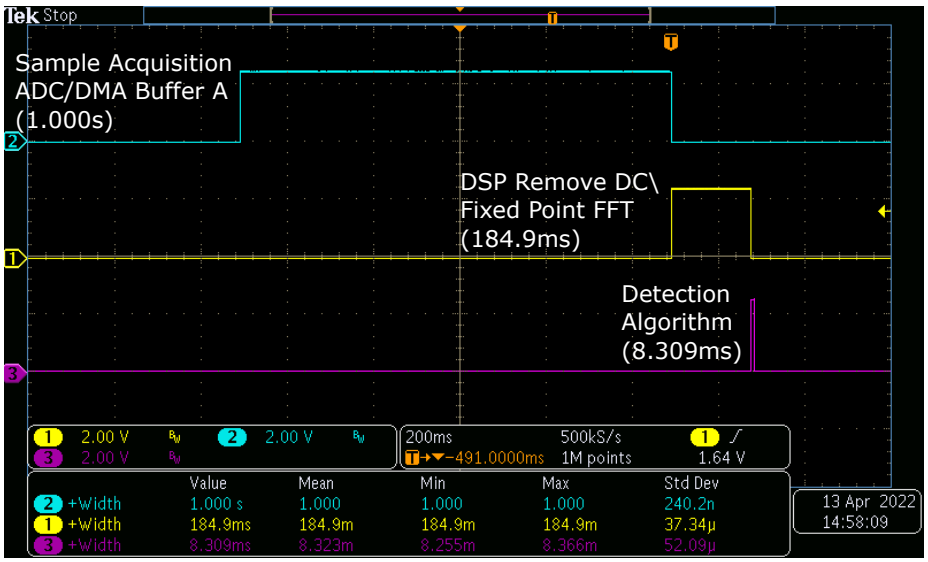

Fig. 5.22 Timing capture of the vessel detectors CADD mode stages for one of the two ADC/DMA buffers.

5.4 Algorithm Field Trial Results

This section contains all of the field trial results related to the development of the vessel detector. This progresses from initial shore based validation results to long duration subsea deployment results. There are results presented in this section which were not an original part of the project plan such as the impact of Covid-19 on North Sea vessel traffic (Section 5.4.6).

5.4.1 River Tyne - Initial System Development

In January to May 2019, the vessel detector was tested on several occasions on the River Tyne in Newcastle Upon Tyne. The purpose of these field trials was to test and validate the detection algorithm once embedded within actual hardware. The MATLAB algorithm previously demonstrated in Section 4.4 has been re-written in C code and embedded within the device's microcontroller using the CADD algorithm described in Section 4.3.1. The field trial location for these initial trials was chosen for two reasons, close proximity to Newcastle University and guaranteed vessel activity. The local Nexus Metro transport system operates a cross river ferry which proved useful for these validation trials. Figure 5.23 illustrates the location where these trials took place and also the route of the passenger ferry.

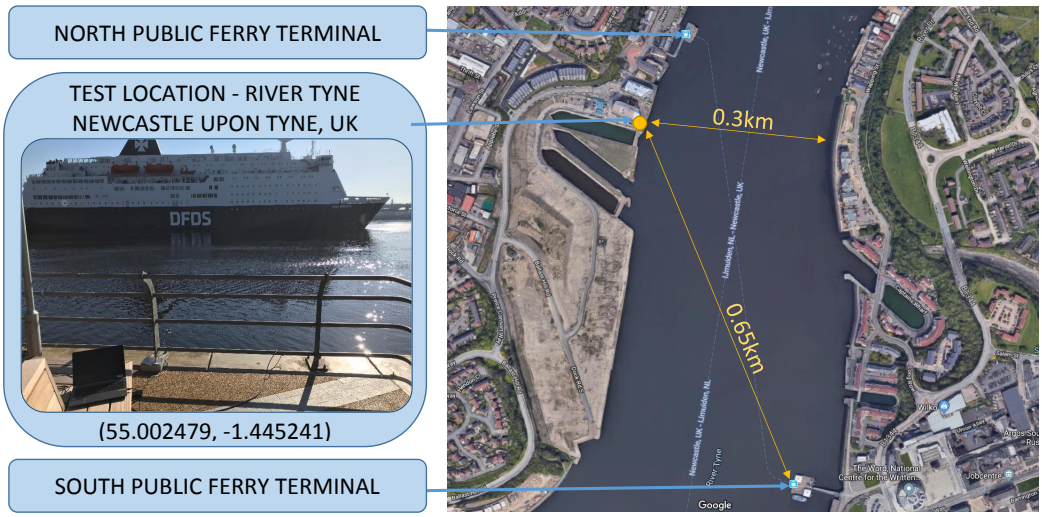

Fig. 5.23 River Tyne Field Trial - Location Map

Figure 5.24 shows the test equipment setup. The setup for this field trial logged the raw audio received by the transducer after amplification, the DEMON spectrum data from the embedded algorithm and any final detection decision made. The detector was setup in its CADD mode for this experiment.

Fig. 5.24 River Tyne Field Trial - System Setup

Using this data it was possible to fine tune the detection algorithm by using the actual spectrum data produced by the fixed-point FFT routine written in software. The system has been tested on several occasions at the location shown in Figure 5.23. To illustrate the results of these field trials, Figure 5.25 shows an example of a positive indication produced

by the detection algorithm. It also shows the vessel which triggered the detection which is the Nexus Passenger Ferry travelling from the North Terminal heading up river to the South Terminal.

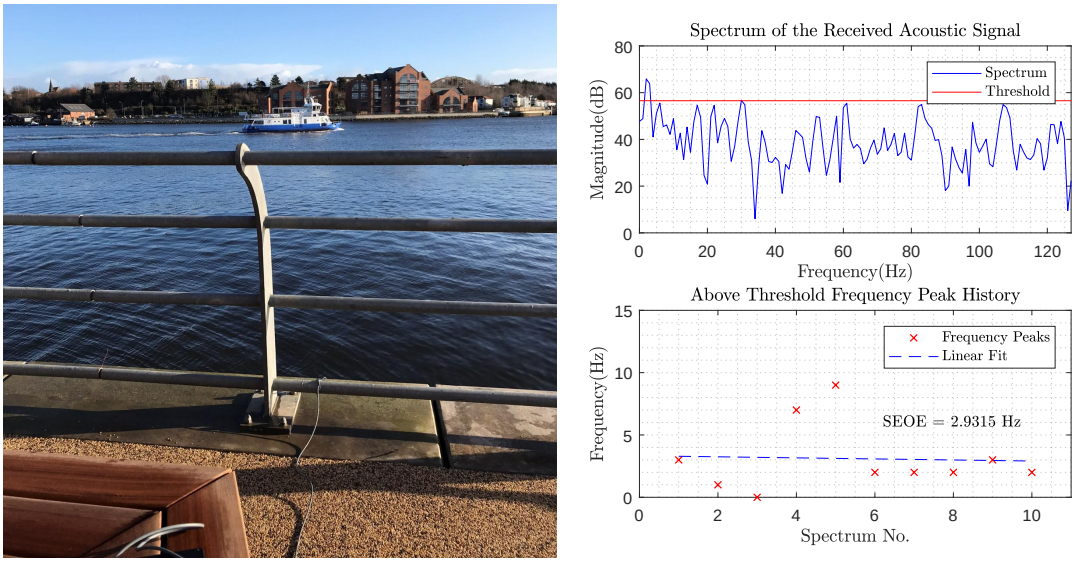

Fig. 5.25 Detection Data Logged During Event

During the vessel's approach, the system is recording any above threshold frequency peaks to establish if a consistent trend in frequency occurs. Figure 5.25 illustrates the last spectrum calculated by the algorithm before a positive detection has been indicated. An above threshold frequency peak has been detected and recorded at 2 Hz. This is reflected in the lower chart which documents historical above threshold frequency peaks ready for further statistical analysis. As indicated in Figure 5.25, a Linear Regression line has been calculated in order to analyse the Standard Error of the Estimate. The SEOE from the linear fit is 2.9315 Hz, which is below the user defined threshold of 5 Hz, therefore a positive detection has occurred.

Once a positive event has been indicated by the detection algorithm, the data must be communicated to achieve a wireless sensor network. This is performed using the NMV3 and is demonstrated in Figure 5.26.

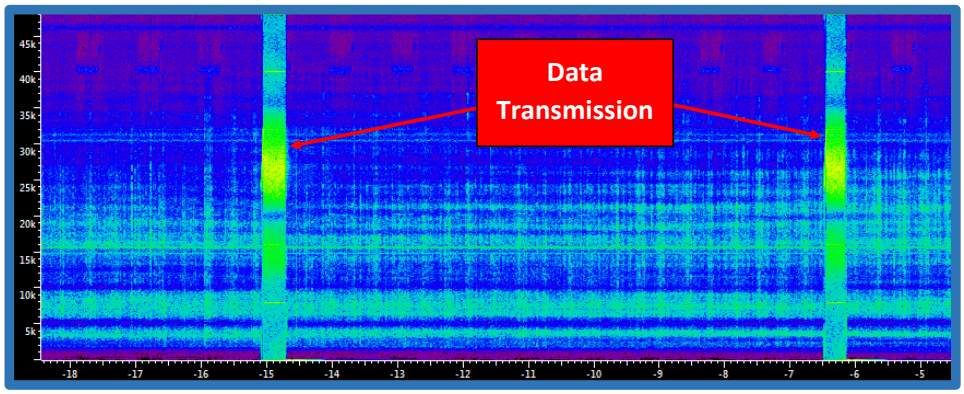

Fig. 5.26 Acoustic Recording of Data Transmission

The spectrogram shown is based on audio recordings taken at the time of deployment. This is another feature added to the system so that the raw acoustic recordings, taken from the same transducer used for detection, can be analysed. As it shows there are two clear short bursts of signal which are related to the acoustic transmission of data from the NMV3. In future field trials, this data would then be received by a second NMV3 stationed at a maximum distance of 3.6 km. During this trial, the data sent is simply a text string to acknowledge that a vessel has been detected. However, in later trials, the data packet contains more useful statistical information and key spectral features based on the detection.

The main aim of this trial was to reproduce a MATLAB based vessel detection algorithm and test whether it could function on a low power microcontroller. As the results show, the system demonstrates the ability to detect a passing vessel and transmit data acoustically. The trial did highlight issues with the sensitivity of the device as other less noisy vessels were missed. This led to a redesign of the analogue amplification stage to increase the gain of the circuit.

5.4.2 Blyth - Rigid-Hulled Inflatable Boat

The vessel detector project is aimed at detecting vessels that potentially don't want to be detected. This may be vessels be used for illegal activities such as drug/human trafficking. The type of vessel used for these activities tends to be cheap and readily available such as a RHIB. To test the vessel detector's ability to detect a RHIB, a trial was carried out using a RHIB owned by Newcastle University. The detector was setup in its CADD mode for this experiment. Figure 5.27 shows the RHIB used during field trials, which is docked at Blyth Marine station. During the trial, the RHIB made several passes at various speeds whilst the vessel detector was deployed from the Marine Station jetty.

Fig. 5.27 RHIB owned by Newcastle University used during vessel detector field trial experiments.

Figure 5.28 shows the associated spectrum captured during recording of the vessel passing. The spectrum shows that the RHIB's cavitation noise contains fairly broadband high frequency components centred around 7 kHz and 26 kHz. (The sharper peaks at 21 kHz and 42 kHz stem from electrical noise within the vessel detector during recording). The next obstacle in the passive acoustic detection of a passing vessel is to make use of the unique high frequency fluctuation that a propeller produces during cavitation.

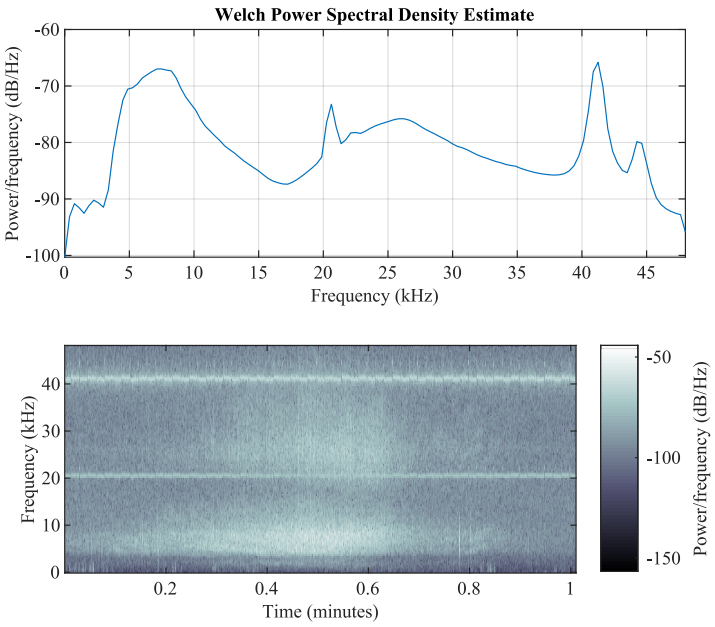

Fig. 5.28 Frequency spectrum and spectrogram of the RHIB recorded using the Vessel Detectors transducer and front end amplifier.

Figure 5.29 shows a positive detection achieved whilst monitoring a RHIB owned by Newcastle University as it travelled past in the Port of Blyth. The two largest peaks in the DEMON spectrum can be found at 19 and 57 Hz.

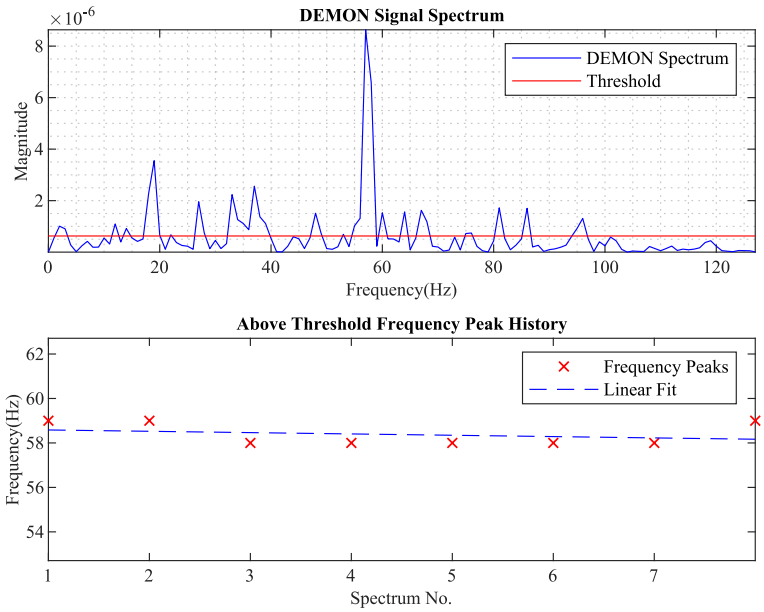

Fig. 5.29 Data produced by the vessel detector whilst monitoring the passing of a RHIB. The plot shows DEMON spectrum data during a positive detection along with historical peak frequency data. The historical peak frequency data has a linear fit applied which if part of the low power detection algorithm.

As introduced in Section 3.2.3.2, the DEMON spectrum peaks are related to the rate of rotation of the propeller shaft and also the blade rate as demonstrated in Equation 3.1. Using the two spectral peaks in Figure 5.29 it is possible to calculate the number of blades on the vessel itself as illustrated below. This information may be useful when it comes to classifying a vessel type.

$$\text{No. Blades}(N) = \frac{\text{Blade Rate}(Fb)}{\text{Shaft Rate}(Fs)} = \frac{57Hz}{19Hz} = 3$$

Using the DEMON peaks in Figure 5.29 the number of blades calculated is shown to be three. This is verified to be a valid calculation by Figure 5.30 which shows there are indeed three blades on the recorded RHIB.

Fig. 5.30 Photo of the detected RHIB showing the number of blades on its propeller.

The aim of this trial was to establish whether the vessel detector could identify its target vessel type. Using the RHIB as a trail vessel, the results show that the vessel was detected successfully. Using the spectral information gained during the field trial, information related to the vessel itself was extracted. As the vessel is known this information was able to be verified by inspecting the number of blades on the RHIB's propeller.

5.4.3 Croatia - Pre-deployment System Validation

The aim of the Croatia trail was to test the vessel detector in a setup which was as close to a full undersea deployment as possible. This was a trial to sign off the design ready for the complete encapsulation and to press ahead with deploying the detector at sea for a long duration. The trial used a version of the vessel detector that was stripped of previous diagnostic features such as real time data acquisition via RS-232. As illustrated in Figure 5.31, the detector was deployed from from a rocky embankment on one end of a bay whilst a standard communication device, connected to a laptop, was monitored on the opposite end of the same bay. This setup mimicked the planned setup at sea with the vessel detector deployed in isolation and a receiving gateway buoy relaying data back to shore. The detector was setup in its CADD mode for this experiment.

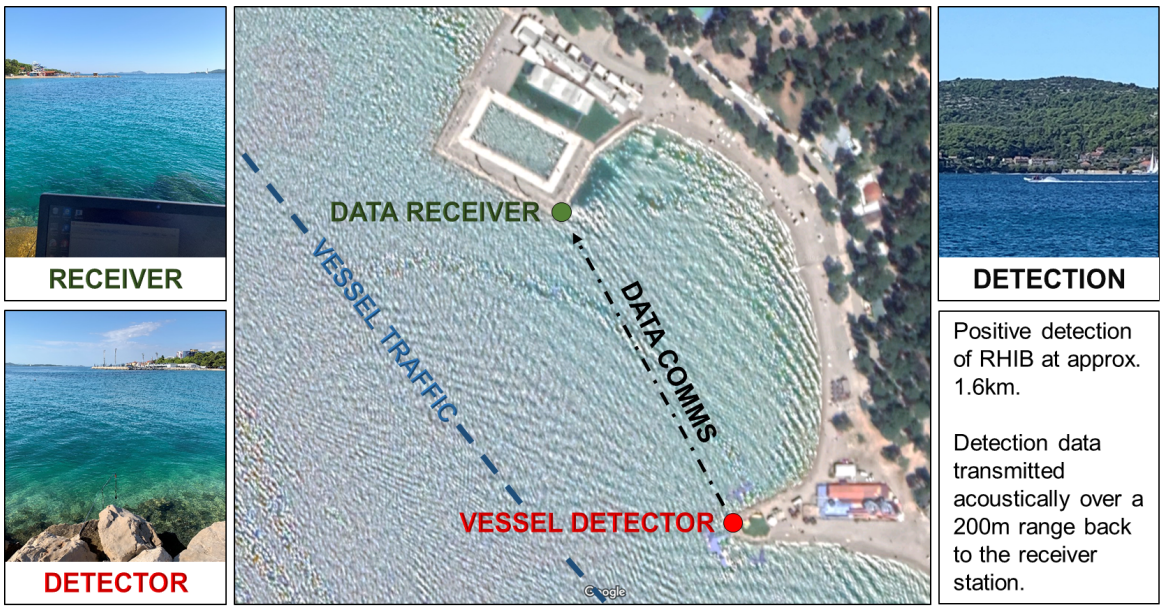

Fig. 5.31 Croatia Field Trial Setup

Using this setup of an isolated detection node and receiver, passing vessel traffic was monitored. As stated in Figure 5.31, a RHIB was detected at an approximate range of 1.6 km. This detection is illustrated by a photo taken at the time of detection as shown in Figure 5.32. The red ring highlights the acoustic transmission being picked up by a hydrophone deployed at the receiver.

Fig. 5.32 Capture of real time vessel detection.

The data travels approximately 200 m from the vessel detector to the receiving acoustic device. The acoustic signal is decoded and displayed in a Termite console window as shown in Figure 5.33.

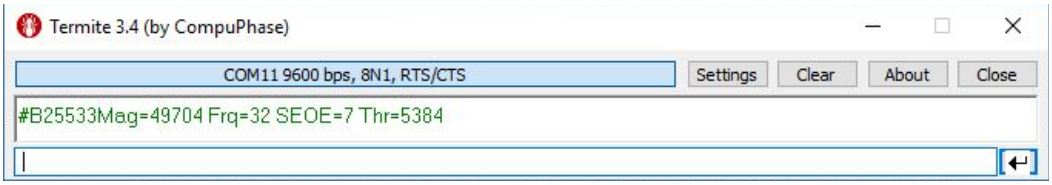

Fig. 5.33 Capture of serial data received from vessel detection during field trials. The serial data includes communication related data such as message type and node address. In addition, detection data is received related to the DEMON spectrum such as SEOE result and magnitude of the peak frequency.

In summary, this field trial provided validation and confidence in the design to press ahead with the more costly long term field trial. The system has shown its ability to operate in a node/gateway configuration with detection data successfully sent through sea water. The system has also managed to detect a key vessel type (RHIB) at a distance of 1.6 km. This shows the system is fit for purpose to satisfy the main aim of the project, which is to detect vessels which may be used for illicit activity such as people/drug trafficking. The next stage of testing will be to put the trial the system over a long period of time in complete isolation.

5.4.4 Blyth - Long Term Open Sea Deployment

5.4.4.1 Introduction

The aim of the Blyth field trial is to test the vessel detector in a realistic offshore environment. Another aim of this trial is to test the reliability of the enclosure, electronics and embedded programming over a long deployment duration. This trial lasted a total of 84 days which provided a large data set with which to analyse performance. Key areas of analysis include the ability of the system to detect vessels and the reliability of these detection results. The trial took place around 3 km off the coast of Blyth as illustrated in Figure 5.34.

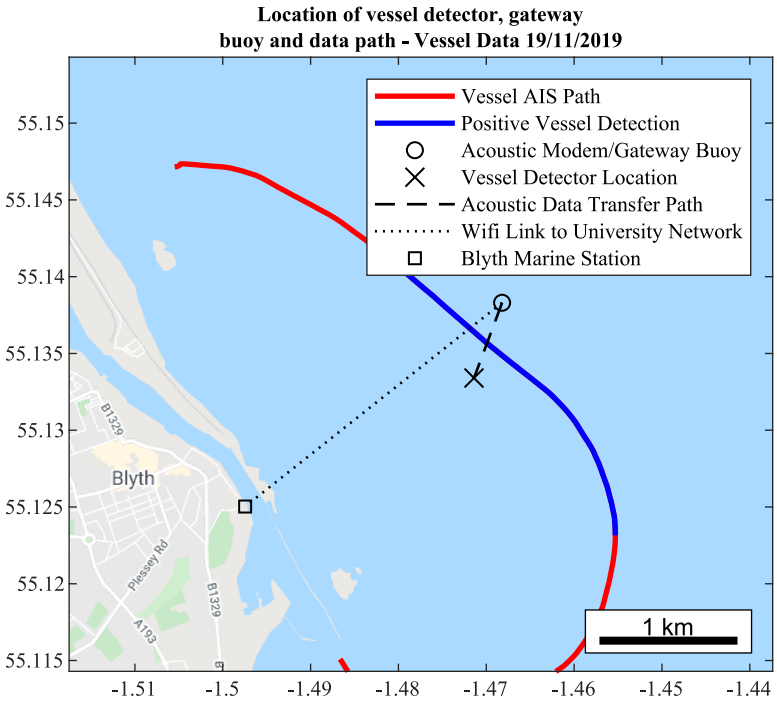

Fig. 5.34 This map shows the location of the vessel detector, gateway buoy and marine station linked to campus. It also gives an example of detection data and local AIS data.

5.4.4.2 Gateway Buoy

A key enabler for the near real time collection of vessel detection data is an off-shore gateway buoy. Designed and commissioned by SEALab, the gateway buoy is complete with a dedicated Wi-Fi link back to the campus network. The gateway buoy is equipped with two hydrophones sampling at 96 kHz which are streamed in near real time back to shore for secure storage on the University network. The buoy also contains two NMV3 devices of the same design as the vessel detectors communication system. This dual-redundancy receiver system allows for reliable collection of vessel detection data over long periods of time. The buoy is powered using external solar panels which charge internal battery packs. Figure 5.35 shows how the gateway buoy is located in relation to the vessel detectors moored deployment.

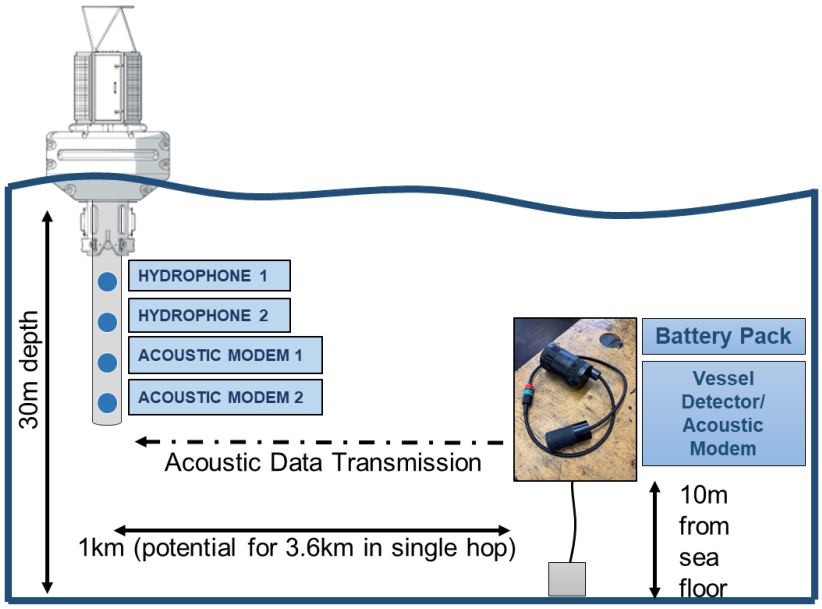

Fig. 5.35 Diagram of the North Sea experimental deployment. The central gateway buoy provides a link back to the University campus network. This affords near real time data from the vessel detector which is located 1 km away from the buoy at a depth of 20m from the surface.

5.4.4.3 AIS Receiver Station

In addition to the gateway buoy, data was collected using a custom Raspberry Pi powered AIS receiver station [91]. The receiver station is positioned on shore near to the Blyth deployment location to collect all vessel traffic data in the area. The Raspberry Pi AIS system was able to receive location data from vessels up to 20 km away from the receiver which more than covered the detection area of interest. Figure 5.36 shows the modified Raspberry Pi alongside the AIS receiving antenna.

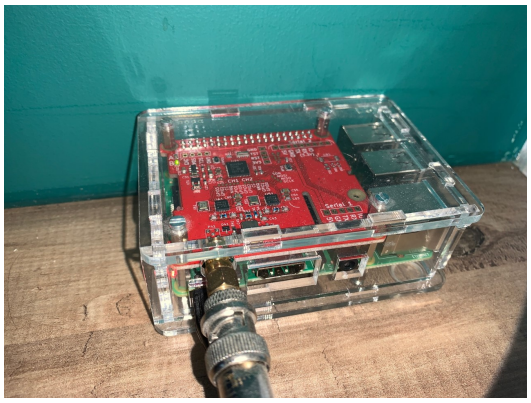

(a) AIS Pi Receiver

(b) AIS Antenna

Fig. 5.36 A photo of the AIS receiver station. Created using a Daisy Hat AIS module attached to a Raspberry Pi alongside an AIS antenna [91].

5.4.4.4 Deployment Duration

The latest deployment of the vessel detector is shown in Figure 5.37. The deployment rig shows the detector and battery pack accompanied by a Soundtrap device used to aid algorithm development in post processing. The Soundtrap is a commercially available underwater recording device capable of sampling data at a rate of up to 576 kHz and storing this data using on board memory [61].

Fig. 5.37 Photo of the vessel detector being deployed in the North Sea. The deployment line contains the vessel detector with battery pack and also a Soundtrap recorder [61].

To maximise the deployment duration, power efficiency of the vessel detector is paramount. Some of the initial power saving methods adopted in the vessel detector's design are documented in previously published research by Lowes et al. [49]. Further refinements have now been made and the vessel detector has been subjected to a long term deployment where power efficiency can be evaluated.

During initial validation field trials there was no restriction on how often the vessel detector could send data when a vessel was detected. One of the modifications made for the long term field trial was to limit this potential continuous stream of data for the same vessel. The main reason being that acoustic transmissions consume significantly higher power (∼1.5 W) than the detection system. To limit unnecessary transmissions, the detector was programmed to only transmit a positive detection every minute unless the peak frequency detected was notably different from the previous detection. The reason for this is that if two vessels pass within the same time period then the detector should ignore the one minute limit restriction and report data. This rule is based on the peak frequencies being different during the time period the two vessels pass. The peak frequency of a vessel's DEMON spectrum is directly related to the rate of rotation of the vessel's propeller and number of blades.

One of the main aims of the vessel detection system is to maintain a low power design approach. The vessel detector operates for the vast majority of time in detection mode as during data transfer the system increases power consumption for only a fraction of a second. Figure 5.38 shows the results from a power consumption test whilst in detection mode. As illustrated the power consumption of the vessel detector is around 11.4mW using a 6V supply.

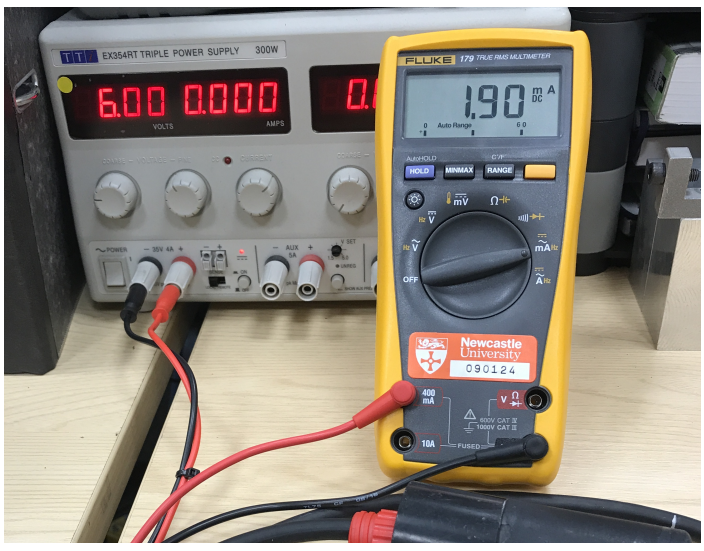

Fig. 5.38 Measured power consumption of vessel detector in CADD detection mode.

Given that the vessel detector is an event-driven system, the total deployment life will depend on the number of data transmissions. Current field trials achieved 84 days of verified functionality. Deployments of less than one month would not provide enough variability in weather conditions and vessel types to effectively evaluate the system. Using the average power consumption while detecting (i.e. 11.4 mW) along with the battery pack power capacity (i.e. 46.8 Wh), an estimated deployment duration of 4–6 months would be reasonable.

5.4.4.5 Retrieval

The vessel detector is deployed twenty metres below the surface in complete isolation. The ability to safely retrieve the device is important both from a cost point of view but also from an environmental aspect. The oceans are already under severe threat from plastics pollution and this project certainly does not want to add to this problem. Two modes of operation have been specifically designed to aid in the retrieval and condition monitoring of the vessel detector when deployed. The first is a 'ping mode' which utilises the integrated NMV3 devices ability to give a point to point range measurement using the acoustic propagation time. This enables a retrieval vessel to triangulate the position of the detector using periodic 'ping mode' range measurements. The second mode is a 'I'm alive' routine which transmits a message acoustically through the water every six hours. This message contains some diagnostics data including the current on-board battery voltage, however, its main function is to periodically check in to confirm the unit is still operational. This is important as the detector is an event driven device so without this mode the detector would only contact the shore if and when a vessel passes its location.

5.4.4.6 Single Vessel Detection

The first result of the long term field trial is validation that the system can detect a single vessel whilst deployed in open water. The vessel detector is setup in CADD mode for this experiment. Figure 5.39 shows a picture of a fishing vessel which was detected during the trial.

Fig. 5.39 Photo of a fishing vessel successfully detected during field trials in the North Sea [33]

To validate the detection, local AIS data is compared with the detection data. The AIS positional data logged for this detection event is illustrated in Figure 5.40.

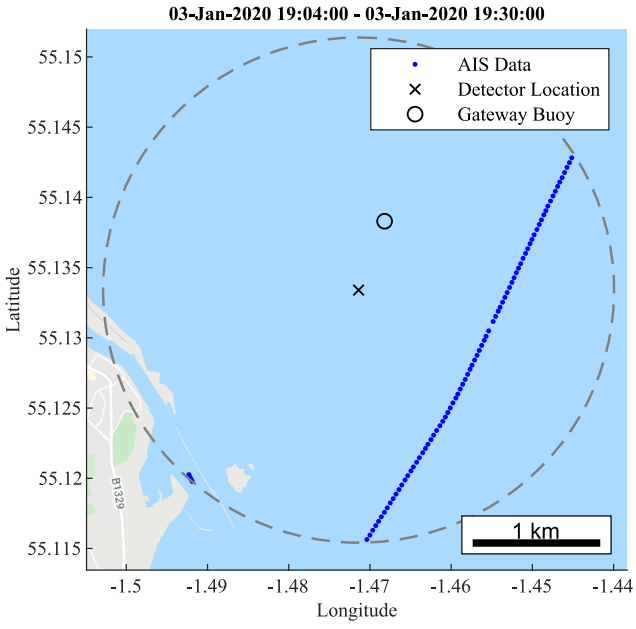

Fig. 5.40 AIS positional data of the detection plotted over a map of the deployment location [41]. The map illustrates the AIS location of the vessel as well as the detector and central gateway buoy. The dashed circle represents a 2 km detection radius around the vessel detectors location.

Figure 5.41 shows a time stamp comparison of vessel detection data and local AIS data to establish any overlap of data points in time. These overlaps represent a true positive detection result as both the vessel detector and local AIS data agree that a vessel was present at that point in time.

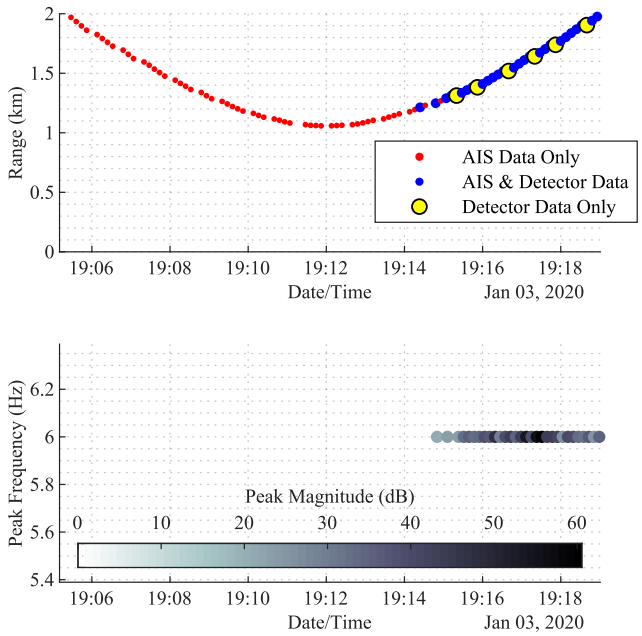

Fig. 5.41 Illustration of a fishing vessel detected by comparing detection time stamps with local AIS data. The first plot shows the DEMON detection data plotted against range provided by the AIS data. The second plot shows the peak frequency and magnitude detected during this period.

Using the AIS positional data in Figure 5.40, a 2km radius is set to filter the AIS data prior to performing a comparison. A 2 km radius has been chosen as this represents a distance where the vessel detector is expected to perform well. Moreover, from a wireless network point of view a 2 km distance between nodes would be well within the communication devices acoustic range capabilities. As the results in Figure 5.41 show, there are occasions where AIS data and detection data do not align in time which is illustrated by the yellow markers. However, it is clear these are true detections as the vessel could not have left the area and returned so quickly.

Figure 5.41 also highlights a detection issue related to the vessels orientation relative to the sensing node. A rear powered vessel will radiate cavitation noise more intensely in the direction away from the rear of the vessel. This is due to the obstruction of the vessel itself in the forward propagation path. This results in vessel detections occurring once the vessel is

orientated so that the propeller faces in the direction of the sensing node. This is illustrated in Figure 5.41 as the vessel is detected after the minimum range is reached at around 1 km. After this point in time the range is increasing which indicates that the vessel is moving away from the sensing node and subsequently positive detections begin to be recorded.

5.4.4.7 Multi-vessel Detection

During field trials there have been numerous occasions where multiple vessels have been present at a similar range within quick succession of each other. An example of this is shown in Figures 5.43 and 5.42. Using the DEMON spectrum detection data provided by the vessel detector in CADD mode, it is possible to make a distinction between these two closely linked events. The peak frequency detected during this time shows two distinctive trends with a note able step change at approximately 03:38.

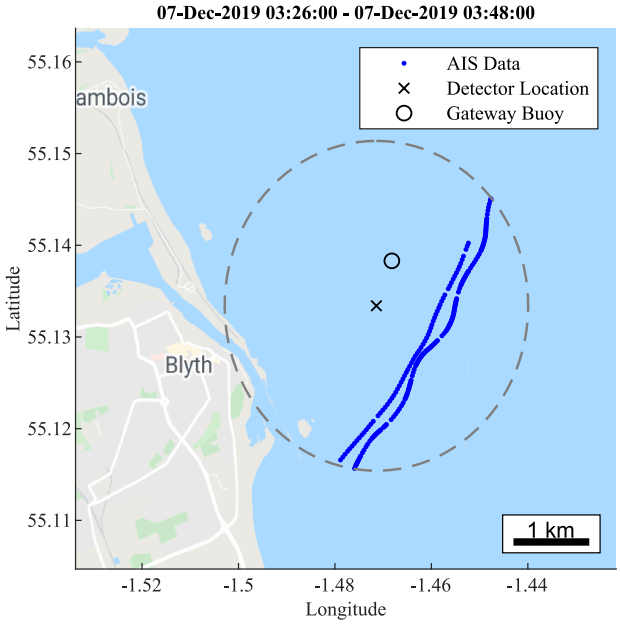

Fig. 5.42 A map of the AIS location data confirms that two vessels were present during the detection time window [41].

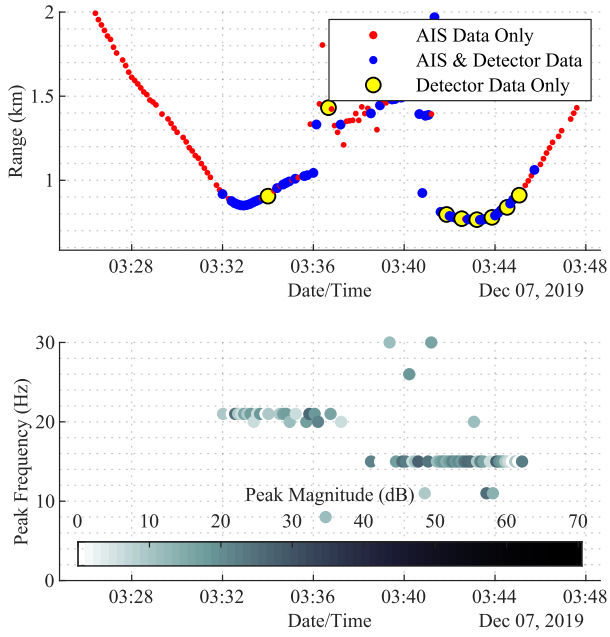

Fig. 5.43 Illustration of two vessels detected within close succession. The first plot shows detection data compared with local AIS data. The second plot shows the DEMON peak frequency and magnitude detected during this period and a clear step change in frequency is observed.

The first peak frequency trend falls around 21 Hz which is then followed by a sudden step change to 15 Hz. This could simply be a change in speed by a sole vessel, however, when the detected magnitude data is also analysed it suggests that two different vessels may be present. When a vessel passes a single monitoring point the magnitude of the cavitation noise would be expected to follow a low-high-low trend over time. This pattern is shown in the magnitude data in Figure 5.43 which is represented by shading, going from light-dark-light over time. As this pattern happens separately for each of the detected frequency pattern this suggest that this is indeed two separate vessels passing the same point of monitoring at a similar distance. This is further validated by AIS positional data which is used in Figure 5.43 to calculate the distance between the vessel detector and surrounding vessels. Relying solely on the data provided by the vessel detector, the results suggest that in its CADD mode, the vessel detector can provide data to distinguish between multiple vessels.

5.4.4.8 Reliability Analysis

The deployment location of the vessel detector, shown in Figure 5.34, is near to the busy Blyth and Tyne estuaries. Within the deployment location, sources of noise stem from both natural and anthropogenic sources. Natural sources of noise include marine life activity and also the changeable North Sea weather conditions. White beaked dolphins and harbour porpoises are regular visitors to the deployment location both of which use high frequency echolocation clicks to navigate. The North Sea weather can be severe and produce significant sources of noise underwater due to strong wind and heavy rain. Sources of anthropogenic noise observed within the deployment area include commercial shipping activity, industrial activity such as offshore wind farm developments, shipping sonar and acoustic marine life deterrent devices. Given the vast sources of noise present in the deployment location, the vessel detector has been designed to isolate only the signal of interest and block out areas of interference. To illustrate the reliability of the vessel detector to isolate the propeller cavitation signal and block out the other sources of noise introduced, detection data is compared with local AIS data. Detection data carries with it a time stamp which can be compared with local AIS data to establish if there are any data matches in time. These matches of detection data and AIS data are considered to be validated true positive detection events.

The first analysis of reliability is related to the severe weather conditions experienced during field trials and how the detector handles these periods of elevated background noise interference. Figure 5.44 shows a 24 hour period where a substantial percentage of the day shows no vessels were detected. During this period the weather conditions were very poor as illustrated by the wave and wind data in Figure 5.44 [20].

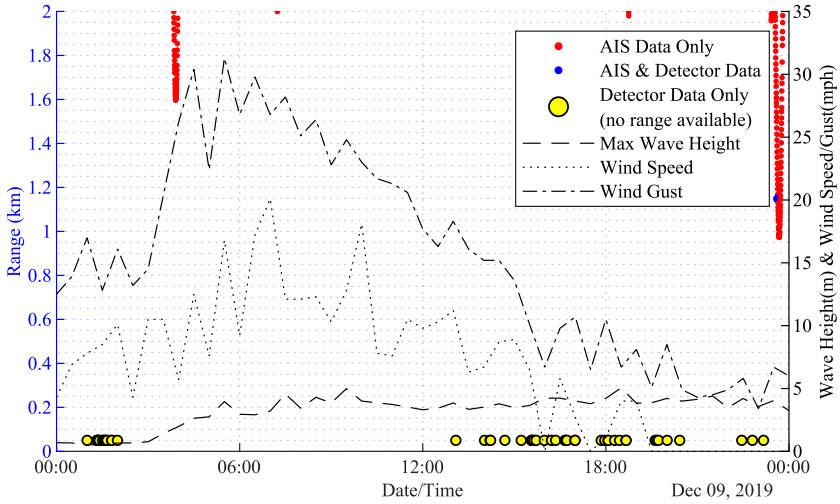

Fig. 5.44 An illustration of the vessel detector operating in adverse weather conditions. The plot shows AIS and detection data plotted alongside meteorological data [20].

During the period between 06:00 and 12:00 the weather was at its most extreme and no detections were produced. This could indicate that during poor periods of weather where interfering noise is likely to be elevated, the vessel detector remains robust against producing false detections due to interfering noise. This is extremely important from a reliability point of view but also from low power perspective as false detections will drain the battery and shorten the deployment duration. Another possibility is that the detection data did not make it back to the gateway buoy, however, using the data sequence identifier in the vessel detector's data payload this has been ruled out. Local AIS data indicates that the results received by the vessel detector during this period of poor weather were accurate as no vessels were reported to be within detection range at the time. However, it must be noted that there is no legal obligation for certain vessels to carry an AIS transmitter therefore an absolute ground truth is very difficult to establish for this field trial.

A second area of analysis, using detection data compared with local AIS data, attempts to quantify the overall reliability of the vessel detector to produce accurate results. Figure 5.45 and 5.46 illustrate the reliability of the vessel detector using 84 days of deployment data. The following list illustrates each of the four possible outcomes when comparing local AIS data (within a 2 km radius of the vessel detector deployment location) against detection results data. As previously stated, there is no legal obligation for all vessel types to carry or use an AIS transmitter. However, for this field trial the AIS data will be used as the best ground truth available and vessel detection data will be compared against the local AIS data.

- True Positive [TP] - Vessel detector data matches with local AIS data (within 2km radius of detector) during the same one minute interval.
- False Positive [FP] - Only vessel detector data present within a one minute interval.
- False Negative [FN] - AIS data detected within a 2 km radius of the detector but no vessel detector data received within the same one minute interval.
- True Negative [TN] - No AIS data or vessel detector received during a one minute interval within the 2km detection radius.

Results are obtained by examining each one-minute interval of the entire 84-day data set. In each of these one-minute intervals, there are four possible outcomes. Figure 5.45 shows each of the outcomes as a percentage for the entire 84 days of data collected. The true negative category implies that no vessels are within the detection area and as expected this commands the majority of the 2,016 hours of monitoring with 94%. This is an incredibly important result, especially from a low power perspective, as it shows that for the majority of time the detector is monitoring but not transmitting data when it is not necessary to do so. The next most frequent outcome is false positive with 5% which covers detections which don't have corroborating AIS data within the same one minute interval. This could be due to a vessel not having an AIS transmitter or it may be that the detection corresponds to a vessel outside of the current 2 km detection radius. The next outcome is a false negative which is when there is AIS data within the detection radius but the vessel detector has not detected anything at the time. This makes up only 1% of the monitoring time during the experiment and could be due to many reasons including distance, signal strength, vessel orientation, sea conditions, vessel type (i.e. sail boat), vessel engine status (i.e. could be idle). A vessels orientation relative to the sensing node has already been illustrated as a detection issue by field trial results presented in Section 5.4.4.6. Another potential reason for the false negative result is that the vessel detection algorithm may require further threshold refinements. However, given that this result constitutes only 1% of 84 days of monitoring it is an encouraging initial deployment result and shows the high detection rate of vessels within 2 km. The final outcome is true positive which represents the times when both the vessel detector and local AIS data agree that a vessel is present within the 2 km detection area.

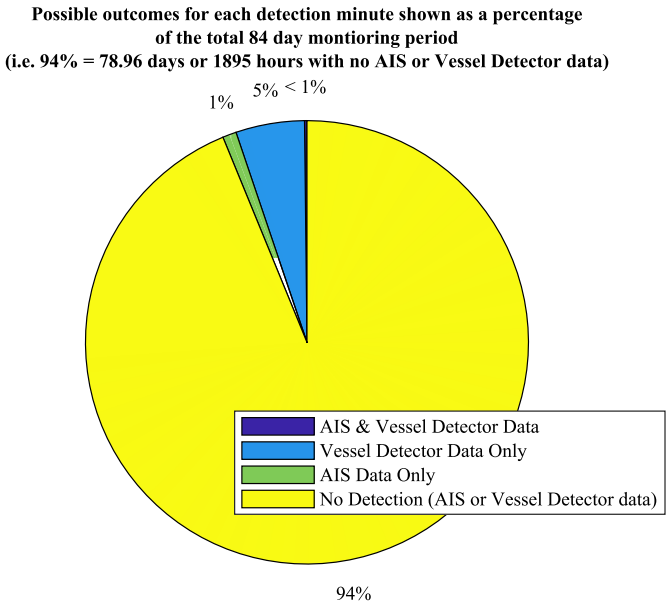

Fig. 5.45 Detection results gathered from 84 days of deployment. The results are based on comparing local AIS data with the vessel detector data within a detection radius of 2 km. The chart shows the percentage for each of the four possible outcomes for the 84 day data set.

Using the data for the four possible outcomes, Figure 5.46 shows the percentage of results that were corroborated by local AIS data. This shows that 94% of the results produced were verified using the best available ground truth.

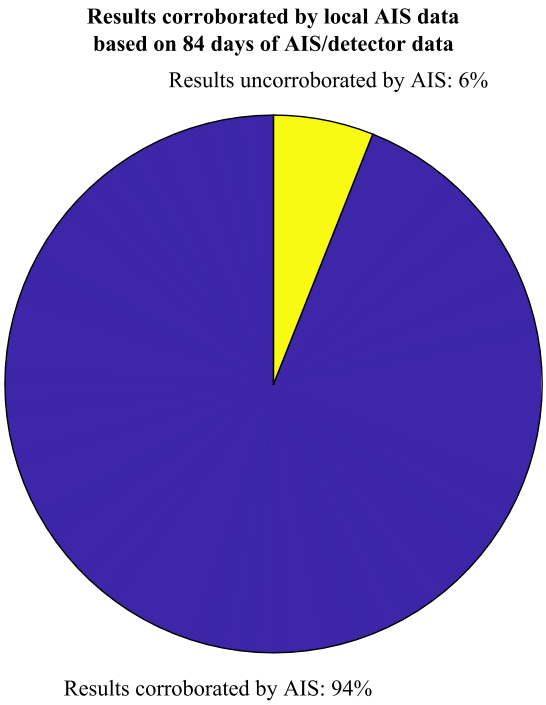

Fig. 5.46 Percentage of results that were corroborated by local AIS data.

As the results in Figure 5.45 show, there are many detections where no AIS data was present during the same one minute time interval. These results have so far been classified as false positives for the purposes of analysing reliability in the absence of a true ground truth. We know that this classification is not completely true as there is no legal requirement for certain vessels to carry AIS transmitters, therefore, a vessel may be present which has no AIS system on board. Many small vessels in the local fishing fleet or leisure users do not carry AIS. The only way that a 100% accurate ground truth could be obtained is by 24hr visual survey which is not practical. Figure 5.47 illustrates the detection data where no AIS was present for various times of day. The plot is created using the total number of non AIS detections for half hour intervals using the entire 84 days of data.

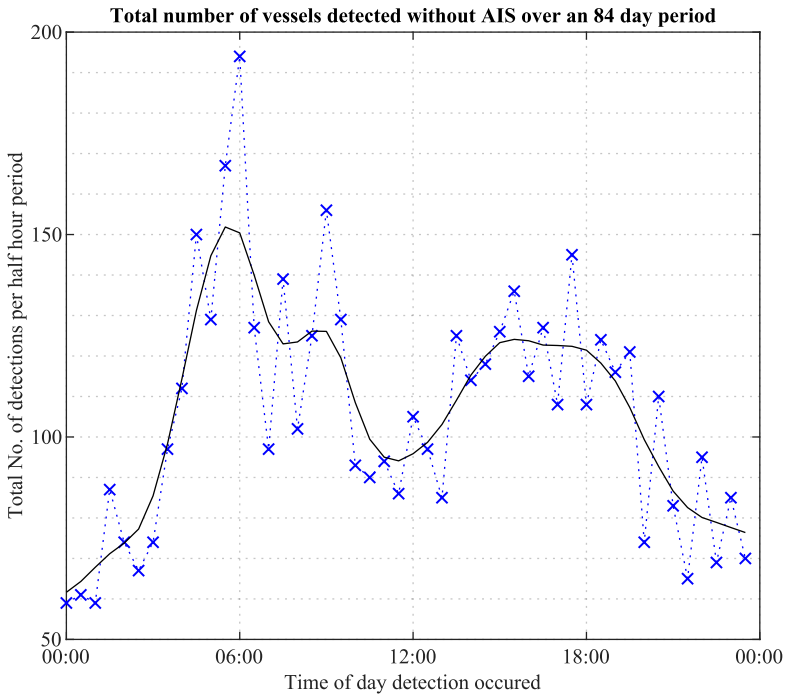

Fig. 5.47 The total number of vessels detected with no corresponding AIS over a 24 h period using 84 days' worth of data.

The trend of Figure 5.47 contains two dominating peaks, one at early morning (06:00) and the other at late evening (17:30). This may correspond with fishing traffic leaving Blyth Port at first light and then returning on an evening before sunset. The data also suggests a higher than expected average of around 100 total detections per half hour period using the entire 84 days of data. Without AIS data it is difficult to say whether this average is accurate or whether there are some false detections within the non AIS detection data.

Reliability is not limited to the detection algorithm itself. The enclosure must operate reliably at a depth of twenty metres (approximately two atmospheres of pressure) in highly changeable North Sea conditions. Moreover, this project is committed to developing a low cost enclosure system which can be made in bulk to form part of an underwater wireless network. The enclosure design previously shown in Figure 5.19 has successfully been deployed at a depth of 20 m on two separate deployments for around six months in total without any failures.

To summarise, the reliability results presented are based on a long term deployment of the vessel detector in harsh North Sea conditions. The detector has been shown to operate in CADD mode during periods of intense weather. It shows that the algorithm is unlikely to produce false detections due to weather related noise. Detection accuracy is an important

factor as any end user wants to have confidence in the detection data produced. In this trial 94% of results were able to be corroborated with the best available ground truth which is local AIS data. As the detector was deployed for a long period of time at depth the enclosure design and integrity was a major consideration. The results show this design and during the field trial the unit did not have any failures.

This field trial has been designed to test the vessel detector in a setup which is representative of its commercial potential. This has involved encapsulating the electronics in a self contained unit and mooring at depth around a busy port. The trial duration has enabled results to be produced to address many of the key project aims. The system has shown the ability to detect a single vessel whilst operating in busy, and noisy, acoustic environment. The data included in the detector's payload has been shown to enable separation of multiple vessels using frequency data. The trial has also provided an indication of the reliability of the vessel detector to detect and operate in a harsh environment for long periods of time. One of the key findings of this trial is shown in the battery voltage which has been monitored over the duration of the trial. A low power device is essential for long term subsea work as there is no external power supply. The results show the ability of the vessel detector to operate for several months before a change of batteries would be needed.

5.4.5 Non-Continuous Digital Detection (NCDD) Analysis

Unfortunately, Covid-19 has had an impact on this project's timeline and ability to carry out all of the intended field trials. The vessel detector's NCDD mode was planned to be deployed in open sea similar to that of the CADD mode. However, initial laboratory based tests have been carried out to explore the NCDD power consumption and sensitivity when compared with the CADD mode. Figure 5.48 shows that both CADD and NCDD modes have been designed to have a matched average level of power consumption.

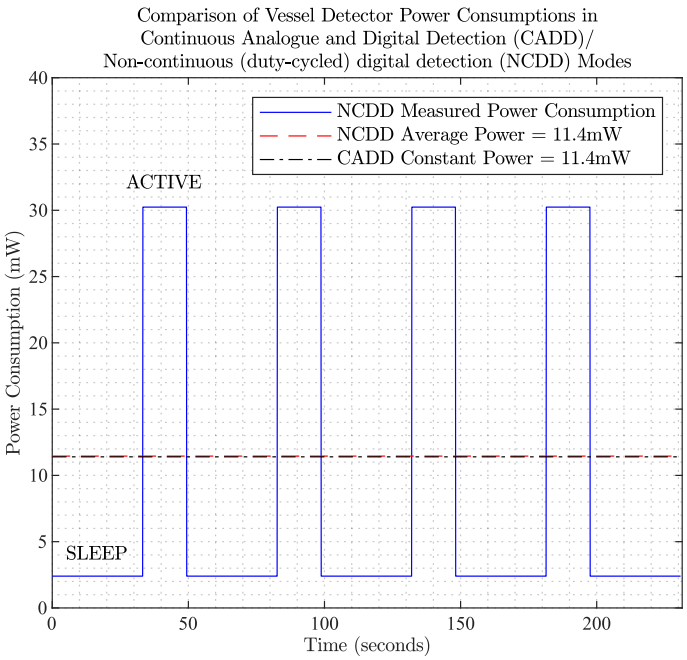

Fig. 5.48 Power consumption comparison between the vessel detectors CADD and NCDD modes.

The reason for this is to explore whether a fully digital duty-cycled approach would perform better or worse than a continuous analogue/digital approach with the same power budget. Although open sea trials have not taken place to fully evaluate this question, Figure 5.49 shows a sensitivity experiment designed to give an indication.

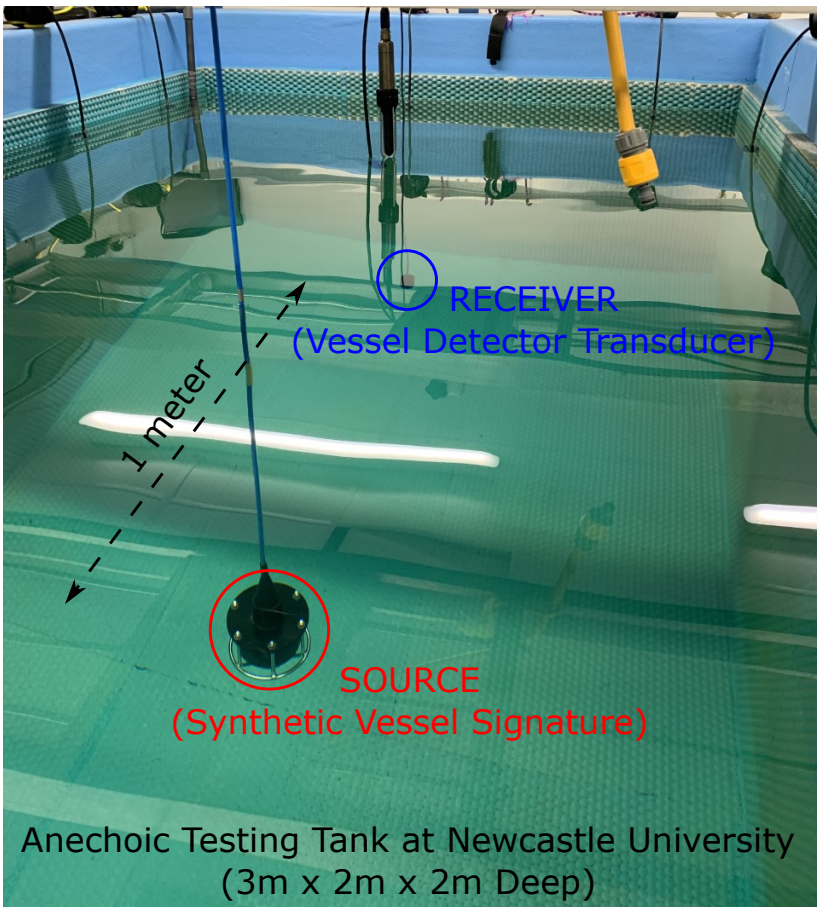

Fig. 5.49 Experimental setup to evaluate the sensitivity difference between the vessel detectors CADD and NCDD modes.

The experiment uses a synthetic vessel signal as the source to trigger the vessel detector at the receiver. The source signal used was a 32 kHz sine wave with 20 Hz sinusoidal amplitude modulation at 100% depth. The source signal remains constant in all aspects aside from the amplitude which is reduced incrementally. Using this gradually attenuated signal, it is possible to measure the point at which the vessel detector fails to detect the synthetic vessel signal. This has been carried out using both NCDD and CADD modes.

As expected, the fully digital version showed a superior minimum detection level of -21.9 dB with the CADD mode at -16.5 dB. This implies that the NCDD mode could achieve a greater detection radius out in open sea for the same power budget. The question still remains what impact a duty cycled approach will have on the accuracy of detection results and this forms part of the future work of this project.

As part of the future work for this project, the NCDD mode should be evaluated on an energy efficiency versus quality of service trade off. This would enable the minimum energy consumption for maximum level of detection service to be calculated. Depending on

the nature of the deployment it may be suitable to prioritise quality of service over energy efficiency and vice-versa.

5.4.6 Impact of Covid-19 on North Sea Vessel Traffic

An interesting result which has emerged from the vessel detector's open sea deployment is the impact of Covid-19 on vessel activity in the North Sea. In March 2020, the UK was placed in lockdown to mitigate the spread of the virus and during this time the detector was still active and communicating data. The results from this time showed there appears to be an abrupt change in the data trend. Figure 5.50 shows that once the lockdown was put in place there was very little vessel activity detected in contrast to the days and weeks prior. This reduction in activity was observed within the detection data for a duration of around two weeks. This detection data has been corroborated with vessel activity observed by the Northumberland Inshore Fisheries and Conservation Authority (NIFCA). The Environmental Inshore Fisheries and Conservation Officer at NIFCA explained the data that the vessel detector was producing around the lockdown period. The reason for the sharp reduction in activity was due to local fisheries markets closing in response to the Covid-19 lockdown. The resurgence of activity after around a two week period of lockdown was due to wholesalers beginning to buy shellfish again from fishermen 4 days per week [32]. This validation by local authorities gives great confidence in the vessel detector's ability to reflect the number of vessels in the area and ultimately its ability to reliably detect vessels.

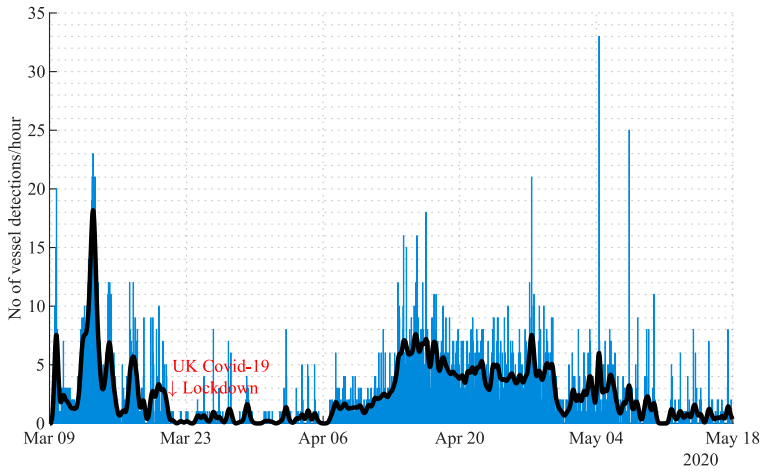

Fig. 5.50 Vessel detection data used to illustrate the impact of Covid-19 on local vessel activity in the Blyth area. The data shows the number of vessels detected per hour over a period of 5 months.

The lockdown presented an otherwise impossible opportunity to operate the detector in open sea with near zero vessel traffic and verify very low false alarm rate under these conditions. This is illustrated in Figure 5.51 which shows the daily false positive rate during the lockdown period. The results assume that there are no fishing/recreational vessels out at sea and that any other industrial vessel would be big enough to require an AIS system in operation.

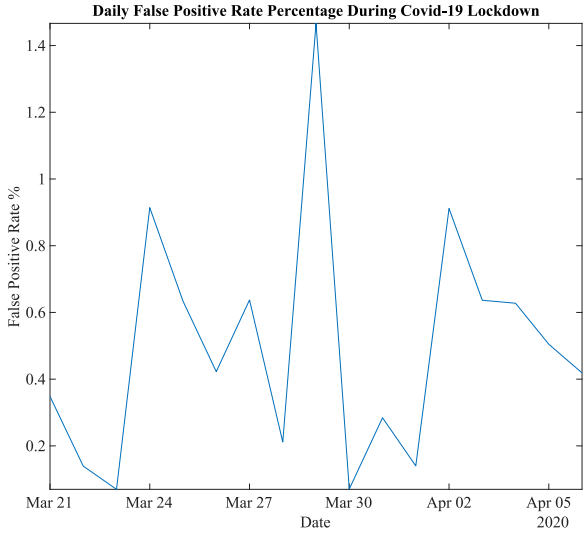

Fig. 5.51 Daily false positive rate during UK Covid-19 lockdown (21/03/2020 to 06/04/2020).

During March 2020, a sister project from SEALab, named NanoPAM, was operating in two locations near to the vessel detector deployment, as shown in Figure 5.52.

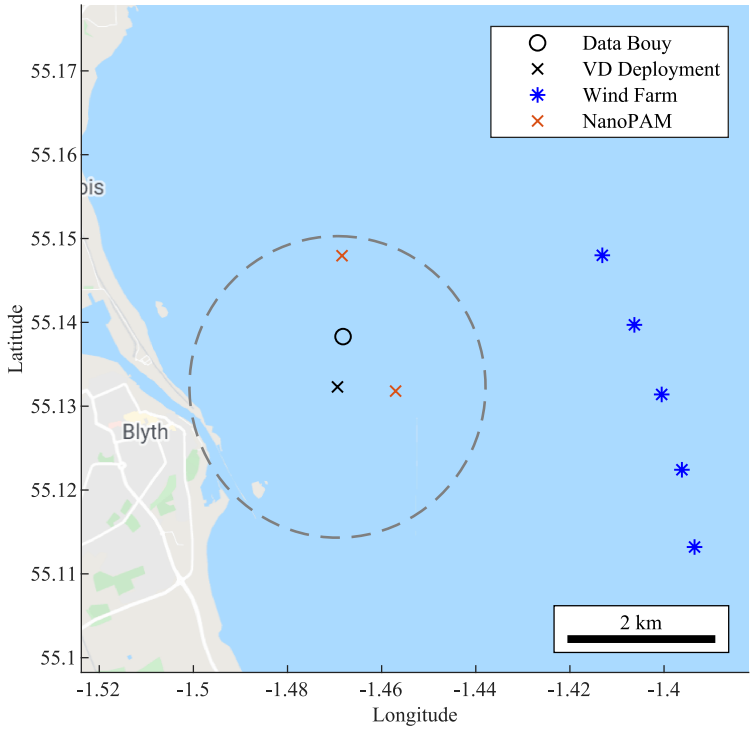

Fig. 5.52 Newcastle University SEALab field trial asset locations alongside the North Sea wind-farm for reference. A 2km radius is provided around the vessel detector's deployment location.

At these locations, two underwater audio recorders were active sampling at 576 kHz. Using this data, the hourly average magnitude of noise in the band 1 to 20 kHz can be calculated. Figure 5.53 shows the mean noise level of each recorder location, alongside the vessel detection data for the same period.

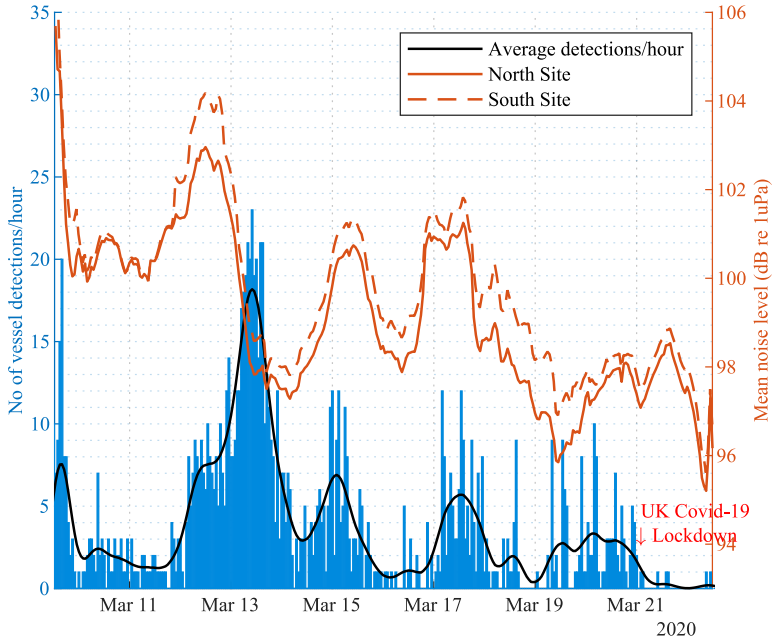

Fig. 5.53 Mean noise levels present during a period of vessel monitoring.

In Figure 5.53, there is a strong correlation between the North and South monitoring sites mean noise level. As these sites are approximately 2 km apart, the data suggests that a single source is dominant in influencing the mean noise level. The most obvious assumption would be the weather conditions as this would likely be consistent over a 2 km area. Comparing the mean noise level with the vessel detection data, there is no consistent correlation between mean noise level and vessels detected. This suggests that noise level alone is not a reliable indicator for vessel activity and the value of the DEMON based detection device is well demonstrated.

5.4.7 Cetacean Click Rejection/Detection

During field trials in the North Sea there have been many cetacean encounters recorded by our gateway buoy. These encounters have been verified by a sister project within the SEALab which attempts to detect cetacean activity based on high-frequency click trains [57]. An interesting outcome of this data verification is that on occasions there is a possibility that the vessel detector may have been fooled by slow cetacean click trains. High energy short duration clicks can still produce an amplitude modulation on the analogue envelope detector output which in turn appears on the DEMON spectrum. It is difficult to say for certain that these slow click trains are producing false positive results as audio recordings are taken 1 km

from the vessel detector's location. Vessels are in the area during the encounter but they are around 13 km south of the vessel detector. Given that there is a possibility of a false positive cause by cetacean activity, there is opportunity to process the recordings offline and attempt to reject these encounters using the vessel detection algorithm.

To develop methods of successfully rejecting slow cetacean clicks, data has been analysed to identify notable features. The first notable feature to distinguish between cetaceans and vessels is the inconsistency in the detected peak frequency. Figure 5.54 shows a period of detection data which is suspected to have been caused by slow cetacean clicks. The data shows that some true positive events are present during the time period, however, the recorded range (i.e. distance between detector and vessel) is quite large at around 13 km. This would suggest that the AIS located vessel is not the source of noise causing a positive detection. It may be that a vessel is closer to the detector without an AIS transmitter on board or that the slow cetacean clicks are indeed causing a problem.

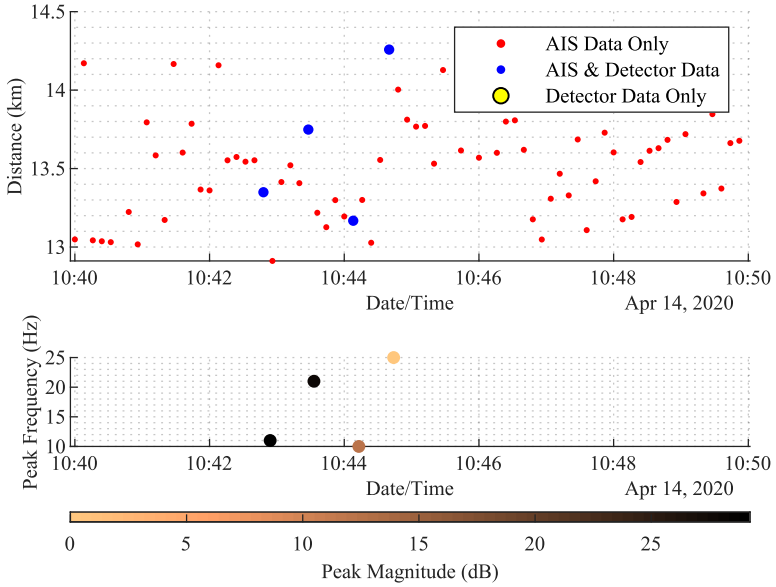

Fig. 5.54 Illustration of a potential false alarm created by nearby cetacean calls. The plot shows detection data along with local AIS data. Note the uncorrelated peak frequency data and high peak magnitude data detected during the event.

Alongside the detection and AIS data there is an audio recording taken from the gateway buoy which is situated approximately 1km north of the vessel detector's location. On this recording there are clearly cetaceans present and they are producing high frequency click trains. Figure 5.55 shows a recording taken by the data buoy of the eight seconds leading up to the potential false positive detection. The plot shows the time domain audio recording

along with a time/frequency spectrogram of the data. Note the high magnitude vertical lines in the spectrogram plot which corresponds to high frequency cetacean clicks.

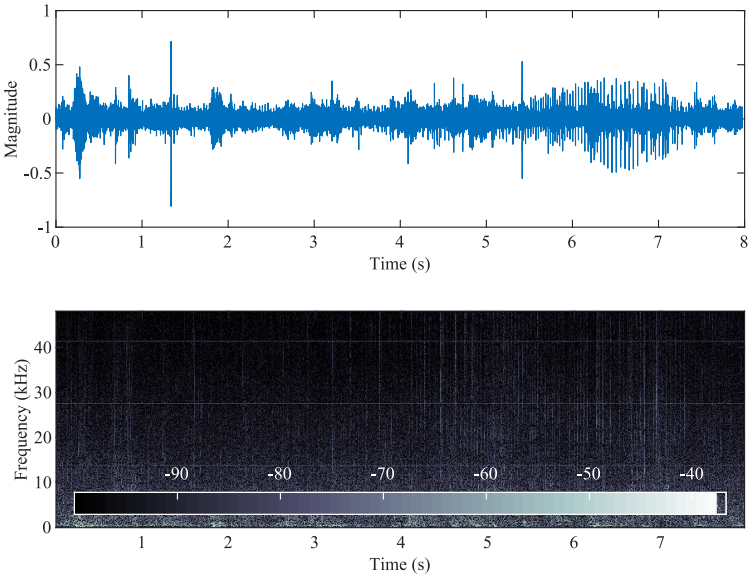

Fig. 5.55 Plot of an audio recording captured by the hydrophones on the gateway buoy during a time of cetacean activity. The plot shows the time domain signal along with a second plot illustrating the spectral content of the captured recording. Note the high intensity (white) vertical lines which correspond to cetacean high frequency clicks.

The reason for analysing eight seconds of audio before a detection is because the detection algorithm searches for eight consecutive DEMON peaks aligned in frequency. If this recording was a vessel, each of these eight one-second periods would tend to show a consistent peak frequency trend over time. This frequency trend can be extrapolated over a longer time duration for a vessel as they tend to be continuously acoustically active for much longer than a cetacean. Dolphins and porpoises rapidly and erratically vary there ICI in response to their environment or prey they are tracking and this would appear on the DEMON spectrum. Such behaviour would be unusual for a vessel propeller (rapid/erratic throttle variations). One method of cetacean rejection may be taking into account historical peak frequency detection results for a suitable period of time. In Chapter 6, a method of detecting cetacean clicks is presented which could equally serve as a method of rejecting false detections within the vessel detection system.

5.4.8 Validation Field Trial - North Sea, December 2020

In this final case study, a field trial was designed with the aim of validating the performance of the vessel detector as close to ground truth as possible. The trial utilised local AIS

data alongside an underwater acoustic recorder situated on the same mooring as the vessel detector. The aim was to capture the raw acoustic signal as received by the vessel detector itself. The recorder also captured acoustic data transmissions and the corresponding acoustic acknowledgement messages from the gateway. This field trial was short in duration due to limited recording capacity and battery life of the Soundtrap acoustic recorder. The setup of the field trial is illustrated in Figure 5.56.

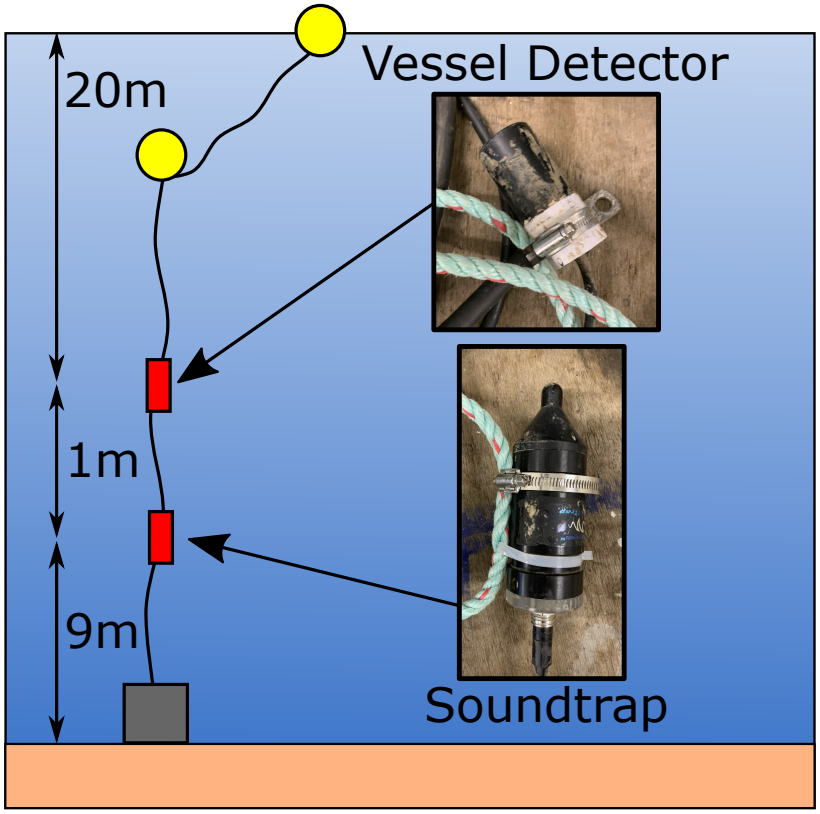

Fig. 5.56 Field trial illustration showing the mooring and equipment deployed.

The trial lasted 12 days in total and during this time there were 697 positive acoustic propeller cavitation events detected. A summary of the detection activity for the trial is shown in Figure 5.57.

To illustrate the ability of the system to reliably detect vessel activity when deployed at sea, one of the many detection events has been chosen to show data from all of the available monitoring equipment. The time period presented is on the 7th December 2020 between 16:23 and 16:48. The first data set to consider is shown in Figure 5.58 which is local AIS data showing vessel activity in the area.

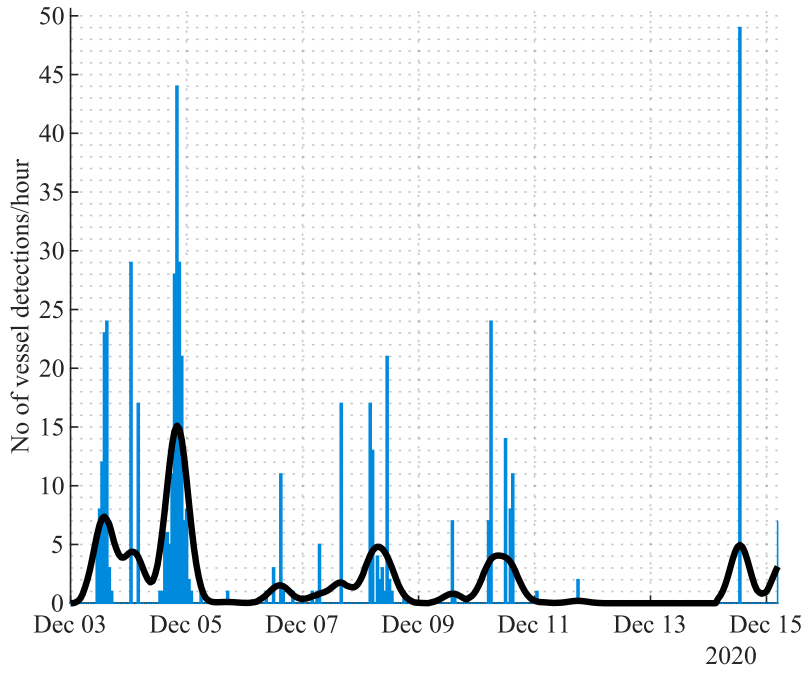

Fig. 5.57 This plot shows the number of vessel detection's per hour for each day of the field trial.

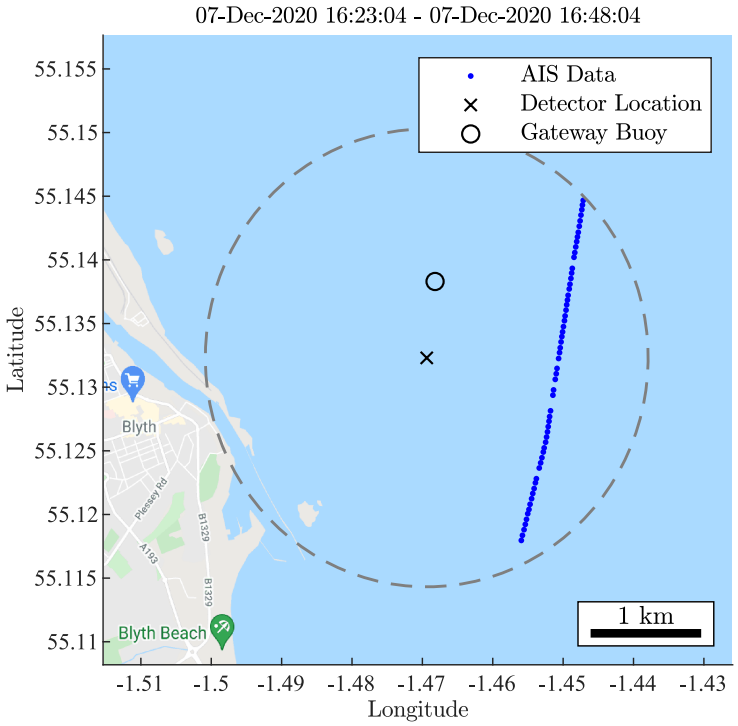

Fig. 5.58 Map of the vessel activity in the North Sea off the coast of Blyth for the given time period.

AIS data also provides information about the vessel itself using the MMSI number. Based on the MMSI number, a picture of the vessel detected is shown in Figure 5.59.

Fig. 5.59 Picture of the vessel detected during the time period of 16:23 and 16:48 on the 7th December 2020 based on the MMSI number provided by AIS data.

The next data set, shown in Figure 5.60, is a combination of the local AIS data and the vessel detection data received back at shore via the gateway buoy. The upper plot shows when both AIS data and vessel detection data is present during the same time period, currently set at eight second intervals. The upper plot also shows the distance of the vessel based on AIS data. The lower plot in Figure 5.60 shows the detected peak frequency as a result of the DEMON algorithm. There is a general trend of 16 Hz and 32 Hz which given their values is likely to be the fundamental and harmonic frequencies. The change in peak magnitude intensity as shown by the colour change from light-dark-light is representative of a boat approaching and then leaving the detector's area.

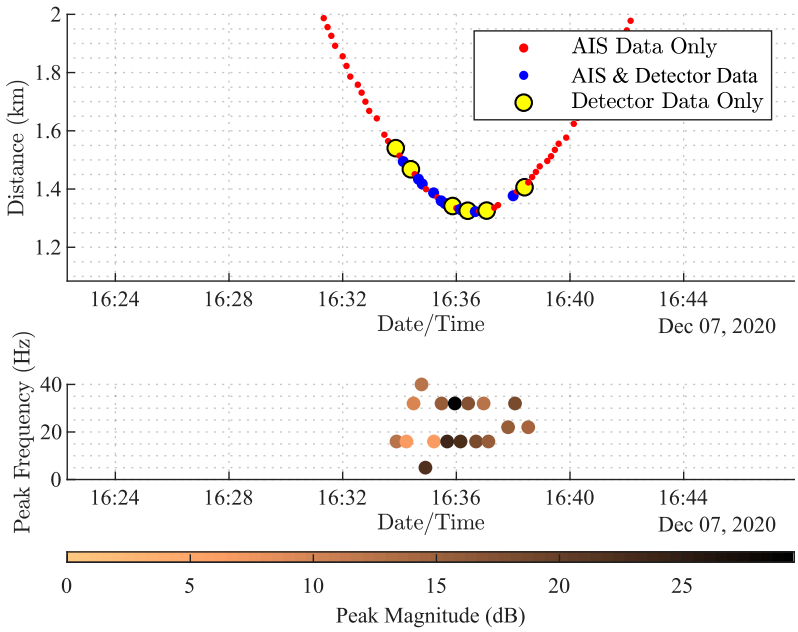

Fig. 5.60 Vessel detection and AIS data for the given time period. The upper plot compares the time stamp data of both the vessel detector and local AIS data. The lower plot shows peak magnitude/frequency data provided by the vessel detector as a result of the DEMON algorithm.

The final data source is the raw audio recorded by the Soundtrap device as shown in the field trial diagram in Figure 5.56. The device was set to record continuously for the duration of the trial at a sample rate of 96 kHz to capture propeller cavitation noise. Figure 5.61 shows a section of audio recorded during the field trial from the same time period as previous data sets. The plot shows both the time domain data as well as the frequency content of the recording. Looking at each plot, the acoustic data transmissions resulting from a positive detection are very apparent. These are the short duration, high magnitude events towards the middle of each plot. The propeller cavitation emitted from the vessel is also visible in the spectrogram by looking for the faint sunburst-like pattern.

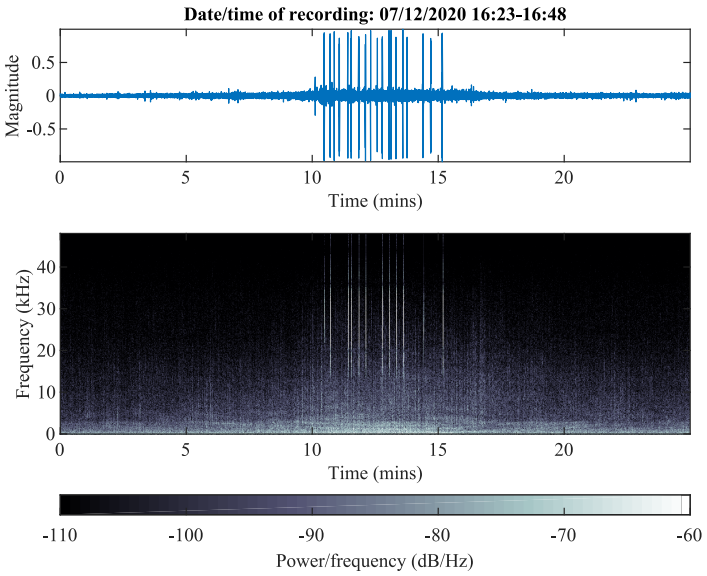

Fig. 5.61 Time/Frequency plot of an audio recording taken during field trials on the 8th December 2020 between 05:22 and 05:37.

This pattern is further illustrated by expanding the spectrogram to look at a lower frequency band as shown in Figure 5.62.

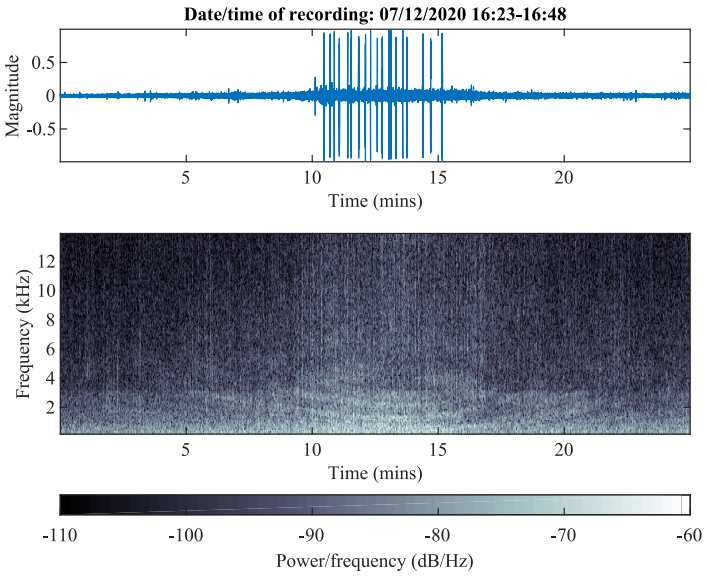

Fig. 5.62 Expanded view of Figure 5.61 to show the sunburst pattern of a vessels propeller cavitation emission.

An additional method of validating the data produced by the vessel detector is to process the same period of raw audio through a Matlab based version of the detection algorithm. The Matlab version of the detection algorithm benefits from a greater degree of FFT resolution as opposed to the fixed point FFT on the vessel detector. Matlab also processes data using floating point arithmetic, therefore a high degree of accuracy is retained during calculation. Figure 5.63 shows a comparison of the Matlab based algorithm and the original vessel detector data produced in the field. As shown, there is alignment for the detected peak frequencies of the vessel at 16 Hz and 32 Hz with few outliers.

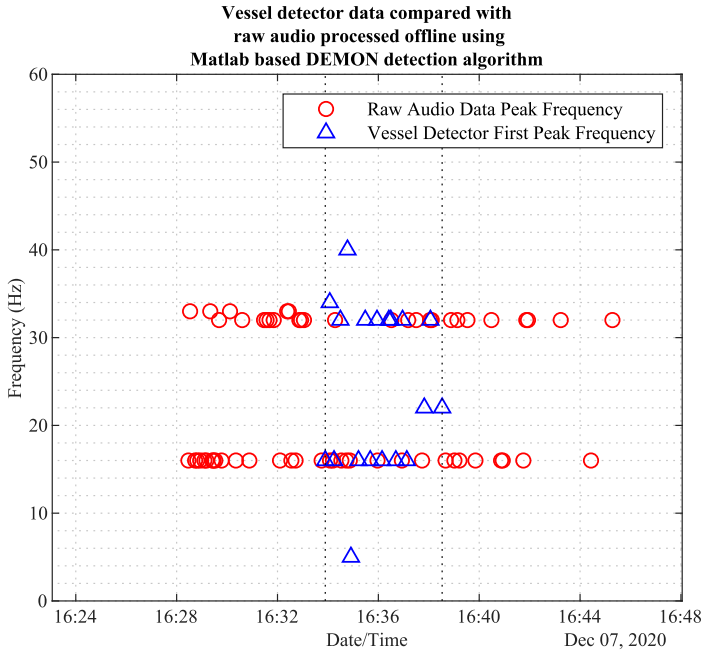

Fig. 5.63 Comparison of vessel detector data with raw audio processed by a Matlab based version of the DEMON detection algorithm.

Using the Matlab based detection algorithm, and the fact that the raw audio processed is time aligned with the field detection data, it is possible to estimate the SNR required to trigger the vessel detector. In Figure 5.64, an estimation of the the signal-to-noise ratio has been calculated for 30 second intervals. The plot shows the timeframe when the hardware detector became active. The results show that an average SNR of 6.872 dB is required for the hardware based detector to identify a vessel's DEMON signature.

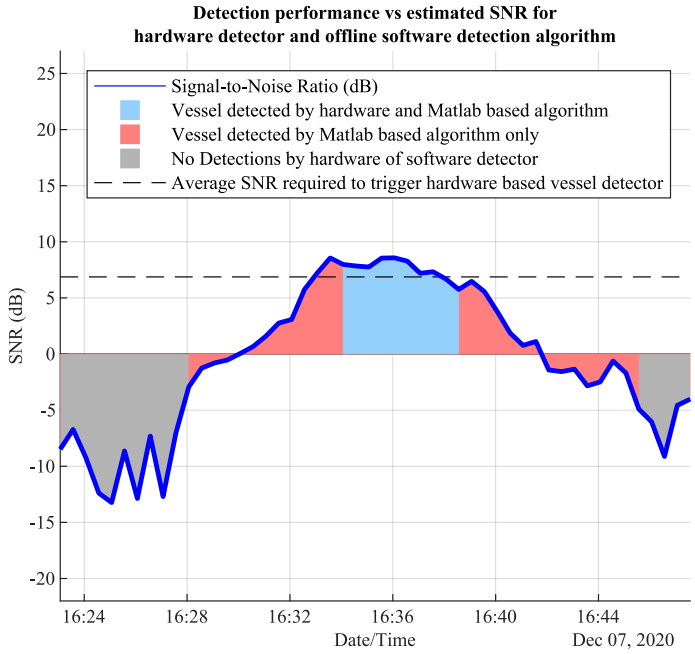

Fig. 5.64 Estimation of the SNR required for the vessel detector to operate.

Figure 5.64 also shows that a Matlab based algorithm is able to detect the vessel much earlier than the vessel detector used in field trials. This is mainly due to the increased resolution and superior performance of the Matlab based DEMON implementation. A low-energy implementation will inherently suffer from power/processing based constraints so there will always be a balance to strike when developing underwater wireless sensors.

As the Matlab algorithm results are based on a similar floating point based arithmetic, the detection results in Figure 5.64 are representative of what the NCDD mode, presented in Section 4.3.2, could achieve in hardware.

In summary, this section shows data from three separate sources, which all provide strong evidence that a vessel was present during the monitoring timeframe. The vessel detector produced positive detections during the same time period in which both the AIS data and raw acoustic recording suggested that a vessel was present.

5.5 Summary

The aim of this section was to produce a low-energy passive acoustic vessel detector which can operate as part of a wireless underwater network.

Results have demonstrated the vessel detector is able to reliably identify passing vessels based solely on the acoustic signature emitted during propeller cavitation. This has included detecting multiple vessels operating during the same time period.

Power consumption measurements alongside periodic battery monitoring data has shown that the vessel detector is capable of deployment lasting several months using only four C cells.

Reliability of the vessel detector has been demonstrated in a variety of ways including noise rejection due to severe weather, detection reliability when compared with local AIS data and enclosure integrity in hard North Sea conditions.

Results have shown that during long term field trials, 94% of results could be corroborated with local AIS data. Local AIS data is used as the best available ground truth accepting that some smaller vessels are not required to transmit AIS data.

Different approaches to vessel detection have been developed using a mixture of analogue/digital signal processing and a continuous/duty-cycled monitoring approach. Unfortunately, due to Covid restrictions, the duty cycled approach has yet to be tested at sea but this forms part of future work. However, a Matlab based algorithm which is representative of the duty-cycled digital approach has been shown to detect vessels much earlier.

Overall, the project has satisfied the overriding goal of developing and testing a low-energy passive acoustic vessel detector. This system has been tested in a realistic offshore environment and showed reliability and resilience in the face of harsh North Sea conditions. The key novelties of the work presented in this chapter are that an energy efficient passive acoustic vessel detection algorithm has been developed in embedded hardware and successfully trialled at sea.

As with a lot of research during a global pandemic, there has been disruption to planned work. This means that some of the initial work planned will now form part of the future work. Planned work includes testing the technology developed as part of a distributed network of underwater sensor nodes. This will give greater spatial data which could offer the ability to not only detect vessels but track them through the network. In addition, further testing of a duty cycled fully digital approach at sea may increase the detection sensitivity for the same energy budget as a continuous analogue/digital approach.

Chapter 6

Cetacean Click Detection/Classification Algorithm

6.1 Introduction

This chapter presents a method of both detecting and classifying cetacean clicks. As with all algorithms presented in this thesis, low power implementation of the algorithm is paramount in its design. The design of the algorithm is not assuming a limitless amount of processing power and is very much tailored to low power embedded devices. It is hoped that by accepting this low energy design caveat, the algorithm could be implemented into a wireless underwater node capable of long term deployments using only battery power.

6.2 Methods

A cetacean 'click' refers to the high frequency (>20 kHz) impulsive sound a cetacean creates to aid navigation and foraging, as described in Section 2.5.1. This section introduces a method to detect cetacean clicks whilst maintaining the overall project goal of low-power, low-cost hardware/software. In addition to the detection of clicks, this section also proposes a method of cetacean species classification based on the detection data collected. As the North Sea region around Blyth, UK, will form the test bed for this project, two species have been chosen for detection and classification field trials as they regularly occupy this area. These are the Harbour Porpoise and the White Beaked Dolphin, based on the Joint Nature Conservation Committee (JNCC) cetacean distribution data for north-west European waters [44]. Figure 6.1 shows the difference in click signals produced by the Harbour Porpoise and the White Beaked Dolphin in both the time and frequency domain.

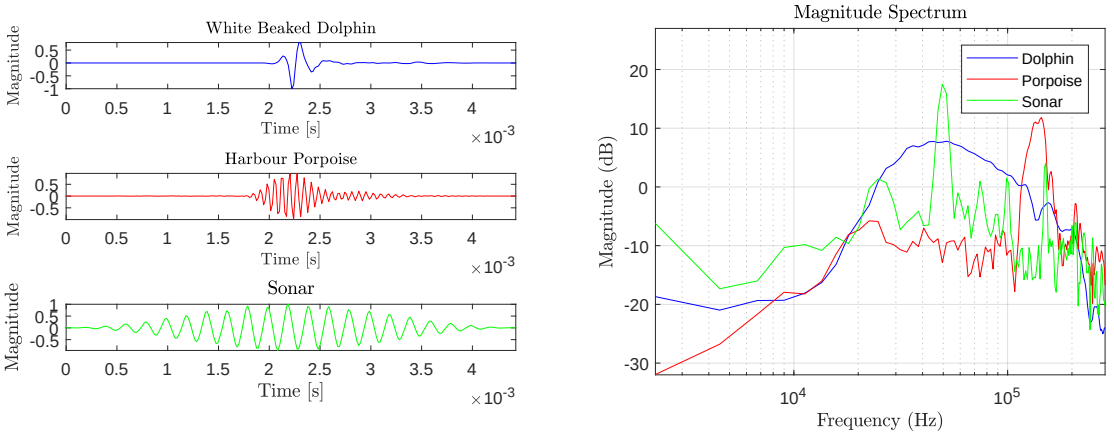

(a) Time domain comparison

(b) Frequency domain comparison

Fig. 6.1 Example of the distinguishing features between cetacean species in both time and frequency. Sonar has also been included to illustrate how synthetic human made signals could be mistaken for cetacean produced signals.

These differences are key to distinguishing between species for the classification part of the algorithm. However, the detection part of the algorithm will exploit similarities between each signal. As observed in Figure 6.1, both signals are high-magnitude impulsive events relative to background noise. To detect these impulsive, high-magnitude events using a low power technique, it is proposed to use a dual analogue low pass filter approach. Using two separate low pass filters, the aim is to track the slow changing background noise level alongside the fast changing cetacean clicks. Using a comparator, it is proposed that click events will be identifiable due to the difference between the slow and fast moving filters. Figure 6.2 provides detail of the overall design of the cetacean click detection and classification system. The following sub-sections provide more detail related to each part of the system.

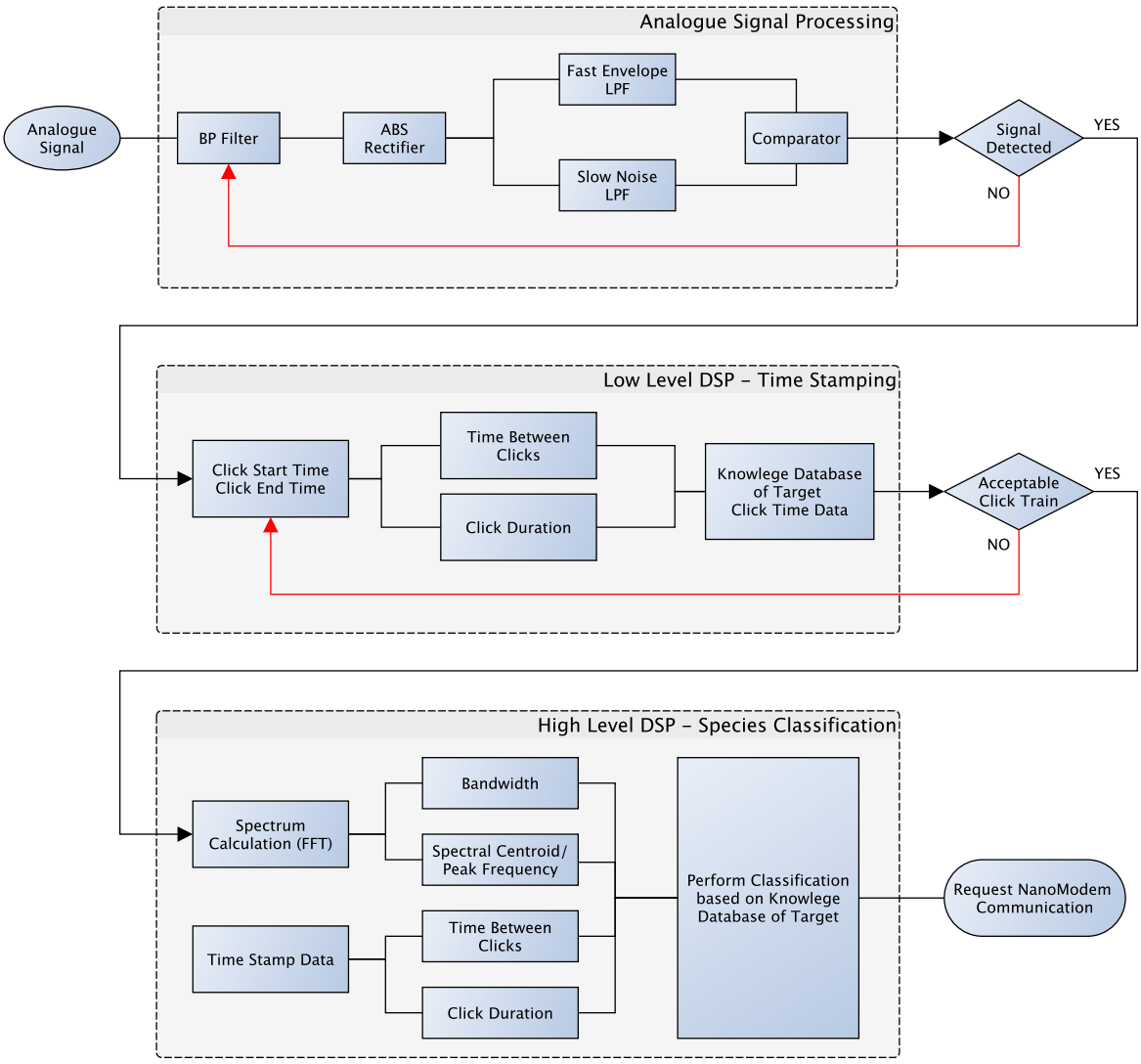

Fig. 6.2 Cetacean click detection and classification system diagram

6.2.1 Analogue Detection

The analogue front end plays a crucial role in regulating the more power hungry digital signal processing algorithms. It essentially acts as a front-line filter which decides which signals may be of interest to investigate further. The balance of which signals are accepted and which are rejected is key, as too robust a system could miss potential targets. The first stage in the system diagram shows that the analogue signal is processed through an analogue band-pass filter. This is currently set up to allow frequencies between 20 to 160 kHz to capture all of the White beaked dolphin and Harbour porpoise click signals. The effect of filtering using a band-pass filter is shown in the time domain in Figure 6.3.

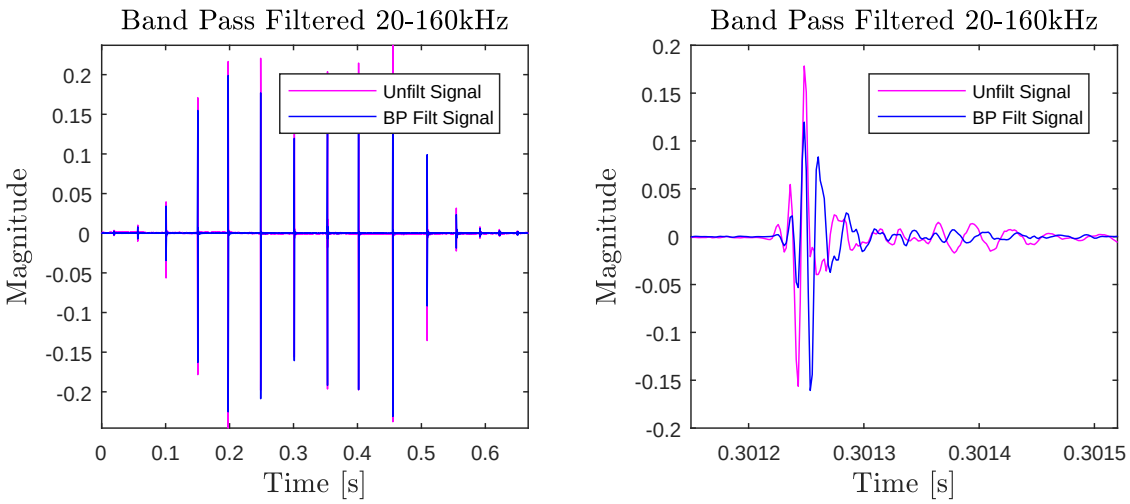

(a) Band Pass Filtered

(b) Band Pass Filtered - Expanded

Fig. 6.3 Initial band limiting stage of the analogue cetacean detection algorithm.

The next stage in the analogue detection process is to rectify the filtered signal and track the envelope in both a fast and slow manner. The speed refers to the cut off frequency of the low pass filter used. A fast filter has a higher cut off frequency and will track fast changing signals more closely whereas the slower filter will act as more of an average line that responds to slower changes in signals such as background noise.

Figure 6.4 show the result of rectification using a fast low pass filter, set at 30 kHz. The filter itself is composed of two first order Butterworth filters cascaded to create a second order filter response. This response is illustrated in the smooth signal envelope shown in red. The reason for detecting this envelope is to allow for comparison with a user defined threshold to establish whether a click event has occurred. It also offers the potential to estimate the start and end time of the individual click event based on the crossing points of the threshold level.

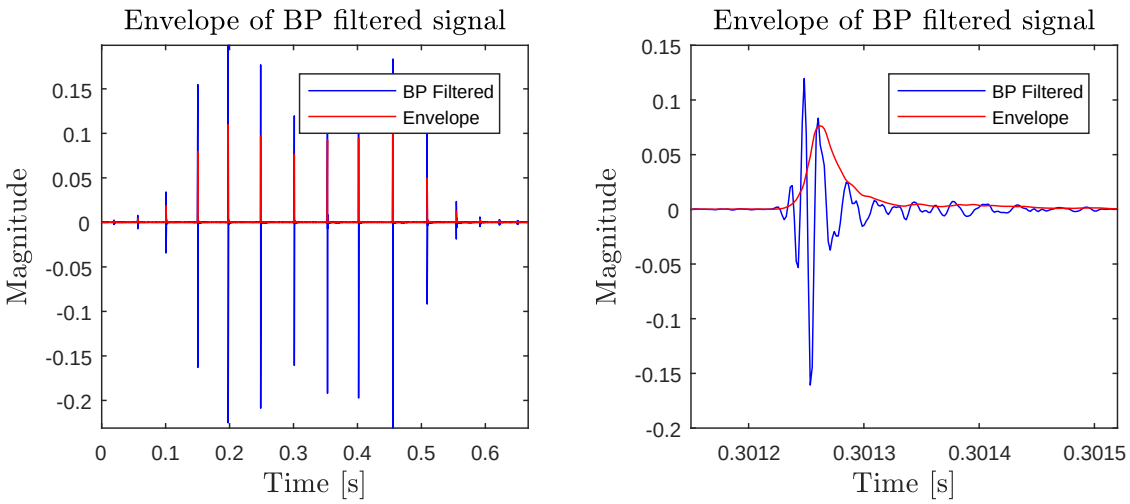

(a) Fast LPF Envelope

(b) Fast LPF Envelope - Expanded

Fig. 6.4 Low pass filter set at 30 kHz cut off frequency. Used to capture the envelope of high frequency click events.

The threshold used to compare against the fast filtered signal is set using a slow low pass filter set at 5 Hz and an optional used defined fixed offset. The reason for the slow low pass filter is that it offers a dynamically changing threshold which responds to changes in the noise floor. In the example shown in Figure 6.5, a fixed gain of 2.5 times the slow filter signal level is used to boost the threshold well above the noise floor.

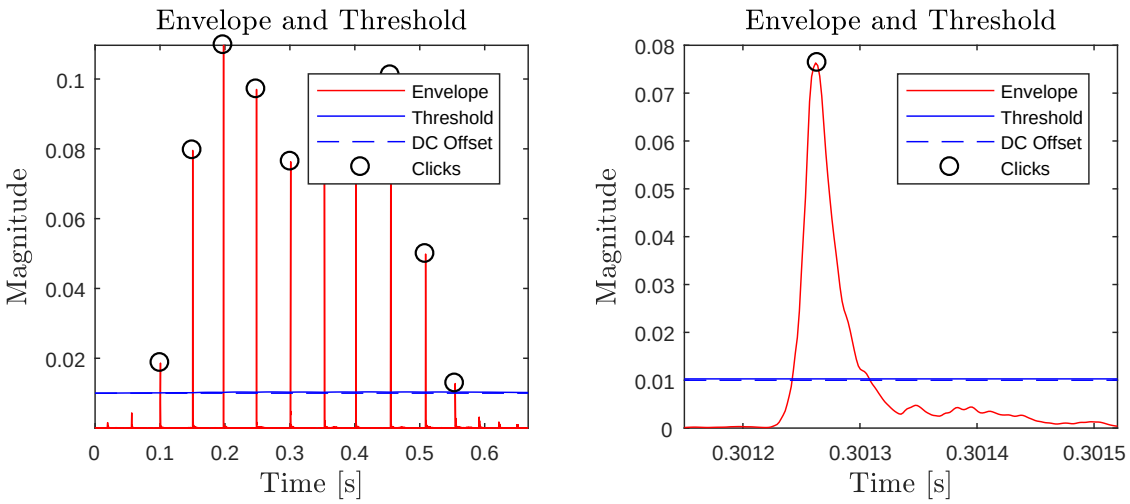

(a) Slow LPF Envelope and Threshold

(b) Envelope and Threshold - Expanded

Fig. 6.5 Illustration of the dynamically changeable threshold based on the average background noise level.

The final stage in the system's diagram in Figure 6.2 is labelled comparator. As the label suggests this is where the fast click envelope is compared with the slower noise tracking envelope to decide whether or not a click has been detected. In Figure 6.5, this is represented by the circle indicators labelled 'Clicks'.

To further demonstrate the slow low pass filter's ability to track the level of the noise floor, white noise has been added to the signal. Figure 6.6 shows that as the noise floor increases in amplitude, the resulting threshold is raised proportionally. Figure 6.6 also demonstrates the limitation of using only a fixed offset as the faster signal tracking envelope (red line) has breached the DC offset (blue dashed line) threshold and would be registering as a positive event unless the offset was adjusted manually.

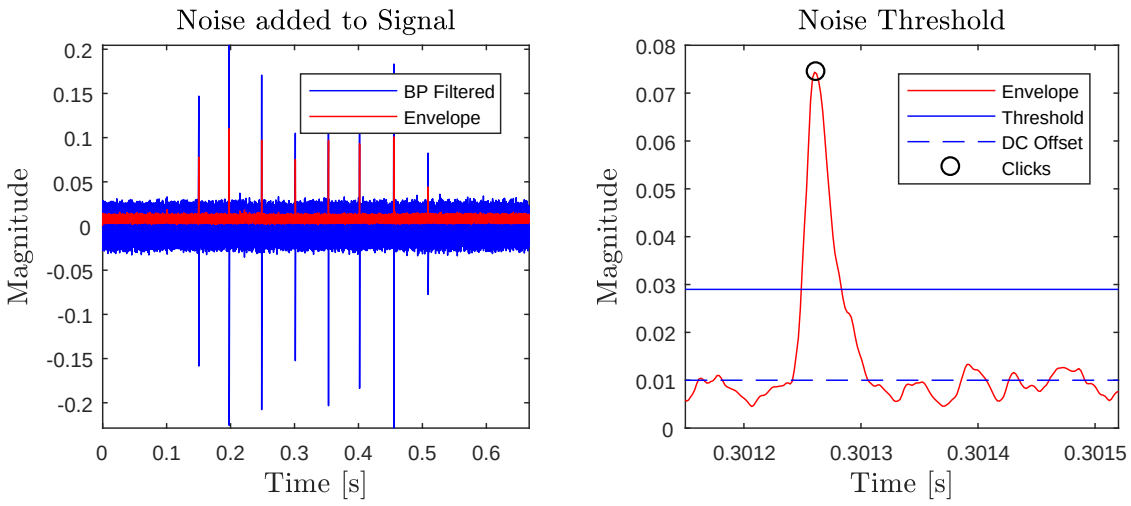

(a) Signal plus Noise

(b) Signal plus Noise - Expanded

Fig. 6.6 Illustration of the dynamically changeable threshold with added white noise.

This concludes the analogue signal processing stage of the detection and classification algorithm as shown in the system diagram in Figure 6.2.

6.2.2 Low Level Digital Signal Processing (DSP) - Time Stamping

The term "low level DSP" refers to operations which use minimal power consumption to further investigate signals of interest received from the analogue front end. This is essentially another gateway to pass through before more power hungry processing is implemented. The aim of this section in the system's diagram (Figure 6.2) is to measure the time data of clicks received. This can then be compared with a knowledge database to determine whether the data represents a signal of interest. This stage is required because the ocean is full of noise sources which initially can mascarade as signals of interest. For example a ship's echosounder would look very similar to that of a cetacean click train in the time domain. By analysing the event duration and repetition rate this could be ruled out due to the potentially evenly spaced sonar emissions in the time domain.

A Matlab based algorithm has been created which identifies the time between each click (Inter-click Interval or ICI) and the duration of each individual click within a train of clicks. 'Click train' is the term used to describe a collection of clicks within quick succession created by cetaceans during navigation and foraging. Figure 6.7 shows the result of processing a real

recording of a cetacean click train using the Matlab based algorithm.

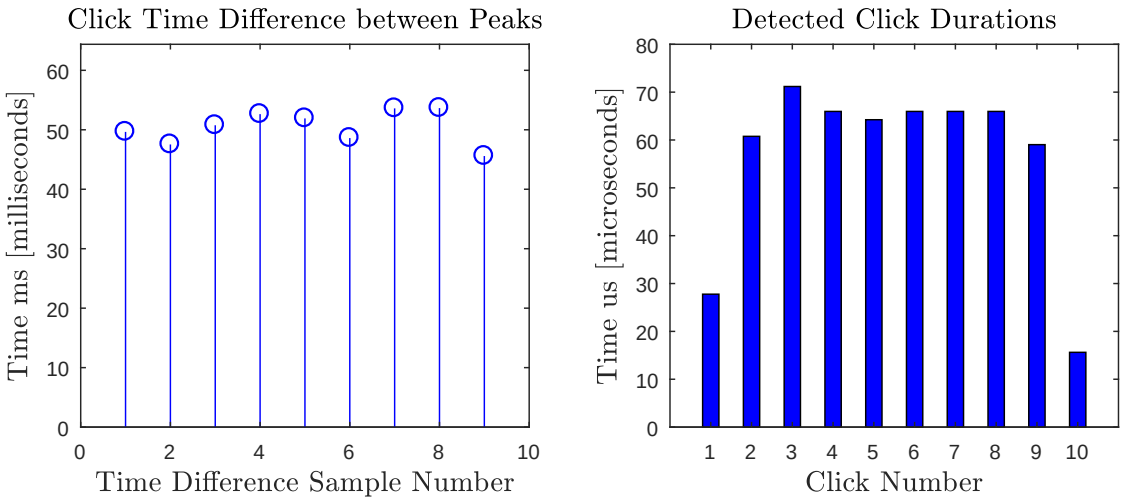

(a) Click Time Interval Plot

(b) Click Duration Plot

Fig. 6.7 Example of the duration and time interval between dolphin click trains.

Using the time stamp data in Figure 6.7 and knowledge about the target, a decision can be made as to whether or not the final high level DSP processing stage (species classification) should be performed.

6.2.3 High Level DSP - Species Classification

This section refers to the higher power digital signal processing which aims to classify the signal as a certain species and communicate this information back to shore. In the White Beaked Dolphin example used in Figure 6.1 there are several features which could be classed as unique identifiers to that species. In this example the bandwidth, peak frequency and click duration have been chosen as unique identifiers. This is because there is a stark contrast in each of these variables when compared with the Harbour Porpoise. The Harbour Porpoise is very narrow band with a long click duration and higher peak frequency than the White Beaked Dolphin [8].

Using the envelope and threshold detection method introduced in Section 6.2.1, it is possible to determine the start and end time of each click event and subsequently calculate the duration. Using many verified clicks of each species, an average can be calculated and

used as an identifier for that specific species.

Bandwidth and peak frequency require a higher level of processing as it requires the use of FFT to calculate the frequency spectrum of each recording. With the frequency spectrum of each of the 26 recordings calculated, a similar envelope and threshold method can be used to estimate the bandwidth and peak frequency unique to a single species. Figure 6.8 shows an example of the frequency spectrum with envelope and threshold taken for one of the White Beaked Dolphin recording sampled at 576 kHz.

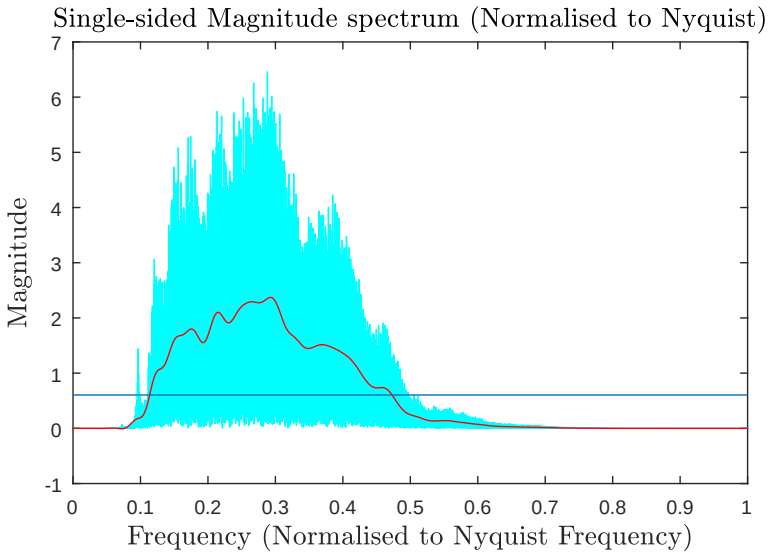

Fig. 6.8 Envelope and threshold applied to a White Beaked Dolphin click spectrum.

By setting a suitable threshold (currently set to the mean of the envelope magnitude) it is possible to obtain the start and end values where the envelope crosses the threshold and hence calculate the estimated bandwidth of the signal. For the example in Figure 6.8 the estimated bandwidth was calculated to be around 100 kHz. Peak frequency is calculated by locating the maximum value in the frequency spectrum envelope plot. This is approximately 84 kHz for the example shown in Figure 6.8.

To better visualise how these three variables can be used for the purposes of classification it is useful to plot each against each other in a three dimensional plot. This allows for a scatter of each of the 26 recordings' average bandwidth, peak frequency and click duration. As Figure 6.9 shows, there is a potential cluster emerging around each of the three variables. Cluster analysis can be used to identify a minimum and maximum value for each variable for the purposes of classification.

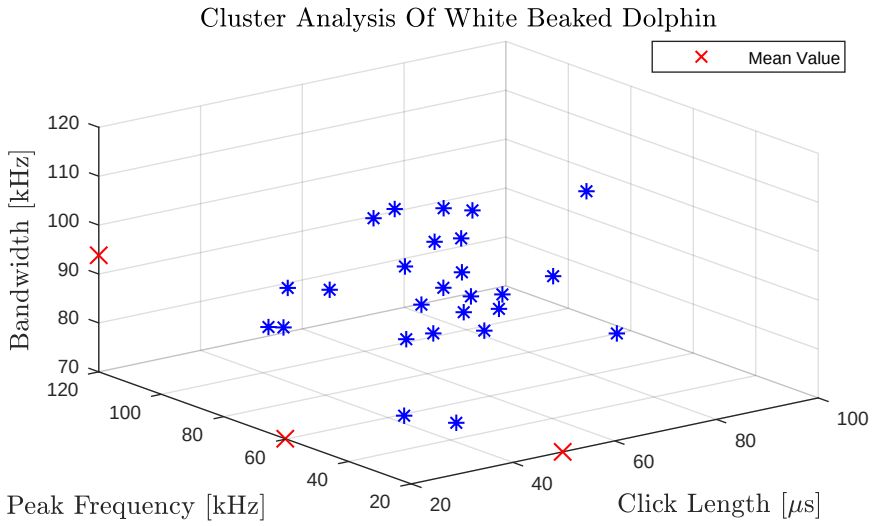

Fig. 6.9 Cluster plot of estimated bandwidth, peak frequency and click duration based on 26 recordings of white beaked dolphin. The red cross on each axis shows the mean value of each variable.

One of the variables used in Figure 6.9 is the peak frequency observed in each recordings' spectrum. Although this is a good indication of where the energy peaks, it does not always portray the whole story. In terms of where the predominantly concentrated energy occurs, a better representation would be to estimate the centroid of the frequency spectrum. This can be calculated using Equation 6.1, where $x(n)$ represents the magnitude and $f(n)$ represents the centre frequency of bin n.

$$Centroid = \frac{\sum_{n=0}^{N-1} f(n)x(n)}{\sum_{n=0}^{N-1} x(n)} \tag{6.1}$$

An example of how the peak frequency and spectral centroid can vary, from very close to widely distanced, is illustrated in Figure 6.10.

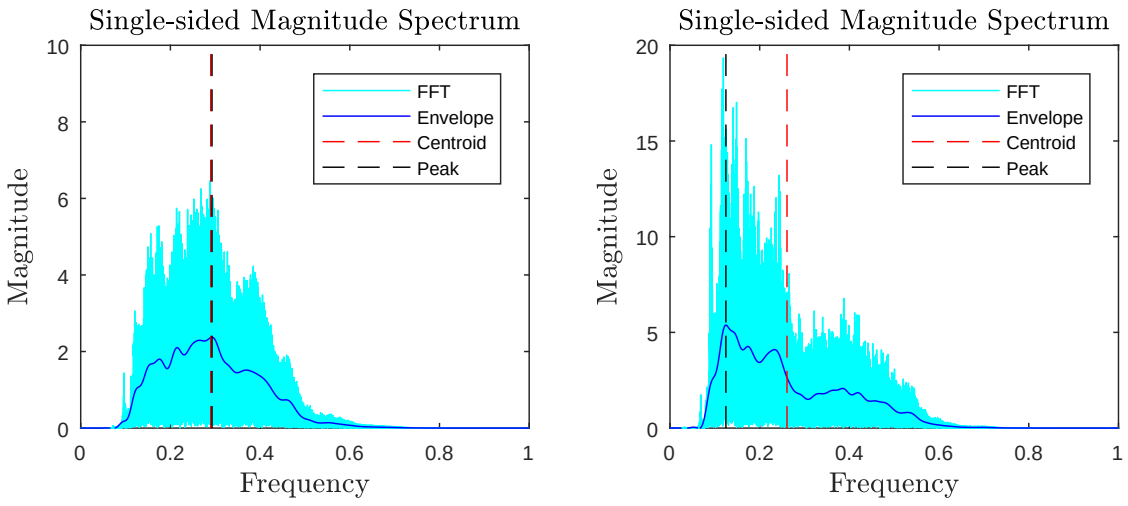

(a) Close Peak and Centroid

(b) Distant Peak and Centroid

Fig. 6.10 Example of the duration and time interval between dolphin click trains.

If we now re-plot the 3D cluster analysis graph (shown in Figure 6.11), this time including spectral centroid estimation instead of peak frequency the resulting mean is very different from the outcome in Figure 6.9. The mean for peak frequency is around 60 kHz whereas the centroid estimation shows a mean of around 80 kHz.

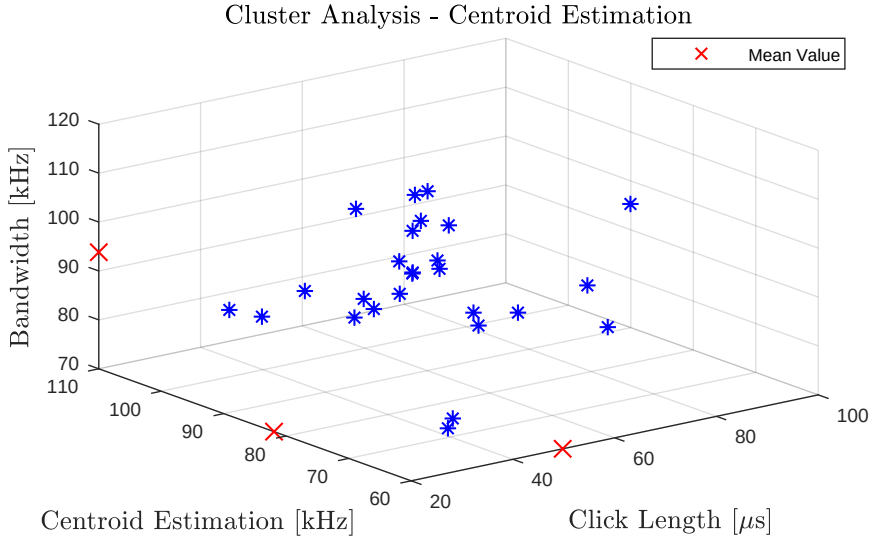

Fig. 6.11 Cluster plot of estimated bandwidth, centroid and click duration based on 26 recordings of white beaked dolphin. The red cross on each axis shows the mean value of each variable.

If we compare the results obtained for peak frequency in Figure 6.9 with what is documented in literature, there is a notable difference. Rasmussen *et al.* conducted open water trials to record White Beaked Dolphin vocalisations, concluding that the average peak frequency occurred around 115 kHz [71]. When this is compared with the results from this project, which indicated a peak at around 60 kHz, there is a clear difference.

One explanation for this discrepancy may be due to the limited number clicks considered for Figure 6.9. Having a greater number of clicks to consider, may lead to a more representative peak frequency for the species. This is of course assuming that the majority of the recording contains the species in question.

In contrast to discrepancies observed with peak frequency, the centroid estimation recorded in this project was similar to the field trials conducted by Rasmussen *et al.* with a frequency of around 80 kHz [71]. This suggests that interfering signals may have caused the shift in peak frequency. The centroid estimation takes into account all energy in the spectrum. The purpose of taking measurements like peak and centroid estimations of frequency content is in the hope of classifying the source reliably.

Classification requires certain boundaries to be set where the algorithm will make a decision based on whether or not the given variable falls within these boundaries. To give an illustration of this method of classifying a target, Figure 6.9 has been adapted to include a three dimensional sphere. The sphere represents the boundaries of classification and is set to have a diameter which is two standard deviations away from the common mean of each variable. The result is illustrated in Figure 6.12.

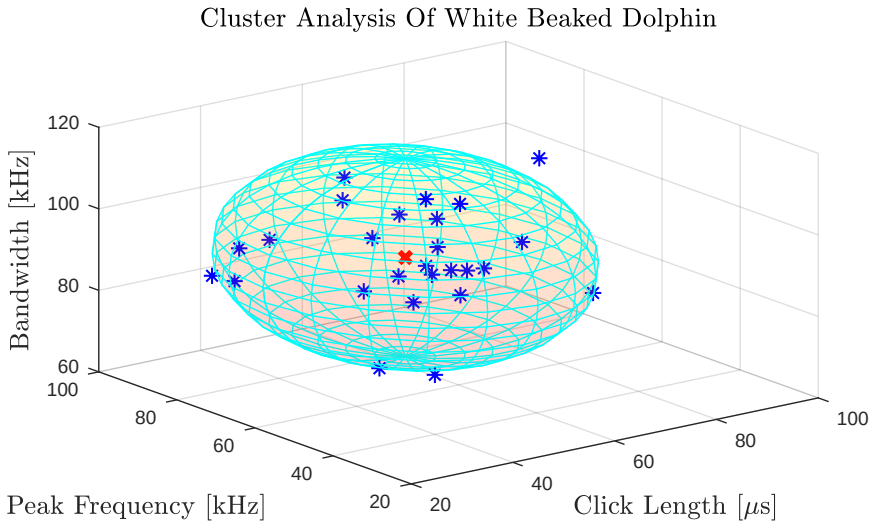

Fig. 6.12 Cluster plot of estimated bandwidth, peak frequency and click duration based on 26 recordings of white beaked dolphin. A sphere is shown which is two standard deviations away from the common mean of each variable.

An alternative method to identify the unique spectral features of the White Beaked Dolphin signal is to consider the FFT of each individual click of a large data set and take an average of the result. This method aims to discount any interfering clicks by assuming that the majority of clicks contained within the recording are from the White Beaked Dolphin. To further increase the probability of gaining an accurate spectrum, any clicks that have been clipped by the receiver are removed from consideration as part of the Matlab based algorithm. The result of the individual click frequency spectrum analysis algorithm is shown in Figure 6.13 and contains approximately 3200 clicks (shown in blue).

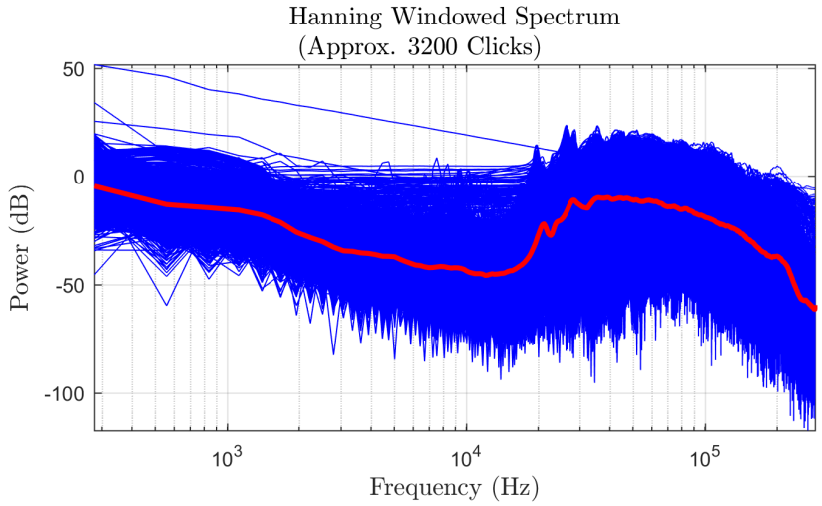

Fig. 6.13 Frequency Spectrum of 3200 Individual Clicks

Figure 6.13 has been constructed using the full spectral content of the recording with no band pass filter applied. To separate each click a moving 1ms pruning window has been used which only considers one high amplitude click per window, therefore discounting any reverberating after-click events. As each click is effectively being cut from the recording and considered independently, a Hanning window has been applied when performing an FFT to ensure the signal starts and finished with a zero value. This is because an FFT assumes that the signal is periodic and any aperiodic truncated signal will cause a non representative frequency spectrum of the original continuous signal. These artificial spectral discontinuities are referred to as spectral leakage.

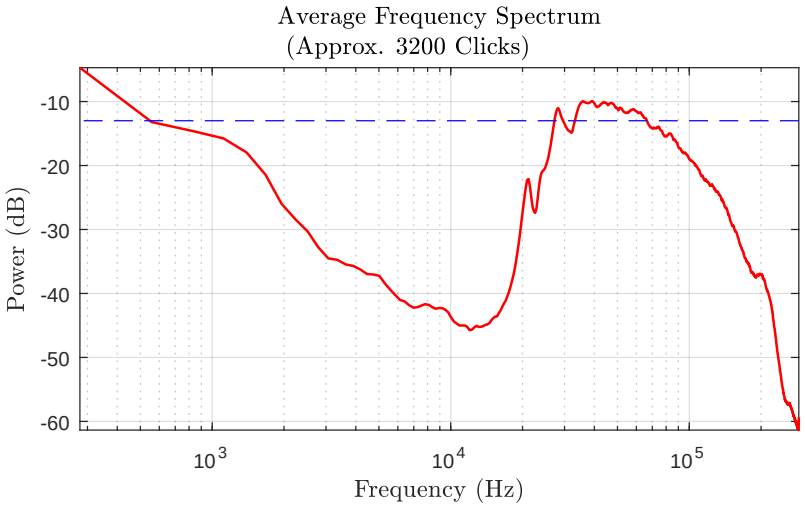

Fig. 6.14 Average Frequency Spectrum of 3200 Clicks

The computed average frequency spectrum for all valid clicks contained within the White Beaked Dolphin recording is shown in Figure 6.14. The blue dashed line refers to the -3dB point from the peak of the 40-160kHz area of interest. Using this as a marker and taking the points of intersection with the spectrum as a measure of bandwidth, the result is around 40kHz. This also agrees with observation made by Rasmussen *et al.* during field trials [71].

In an attempt to further investigate the peak frequency anomaly discussed in Figure 6.9, we will now consider the entire White Beaked Dolphin recording band limited from 40 to 160 kHz. The aim of this is to gain an average click frequency spectrum across the entire recording, limited to the band of interest, and gain a peak frequency value. This is illustrated in Figure 6.15, where the black cross shows a peak of around 50 kHz.

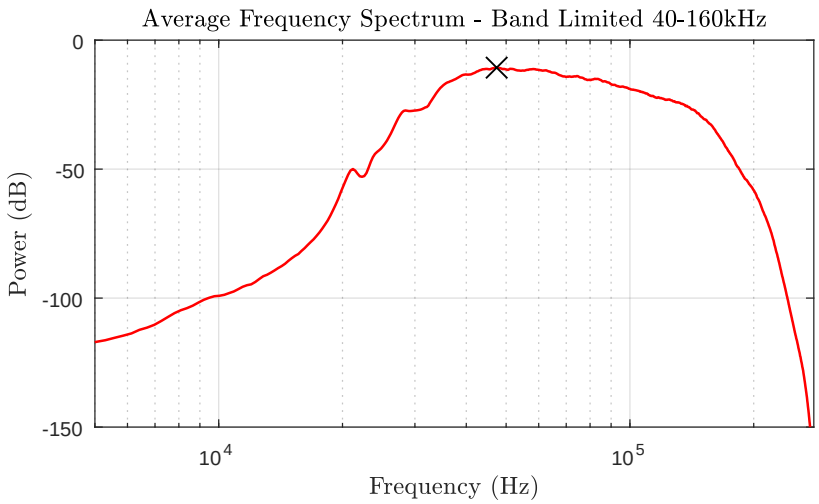

Fig. 6.15 Average Band Limited Frequency Spectrum

To explain this difference from the 115 kHz peak experienced in literature, the White Beaked Dolphin's beam pattern may be a contributing factor. In 2004, Rasmussen *et al.* conducted field trials to estimate the transmission beam patter of White Beaked Dolphin clicks in Icelandic waters [72]. Findings indicated that at an off-axis angle of only $\pm 10^{\circ}$ results in a minus 18 dB attenuation in the signal's intensity compared with an on axis 0° transmission. This indicated that White-Beaked Dolphins emit a highly directional vocalisation. This directivity may explain the shift in peak frequency, as in the event of an off axis signal being received, the higher frequency components will be lost before the lower frequencies.

Another explanation may be that the frequency content has been effected simply by the distance between the receiver and the animal. Higher frequency content suffers much worse than lower frequency components over distance due to propagation losses, therefore a shift in peak frequency may be observed in spectral analysis.

6.2.4 Detection and Classification Algorithm Overview

In this section, the complete cetacean detection and classification algorithm is summarised using Figure 6.16 alongside a brief description of each stage.

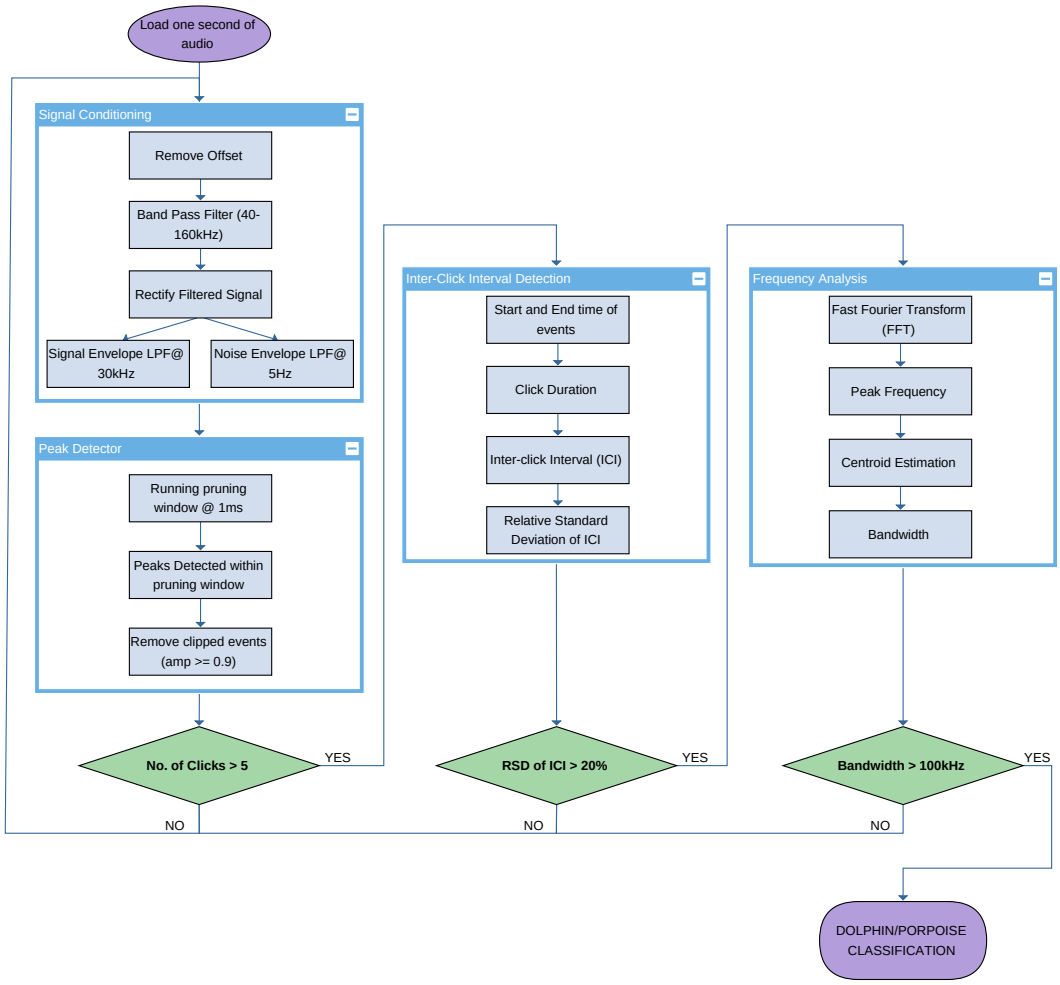

Fig. 6.16 Cetacean detection and classification algorithm produced in Matlab.

To process the audio recording in a manner which resembles a real time system, the Matlab-based algorithm considers one second windows of data. The first stage in processing involves the signal conditioning, which filters the signal to a stage where a slow noise tracking and fast signal tracking envelope are produced. These two outputs form the method of detecting click events (i.e. when the signal envelope exceeds the noise tracking envelope).

The second stage is the detection of the signal peaks above the threshold. To refine this data the algorithm uses a 1ms pruning window to return only the highest amplitude peaks in each given window. The reason for this is to discount any reverberating signals which may follow an impulsive click event. At this stage, a conditional threshold is applied to remove

any clicks which may have been clipped by the receiver. In this instance, any amplitude which exceeds 0.9 (positive dynamic range of Wav file is 0 to 1.0) is considered a clipped audio event and removed from further calculations.

The third stage in the detection and classification algorithm is the first of three major thresholds. The first is based simply on the number of click events in the one second time window. In this instance, a value of five has been chosen to ensure there are sufficient clicks to consider the event as a click train.

After successfully satisfying the number of clicks threshold, the fourth stage of the detection process refers to the time stamping and analysis of ICI. To obtain this time stamp data, the previously detected peaks are used as references to search for the start and end time of each peak event (i.e. the point at which the signal envelope moves above and below the noise threshold). With this data the standard deviation relative to the mean is calculated. The reason for relating the standard deviation to the mean is to provide a normalised threshold percentage which will be consistent for all extremes in timing data. These extremes refer to the wide dynamic range of click rate that Cetaceans are capable of producing.

The fifth stage is the next major threshold of the algorithm, where the calculated relative standard deviation of ICI is used. In this case, a value of less than 20% is deemed as acceptable, as the aim is to find consistent clicks with no interfering click signals present.

Upon successful ICI data, the next stage is the calculation of the frequency content for the successful click events in the one second window. Using an FFT, with Hanning window function, the spectrum for each click is evaluated to find the peak, centroid and bandwidth in similar methods described earlier in this Chapter.

The final stage of the detection and classification algorithm is to place a threshold on the bandwidth, which is a big indicator for dolphin/porpoise classification. For this example a value of 100 kHz has been chosen to ensure a broadband signal, characteristic of a dolphin acoustic signature.

For the Matlab-based algorithm presented in Figure 6.16, only positive detections are recorded. If no detection is established the algorithm moves onto the next block of data as shows by the 'NO' path back to the start of the diagram.

6.3 Results

In this section, results of the cetacean click detection/classification algorithm are presented. The first subsection of the results demonstrates the algorithm's ability to detect cetacean clicks and also its ability to classify these clicks into separate species. The final part of the results section compares the algorithm against the most widely adopted commercial system used amongst marine biologists, which is the previously introduced C-POD [21]. The C-POD is a device which monitors the presence of cetaceans by detecting echo-location click trains.

6.3.1 Dolphin/Porpoise/Sonar Detection and Classification

The click detection algorithm is set up to classify incoming signals into three categories which are dolphin, porpoise or sonar. A dolphin has the following classification features:

- Bandwidth > 26 kHz.
- Centroid < 110 kHz.
- Peak Frequency < 110 kHz.
- Minimum number of clicks = 4.
- Relative Standard Deviation (RSD) of ICI < 60% (see Equation 6.2).

$$RSDofICI = \frac{\sigma(ICI)}{\mu(ICI)} * 100 \tag{6.2}$$

An illustration of a positive dolphin detection/classification is shown in Figure 6.17. The algorithm looks in each one second window for cetacean click activity and then displays the results. The first of three subplots shows the spectrum of each identified click (blue plots) overlayed within the one second detection period. The black line is the average of all of these detected clicks. A smoothing filter is applied to the average click spectrum to help estimate the bandwidth. The red line shows the filtered average click spectrum. Taking the maximum of the red line, bandwidth is estimated to be at the crossing points of -3 dB from this maximum value, as shown by the dashed cyan coloured line. The second subplot shows the envelope of the clicks detected. Each black circle represents an above threshold click event. The final plot shows the band limited input signal which has been processed through the detection/classification algorithm. This format of subplot is the same for the next three Figures in this section.

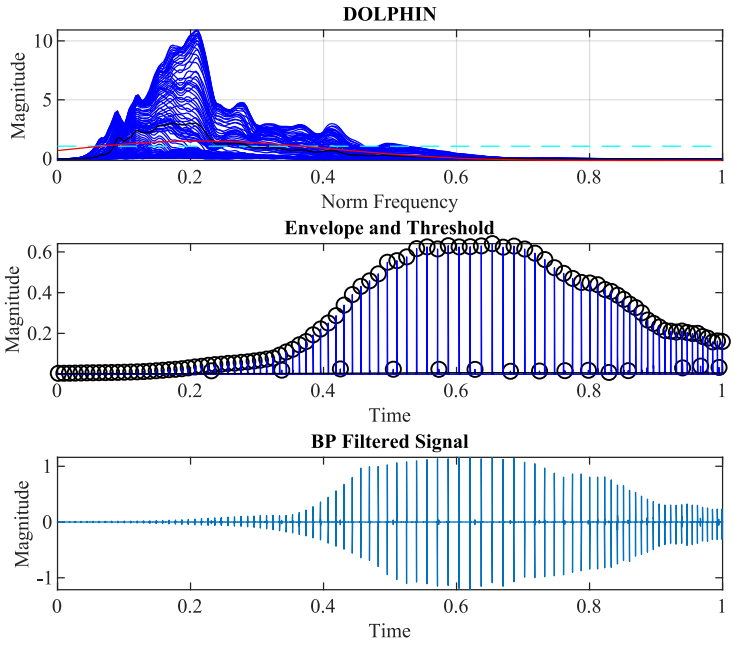

Fig. 6.17 Example of a positive dolphin detection/classification.

The next example refers to a successful porpoise detection/classification. A porpoise has the following classification criteria:

- Bandwidth < 26 kHz.
- Centroid > 110 kHz.
- Peak Frequency > 110 kHz.
- Minimum number of clicks = 4.
- RSD of ICI < 60% (see Equation 6.2).

An example of a positive detection/classification of a porpoise is shown in Figure 6.18. The most immediate distinction when compared to a dolphin result is that the porpoise has a much narrower bandwidth than a dolphin. This is illustrated in the first subplot of Figure 6.18.

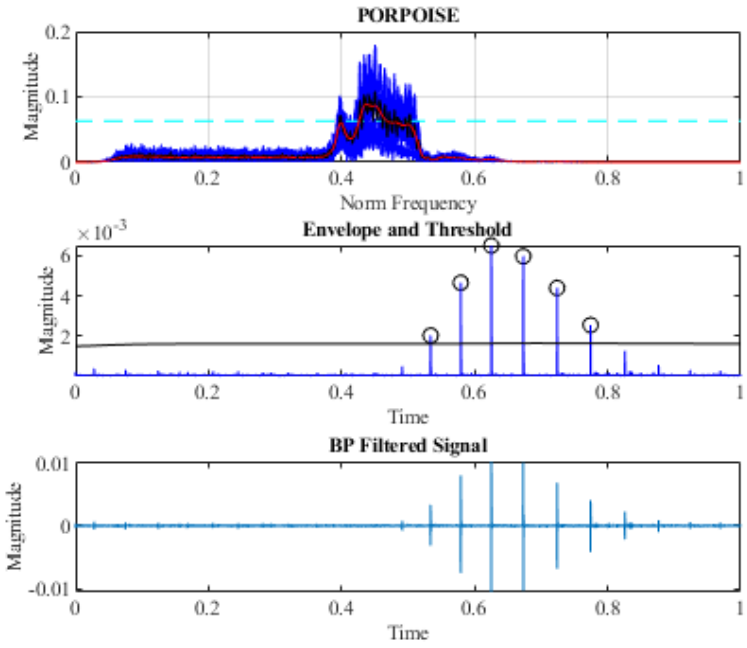

Fig. 6.18 Example of a positive porpoise detection/classification.

The final example is related to detection/classification of sonar. The following criteria is an example of classifying a specific sonar signal around 50 kHz.

- Bandwidth < 26 kHz.
- Centroid < 110 kHz.
- Peak Frequency > 45 kHz and < 55 kHz.
- Minimum number of clicks = 4.
- RSD of ICI < 60% (see Equation 6.2).

Figure 6.19 shows an example of a detected sonar event. As illustrated in the first subplot the signal produced contains a very narrow band signal. In comparison to a porpoise it is notable narrower in frequency.

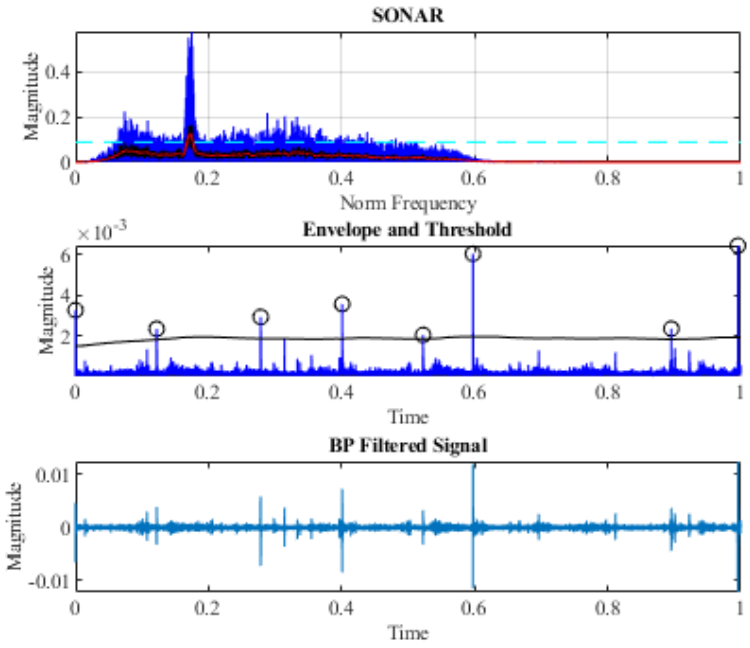

Fig. 6.19 Example of a positive sonar detection/classification.

6.3.2 Detection algorithm/C-POD comparison

In order to provide a meaningful result on the accuracy of the detection algorithm, a ground truth is required. As introduced in Section 3.3.1.2, the C-POD system is used to automatically monitor cetacean activity [21]. It has been widely used by researchers to capture and store cetacean detection data. This data can then be retrieved from the deployment location and downloaded for processing offline. Figure 6.20 shows the C-POD deployed alongside a Soundtrap acoustic recorder.

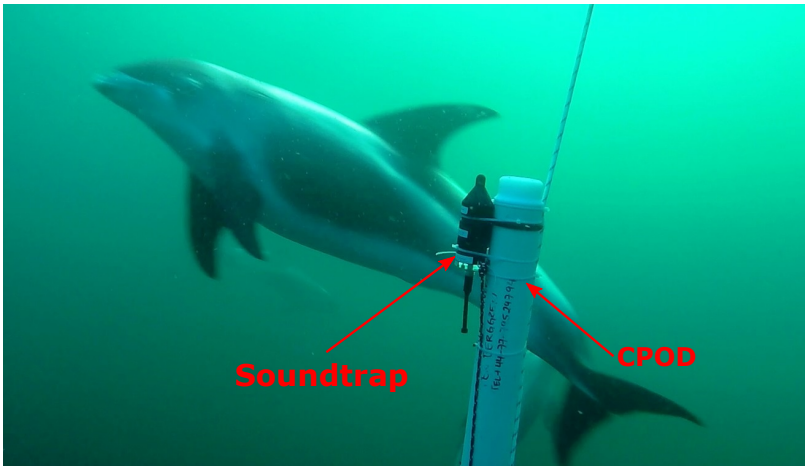

Fig. 6.20 Deployment of Soundtrap acoustic recorder alongside a C-POD cetacean monitoring system.

In this experiment, an underwater acoustic recorder has been deployed to capture the signal that the C-POD has received during its detection period. Using this data a direct comparison between the C-POD detection results and the detection algorithm results can be evaluated. The recordings are processed offline using the Matlab based cetacean detection algorithm (CDA). The daily results for each method of detection are summarised in Figure 6.21.

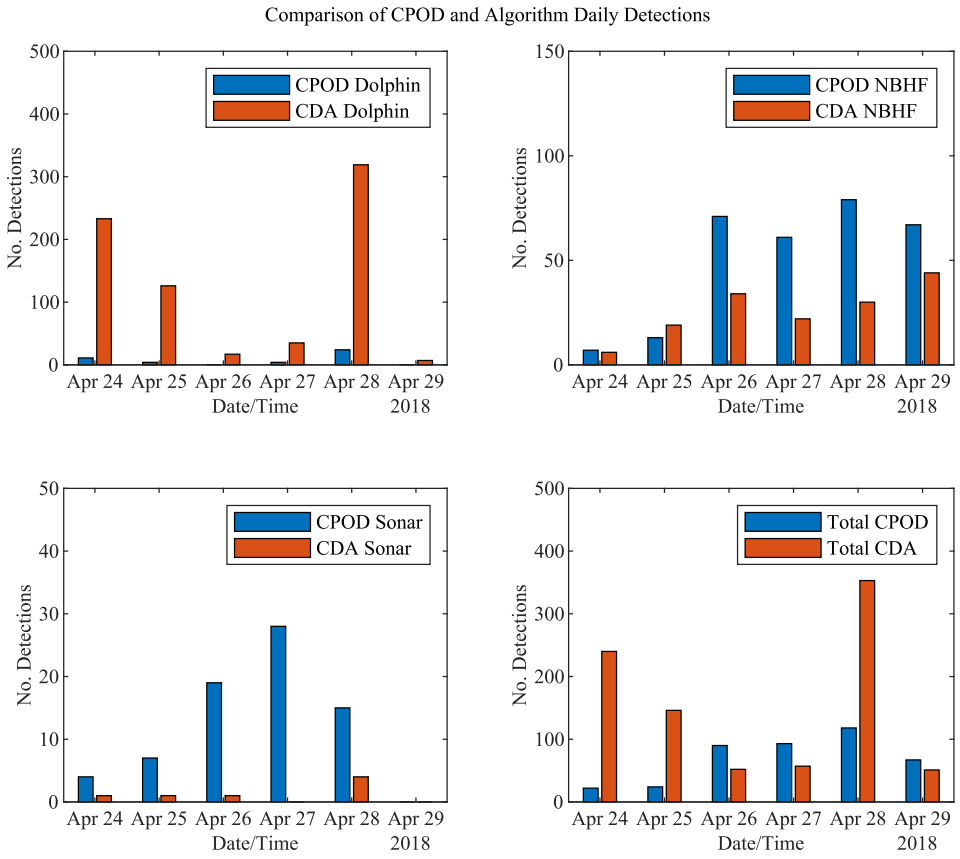

Fig. 6.21 Daily detection results of a C-POD device and offline processing of acoustic recordings by the CDA.

Figure 6.21 shows a high correlation between the CPOD and CDA for both dolphin and porpoise with a proportional shift in detection numbers for each species.

Figure 6.22 shows a comparison of detection results within five minute periods for both the C-POD and the CDA. The reason for choosing a five minute period is to protect against the misalignment of the C-POD and acoustic recorder's date/time source. The second reason is based on knowledge of the C-POD, in that it logs detection positive minutes. Therefore, cetaceans detected between minutes can cause ambiguity when comparing against another system (i.e. the acoustic recorder). The results for dolphin and porpoise (C-POD refers to these results as narrow band high frequency (NBHF)) show that the C-POD and CDA agree on detection results 91% and 92% respectively.

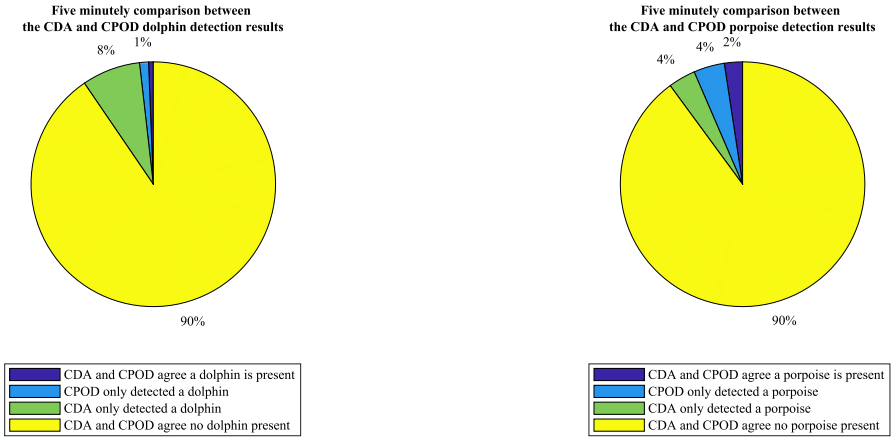

(a) C-POD and CDA dolphin results.

(b) C-POD and CDA porpoise (NBHF) results.

Fig. 6.22 Comparison of the C-POD/CDA detection results for dolphin and porpoise within five minute windows.

To further investigate performance, recordings of individual cetacean detection events can be manually scrutinised. These recordings have all been high pass filtered at 5 kHz to remove low frequency noise which is not of interest in the analysis of cetacean recordings. In Figures 6.23, 6.24, 6.25 and 6.26 recordings are analysed to show occasions where dolphins and porpoises were detected by both the C-POD and CDA but also occasions where only the CDA detected. In each of the four figures presented, there is a strong indication the dolphin/porpoise were indeed present. This is based on knowledge of each species with dolphin clicks having a broadband spectrum between 40 and 130 kHz and porpoise having a NBHF click spectrum between 120 and 150 kHz. In the events where only the CDA detected (Figures 6.24 and 6.26), it is clear to see the spectrum of an individual click is closely matched to the occasions where the CDA and C-POD agreed (Figures 6.23 and 6.25). The main difference in clicks that are detected solely by the CDA appears to be the magnitude of the click itself. In the dolphin click frequency band detected by the the CDA only, there is a peak frequency reduction of approximately 20 bB/Hz when compared to the C-POD/CDA result. This is echoed in the porpoise results where there is a peak frequency reduction of approximately 15 bB/Hz when compared to the C-POD/CDA result. This implies that there is a greater sensitivity in dolphin/porpoise detection when processed by the CDA.

At present the algorithm is designed to mimic the true low power hardware/software implementation by using analogue modelled filters. However, the algorithm is still Matlab

based and an increase in sensitivity cannot be ruled out to be a result of the increased resolution achievable with full floating point arithmetic. There will always be sacrifices when fully implementing an algorithm in a low power embedded system. However, the results do show that the algorithm design is capable of detecting cetaceans that the C-POD has missed which in itself is a positive result to take into a fully embedded implementation. This implementation forms the key future work for the cetacean click detection part of this project.

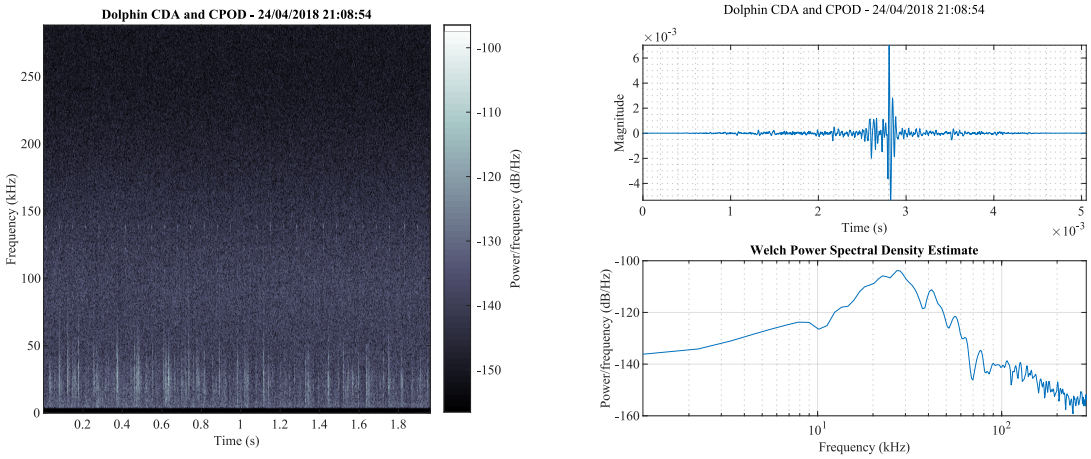

(a) Spectrogram of event.

(b) Individual click analysis.

Fig. 6.23 Recording of positive dolphin detection result showing an agreement between C-POD and CDA algorithms.

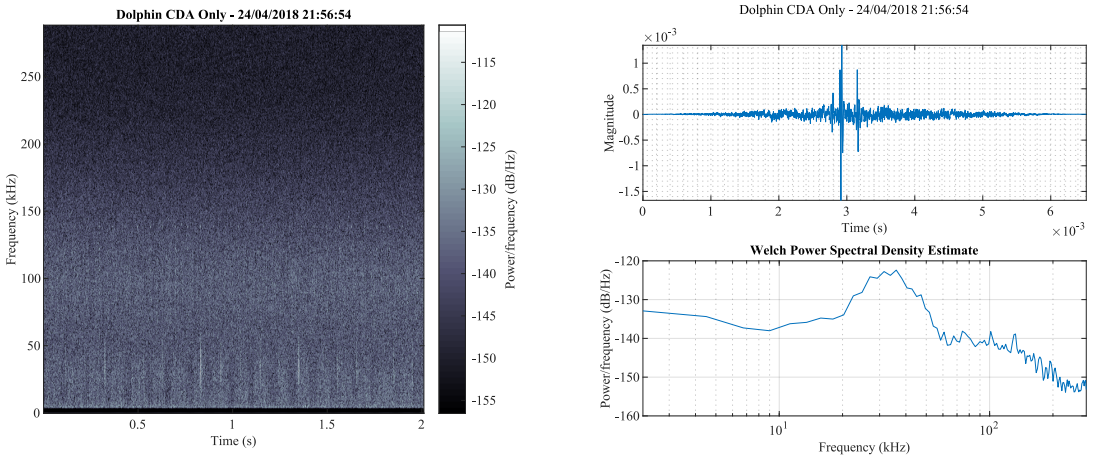

(a) Spectrogram of event. (b) Individual click analysis.

Fig. 6.24 Recording of positive dolphin detection result detected by the CDA algorithm only.

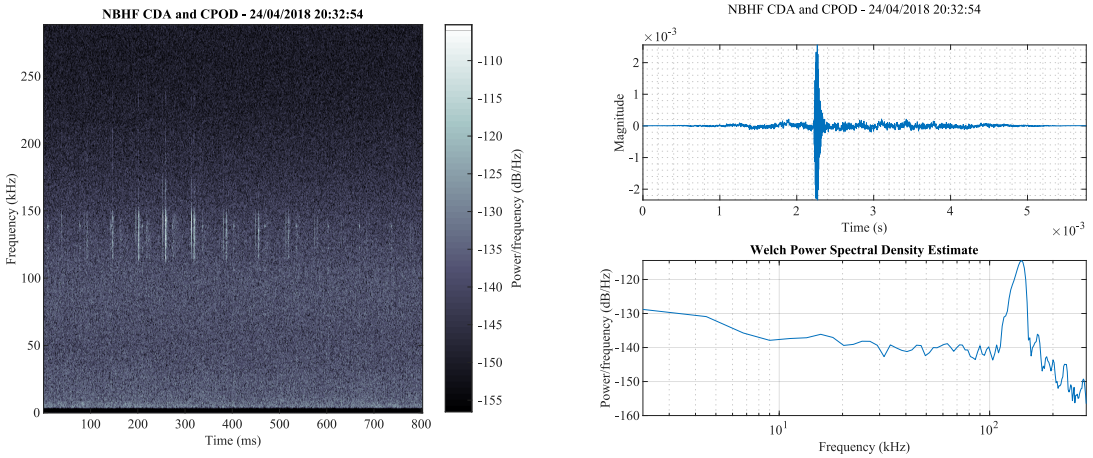

(a) Spectrogram of event. (b) Individual click analysis.

Fig. 6.25 Recording of positive porpoise (NBHF) detection result showing an agreement between C-POD and CDA algorithms.

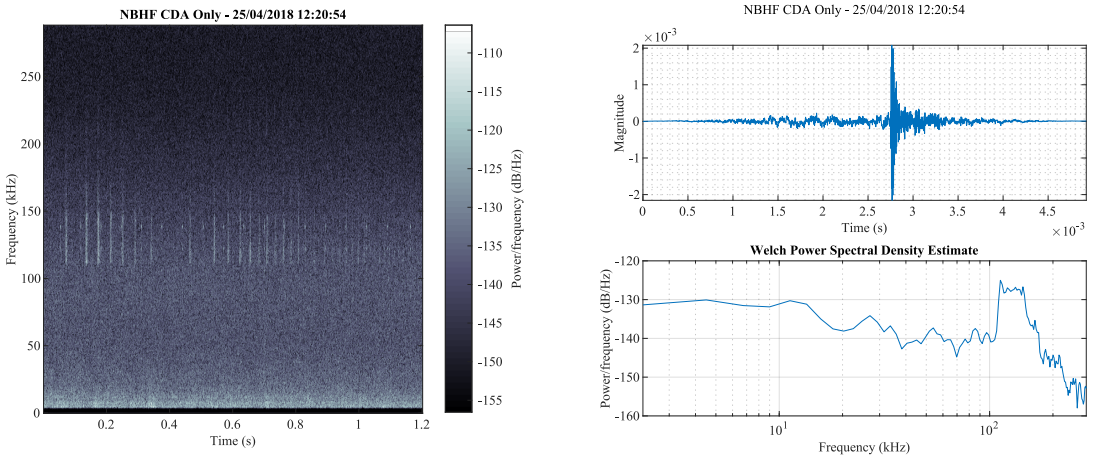

(a) Spectrogram of event.

(b) Individual click analysis.

Fig. 6.26 Recording of positive porpoise (NBHF) detection result detected by the CDA algorithm only.

6.4 Summary

This section has shown a cetacean click detection and classification algorithm. The system presented has been specifically designed to have the potential for a low energy application by using analogue electronics. This is shown by the analogue method of signal processing in the first stage of detection. Using an analogue fast and slow filter is an energy efficient way of processing a high frequency signal. Comparison of these slow and fast signals could also be achieved using an electronic comparator, thereby saving the more energy hungry digital processing to the latter stages of the algorithm. In the digital stages of the detection and classification algorithm, there are again efforts to conserve energy hungry processing. A low energy digital processing stage controls access to the higher energy stage to maximise efficiency when signals are not deemed to be suitable for access to the next stage of processing. The highest energy stage of the algorithm is the final classification based on the frequency spectrum of the signal.

Testing of the algorithm was completed using recordings of cetacean encounters. Results have shown that the algorithm is capable of detecting and isolating cetacean clicks for analysis. Detection's have then been shown to be classified into either dolphin, porpoise or sonar. Every effort in the algorithm design has been made to ensure a realistic transition to a physical system. Results have shown that when compared to a realistic system, i.e. the C-

POD, the algorithm achieved comparable results and on occasions detected more encounters. This result is debatable as there is not a definitive ground truth but the fact that the algorithm is detecting alongside the C-POD, is an encouraging result. Further investigation of the C-POD and CDA results was carried out using the time aligned audio recordings of positive events. Results have shown a strong agreement between dolphin and porpoise events when comparing the C-POD and CDA. The results have also suggested an increase in detection sensitivity for the CDA when comparing against the C-POD.

The algorithm presented is still in a Matlab phase of development and only full production into a deployable device would bring with it greater confidence in the results. This forms the future work of this section as a practical deployment alongside a ground truth would be the ultimate test of reliability and functionality. The results have shown potential when processed with real cetacean recordings.

6.5 Associated Work - NanoPAM Project

Please note - The work presented in this section was not completed by the author. However, the algorithms presented in Chapter 6 were used in the initial stages of development for the Natural Environment Research Council (NERC) sponsored NanoPAM project.

This section is included for the purposes of providing the reader with some brief context about the contribution this section has made to an associated project. The NERC sponsored NanoPAM project took place alongside the research conducted in this Chapter. The cetacean click detection algorithms investigated in Chapter 6 were further developed by research staff within SEALab. This led to the creation of custom hardware and successful sea trial [57].

Figure 6.27 shows the low power cetacean detector which is built around the NMV3 to relay data back to shore every hour. The NanoPAM was successfully deployed on several occasions in the North Sea for periods of months and produced very promising results in detecting both dolphin and porpoise.

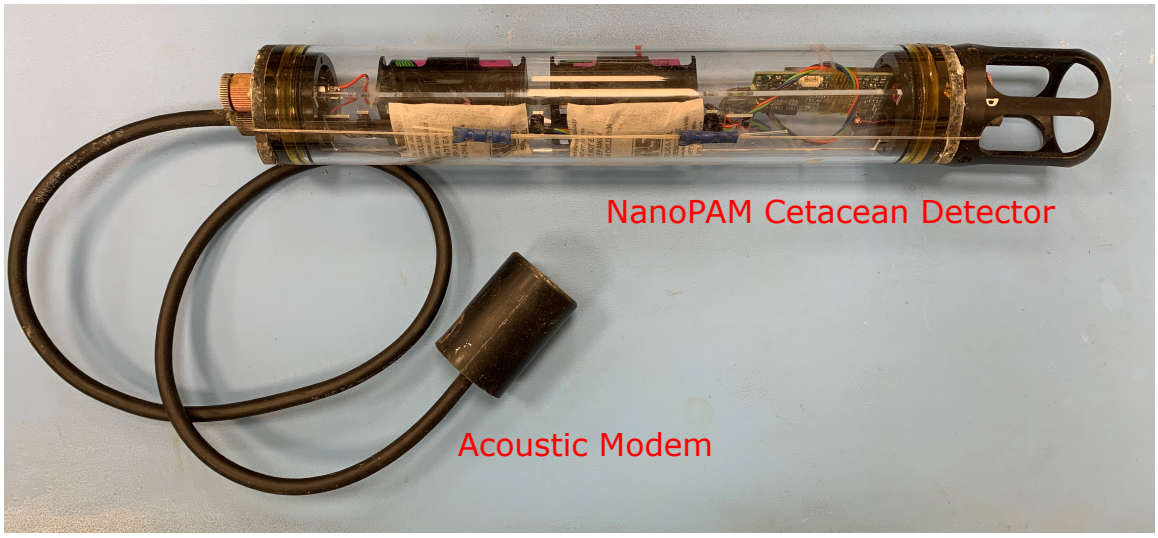

Fig. 6.27 NanoPAM Cetacean Detector with acoustic communication capabilities.

To illustrate the energy-efficiency achieved in the NanoPAM project, Figure 6.28 shows the system in detection mode under test. The figure shows that a detection algorithm based on the research presented in this Chapter has been successfully developed into workable hardware with very low power consumption. Figure 6.28 shows the detection mode consumes only 2 mW of power, which would be capable of long term deployments using only battery power.

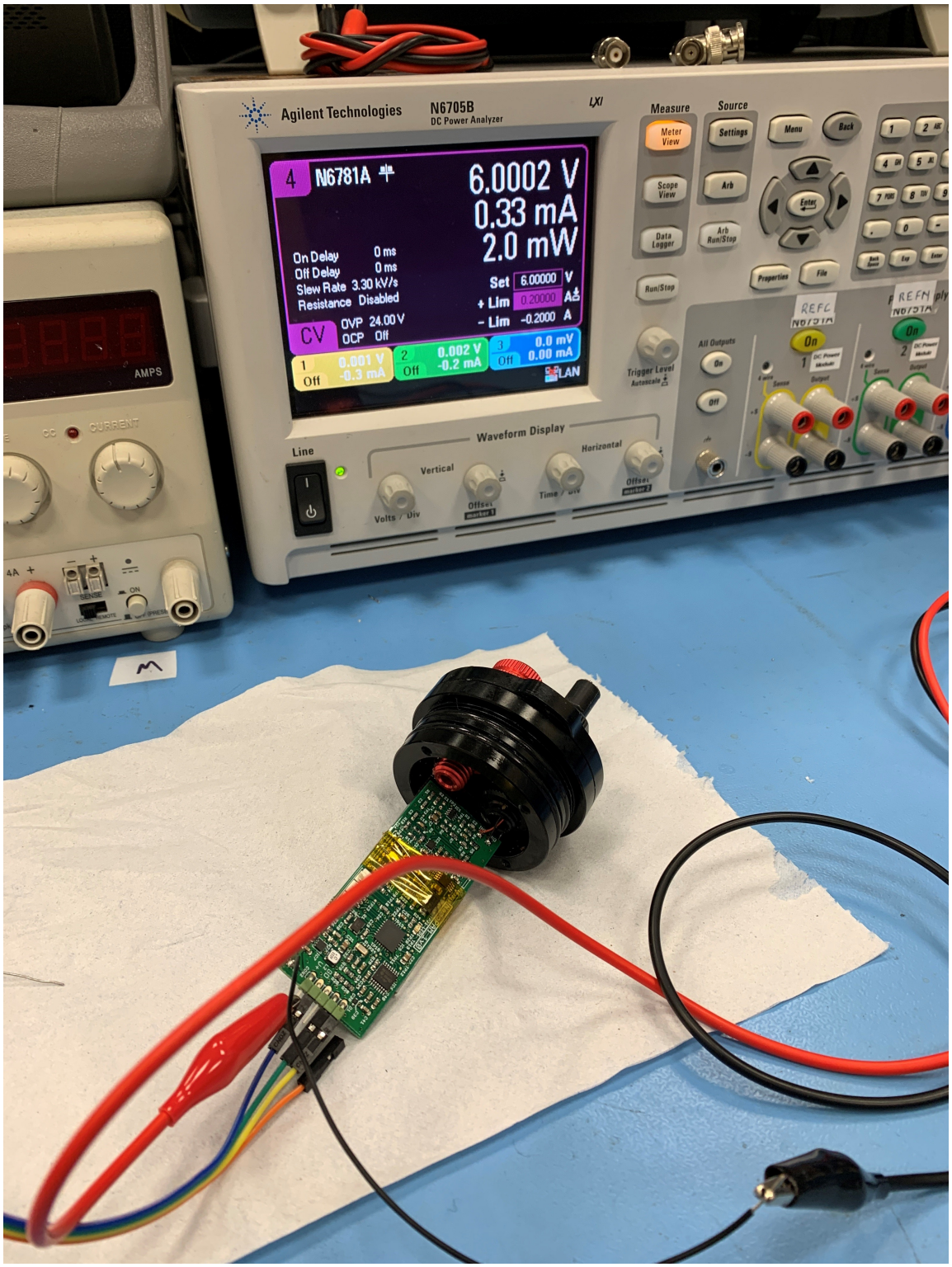

Fig. 6.28 NanoPAM PCB power consumption analysis during detection mode.

Chapter 7

Cetacean Whistle Detection Algorithm

7.1 Introduction

This chapter will present a method of automatically detecting cetacean whistles. The method presented is based on Phase Locked Loop (PLL) which has been chosen to align with the potential low-energy implementation a PLL offers. A PLL is an electronic feedback control system which enables an input signal characteristic to be matched at the output of the PLL. This is achieved by the PLL constantly adjusting to minimise the input to output error. PLL's are often used in communication to modulate/demodulate a signal, which involves minimising the phase error to synchronise transmitted and received signals.

A PLL based approach offers a realistic implementation onto a low-energy embedded processor similar to the Arm Cortex M0+ used in Chapters 4 and 5. A PLL can be implemented digitally but also in custom analogue circuits, both approaches have potential to achieve a very low power detection system.

7.2 Methods

As introduced in Section 3.3.2.2, cetacean whistle detection is an active area of research in the marine biology community. Current research tends to focus on fairly power hungry detection methods such as spectrogram image-based edge detection and data training of neural networks. This section proposes a method based on a lower power PLL approach.

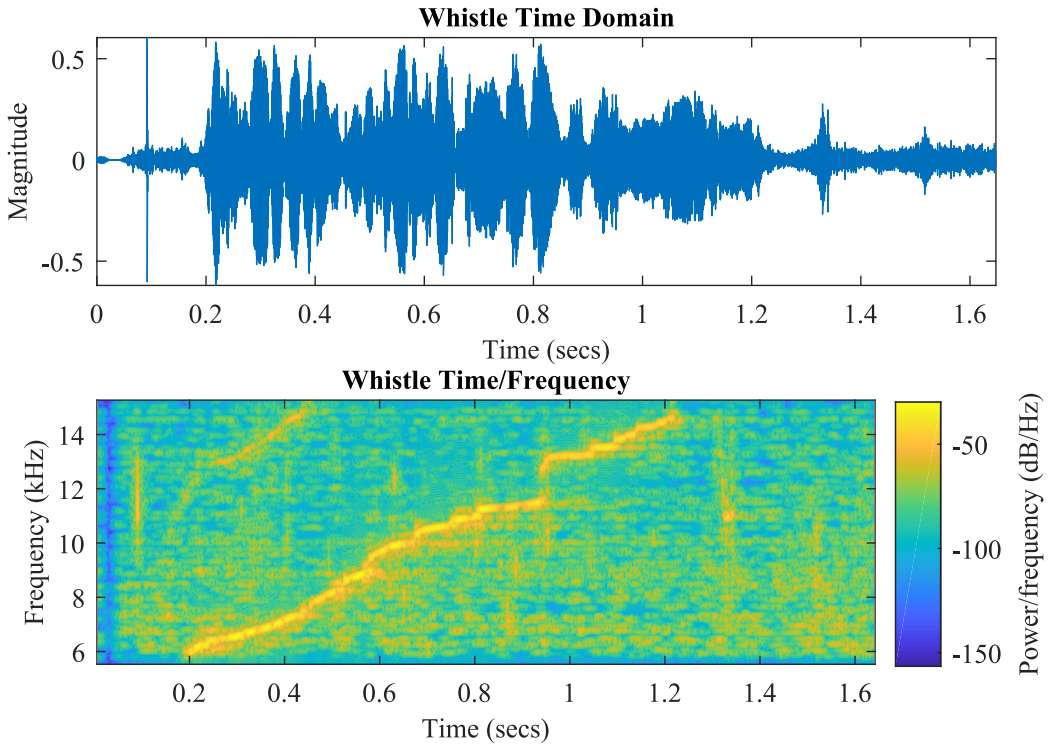

Fig. 7.1 Example of a single whistle.

As Figure 7.1 shows, a whistle consists of a fairly linear sweep in frequency over a short time period. Designing an algorithm which can track this frequency sweep in real time could enable automated detection of the whistle. This is where a PLL comes into the design of a whistle detection algorithm. A simplified block diagram of a PLL is shown in Figure 7.2.

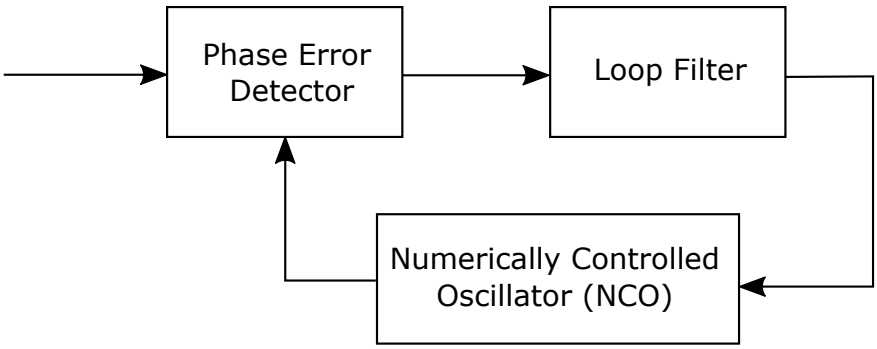

Fig. 7.2 Basic phase locked loop (PLL) diagram.

A PLL is a feedback loop control system which forces a numerically controlled oscillator (NCO) to replicate and track the frequency and phase at the input when locked. A locked

state refers to the point at which the input phase is equal to the feedback loop phase resulting in a zero phase error. At this point of lock, the input frequency must equal the feedback loop frequency. This means that a PLL alongside a custom detection algorithm has the potential to track and classify a cetacean whistle.

7.2.1 Whistle frequency tracking using Phase Locked Loop technique

Figure 7.3 shows an overall diagram of the signal conditioning and PLL stages of the Matlab based whistle detection algorithm. This diagram is broken up in subsequent sections to provide more detail, which then leads on to the detection algorithm itself.

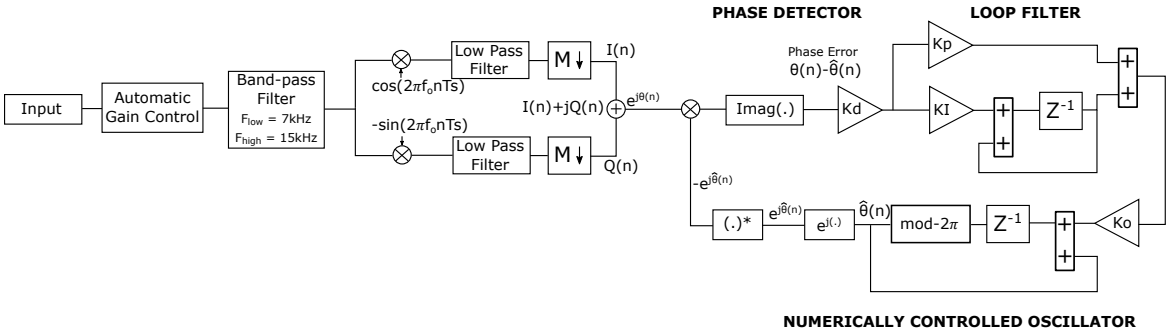

Fig. 7.3 System diagram of the signal conditioning and PLL stages of a Matlab based cetacean whistle detection algorithm.

- Input Signal - The input stage represents the sampled audio signal which is set up to capture all of the whistle frequency band. In this example the sample rate is set at 96 kHz which captures all of the energy upto the 48 kHz Nyquist limit.
- Automatic Gain Control (AGC) - During testing of the whistle detection algorithm, it was observed that one of the limiting factors was frequency selective fading in the input signal. Frequency selective fading is when the input signal reaches the receiver via multiple paths causing partial cancellation of the signal. Figure 7.4 shows how fading can impact the performance of the PLL to track the frequency. The red circle in Figure 7.4 show the point in which the PLL loses its lock due to a fade in the spectrogram.

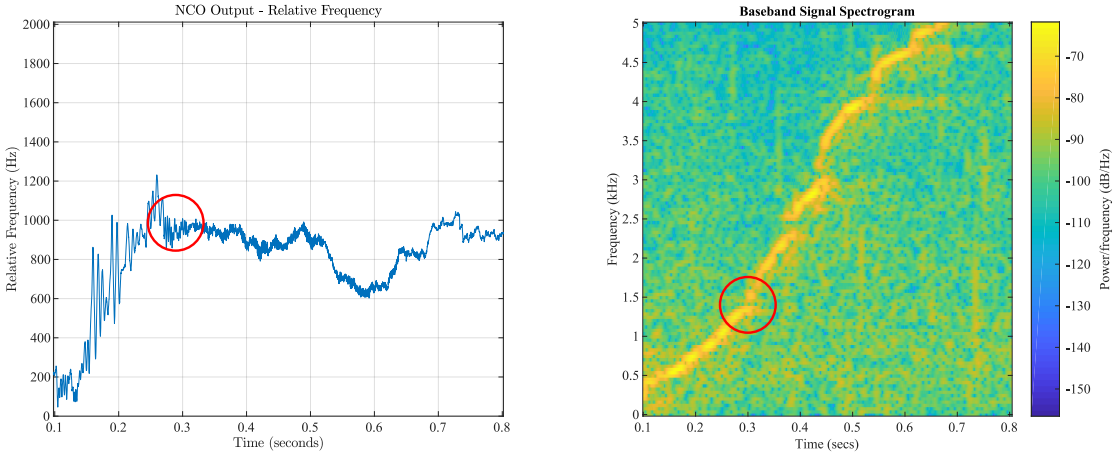

(a) Tracked frequency of the PLL

(b) Spectrogram of the input signal

Fig. 7.4 Cetacean whistle processed by PLL without using AGC on the input signal.

Using AGC, the input signal is amplified during this period of fading, which aims to keep the PLL in a locked state. When the PLL is locked, it is tracking the frequency of the whistle, which is the basis of the later described detection algorithm. Using the same input signal, this time modified to include AGC, Figure 7.5 shows that the entire whistle is now successfully tracked.

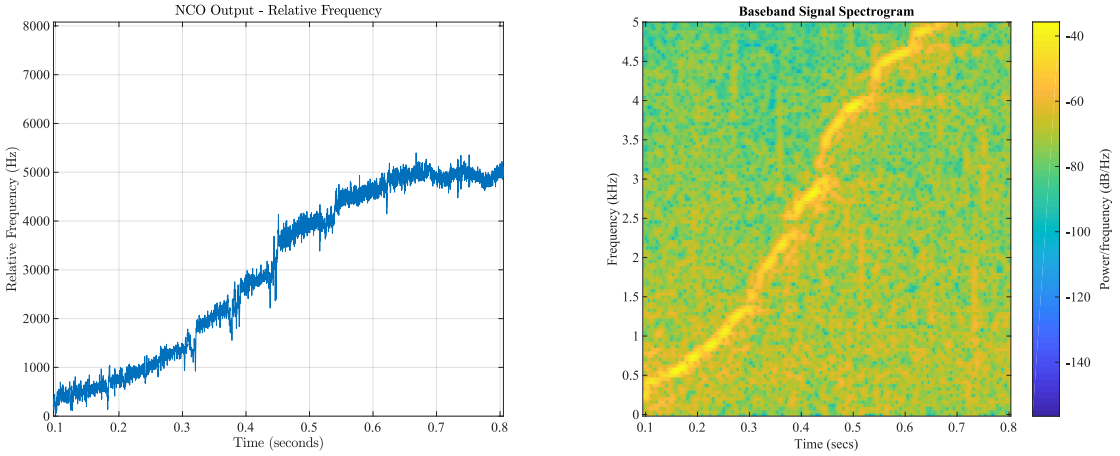

(a) Tracked frequency of the PLL

(b) Spectrogram of the input signal

Fig. 7.5 Cetacean whistle processed by PLL with AGC added to the input signal.

- Band Pass Filter - This stage is used to isolate the band of interest for the whistle the user is aiming to detect. There are many variations of the whistle signals created by different cetacean species [88]. This is one of the stages which can be used to tailor the algorithm to a specific species of interest.

- Complex Baseband Signal - In this stage the input signal is passed through a quadrature modulator. Using two orthogonal signals ($cos(2\pi f_o nTs)$ and $-sin(2\pi f_o nTs)$) ensures that all of the input signal energy is received. The term f_o refers to the local oscillator frequency, which is set to the lowest frequency that the PLL is required to lock onto (7 kHz in this example). The two low pass filters are required to remove the high frequency component resulting from the previous stage's orthogonal signal multiplications. The low pass filter stop band is set just above the signal bandwidth of input signal ($F_{high} - F_{low} = 6$ kHz in this example).

- Phase Detector - The phase detector is implemented using a complex multiplication of $e^{j\theta(n)}$ and $e^{-j\hat{\theta}(n)}$, as illustrated in Figure 7.6. The imaginary part of the multiplication result represents the phase difference of $\theta(n) - \hat{\theta}(n)$. The final term K_d is phase detector gain which can be set by the user during the tuning process of the PLL.

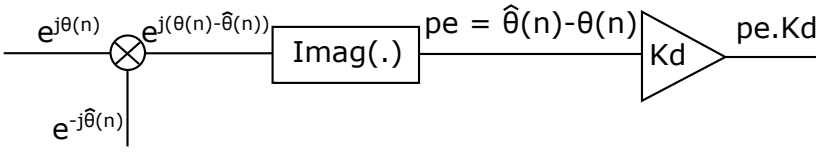

Fig. 7.6 Phase detector stage of the cetacean whistle detection algorithm.

- Loop Filter - As shown in Figure 7.7, the loop filter is a proportional-plus-integral second order filter. Terms K_p and K_i are the proportional and integral gain of the loop filter respectively. These are set as part of the tuning process which is covered next in Section 7.2.2. The output of Figure 7.7 is $V(n)$, which is the control signal which drives the next stage.

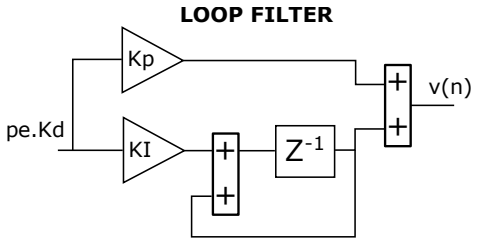

Fig. 7.7 Loop filter stage of the cetacean whistle detection algorithm.

- Numerically Controlled Oscillator (NCO) - The NCO contains an integrator (alongside the loop filter integrator which means this is a Type 2 PLL) which accumulates the phase difference from the previous stage. This produces a local copy of the phase of the incoming signal, which is then made to be a complex conjugate ready to feedback to the phase difference multiplier.

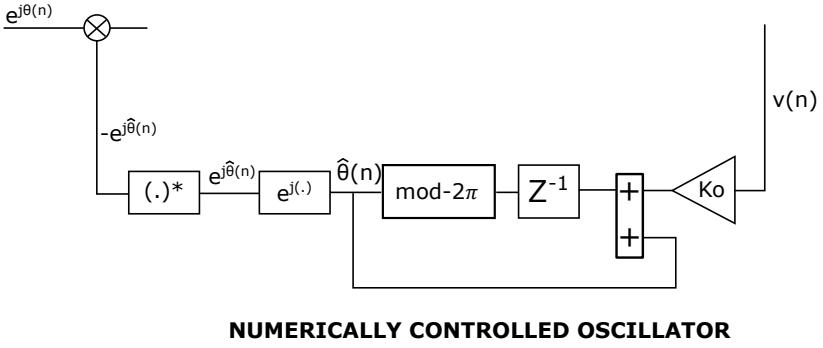

Fig. 7.8 Numerically controlled oscillator stage of the cetacean whistle detection algorithm.

7.2.2 Phase Locked Loop Tuning

Tuning of the PLL is essential to control the response at the output and to minimise the phase error. There are four tuning parameters used in the whistle detection algorithm:

- Phase detector gain K_d.
- NCO gain factor K_o.
- Loop Noise Bandwidth B_n.
- Damping factor ζ.

The relationship between these tuning parameters must now be derived so that they can be understood and used within the whistle detection algorithm. The diagram in Figure 7.9 shows a second order digital PLL with proportion plus integral loop filter derived using Figure 7.3. Using the basic relationship between input and output, the open loop transfer function can be derived as shown in 7.1.

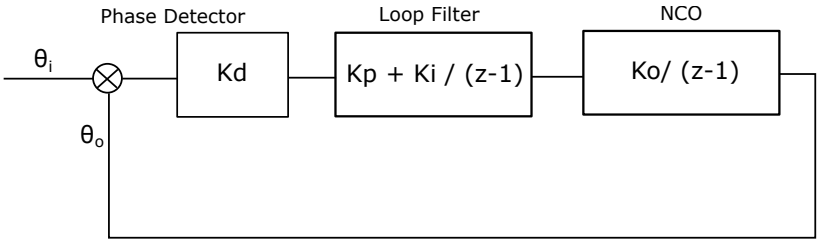

Fig. 7.9 Digital PLL with proportional plus integral loop filter in z-domain.

$$G(z) = \frac{K_d K_p K_o}{(z-1)} + \frac{K_d K_i K_o}{(z-1)^2} \tag{7.1}$$

Using basic control theory, the closed-loop transfer function of the PLL can be expressed using equation 7.2.

$$H(z) = \frac{\theta_o(z)}{\theta_i(z)} = \frac{G(z)}{1+G(z)} = \frac{\frac{K_d K_p K_o}{(z-1)} + \frac{K_d K_i K_o}{(z-1)^2}}{1 + \frac{K_d K_p K_o}{(z-1)} + \frac{K_d K_i K_o}{(z-1)^2}} \tag{7.2}$$

To find expressions for K_p and K_i, the discrete open loop transfer function in equation 7.1 is equated with a continuous-time equivalent second order system which has been converted to z-domain. The s to z domain conversion of the loop filter and NCO are shown in equations

7.3 and 7.4. The s to z domain was carried out using the backward difference method shown in equation 7.5.

$$LoopFilter = \frac{2\zeta\omega_n + \omega_n^2}{s} = \frac{2\zeta\omega_n + T_{s(filt)}\omega_n^2}{(z-1)} \tag{7.3}$$

$$NCO = \frac{1}{s} = \frac{T_{s(nco)}}{(z-1)} \tag{7.4}$$

$$s \rightarrow \frac{(z-1)}{T_s} \tag{7.5}$$

The open loop transfer function of the continuous-time second order system converted to z-domain is shown in equation 7.6.

$$G(z) = \frac{2\zeta\omega_n T_{s(nco)}}{(z-1)} + \frac{T_{s(filt)}T_{s(nco)}\omega_n^2}{(z-1)^2} \tag{7.6}$$

Equating equations 7.1 and 7.6 gives the relationship in equation 7.7.

$$\frac{K_d K_p K_o}{(z-1)} + \frac{K_d K_i K_o}{(z-1)^2} = \frac{2\zeta T_{s(nco)}}{(z-1)} + \frac{T_{s(filt)}T_{s(nco)}\omega_n^2}{(z-1)^2} \tag{7.7}$$

Equating each side of equation 7.7 enabled expressions to be formed for K_p and K_i as shown in equations 7.8 and 7.9.

$$K_p = \frac{2\zeta\omega_n T_{s(nco)}}{K_d K_o} \tag{7.8}$$

$$K_i = \frac{\omega_n^2 T_{s(nco)} T_{s(filt)}}{K_d K_o} \tag{7.9}$$

A second order, type 2 (number of intergals) PLL has a noise bandwidth defined by equation 7.10 [34].

$$B_n = \frac{\omega_n}{2}\left(\frac{1}{4\zeta} + \zeta\right) \tag{7.10}$$

Substituting equation 7.10 into equations 7.8 and 7.9 results in an expression for K_p and K_i in terms of the loop noise bandwidth B_n and damping factor ζ. This is shown in equations 7.11 and 7.12.

$$K_p \approx \frac{1}{K_d K_o} . \frac{4\zeta B_n T_{s(nco)}}{\zeta + \frac{1}{4\zeta}} \tag{7.11}$$

$$K_i \approx \frac{1}{K_d K_o} . \frac{4\zeta B_n T_{s(nco)} T_{s(filt)}}{\left(\zeta + \frac{1}{4\zeta}\right)^2} \tag{7.12}$$

The PLL can now be tuned using phase detector gain K_d, NCO gain factor K_o, loop noise bandwidth B_n and damping factor ζ. The first two tuning parameter offer fixed gain control whereas the impact of changing tuning parameters B_n and ζ is illustrated in Figure 7.10.

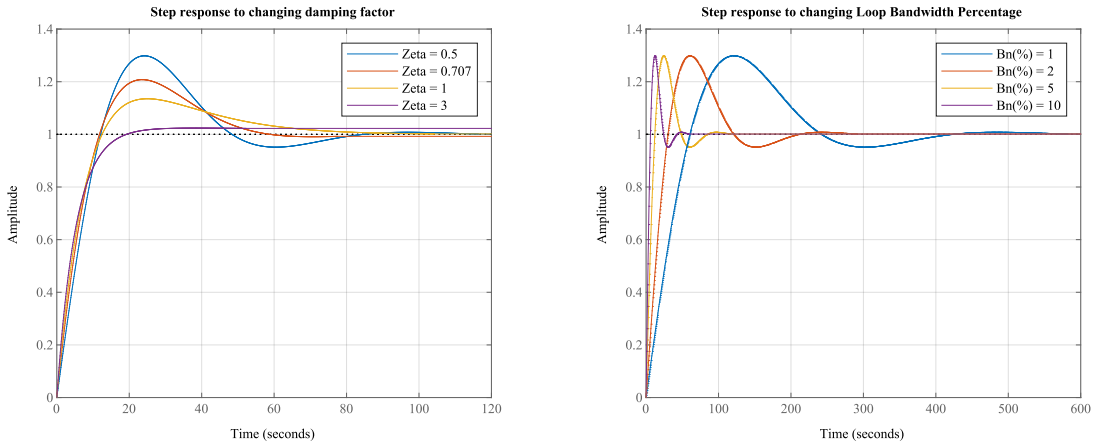

(a) Step response - damping factor ζ (b) Step response - loop bandwidth B_n

Fig. 7.10 Illustration showing the impact of changing whistle detection tuning parameters B_n and ζ.

The impact of changing B_n and ζ can be summarised as follows:

- A small B_n rejects more noise but limits the frequency range that can be tracked.
- A large B_n acts in opposite manner, rejects less noise but can track greater frequency range.
- A large ζ reduces overshoot but increases convergence time in the PLL frequency response.
- A small ζ converges faster but increases overshoot.

7.2.3 Whistle Detection Algorithm

Using a PLL to track the incoming signal frequency is not enough to automate the detection of whistles. This section presents the whistle detection algorithm decision making process and user controlled thresholds. The thresholds included in the algorithm enable the user to tailor detections to specific cetacean signature whistles. The user defined thresholds are as follows:

- Linger frequency threshold - frequency at which a timer is started to track how long a frequency is lingering.
- Linger duration - time at which to reset the PLL as the frequency has lingered for too long above the set threshold.
- Minimum Duration Threshold - this is used to stop detection arrays which are too short to be a whistle being passed to the SEOE test and therefore discounting them from progressing any further.
- Reset frequency - PLL is reset if frequency reaches this limit (i.e. if the whistle is tracked to its expected highest frequency it will reset the PLL).
- SEOE - when a linear fit is applied to a tracked frequency sweep, the SEOE is a measure of how well the linear fit matches the data.
- Linear Fit Gradient - the linear fit must have a gradient representative of a whistle (i.e. if the fit was horizontal it would be a tone and not a frequency sweep).

To best explain what each of the user defined thresholds relate to, Figure 7.11 shows an example whistle with illustrations for each threshold.

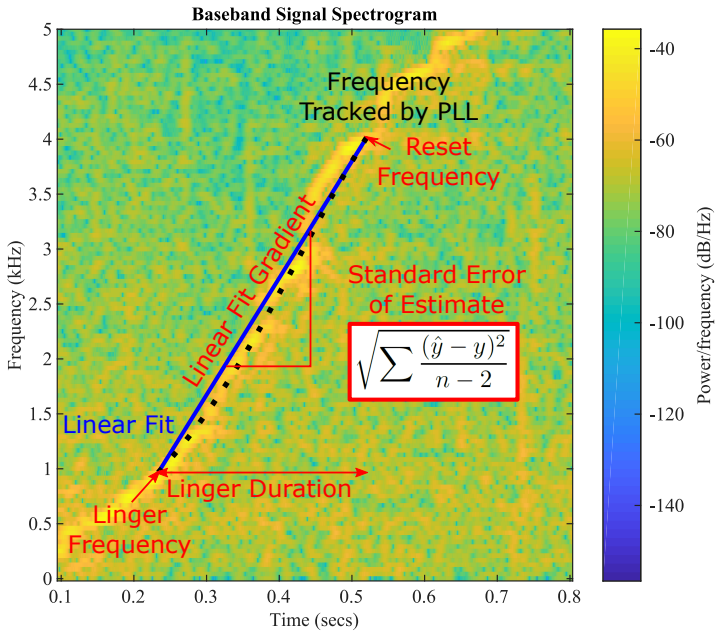

Fig. 7.11 Illustration of the user defined tuning parameters for the whistle detection algorithm.

The decision making process is best described in Figure 7.12. This shows the NCO relative frequency input with each of the decisions made. The final result is a whistle detection once each stage has been satisfied.

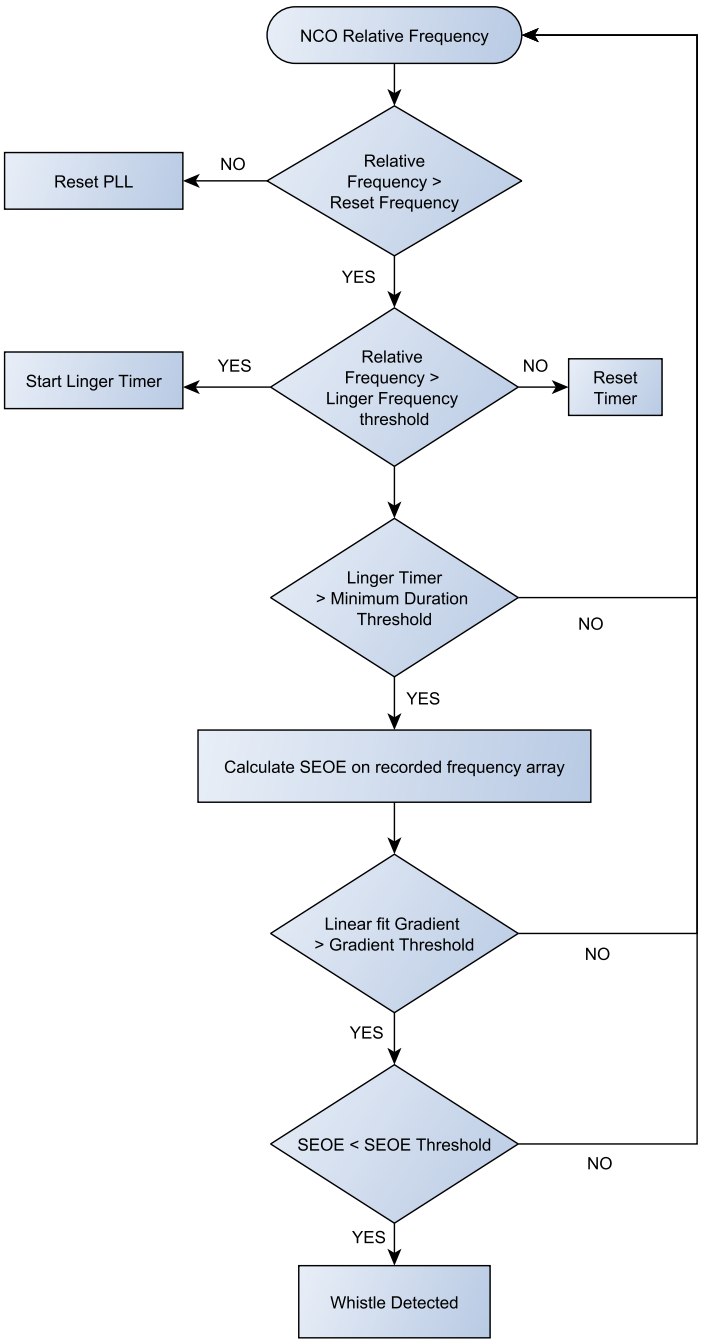

Fig. 7.12 Flowchart showing the decision making process of the whistle detection algorithm.

7.3 Results

The results presented for whistle detection are all based on offline processing of signals. In the first instance a artificial signal has been created to help develop the detection algorithm.

In the second instance, a recording of cetacean activity is processed using the detection algorithm.

7.3.1 Artificial Cetacean Whistles

In this section, an artificial whistle has been created with similar attributed to actual cetacean whistle. As shown in Figure 7.13, a repeating frequency sweep ranging from 7 to 14 kHz, each lasting 0.6 seconds, has been created. The sample rate for the artificial signal is 96 kHz. A real cetacean whistle may vary in frequency and linearity, but this signal is a good representation of the general shape of a whistle in the frequency domain.

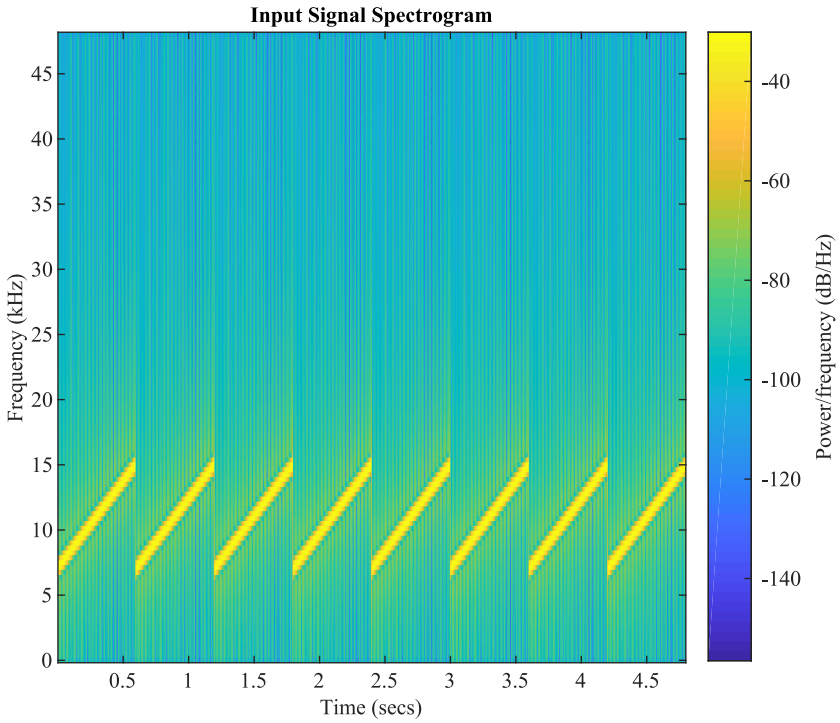

Fig. 7.13 Spectrogram of a artificially created cetacean whistle. It is a linear sweep in frequency between 7 and 14 kHz lasting 0.6 seconds.

Once the signal has been processed through the first stages of the detection algorithm (as discussed in Section 7.2.1), the signal is now at baseband. This is illustrated in the spectrogram in Figure 7.14. The previous frequency sweep in Figure 7.13 is now in the 0 to 7 kHz range.

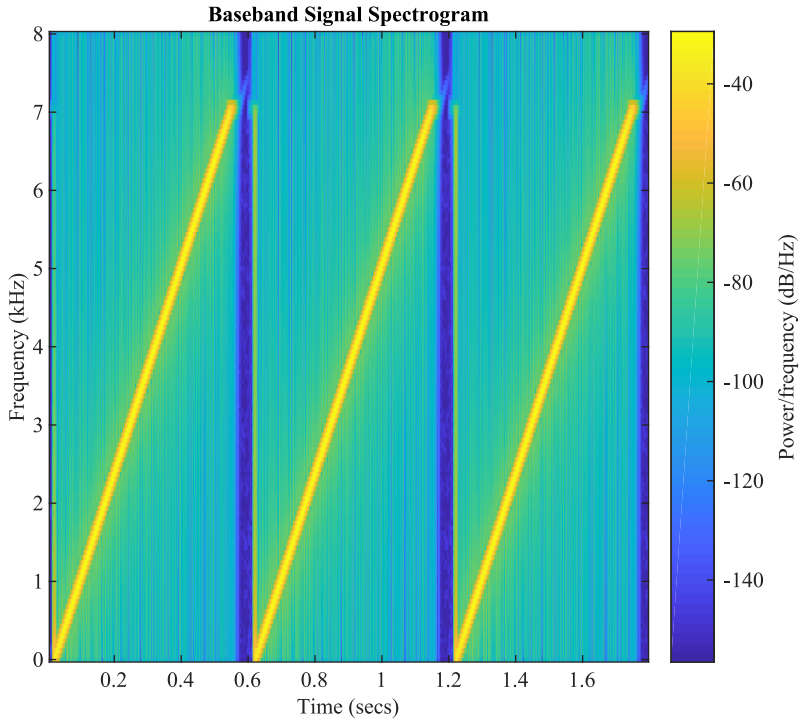

Fig. 7.14 Spectrogram of the input signal once processed by the detection algorithm. The frequency sweep is now at baseband and has been downsampled.

Detection of the artificial whistles is illustrated in Figure 7.15. The results show the output at various stages of the PLL, with a positive result indicated by the red lines in the lower plot. Each of the red lines represents a linear fit, which was deemed acceptable by each of the user defined threshold built into the algorithm. An acceptable linear fit indicates a positive whistle detection.

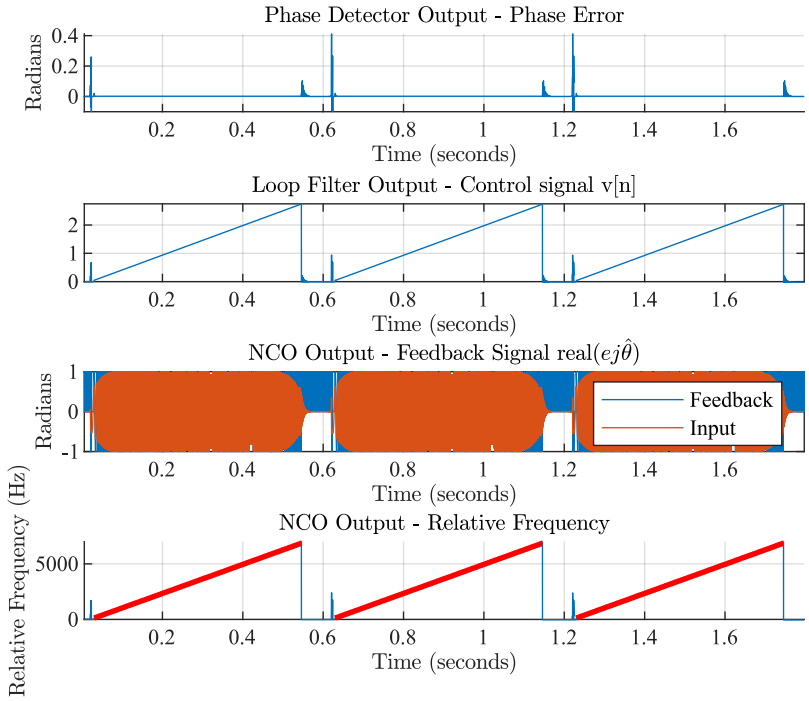

Fig. 7.15 Whistle detection algorithm result using artificially created whistle like signals.

Using artificial whistles has helped to develop and test the detection algorithm. However, it is no substitute for using real cetacean signals which are often filled with challenges such as noise interference.

7.3.2 Real Cetacean Whistles

In this section a real recording of cetacean activity is processed using the detection algorithm. Figure 7.16 shows the spectrogram of the recording with a zoomed in view to confirm there are whistles present.

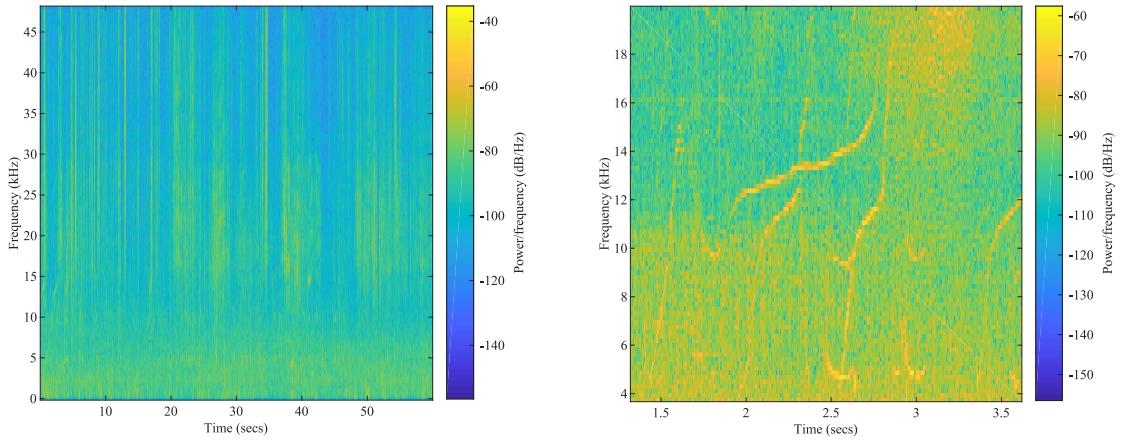

(a) Cetacean Activity

(b) Expanded Cetacean Whistle

Fig. 7.16 Spectrogram of cetacean activity including a expanded view of a cetacean whistle.

The recording is extremely active with whistles and click trains often overlapping in time. To evaluate the effectiveness of the detection algorithm the recording has been manually examined to determine how many clear whistles are present. The examination revealed 25 whistles were present and thought to be detectable. Figure 7.17 shows the result of processing the recording through the detection algorithm. The red lines in the lower plot show that 19 out of 25 whistles where detected using the algorithm.

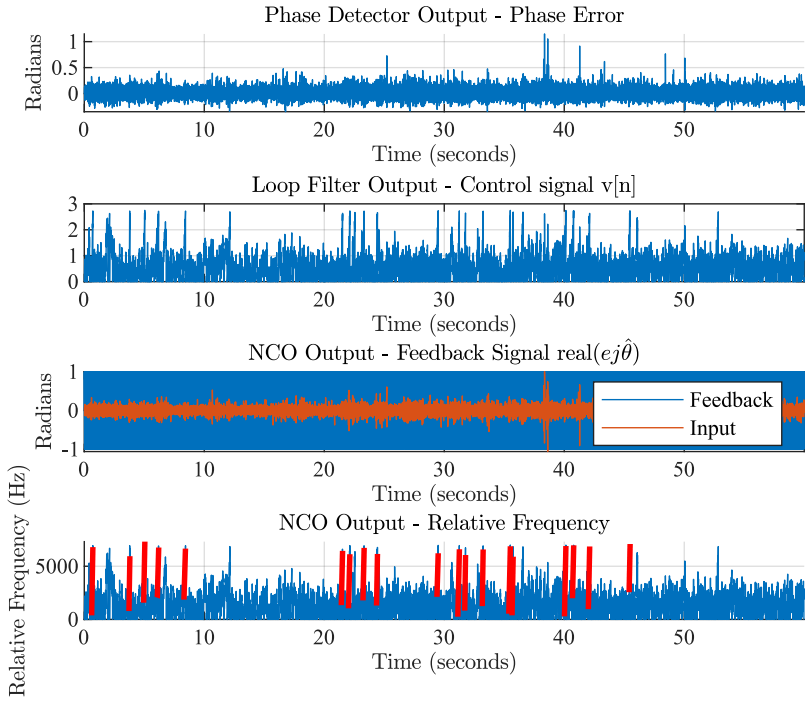

Fig. 7.17 Whistle detection algorithm result using a real recording of cetacean activity.

To highlight what a single whistle detection looks like at each stage of the PLL, Figure 7.18 contains an expanded view on one of the 19 whistles detected. As shown, the PLL tracked the frequency of the whistle between approximately 100 Hz and 55.5 kHz.

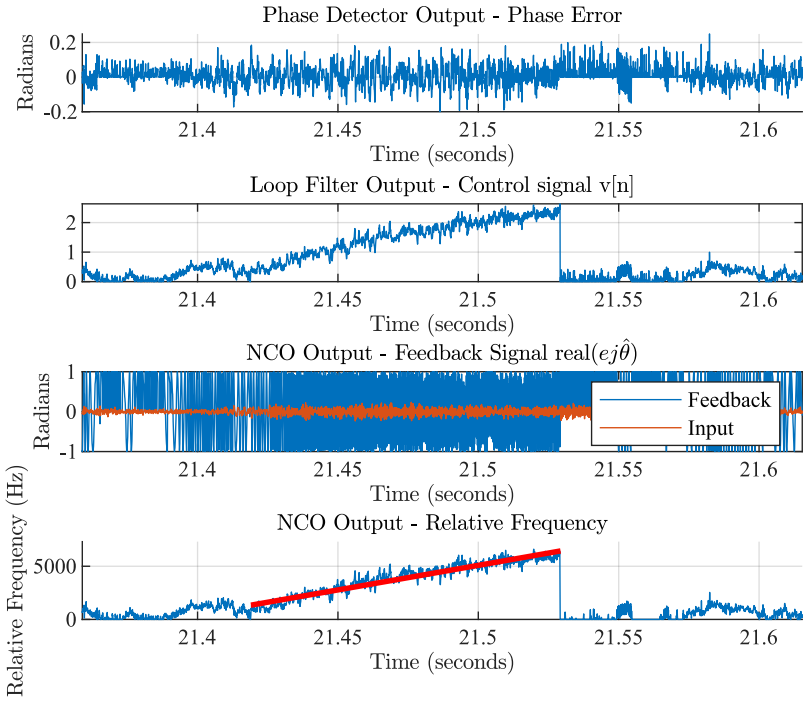

Fig. 7.18 Example of a successfully detected whistle result.

The detected whistle relating to Figure 7.18 is shown in the spectrogram in Figure 7.19. This shows the frequency versus time of the actual signal that the PLL has successfully locked onto and tracked.

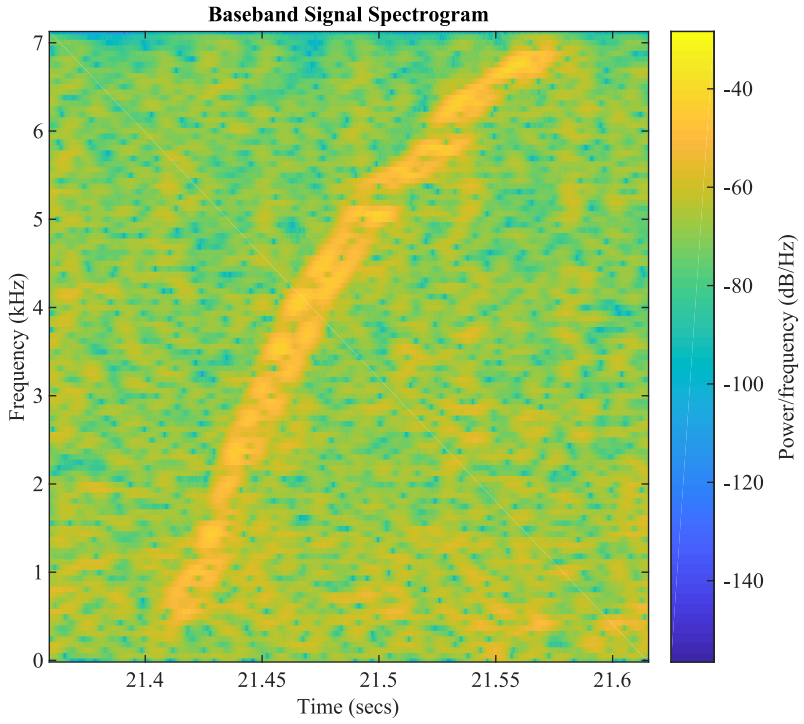

Fig. 7.19 Spectrogram of a detected whistle.

As previously stated the detection algorithm missed 6 out of 25 whistles. An example of a missed whistle is shown in the result in Figure 7.20. As the NCO output relative frequency shows, the PLL lost its locked state around 23.36 seconds.

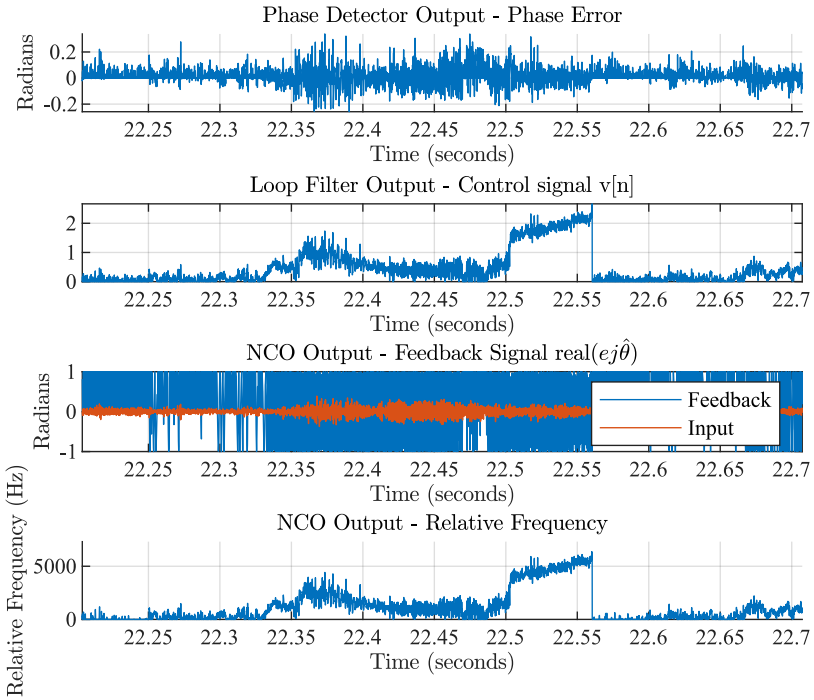

Fig. 7.20 Example of a missed whistle event result.

To further investigate why the PLL lost its locked state, Figure 7.21 shows the spectrogram of the missed whistle event. The spectrogram shows an overlap of a downward frequency sweep closely followed by the upward whistle. This close proximity of high magnitude event has caused the PLL to lock onto the whistle at around 22.5 seconds. This has shortened the length of the whistle in the eyes of the algorithm and placed the event over the minimum threshold for a positive whistle event. Therefore, further tuning of the algorithm's thresholds could help to resolve this missed whistle. However, a balance must always be struck to mitigate against potential false positive events.

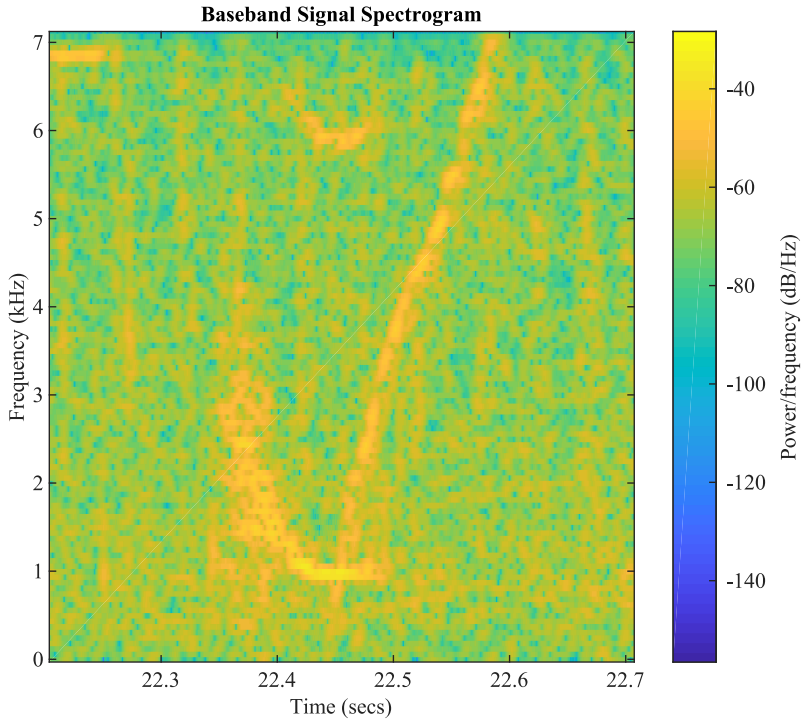

Fig. 7.21 Spectrogram of a missed whistle event.

7.4 Summary

This section has shown an automated whistle detection algorithm based on a PLL methodology. The PLL has been used as a low-energy means of tracking the frequency of an input signal. Using this tracking feature a detection algorithm has been built to identify whistle-like signals.

The results have shown the ability of the detection algorithm to track and single out artificially created whistles. These are signals representative of a whistle that are free from noise and interference. This allowed the refinement of the algorithm but did not provide confidence in a realistic environment. To achieve this confidence, real recordings of cetacean activity are used in offline processing of the algorithm. These recordings contain whistles but also high frequency clicks as well as general background noise. Results showed that when a recording of 25 identifiable whistles was processed, 19 whistles where automatically detected by the algorithm. This is an encouraging result as over 75% of the whistles where identified amongst all of the interfering signals. Results also showed examples of the missed whistles and offered potential explanations for these results.

One of the most difficult scenarios for whistle detection is when multiple whistles overlap each other. This causes a very random spectrogram with no single, trackable sweep in frequency. This is one area which forms part of the future work for this project. This is an important area to research further as we cannot assume a single whistle will occur.A method of dealing with multiple whistles would reduce the chance of producing a false negative result.

The strengths of this experiment are the realistic low-energy methodology used for detection and the production of results using real cetacean recordings. Due to the time constraints of this project, a physical device has not been created to deploy at sea. This would have enabled long term deployment and much larger data sets to analyse. As with all passive detection algorithms, the performance must always be measured with the best ground truth available. Although this experiment was measured against human analysis of the recording to measure the number of whistles, a more robust ground truth would have been more favourable. There are detection algorithms in literature which use high processing powered image recognition methods for detection whistles. This may be a better less debatable ground truth as two human operators may have different interpretations of identifying a positive whistle event.

The future work for cetacean whistle detection would be to produce a deployable piece of hardware which encompasses the detection algorithm. Long term deployment of this system would provide large data sets with which to analyse and improve upon the method of detection.

Chapter 8

Conclusion

This chapter brings together all of the results and conclusions of the technical chapters included within the thesis. A discussion of the thesis as a whole is included alongside the identified future works of this project.

The overall aim of the project is to investigate and design low energy passive acoustic detection algorithms for underwater acoustic targets. These are algorithms which can be implemented in hardware and achieve long duration deployments in harsh sea conditions. The systems are to be integrated with the NMV3 to afford real time communication of data through a network of underwater nodes. Evaluation of the algorithms is completed by measuring against the best available ground truth. This is to gain confidence in the results produced during field trials. The conclusions drawn from this research have been grouped into the two main detection/classification targets.

8.1 Vessel Detection/Classification

The main aims of the vessel detection/classification research presented in this thesis are:

- Develop passive acoustic vessel detection algorithms that can be implemented with very low energy processing (of the order of 10 mW).
- Compare different approaches with mixtures of analogue and digital processing, continuous and duty-cycled sampling/processing.
- Adapt an existing low cost/power acoustic modem platform (NMV3) to implement a wireless vessel detection device.
- Demonstrate underwater acoustic transmission of vessel detection information.

- Evaluate system performance in a realistic offshore environment.

The background research in Chapter 2 shows that sound is created by a propeller during cavitation and this signal can be exploited for the purposes of passive acoustic detection/classification of vessels. Current technology such as the AIS is shown to lack the ability to identify vessels which may not want to be visible. The motivation for this research is shown to be predominantly related to safety. This is safety for humans in vessels and also to protect shorelines from potential threats. If you know a vessel is there, action can be taken if required.

The literature review in Chapter 3 shows a detailed overview of the current vessel detection instrumentation used by end users. As stated there are a variety of approaches to detect/track a vessel such as RADAR, air surveillance, passive acoustics, AIS and Active SONAR. The review presented aims to focus on approaches which are realistic for low energy applications. Passive acoustics is identified as the most suitable methodology for low energy. The review shows both wired and wireless passive acoustic monitoring systems which have been targeted to vessel detection. It is shown that there are limiting factors in both approaches. A wired system has a limited deployment area and can often be expensive to install. A wireless approach allows for a wider deployment range, however, if data is stored locally then it has the potential to get lost at sea. A system which relays data in near real time would address this problem.

Chapter 3 also contains a review of the latest detection/classification algorithms used by researchers for passive acoustic vessel monitoring. The review shows that there are two main approaches to vessel detection which are wavelet analysis and DEMON. Both approaches show that they are both capable of detecting vessels and can do so in a reasonably reliable manner. The main caveat identified is that wavelet analysis does not easily fit within a low energy system. The DEMON method is shown to be a reliable method of detecting vessels and has the potential to be applied using carefully designed low energy signal processing techniques. On the classification side of vessel monitoring, the literature review shows that a neural network approach can identify distinguishing features using a large training data set. However, this approach would not be realistic on a battery powered device and the DEMON method looks to be a better option. The review shows that features related to the vessel such as shaft/engine rate, number of propellers and blades, and engine firing rate can be identified using the spectral data.

The results presented in Chapter 4 and 5 shows that vessels can be detected using a low energy passive acoustic detection algorithm. The majority of the results relate to the CADD mode. In this mode results have shown that the system is capable of detecting the key target vessel type which is a RHIB. In this controlled experiment, passive detection

was achieved by the algorithm with the additional benefit of extracting classification related information. Results showed that the DEMON spectrum peaks indicated the number of blades and inspection of the vessel confirmed this was accurate.

After numerous shoreline deployments, the system was deployed in open water for the first long duration field trial which provided 84 days of data. This was enabled using an array of custom infrastructure such as AIS received station and Wi-Fi enabled data buoy. The results showed that the detection of a single vessel was achieved. The data received by the detection algorithm also showed that separation of multiple vessels in the same time period was a possibility by interpreting the peak frequency data. It was shown that two vessels can show notable different consistent peak frequency data in the DEMON spectrum. This allows for a decision to be made that there two signals are likely to be coming from two different vessels. Using the AIS data as a ground truth this was confirmed to be the case.

The most important factor to an end user when choosing a passive acoustic vessel detection system is whether or not the system is reliable. This is reliability both in the detection results but also includes the enclosure and resilience against external factors such as weather related noise. Using the detection data collected, cross referenced with local meteorological data, results showed that the detection algorithm performed well under severe weather conditions.

The overall reliability of the system in terms of detection results is measured using the best available ground truth, which is AIS data. This showed that for the 84 days of data, 94% of detection results could be corroborated with local AIS data. This is a very encouraging result but there is not legal requirement for certain vessels to carry and AIS system. This creates a margin of potential error, however, in the absence of a absolute ground truth the use of AIS is seen to be the best available for a long duration field trial.

The system was deployed for a total of 84 days and in this time there were no failures of the enclosure. Moreover, the embedded software and custom circuitry proved robust over the duration of the field trial without any human intervention required. The results also confirmed one of the key factors in this project which is that the system is indeed low energy. The results showed that the detector could be deployed for several months using only four C battery cells. The average power consumption was measured to be 11.4mW during detection mode. This confirmed that all of the low energy design constraints had been successful.

As the vessel detector was designed to operate as part of a distributed underwater network, cost was a key factor. The results have shown the re-purposing/sharing of the SEALab developed acoustic modem. Only a small addition signal processing PCB was added to convert a communication only device into a dual purpose passive sensing/communication system.

An alternative mode from the previously presented CADD mode was also developed and is shown in Chapter 4. The NCDD mode is shown to operate in a duty cycled approach using a full digital signal processing detection method. Although the impact of Covid-19 hampered the planned open sea field trials of this mode, there were some laboratory based experiments carried out. Results showed that for the same average power consumption as the CADD mode, the NCDD mode was able to detect vessel like signals at a level 5.4 dB lower than the CADD mode. This is due to the improved performance of the digital envelope detection and filtering stages in the NCDD mode. This improved sensitivity has the potential to increase the detection radius and identify vessels further away from the node. In addition, an NCDD representative Matlab based algorithm has been shown to detect vessels much earlier than the CADD mode. This shows the potential for improved detection performance in the NCDD approach.

The results in Chapter 5 show an example of the vessel detector capturing a real world event. The United Kingdom was placed into lockdown in March 2020 and the detector was still deployed in the North Sea communicating its detection data. The results show that the number of vessels detected greatly reduced when lock down was enforced. This reduction was corroborated by the NIFCA who aligned this event with the closure of local fisheries markets.

One of the main pitfalls in PAM is false positive results where a non vessel signal source is able to fool the detector. Chapter 5 shows an example of a potential false positive created by a cetacean vocalising slowly spaced clicks. The discussion suggest the potential methods of rejecting these potential false positive events. It also shows that if these false positive cetacean related events are consistent it may afford the possibility to include this as a detectable target within the detection algorithm.

The final section of Chapter 5 attempts to validate the vessel detector using all available ground truth sources of data. This includes the use of local AIS data alongside an underwater acoustic recorder situated on the same mooring as the vessel detector. Results show that in one of the positive detection events received by the algorithm, there is positive corroboration with local AIS data as well as off-line processing of the raw acoustic recording. This agreement between detection algorithm, local AIS and off-line processing of the raw data is the best available means of validation possible in this experiment. The results also gave an indication on the SNR required by the vessel detector to trigger a positive event. Results also showed how this compared with the offline processing of the raw audio carried out in Matlab. As expected the Matlab based algorithm was shown to detect the vessel at an earlier point in time and at a lower SNR.

8.2 Cetacean Monitoring

The main aims of the cetacean detection/classification research presented in this thesis are:

- Reliably detect cetacean acoustic signals (whistles or clicks).
- Transmit detection results acoustically and in a bio-friendly manner.
- Distinguish between species based on the acoustic signals received.
- Achieve a low power design to enable units to remain deployed for long periods.
- Maintain a low-cost design approach throughout.

The background research in Chapter 2 introduces the problem statement surrounding cetacean monitoring as a whole. Vocalisations from these animals are shown to be high frequency signals which can require significant computational power and memory facility to process digitally. The current available PAM technology is shown to lack the freedom to deploy and receive data in any ocean location. Systems tend to be either wireless loggers which risk data being lost at sea and wired systems which are restricted to shoreside locations. There is a real motivation to address limitations of this technology by producing a low energy wireless system capable of transferring data in near real time. The motivation for this research is to provide a tool to enable marine biologists and conservationists to monitor these animals without the need for invasive tagging or adding to ocean pollution.

The literature review in Chapter 3 shows the instrumentation and detection/classification methods used by researchers. The instrumentation presented goes into further detail than Chapter 2 by looking at the specific details of each system used for PAM of cetacean. The review highlights the potential advantages of using a low-energy underwater network of nodes as opposed to a single fixed system. Receiving data in near real time eliminates the risk of data loss from isolated logging systems.

Chapter 3 reviews the methods of detecting and classifying cetaceans used by researchers in the field. Many of the methods of detecting/classifying cetaceans have been shown to rely on commercial products. The issue with some of these systems is that the specific method is protected intellectual property. This means that there is little known about the inner workings but as the product is used heavily by researchers it does provide a system with which to compare against. Other commercial products have been shown to be highly customisable digital processing software. These systems are only as good as the threshold data provided by the user. There are examples of systems based on custom detection algorithms but they tend to consist of hydrophones connected to laptops running software. In the whistle detection

research, systems are shown to be very processor intensive using neural networks and image recognition. Neither of these would be realistic in a battery operated isolated PAM node. The review shows the lack of an open source low-energy cetacean detection/classification capable of relaying data in near real time.

8.2.1 Cetacean Click Detection/Classification

The method presented in Chapter 6 shows a cetacean click detection system using a mixture of analogue and DSP. The power efficiency consideration is evident in the algorithms layered approach where the very low power system controls access to the next higher power layer. This has been shown to only allow access to the most power hungry level of DSP when there is a significant possibility that the signal is indeed from a cetacean. This high level DSP stage involves species classification and results have shown that this can be achieved using key characteristics related to each species. Examples of these characteristics are shown to be estimated bandwidth, peak frequency, inter-click-interval and spectral centroid.

Chapter 6 shows the results of comparing the developed detection algorithm with a ground truth device used by researchers call the C-POD. Whilst the number of detections are comparable with the C-POD, a definitive measure of detection reliability is difficult due to the 'black-box' nature of the C-POD. The method it uses is not in the public domain. Producing a device in hardware which houses the detection algorithm would allow for more realistic evaluation. A superior ground truth would also need to be in place so that results can be compared against. At present, using acoustic recordings with manual analysis is the best available ground truth but it is a very labour intensive method.

8.2.2 Cetacean Whistle Detection

The results in Chapter 7 show that whistles can be identified using a PLL based detection algorithm. The use of PLL is shown to be selected based on its potential to satisfy the low energy requirement of this project. The method created shows that a tuned PLL can track the frequency of a whistle. The introduction of AGC to the beginning stage of the signal processing helped to maintain the PLL in its locked state when fading occurred. Processing synthetically created whistles showed that the algorithm was able to both track the single out the whistle like signals. The performance evaluation of the cetacean algorithm in Chapter 7 shows that 19 out of 25 real cetacean whistles were detected. The total number of cetacean whistles was verified manually by the author audibly and by analysing the spectrogram of the cetacean recording. Ideally the algorithm could be evaluated against a ground truth adopted by the research community but there are a variety of methods and no definitive commercial

standard product. A long duration field trial with accompanying audio recordings would allow for further performance based analysis of the cetacean whistle detection algorithm.

8.3 Concluding Remarks

The passive acoustic monitoring algorithms presented in this thesis have shown the ability to detect the target signals. In each of the three target areas, cetacean clicks, cetacean whistles and surface vessels every effort has been made to compare the detection/classification results against the best available ground truth. The results have been promising throughout with good levels of detection using passive acoustics. The PAM methodologies presented have either been chosen for their low energy potential or ability to be physically implemented in custom hardware. In the vessel detection sections of this thesis there has been a greater level of development of hardware. This has resulted in a deployable device which has been successfully integrated with the NMV3. Detection results have been transmitted acoustically during long deployment duration's back to a shore side base station. Deployment in a realistic environment is one of the key aims for this project and this has been achieved. The North Sea can be a severe environment to conduct long term experiments so the robust enclosure design and low energy ethos have been key enablers to achieve this goal. Overall this project has shown promising results in the field of low energy passive acoustic monitoring.

8.4 Future Work

A number of further areas of research have been identified as a result of the work in this thesis. The vessel detection algorithm has been developed into a physical device which can be deployed in open sea. One area of further research would be beneficial is the used of the device to test the NCDD mode. Comparing this mode against the most exhaustively tested CADD would provide an answer as which would is the better performing method. Early indications suggest that the NCDD mode would provide better sensitivity in detecting vessels but the main question would be what impact a duty cycled approach has the the detection results.

Another area of further research related to the vessel detection algorithms would be the inclusion of a localisation facility. Knowing a vessel is present is only half of the battle because if the end user wishes to act on the detection they would need to be aware of the location where it occurred. Therefore, a method of localisation would be a valuable feature. The aim of achieving this would be a mixture of the base detection algorithm which controls

a localisation mode. This mode could be implemented using a combination a spacial network data and potentially on node acoustic positioning.

The research on cetacean clicks has shown great promise in Matlab but the true test is to develop deployable hardware and embedded software. Although the author would have liked to continue with this area, a sister project has utilised much of this research to achieve workable hardware. The NanoPAM project has achieved successful detection of cetacean clicks whilst deployed in the North Sea [57]. The cetacean whistle detection research has shown great promise in detecting whistles without the need for heavy processing power. The use of PLL is not a common approach within research and a greater level of testing would provide a more in depth evaluation of its performance. Development of a deployable piece of hardware would provide a better test bed for the system.

In evaluating this project, a key area for improvement in future work would be to establish a more robust ground truth. The current ground truth for vessel detection uses AIS data which is not definitive as some vessel types are not required to carry an AIS system. An absolute ground truth would enable more accurate analysis of reliability and potentially provide additional data to refine the detection algorithm. In order to facilitate long term ground truth monitoring, one solution would be to use a combination of devices such as visual survey, video capture, acoustic recording, AIS data and RADAR. This would require significant investment to setup but would improve the accuracy of detection results.

This project has shown potential methods of detecting both vessel and cetacean activity using low-energy passive acoustic monitoring techniques. One interesting area of future work would be to integrate these different detection targets into a single multi-modal sensing device. Having a device that could detect both vessel and cetacean activity would provide a great data set for marine biologists to evaluate the impact of shipping on migration patterns of cetaceans. This could inform governments on methods of limiting the impact of shipping on marine life. In addition to creating a multi-modal device, integrating networking capabilities would increase the detection area and also improve data transfer reliability as detection results could be transferred through the network using the most reliable path. This data path could be monitored using acoustics and the preferred route updated based on the changing channel conditions.

References

[1] (2011). *Computational ocean acoustics*. Modern acoustics and signal processing. Springer Science+Business Media, LLC, New York, 2nd ed.. edition.

[2] Abrahamsen, K. (2012). The ship as an underwater noise source. In *Proceedings of Meetings on Acoustics ECUA2012*, volume 17, page 070058. ASA.

[3] Akyildiz, I. F., Pompili, D., and Melodia, T. (2005). Underwater acoustic sensor networks: research challenges. *Ad hoc networks*, 3(3):257–279.

[4] Alvarado-Rybak, M., Toro, F., Escobar-Dodero, J., Kinsley, A. C., Sepúlveda, M. A., Capella, J., Azat, C., Cortés-Hinojosa, G., Zimin-Veselkoff, N., and Mardones, F. O. (2020). 50 years of cetacean strandings reveal a concerning rise in chilean patagonia. *Scientific Reports*, 10(1):1–10.

[5] Andrews, R. D., Baird, R. W., Calambokidis, J., Goertz, C. E., Gulland, F., Heide-Jorgensen, M.-P., Hooker, S. K., Johnson, M., Mate, B., Mitani, Y., et al. (2019). Best practice guidelines for cetacean tagging. *Journal of Cetacean Research and Management*.

[6] Aroyan, J. L. (1996). *Three-dimensional numerical simulation of biosonar signal emission and reception in the common dolphin*. University of California, Santa Cruz.

[7] Au, W. W. (2012). *The sonar of dolphins*. Springer Science & Business Media.

[8] Au, W. W., Kastelein, R. A., Rippe, T., and Schooneman, N. M. (1999). Transmission beam pattern and echolocation signals of a harbor porpoise (phocoena phocoena). *The Journal of the Acoustical Society of America*, 106(6):3699–3705.

[9] Averbuch, A., Zheludev, V., Neittaanmäki, P., Wartiainen, P., Huoman, K., and Janson, K. (2011). Acoustic detection and classification of river boats. *Applied Acoustics*, 72(1):22–34.

[10] Axelsson, O. and Rhén, C. (2020). Neural-network-based classification of commercial ships from multi-influence passive signatures. *IEEE Journal of Oceanic Engineering*, 46(2):634–641.

[11] Barnes, C. R., Best, M. M., Johnson, F. R., Pautet, L., and Pirenne, B. (2012). Challenges, benefits, and opportunities in installing and operating cabled ocean observatories: Perspectives from neptune canada. *IEEE Journal of Oceanic Engineering*, 38(1):144–157.

[12] Bouffaut, L., Dréo, R., Labat, V., Boudraa, A.-O., and Barruol, G. (2018). Passive stochastic matched filter for antarctic blue whale call detection. *The Journal of the Acoustical Society of America*, 144(2):955–965.

[13] British Broadcasting Corporation (2019). Migrants found in english channel boats. https://www.bbc.co.uk/news/uk-england-kent-47668296. [Online; accessed March 26, 2019].

[14] Brunoldi, M., Bozzini, G., Casale, A., Corvisiero, P., Grosso, D., Magnoli, N., Alessi, J., Bianchi, C. N., Mandich, A., Morri, C., et al. (2016). A permanent automated real-time passive acoustic monitoring system for bottlenose dolphin conservation in the mediterranean sea. *PloS one*, 11(1):e0145362.

[15] Burdic, W. S. (1991). *Underwater acoustic system analysis*. Prentice Hall signal processing series. Prentice Hall, Englewood Cliffs, N.J., 2nd ed.. edition.

[16] Caldwell, M. C. and Caldwell, D. K. (1965). Individualized whistle contours in bottlenosed dolphins (tursiops truncatus). *Nature*, 207(4995):434–435.

[17] Carlton, J. S. J. S. (2007). *Marine propellers and propulsion*. Butterworth-Heinemann, Oxford, 2nd ed.. edition.

[18] Carstensen, J., Henriksen, O., and Teilmann, J. (2006). Impacts of offshore wind farm construction on harbour porpoises: acoustic monitoring of echolocation activity using porpoise detectors (t-pods). *Marine Ecology Progress Series*, 321:295–308.

[19] Castellote, M., Leeney, R. H., O'Corry-Crowe, G., Lauhakangas, R., Kovacs, K. M., Lucey, W., Krasnova, V., Lydersen, C., Stafford, K. M., and Belikov, R. (2013). Monitoring white whales (delphinapterus leucas) with echolocation loggers. *Polar biology*, 36(4):493–509.

[20] Channel Coastal Observatory (2020). Channel coastal observatory. http://www.channelcoast.org/.

[21] Chelonia Limited (2020a). Cetacean monitoring systems. http://www.chelonia.co.uk/index.html. [Online; accessed November 20, 2020].

[22] Chelonia Limited (2020b). Cetacean publications. https://www.chelonia.co.uk/publications.htm. [Online; accessed November 20, 2020].

[23] Chung, K. W., Sutin, A., Sedunov, A., and Bruno, M. (2010). Cross-correlation method for measuring ship acoustic signatures. In *Proceedings of Meetings on Acoustics 160ASA*, volume 11, page 055002. Acoustical Society of America.

[24] Chung, K. W., Sutin, A., Sedunov, A., and Bruno, M. (2011). Demon acoustic ship signature measurements in an urban harbor. *Advances in Acoustics and Vibration*, 2011.

[25] Clark, C. W., Charif, R., Mitchell, S., and Colby, J. (1996). Distribution and behavior of the bowhead whale, balaena mysticetus, based on analysis of acoustic data collected during the 1993 spring migration off point barrow, alaska. *Report-International Whaling Commission*, 46:541–554.

[26] Clark, P., Kirsteins, I., and Atlas, L. (2010). Multiband analysis for colored amplitude-modulated ship noise. In *2010 IEEE International Conference on Acoustics, Speech and Signal Processing*, pages 3970–3973. IEEE.

[27] Council, N. R. et al. (2003). *Ocean noise and marine mammals*. National Academies Press (US).

[28] Cranford, T. W. (2000). In search of impulse sound sources in odontocetes. In *Hearing by whales and dolphins*, pages 109–155. Springer.

[29] Datta, S. and Sturtivant, C. (2002). Dolphin whistle classification for determining group identities. *Signal processing*, 82(2):251–258.

[30] Díaz, H. and Soares, C. G. (2020). Review of the current status, technology and future trends of offshore wind farms. *Ocean Engineering*, 209:107381.

[31] Evans, P. G. and Hammond, P. S. (2004). Monitoring cetaceans in european waters. *Mammal review*, 34(1-2):131–156.

[32] Fisheries, N. I. and (NIFCA), C. A. (2020). https://www.nifca.gov.uk/about/.

[33] FleetMon (2020). Live ais vessel tracker with ship and port database. https://www.fleetmon.com/.

[34] Gardner, F. M. (2005). *Phaselock techniques*. John Wiley & Sons.

[35] Garrod, A., Fandel, A. D., Wingfield, J. E., Fouda, L., Rice, A. N., and Bailey, H. (2018). Validating automated click detector dolphin detection rates and investigating factors affecting performance. *The Journal of the Acoustical Society of America*, 144(2):931–939.

[36] Gillespie, D. (2004). Detection and classification of right whale calls using an'edge'detector operating on a smoothed spectrogram. *Canadian Acoustics*, 32(2):39–47.

[37] Gillespie, D. and Caillat, M. (2008). Statistical classification of odontocete clicks. *Canadian Acoustics*, 36(1):20–26.

[38] Gillespie, D., Caillat, M., Gordon, J., and White, P. (2013). Automatic detection and classification of odontocete whistles. *The Journal of the Acoustical Society of America*, 134(3):2427–2437.

[39] Gillespie, D. and Chappell, O. (2002). An automatic system for detecting and classifying the vocalisations of harbour porpoises. *Bioacoustics*, 13(1):37–61.

[40] Gillespie, D., Mellinger, D., Gordon, J., Mclaren, D., Redmond, P., McHugh, R., Trinder, P., Deng, X., and Thode, A. (2008). Pamguard: Semiautomated, open source software for real-time acoustic detection and localisation of cetaceans. *Journal of the Acoustical Society of America*, 30(5):54–62.

[41] Google (2020). Google maps. https://www.google.com/maps/.

[42] Holmes, J. J. (2006). Exploitation of a ship's magnetic field signatures. *Synthesis Lectures on Computational Electromagnetics*, 1(1):1–78.

[43] IMO (International Maritime Organisation (2020). Regulations for carriage of ais. https://www.imo.org/fr/OurWork/safety/navigation/pages/ais.aspx. [Online; accessed November 19, 2020].

[44] James Reid (2003). Atlas of cetacean distribution in north-west european waters. [Online; accessed April 04, 2018].

[45] Jiang, J.-j., Bu, L.-r., Duan, F.-j., Wang, X.-q., Liu, W., Sun, Z.-b., and Li, C.-y. (2019). Whistle detection and classification for whales based on convolutional neural networks. *Applied Acoustics*, 150:169–178.

[46] Ketten, D. R. (2005). Beaked whale necropsy findings for strandings in the bahamas, puerto rico, and madeira, 1999-2002. Technical report, WOODS HOLE OCEANOGRAPHIC INSTITUTION MA.

[47] Leal, N., Leal, E., and Sanchez, G. (2015). Marine vessel recognition by acoustic signature. *ARPN J. Eng. Appl. Sci*, 10(20):9633–9639.

[48] Lowes, G. J., Neasham, J., Burnett, R., Sherlock, B., and Tsimenidis, C. (2022). Passive acoustic detection of vessel activity by low-energy wireless sensors. *Journal of Marine Science and Engineering*, 10(2):248.

[49] Lowes, G. J., Neasham, J. A., Burnett, R., and Tsimenidis, C. C. (2019). Low energy, passive acoustic sensing for wireless underwater monitoring networks. In *OCEANS 2019 MTS/IEEE SEATTLE*, pages 1–9. IEEE.

[50] Lurton, X. (2010). *An introduction to underwater acoustics : principles and applications*. Springer-Praxis books in geophysical sciences. Springer, Berlin ; London, 2nd ed.. edition.

[51] Marine, T. (2020). Slocum g3 glider. http://www.teledynemarine.com/slocum-glider. [Online; accessed January 04, 2021].

[52] Matsumoto, H., Turpin, A., Haxel, J., Meinig, C., Craig, M., Tagawa, D., Klinck, H., and Hanson, B. (2016). A real-time acoustic observing system (raos) for killer whales. In *OCEANS 2016 MTS/IEEE Monterey*, pages 1–6. IEEE.

[53] McFee, J., Das, Y., and Ellingson, R. (1990). Locating and identifying compact ferrous objects. *IEEE Transactions on Geoscience and Remote Sensing*, 28(2):182–193.

[54] Mellinger, D. (2002). Ishmael: 1.0 user's guide; ishmael: integrated system for holistic multi-channel acoustic exploration and localization.

[55] Mellinger, D. K. and Clark, C. W. (2000). Recognizing transient low-frequency whale sounds by spectrogram correlation. *The Journal of the Acoustical Society of America*, 107(6):3518–3529.

[56] Munger, L. M., Mellinger, D. K., Wiggins, S. M., Moore, S. E., and Hildebrand, J. A. (2005). Performance of spectrogram cross-correlation in detecting right whale calls in long-term recordings from the bering sea. *Canadian Acoustics*, 33(2):25–34.

[57] NanoPAM (2020). Nerc. https://gtr.ukri.org/projects?ref=NE%2FR014884%2F1.

[58] NURC (2008). *Sonar Acoustics Handbook*. NURC. La Spezia, Italy. 2008.

[59] Nuuttila, H. K., Thomas, L., Hiddink, J. G., Meier, R., Turner, J. R., Bennell, J. D., Tregenza, N. J., and Evans, P. G. (2013). Acoustic detection probability of bottlenose dolphins, tursiops truncatus, with static acoustic dataloggers in cardigan bay, wales. *The Journal of the Acoustical Society of America*, 134(3):2596–2609.

[60] NXP (2021). Mkl16z256vlh4. https://www.nxp.com/part/MKL16Z256VLH4#/. [Online; accessed January 28, 2021].

[61] Ocean Instruments (2020). Soundtrap 300. http://www.oceaninstruments.co.nz/soundtrap-300/. [Online; accessed November 16, 2020].

[62] Pamguard (2020). Open source software for passive acoustic monitoring. https://www.pamguard.org/. [Online; accessed December 02, 2020].

[63] Panigada, S., Lauriano, G., Burt, L., Pierantonio, N., and Donovan, G. (2011). Monitoring winter and summer abundance of cetaceans in the pelagos sanctuary (northwestern mediterranean sea) through aerial surveys. *PloS one*, 6(7):e22878.

[64] Parsons, E., Dolman, S. J., Wright, A. J., Rose, N. A., and Burns, W. (2008). Navy sonar and cetaceans: Just how much does the gun need to smoke before we act? *Marine pollution bulletin*, 56(7):1248–1257.

[65] Pollara, A., Sutin, A., and Salloum, H. (2016). Improvement of the detection of envelope modulation on noise (demon) and its application to small boats. In *OCEANS 2016 MTS/IEEE Monterey*, pages 1–10. IEEE.

[66] Pollara, A., Sutin, A., and Salloum, H. (2017a). Modulation of high frequency noise by engine tones of small boats. *The Journal of the Acoustical Society of America*, 142(1):EL30–EL34.

[67] Pollara, A., Sutin, A., and Salloum, H. (2017b). Passive acoustic methods of small boat detection, tracking and classification. In *2017 IEEE International Symposium on Technologies for Homeland Security (HST)*, pages 1–6. IEEE.

[68] Potter, J. R., Mellinger, D. K., and Clark, C. W. (1994). Marine mammal call discrimination using artificial neural networks. *The Journal of the Acoustical society of America*, 96(3):1255–1262.

[69] Quick, N. J., Cioffi, W. R., Shearer, J. M., Fahlman, A., and Read, A. J. (2020). Extreme diving in mammals: first estimates of behavioural aerobic dive limits in cuvier's beaked whales. *Journal of Experimental Biology*, 223(18).

[70] Randall, R. B. (2017). A history of cepstrum analysis and its application to mechanical problems. *Mechanical Systems and Signal Processing*, 97:3–19.

[71] Rasmussen, M. H. and Miller, L. A. (2002). Whistles and clicks from white-beaked dolphins, lagenorhynchus albirostris, recorded in faxaflói bay, iceland. *Aquatic Mammals*, 28(1):78–89.

[72] Rasmussen, M. H., Wahlberg, M., and Miller, L. A. (2004). Estimated transmission beam pattern of clicks recorded from free-ranging white-beaked dolphins (lagenorhynchus albirostris). *The Journal of the Acoustical Society of America*, 116(3):1826–1831.

[73] Roberts, B. L. and Read, A. J. (2015). Field assessment of c-pod performance in detecting echolocation click trains of bottlenose dolphins (tursiops truncatus). *Marine Mammal Science*, 31(1):169–190.

[74] Roch, M. A., Klinck, H., Baumann-Pickering, S., Mellinger, D. K., Qui, S., Soldevilla, M. S., and Hildebrand, J. A. (2011). Classification of echolocation clicks from odontocetes in the southern california bight. *The Journal of the Acoustical Society of America*, 129(1):467–475.

[75] Ross, D. (1987). *Mechanics of underwater noise*. Peninsula, Los Altos, CA.

[76] Ryan, J., Cline, D., Dawe, C., McGill, P., Zhang, Y., Joseph, J., Margolina, T., Caillat, M., Fischer, M., DeVogelaere, A., et al. (2016). New passive acoustic monitoring in monterey bay national marine sanctuary. In *OCEANS 2016 MTS/IEEE Monterey*, pages 1–8. IEEE.

[77] Sarnocinska, J., Tougaard, J., Johnson, M., Madsen, P. T., and Wahlberg, M. (2016). Comparing the performance of c-pods and soundtrap/pamguard in detecting the acoustic activity of harbor porpoises (phocoena phocoena). In *Proceedings of Meetings on Acoustics 4ENAL*, volume 27, page 070013. Acoustical Society of America.

[78] Sheinker, A., Salomonski, N., Ginzburg, B., Shkalim, A., Frumkis, L., and Kaplan, B.-Z. (2006). Network of remote sensors for magnetic detection. In *2006 International Conference on Information Technology: Research and Education*, pages 56–60. IEEE.

[79] Sierra, E. and Contreras, J. (2015). Classification of small boats using fuzzy classifier. In *2015 Annual Conference of the North American Fuzzy Information Processing Society (NAFIPS) held jointly with 2015 5th World Conference on Soft Computing (WConSC)*, pages 1–5. IEEE.

[80] Sky News - Emily Mee (2019). Two boats of suspected iranian migrants picked up in english channel. https://news.sky.com/story/two-boats-of-suspected-iranian-migrants-picked-up-in-english-channel-11648301. [Online; accessed March 26, 2019].

[81] Soldevilla, M. S., Henderson, E. E., Campbell, G. S., Wiggins, S. M., Hildebrand, J. A., and Roch, M. A. (2008). Classification of risso's and pacific white-sided dolphins using spectral properties of echolocation clicks. *The Journal of the Acoustical Society of America*, 124(1):609–624.

[82] Sorensen, E., Ou, H. H., Zurk, L. M., and Siderius, M. (2010). Passive acoustic sensing for detection of small vessels. In *OCEANS 2010 MTS/IEEE SEATTLE*, pages 1–8. IEEE.

[83] Sozer, E. M., Stojanovic, M., and Proakis, J. G. (2000). Underwater acoustic networks. *IEEE journal of oceanic engineering*, 25(1):72–83.

[84] Stafford, K. M. (1995). Characterization of blue whale calls from the northeast pacific and development of a matched filter to locate blue whales on the us navy sosus (sound surveillance system) arrays.

[85] Stafford, K. M., Fox, C. G., and Clark, D. S. (1998). Long-range acoustic detection and localization of blue whale calls in the northeast pacific ocean. *The Journal of the Acoustical Society of America*, 104(6):3616–3625.

[86] Sutin, A., Salloum, H., DeLorme, M., Sedunov, N., Sedunov, A., and Tsionskiy, M. (2013). Stevens passive acoustic system for surface and underwater threat detection. In *2013 IEEE International Conference on Technologies for Homeland Security (HST)*, pages 195–200. IEEE.

[87] Tesei, A., Been, R., Williams, D., Cardeira, B., Galletti, D., Cecchi, D., Garau, B., and Maguer, A. (2015). Passive acoustic surveillance of surface vessels using tridimensional array on an underwater glider. In *OCEANS 2015-Genova*, pages 1–8. IEEE.

[88] Todd, V., Todd, I., Gardiner, J., and Morrin, E. (2015). *Marine mammal observer and passive acoustic monitoring handbook*. Pelagic Publishing Ltd.

[89] University, N. (2020). Usmart project. https://research.ncl.ac.uk/usmart/. [Online; accessed December 02, 2020].

[90] Urick, R. J. (1983). *Principles of underwater sound*. McGraw-Hill, New York, 3rd ed.. edition.

[91] Wegmatt LLC (2020). daisy hat - ais receiver for raspberry pi. https://www.tindie.com/products/astuder/daisy-hat-ais-receiver-for-raspberry-pi/. [Online; accessed March 08, 2020].

[92] Wenz, G. M. (1962). Acoustic ambient noise in the ocean: spectra and sources. *The Journal of the Acoustical Society of America*, 34(12):1936–1956.

[93] Wiggins, S. M. and Hildebrand, J. A. (2007). High-frequency acoustic recording package (harp) for broad-band, long-term marine mammal monitoring. In *2007 Symposium on Underwater Technology and Workshop on Scientific Use of Submarine Cables and Related Technologies*, pages 551–557. IEEE.

[94] Witzany, G. (2013). *Biocommunication of Animals*. Springer Science & Business Media.

[95] Zimmer, W. M. (2011). *Passive acoustic monitoring of cetaceans*. Cambridge University Press.